Western Australian School of Mines: Minerals, Energy and Chemical Engineering
Faculty of Science and Engineering

Solubility Kinetics Study of Organic and Inorganic Mercury Species in Reservoir Fluids and Their Behaviour in Aqueous Environments

Fenny Anggreni Kho

This thesis is presented for the Degree of
Doctor of Philosophy
of
Curtin University

August 2018

DECLARATION

To the best of my knowledge and belief this thesis contains no material previously published by any other person except where due acknowledgment has been made.

This thesis contains no material which has been accepted for the award of any other degree or diploma in any university.

Signature: …….

Date: 30 August 2018

This thesis is dedicated to my family,

My parents, Lisma Carina and Augus Tendy Kho

And my brother, Ryan Anggada Kho

For their continuous love, prayers and encouragements.

ACKNOWLEDGEMENTS

I would like this opportunity to express my deepest appreciation to my principal supervisor, Dr. Gia Hung Pham. Throughout this project, Dr. Gia Hung Pham has been a wonderful example to learn from in all aspects of life and without his utmost support, this work wouldn't have been possible. The knowledge, skill and dedication of Dr. Gia Hung Pham as a researcher is an inspiration and I could not have hoped for a better advisor. I cannot thank Dr. Gia Hung Pham enough for his advice, encouragement, consideration and guidance that enabled me to persevere and complete this PhD research program.

I would like to thank my co-supervisor, Prof. Vishnu Pareek for his kind suggestions, encouragement and support during my project.

I would also like to acknowledge the encouragement and support given by the chairman of the thesis committee, Prof. Shaomin Liu.

In addition, I would like to thank my industrial co-supervisor, Mr. Thor Frette for his kind suggestions and support during this PhD research project. His comments and experience from the industrial aspect of the project have been extremely valuable and become one of the main motivation to complete this thesis.

I would like to gratefully acknowledge Shell Development Australia Pty Ltd and Department of Chemical Engineering of Curtin University, Perth for providing the financial support and the necessary research facilities for making the completion of this PhD research program possible.

My heartfelt thanks go to all my friends, colleagues and lab technicians at Curtin University. Thank you for your help during my experiments as well as the moral support and encouragements everyone have given to me.

Finally, I would like to take this opportunity to express my sincerest love and gratitude to my parents. I truly thank them for their support during this PhD program. Thank you for always looking after my health and wellbeing even though they are not here in Australia. I would not be where I am today without your continuous prayers and encouragements.

ABSTRACT

Mercury is a highly toxic contaminant that exist in trace quantities naturally occurring trace contaminant in hydrocarbon reservoirs and is distributed in multiple (oil, gas and water) phases. Multiple mercury species namely elemental, inorganic and organic mercury have been detected to co-exist within different sections of the pipeline and waste streams within a gas processing facilities. Knowledge on the behaviour of mercury, especially inorganic and organic is substantially limited, thus making it difficult to predict its distribution and reaction mechanisms within the process system and during release as waste into the environment. While there is an abundance of data available on the solubility of varying mercury species at different conditions, those data only cover the equilibrium/saturated portion. Transient information such as absorption rate and reaction kinetics of mercury species with the compounds present at reservoir fluids at transient conditions are crucial to enable accurate prediction models. Currently, very limited sources are found, in which those transient conditions have been investigated.

The aim of this research project is to study solubility kinetics study of several selected mercury species in fresh and sea water, along with addition of impurities that is commonly injected into the pipeline. The solubility kinetics study was conducted on selected inorganic; mercury (II) chloride $HgCl_2$ and organic; diphenyl mercury Ph_2Hg mercury that has been detected in the oil and gas process. The solid vaporization method is applied to generate mercury gas at different concentrations for this study. The absorption and kinetic parameters of $HgCl_2$ and Ph_2Hg into various aqueous solutions was measured in a temperature controlled semi-batch stirred cell reactor at temperature of 283 – 333 K.

The kinetic parameters of the reaction between $HgCl_2$ and sodium chloride (NaCl) is reported for the first time. At the same hydrodynamic condition, the absorption flux of $HgCl_2$ into water increases from 6.02×10^{-6} to 10.26×10^{-6} mol/m^2.h when absorption temperature is increased from 298 to 333 K. Applying the two-film theory, the absorption of $HgCl_2$ into water is controlled by the gas phase resistance. The gas phase mass transfer coefficient; k_G does not change with the $HgCl_2$ concentration in the gas phase significantly, but is affected by the absorption temperature. For the case of absorption of $HgCl_2$ into aqueous NaCl solution, the absorption flux increases with

increasing NaCl concentration and absorption temperature. The mechanism of reaction between $HgCl_2$ and NaCl is proposed and the reaction rate law follows second order; first order with respect to $HgCl_2$ and Cl^- with the reaction rate constant $k_2 = 1.09 \times 10^9 \exp(\frac{-123.32\ \mathrm{kJ/mol}}{\mathrm{RT}})$ m^3/mol.s.

Absorption of $HgCl_2$ into monoethylene glycol (MEG) solutions was comparable to absorption in pure water and effect of MEG was not seen for MEG concentrations of 2 – 30 v/v%. The absorption flux was mainly affected by the absorption temperature and the concentration of $HgCl_2$ in the gas phase. Utilisation of several mercury analysis techniques such as flow injection mercury spectroscopy (FIMS), inductively couple plasma-mass spectroscopy (ICP-MS), Fourier-transform infrared spectroscopy (FTIR) and Raman spectroscopy show that no interactions between $HgCl_2$ and MEG were detected for the test parameters studied.

Ph_2Hg is barely soluble in water, its solubility is found to be 10.43 mg/L at 293 K. Absorption of Ph_2Hg into aqueous NaCl solutions show decrease in absorption flux with increase NaCl concentration. This depression in absorption flux is related to the effect of salting-out as NaCl concentration was increased up to 3.5 wt.%. The interaction between Ph_2Hg and NaCl is purely physical as product of chemical reaction was not detected to overcome the salt effect on the absorption process.

Ph_2Hg is 20 times more soluble in solution containing 50 v/v% MEG compared to in fresh water. Absorption of Ph_2Hg into aqueous 10 – 30 v/v% MEG solutions are comparable to its absorption in fresh water. Further increase of MEG to 50 v/v% show a slight decrease in overall absorption flux of Ph_2Hg, indicating that liquid phase resistance; k_L is dominating. Interaction between Ph_2Hg and MEG also did not yield in a chemical-reaction enhanced absorption and that it is mostly physical. The absorption flux was mainly affected by the absorption temperature and the concentration of Ph_2Hg in the gas phase.

Evaluation of the absorption of Hg^0, $HgCl_2$ and Ph_2Hg suggest that vapour/liquid equilibrium within the different sections of the oil and gas processes will be first reached by Hg^0, followed by Ph_2Hg and $HgCl_2$. Temperature has a positive effect on the absorption of $HgCl_2$ and Ph_2Hg into various aqueous solutions, hence absorption flux will be highest at sections of the process operating at higher temperature such as the MEG and amine regeneration columns. Regarding the effect of impurities, $HgCl_2$

will be most prevalent in process streams containing high NaCl concentration, which is mainly in produced and waste water streams. Ph_2Hg will be less likely to partition into the mentioned streams due to the depressing effect of NaCl on its absorption. Since Ph_2Hg is 20 times more soluble in MEG compared to water, higher concentration of this compound will prevail within the 'rich' MEG streams that is re-circulated back into the pipeline.

In summary, the findings from this work helps to improve the knowledge on behaviour of $HgCl_2$ and Ph_2Hg within the natural gas processing facilities, especially during transportation in pipelines and the MEG regeneration process. Moreover, behaviour of $HgCl_2$ and Ph_2Hg in aqueous environment is also addressed. The result of this project will ultimately deliver key information in the development of improved strategies for mercury treatment and handling in existing and future oil and gas facilities along with other related fields.

LIST OF PUBLICATIONS

Published Paper:

1. **Kho, Fenny**, and Gia Hung Pham. 2018. "Absorption kinetics of mercury (II) chloride into water and aqueous sodium chloride solution." *Fuel Processing Technology* no. 174:78-87. doi: 10.1016/j.fuproc.2018.02.017.
2. **Kho, Fenny**, and Gia Hung Pham. 2019. Absorption kinetics of mercury (II) chloride into mono-ethylene glycol (MEG) solution. *Fuel Processing Technology* no. 185:46-55. doi: 10.1016/j.fuproc.2018.11.018.

Manuscripts Submitted or in Preparation:

3. **Kho, Fenny**, and Gia Hung Pham, Absorption of various mercury species in water at trace concentration **(in preparation)**.
4. **Kho, Fenny**, and Gia Hung Pham, Absorption of diphenyl mercury into water and aqueous solutions **(in preparation)**.

Conference:

5. **Kho, Fenny**, and Gia Hung Pham. 2017. Absorption of Hg^0 and $HgCl_2$ in water at 25°C at trace concentration. Chemeca, 23 – 26 July 2017, Melbourne, Australia (**Oral Presentation)**.

TABLE OF CONTENT

LIST OF FIGURES

LIST OF TABLES

NOMENCLATURES

A	Surface area of contact
a	Ratio between gas/liquid interface area and volume of reactor
$C_{A,L}$	Concentration of A in the bulk liquid side
$C_{A,L}^{*}$	Equilibrium concentration of A at liquid side interface
C_{Cl^-}	Concentration of Cl^- ions in the liquid
D	Diffusion coefficient
E	Enhancement factor
E_a	Activation energy
f_l	Ratio between volume of liquid and reactor
H	Henry coefficient
H_T	Henry coefficient at temperature T
J	Absorption flux
k_2	Second order rate constant
K_L	Overall liquid mass transfer coefficient
K_G	Overall gas mass transfer coefficient
k_L	Liquid side mass transfer coefficient
k_G	Gas side mass transfer coefficient
N	Absorption rate
$P_{A,g}$	Partial pressure of A in the bulk gas side
$P_{Ag,i}$	Partial pressure of A at the gas side interface
$P_{A,g}^{*}$	Equilibrium partial pressure of A at gas side interface
R	Gas Constant
$-r_A'''$	Rate of absorption of A into the liquid
T	Temperature
t	Absorption time
t_s	Surface renewal rate
δ_G	Gas film thickness
δ_L	Liquid film thickness

CHAPTER 1:
INTRODUCTION

1.1 Background and Motivation

Mercury is a well-known pollutant that are released into the environment from natural and anthropogenic sources. In recent years, there has been a growing number of interests and studies on mercury and its species within the oil and gas industry due to increasing industrial activities from drilling into new and deeper gas reservoirs. Mercury and its various species have been reported to be present naturally as trace contaminants in the oil and gas reservoirs [1]. Mercury species distribution and concentration levels are difficult to anticipate as they vary greatly depending on the locations of extraction [2].

Mercury species exist in the natural gas and crude oil in three main groups, namely elemental mercury (Hg°), organic mercury such as dimethyl mercury (DMM) and inorganic mercury such as mercury (II) chloride ($HgCl_2$) and mercury (II) sulphide (HgS) [2, 3]. The physical and chemical properties of mercury species are different, therefore they behave differently in oil and gas processes. In addition, other common anthropogenic emission of mercury also derives from incineration of municipal solid waste and coal [4, 5]. At high temperature (>1073K), mercury exists in the flue gas as Hg^0 as this mercury species is reactive and react with available Cl_2 in the flue gas to yield inorganic Mercury. The flue gas escapes the incineration process at about 573 K with the typical mercury concentration ranges between 200 and 2000 $\mu g/Nm^3$ [6, 7].

Mercury species can be transferred between gas and water phase in the liquefied natural gas (LNG) process at different stages such as gas separation in slug catcher, monoethylene glycol (MEG) regeneration and acid gas removal using amine solution. Primarily, after the slug catcher, mercury species have been detected in all three phases (gas, condensate and water phase). The total mercury in the gas, condensate and water phase have been reported to vary widely from <0.015-1930 $\mu g/Nm^3$, <0.001-1.2 mg/l and <0.001-0.3 mg/l respectively in several well-known gas fields [8-12].

The mercury species detected in the gas phase are namely, Hg°, DMM, dibutyl mercury, diphenyl mercury and $HgCl_2$; Hg° being the dominant species [3, 13, 14].

The main mercury species detected in the condensate phase are Hg°, DMM, $HgCl_2$, suspended HgS and CH_3HgCl; $HgCl_2$ has been found to be the dominant species [2, 3, 15, 16]. In the water phase, $HgCl_2$ was found as the main mercury species existed [17]. Usually, untreated water phase is released from natural gas process and this becomes one of the major way of mercury enter the environment [17]. Although the concentration is quite low, mercury species have the tendency to accumulate in the process by adsorption, chemical reaction, dissolution in sludge and condensation [1], causing several detrimental effects such as liquefaction of aluminium heat exchangers, corrosion, catalyst poisoning, and technical plant maintenance.

In an attempt to negate these issues, academics and industrial researchers have been investigating mercury behaviours in oil and gas process. Having said that, the knowledge about mercury partitioning within oil and gas processing still needs to be improved. This is because most mercury partitioning studies and predictions within the oil and gas processes assumed that mercury species reach vapour-liquid equilibrium.

Furthermore, being the major species found in the fossil fuels and environment, Hg° is very well studied [18, 19], however there is a lack of information about organic and inorganic mercury available. Several work has been done to close the knowledge gap with regards to inorganic and organic Mercury, however current work are limited to the saturated solubility in different solvents [20-22], distribution between gas and liquid system and henry coefficient [23, 24]. To the best of our knowledge, current information are limited to either saturated or equilibrium condition, and no information available for its absorption kinetics

It is important to conduct complete mercury mapping and perform mercury balance for oil and gas processes to determine the mercury pathway in the process and their impact on the different products (gas and condensate) and waste streams. Understanding how each of the mercury species behave at different stages is also critical to make sure the safeguards are put in place to perform operations and maintenance in the field as well as environmental protection strategy if required.

With the current mercury problems and knowledge standpoint, the information with regards to the kinetics of absorption of each mercury species, especially inorganic and organic mercury are needed urgently to enable the prediction of the dynamics of

mercury accumulation in oil and gas processing equipment using absorption technique at any given time. The mentioned knowledge gaps are the main motives of this research.

1.2 Scope and Objectives

A number of research challenges for studying solubility kinetics mercury have been identified. The main objective of the current study will focus on the study of absorption process of gaseous inorganic and organic mercury in aqueous solutions. This research also aims to identify possible reactions that might occur in the presence of common contaminants within the reservoir fluids along with kinetics parameter to provide insights into mercury pathways and possible speciation upon release into aqueous environment.

The main objectives of the current study are listed:

- Study the physical and chemical solubility kinetics of both organic and inorganic mercury in 'pure' water and water with equivalent salinity of sea water by measurements.
- Investigation on the effect of temperature and impurities on the mechanism and solubility kinetics of mercury (NaCl and monoethylene glycol; MEG).
- Development of reaction mechanism and pathway of selected mercury species in fresh and sea water.
- Development of mathematical modelling to validate the solubility kinetics data achieved.
- Assessment on the effects of solubility kinetics of varying mercury species on dispersion into aquatic environment upon disposal.

Mercury species to focus on include:

- Inorganic mercury; mercury (II) chloride $HgCl_2$
- Organic mercury; diphenylmercury $Hg(C_6H_5)_2$ or equivalent non-volatile organic mercury species
- Elemental mercury; Hg^0 to validate proof of concept

1.3 Significance

There have been great complications in the oil and gas facilities in which impact of mercury within the process and end product is little understood and yet possessing detrimental effects. Unknown impact of mercury within the process and the end product include corrosion of heat exchangers and other main equipment, speciation (both qualitatively and quantitatively), leading to insufficient information to design better mercury treatment and handling system.

This research work intends to improve the understandings of the solubility kinetics of several different occurring species which will assist to:

1. Deliver the missing information, which is the transient solubility state.
2. Modelling and prediction of mercury's reaction pathways in the process system (processing of oil and gas products) which will help identify specific locations in which mercury will condensate or accumulate.
3. Calculating the distribution and speciation of the various mercury species at different sections of the process, the downstream products and environmental releases.
4. Development of effective strategies to prevent corrosion and mercury disposal plan as pollution control.
5. Insight into the fundamental mechanisms controlling the kinetics of mercury solubility.
6. Extensive insight gained on the partitioning and reaction mechanisms of mercury with other compounds to assist in improving efficiency and safety of future design of oil and gas processes and equipment.
7. Understanding of behaviour of different mercury species in aqueous environment.

1.4 Thesis Organisation

This thesis has been organised into 7 chapters that cover the details of this research work. An overview of each chapter in this thesis is as outlined below:

- **Chapter 1: Introduction**

  This chapter outlines a brief introduction to the project background. The aim and objectives of this research project are also discussed in this chapter.

- **Chapter 2: Literature Review**

  This chapter outlines a current literature reviews on the topic of mercury problem and their behaviour within the oil and gas industry. This includes the presence and distribution of various mercury species at different parts of the oil and gas processes. The review also concentrates on removal and measurement techniques commonly utilised to deal with mercury related issues. Finally, current information available on parameters such as reactions kinetics, absorption and solubility characteristics were evaluated. This leads to the identification of existing research gaps and suitable research methods for the present work.

- **Chapter 3: Research Methodology and Analytical Techniques**

  This chapter outlines the method employed to generate mercury test gases, sample preparation, experimental set-ups and analytical instruments utilised to achieve the research objectives. Later sections include Proof-of-concept test to validate the research methodology selected.

- **Chapter 4: Dynamic Solubility of Inorganic Mercury in Water**

  This chapter outlines the research findings on the solubility kinetics of inorganic mercury species ($HgCl_2$) in fresh water. Effect of temperature on $HgCl_2$ absorption characteristics are further discussed. Effect of NaCl and MEG on chemical-reaction enhanced absorption are also included.

- **Chapter 5: Dynamic Solubility of Organic Mercury in Water**

  This chapter outlines the research findings on the solubility kinetics of organic mercury species (Ph_2Hg) in fresh water and reservoir fluids (addition of NaCl and MEG). Effect of temperature on the absorption process are further evaluated. Finally, the absorption characteristics of various mercury species (elemental, inorganic and organic) are compared and their implications on the oil and gas processes discussed.

- **Chapter 6: Behaviour of Inorganic and Organic Mercury in Aqueous Environment**

  This chapter consolidates and applies the research findings obtained from the proceeding chapters to predict mercury species behaviour within aqueous environment. Possible emission pathways and behaviour within the reservoir fluids and several waste streams are addressed.

- **Chapter 7: Conclusion and Recommendation**

  This chapter concludes the major findings drawn from all chapters within the thesis, based on research findings from the data obtained. Recommendations for future research work are also provided.

1.5 Reference

[1] Shafawi, Azman Bin. 1999. *Mercury Species in Natural Gas Condensate* Department of Environmental Sciences, University of Plymouth Plymouth

[2] Wilhelm, S. Mark, and Nicholas Bloom. 2000. "Mercury in Petroleum." *Fuel Processing Technology* no. 63 (2000):1-27.

[3] Wilhelm, S. Mark. 2001. Mercury in Petroleum and Natural Gas: Estimation of Emissions from Production, Processing, and Combustion. Tomball, Texas.

[4] Pacyna, Jozef M., Oleg Travnikov, Francesco De Simone, Ian M. Hedgecock, Kyrre Sundseth, Elisabeth G. Pacyna, Frits Steenhuisen, Nicola Pirrone, John Munthe, and Karin Kindbom. 2016. "Current and future levels of mercury atmospheric pollution on a global scale." *Atmospheric Chemistry and Physics* no. 16:12495–12511. doi: 10.5194/acp-16-12495-2016.

[5] UNEP. 2013. Global Mercury Assessment - Sources, Emissions, Releases and Environmental Transport.

[6] Carey, Todd R., Jr. Oliver W. Hargrove, Carl F. Richardson, Ramsay Chang, and Frank B. Messerole. 1998. "Factors Affecting Mercury Control in Utility Flue Gas Using Activated Carbon." *Journal of the Air & Waste Management Association* no. 48:1166-1174.

[7] Lancia, A., D. Musmarra, F. Pepe, and G. Volpicelli. 1993. "Adsorption of Mercuric Chloride Vapours from Incinerator Flue Gases on Calcium Hydroxide Particles." *Combustion Science and Technology* no. 93 (1):277-289. doi: 10.1080/00102209308935293.

[8] Zettlitzer, M., R. Scholer, and R. Falter. 1997. Determination of elemental, inorganic and organic mercury in North German gas condesates and formation brines. In *SPE International Symposium on Oilfiled Chemistry*. Houston, Texas: Society of Petroleum Engineers, Inc. .

[9] Carnell, Peter J H, Vince Atma Row, and R McKenna. 2007. A re-think of the mercury removal problem for LNG plants. In *LNG15*. Barcelona, Spain.

[10] Ahmadun, Fakhru'l-Razi, AlirezaPendashteh, Luqman Chuah Abdullah, Dayang Radiah Awang Biak, Sayed Siavash Madaeni, and Zurina Zainal Abidin. 2009. "Review of technologies for oil and gas produced water treatment." *Journal of Hazardous Materials* no. 170 (2-3):530-551. doi: 10.1016/j.jhazmat.2009.05.044.

[11] Pichtel, John. 2016. "Oil and Gas Production Wastewater: Soil Contamination and Pollution Prevention." *Applied and Environmental Soil Science* no. 2016:1-24. doi: 10.1155/2016/2707989.

[12] Sainal, Muhamad Rashid, Azman Shafawi, and Abdul Jabar Hj. Mohamed. 2007. Mercury Removal System for Upstream Application: Experience in Treating Mercury From Raw Condensate In *E&P Environmental and Safety Conference*. Galveston, Texas, U.S.A. : Society of Petroleum Engineers.

[13] Abbas, Tauqeer, Girma Gonfa, Kallidanthiyil Chellappan Lethesh, M.I. Abdul Mutalib, Mahpuzah bt Abai, Kuah Yong Cheun, and Eakalak Khan. 2016. "Mercury capture from natural gas by carbon supported ionic liquids: Synthesis, evaluation and molecular mechanism." *Fuel* no. 177:296-303. doi: 10.1016/j.fuel.2016.03.032.

[14] Frech, Wolfgang, Douglas C. Baxter, Berit Bakke, James Snell, and Yngvar Thomassen. 1996. "Determination and Speciation of Mercury in Natural Gases and Gas Condensates." *Analytical Communications* no. 33:7H-9H.

[15] Tao, Hiroaki, Tadahiko Murakami, Mamoru Tominaga, and Akira Miyazaki. 1998. "Mercury speciation in natural gas condensate by gas chromatography-inductively coupled plasma mass spectrometry." *Journal of Analytical Atomic Spectrometry* no. 13 (1998):1086-1093.

[16] Wilhelm, S. Mark, Lian Liang, and David Kirchgessner. 2006. "Indentification and Properties of Mercury Species in Crude Oil." *Energy & Fuels* no. 20 (1):180-186.

[17] Gallup, Darrell L. 2014. Removal of mercury from water in the petroleum industry. Paper read at 21st International Petroleum Environmental Conference

[18] Zhao, Lingbing. 1997. *Mercury Absorption in Aqueous Solutions* The University of Texas, Austin.

[19] Iverfeldt, Åke, and Oliver Lindqvist. 1984. "The Transfer of Mercury at the Air/Water Interface." In *Gas Transfer at Water Surfaces*, 533-538. Springer Netherlands.

[20] Clever, H. Lawrence, Susan A. Johnson, and M. Elizabeth Derrick. 1985. "The Solubility of Mercury and Some Sparingly Soluble Mercury Salts in Water and Aqueous Electrolyte Solutions." *Journal of Physical and Chemical Reference Data* no. 14 (3).

[21] Gallup, Darrell L., Dennis J. O'Rear, and Ron Radford. 2017. "The behavior of mercury in water, alcohols, monoethylene glycol and triethylene glycol." *Fuel* no. 196:179-184. doi: 10.1016/j.fuel.2017.01.100.

[22] Khalifa, Mansour, and Leo Lue. 2017. "A group contribution method for predicting the solubility of mercury." *Fluid Phase Equilibria* no. 432:76-84. doi: doi.org/10.1016/j.fluid.2016.10.025.

[23] Sommar, Jonas, Oliver Lindqvist, and Dan Strömberg. 2000. "Distribution Equilibrium of Mercury (II) Chloride between Water and Air Applied to Flue Gas Scrubbing." *Journal of the Air & Waste Management Association* no. 50 (9):1663-1666. doi: 10.1080/10473289.2000.10464192.

[24] Bernard, L., K. Awitor, J. Badaud, O. Bonnin, B. Coupat, J. Fournier, and P. Verdier. 1997. "D´etermination de la pression de vapeur de HgCl2 par la m´ethode d'effusion de Knudsen." *Journal de Physique III* no. 7 (2):311-319. doi: 10.1051/jp3:1997124.

CHAPTER 2:
LITERATURE REVIEW

2.1 Introduction

In 2017, the US Government Agency for Toxic Substances and Disease Registry (ATSDR) has ranked mercury to be third amongst the other 274 substances in terms of degree of toxicity and potential for human exposure [1]. Mercury are released into the environment via natural and anthropogenic sources, while existing mercury are re-emitted and circulated within the ecosystem.

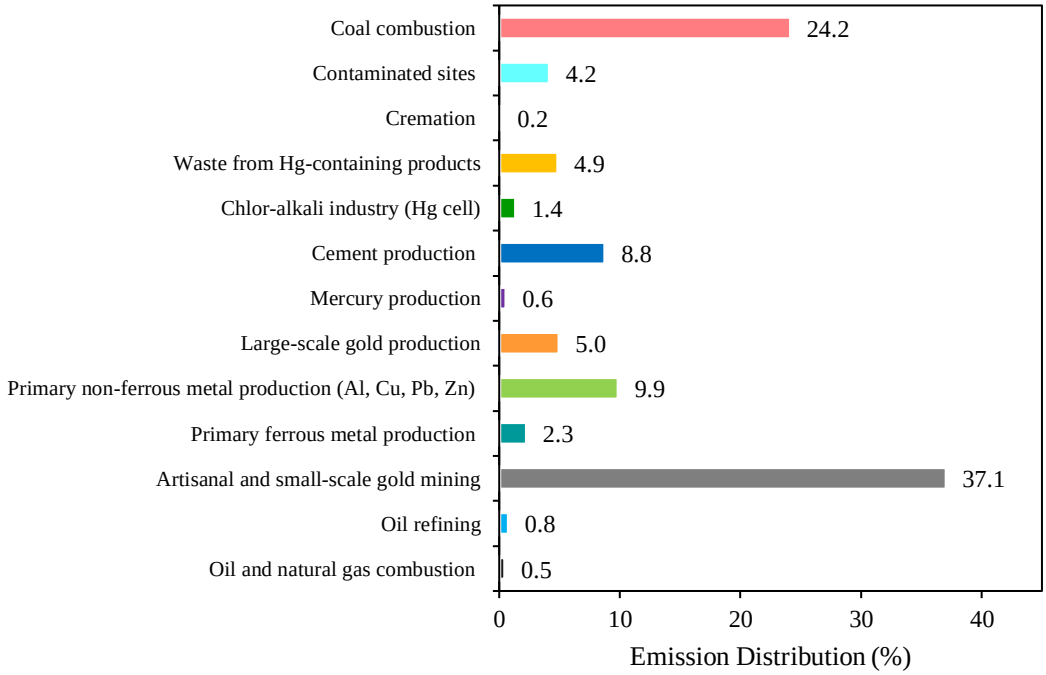

Fig. 2.1 Distribution of Global Mercury Emission from Anthropogenic Sources in 2010 [2]

Mercury are released naturally, varying from volcanic and geothermal activities, marine environments and forest fires. With the increase in human activities since the start of the industrial era (recorded since 1800) [2, 3], it has substantially resulted in increased mercury load into the environment, thus raising its concentration in both aquatic and soil ecosystems by 1.5% per year [4]. Recent studies have shown that approximately 30% of mercury entering the atmosphere per year comes from anthropogenic origins. Combustion of fossil fuels and emission from artisanal and small-scale gold mining were identified to be the major sources for mercury emission, having contribution of 37% and 25% respectively to the total anthropogenic sources

[2, 5]. Fig. 2.1 shows the global mercury emissions from several anthropogenic sources estimated in 2010 [2].

With the current energy demand, an increasing number of LNG plants are in operation around the world. The recent BP Statistical Review of World Energy reviewed that in 2016, oil and natural gas still remained the world's leading fuel source, despite the 14.1% growth of renewable energy sources [6]. The world production of natural gas increased by 21 billion cubic meters (bcm), 19 bcm of which were produced in Australia alone [6].

So, although anthropogenic mercury emission from oil and gas processes and products are fairly small; 1.3% of the total anthropogenic emissions, it is still contributing to 11.8-42.7 tonnes as of 2010 [7]. Furthermore, according to the recent statistical annual review of the world energy in 2017, it is predicted that consumption of petroleum liquids and especially natural gas will keep on increasing by 2040 [8]. The increasing volume of natural gas being extracted, and petroleum products being produced will contribute to the increasing mercury level in the environment [9, 10].

The objective of this chapter is to review the current knowledge status on mercury in the oil and gas industry and their behaviour in aqueous environment. The review will concentrate on the presence, properties and distribution of the different mercury species detected within the oil and gas processes, mainly in reservoir fluids and released water streams. The review starts with an introduction about the presence and fate of mercury in the oil and gas industry in section 2.2 along with present methods to remove mercury detected in different phases in section 2.3. Section 2.4 evaluates existing mercury involved reactions to help identify possible reaction pathways of identified mercury with chemicals present in the oil and gas processes along with species interconversion to identify knowledge gap on mercury speciation. Behaviour of mercury within the aquatic environment upon release from the oil and gas processes is also discusses. Finally, section 2.5 identifies the challenges, standpoints and objectives of performing solubility kinetics study to close in on the current knowledge gap.

2.2 Mercury in the Oil and Gas Processes

2.2.1 Origin of Mercury

Mercury is well known to be a trace component present in oil and gas reservoirs around the world. It is believed that the primary natural source of mercury comes from the rocks located in the Earth's crust and its concentration has been reported [11]. There have been a few attempts to investigate how mercury come about in the oil and gas processes and this can be caused by a number of factors.

One possibility would be through atmospheric deposition of mercury [10, 12] whereby the deposited mercury are consumed by organic matters. These mercury bound organic matters then decomposed and buried overtime which account for the formation of natural gas and hydrocarbons found in the reservoirs [13].

Some suggest that mercury migration into the oil and gas reservoirs occurred from source rocks and ore-forming fluids containing mercury. The migration process is encouraged by secondary processes such as geological and geothermal activities [14, 15]. Several authors believe that regions with higher tectonic and geological activity are responsible for higher mercury content within the natural gas reservoirs [13, 14, 16]. Consequently, interaction with rich metal fluids, mineral matters and formation waters also have a relationship with elevated mercury content [17].

Based on the possible origins of mercury, it is clear that the mercury content and distribution varies not only within the reservoirs itself but also with its geological location [18]. These variation have been reported by Ryzhov et al. [19], whereby levels of mercury vary considerably in natural gases for a period of 20 years within the same location. Other authors have also examined that in sour gas reservoirs, mercury that are usually detected are its sulphur bound species (HgS, HgS_x^{y-}). On the other hand, mainly elemental mercury (Hg^0) and several other species are usually detected in sweet gas reservoirs [16]. Furthermore, mercury concentration within the oil and gas processes from different parts of the world are shown in Table 2.1. The variations in mercury content and distribution globally may be affected by geographical location, geology, structure and age of the gas reservoirs as well as tectonic and seismic activity of the region [19].

Table 2.1 Mercury Concentration within Oil and Gas Processes at Different Geological Region

Region	**Natural Gas ($\mu g/m^3$)**	**Condensate ($\mu g/kg$)**	**Crude Oil ($\mu g/kg$)**
Europe	<0.1 - 450	-	3.6 - 19.5
Norway	0.5 - 30	-	19.5
Mexico	0.02 - 0.4	-	1.3
South America	0.01 - 120	-	5.3
Thailand	100 - 400	400 - 1200	593.1
Malaysia	1 - 200	10 - 100	-
Indonesia	0.1 - 300	10 - 500	-
Australia	38 - 83	0.035 - 0.041	0.8
China	0.015 - 1930	-	-
Middle East	1 - 9	-	0.8
Africa	1.25 - 200	20 - 1117	0.3 - 13.3

From Table 2.1, it can be seen that mercury as a global pollutant exist at a very wide range; ranging from as little as 0.01 $\mu g/m^3$ in South America to as high as 1930 $\mu g/m^3$ in China [13, 14, 20-25]. The reported variation in mercury concentration at different geological location is consistent with the origin of mercury studied by many researchers.

An interesting point that could be seen in Table 2.1, would be the variety in the mercury contents at different geological locations. Table 2.1 shows that mercury content reported in Thailand and Africa show similar magnitude in natural gas and condensate. However, the mercury content found in crude oil highly varies by an order of magnitude (0.3 – 13.3 and 593.1 $\mu g/kg$). It has been reported by Wilhelm and Bloom [18] that $HgCl_2$ is the prevailing species in the crude oil samples. The results suggest that majority of mercury species present in Thailand would be inorganic mercury due to the high concentration detected in the crude oil. On the other hand, the mercury content in Australia show very small concentration in both condensate and crude oil phase, suggesting that majority of the mercury is present as Hg^0. Hg^0 is one of the more volatile mercury species around and is less likely to partition into the condensate and crude oil phase due to its low solubility in those two phases. The distribution data in Table 2.1 shows a good indication that mercury exists in different species at its geological source.

2.2.2 Mercury Species Distribution

The presence of mercury within the oil and gas reservoirs can be classified into three main forms, namely elemental (Hg^0), organic (example: $HgCH_3$, $Hg(C_6H_5)_2$, $ClHgCH_3$) and inorganic mercury (example: $HgCl_2$, Hg_2Cl_2, HgS) [12, 18]. The various species of mercury within the oil and gas processes differ in their physical and chemical behaviour; including adsorption, amalgamation, solubility, volatility and phase partitioning (gas/liquid) [26]. In the liquefied natural gas (LNG) processing, after the natural gas primary separation in a slug catcher, various mercury species partitioned and have been detected in all three phases (gas, water and condensate phase). In a multi-phase environment, organic mercury compounds have a tendency to partition to heavy liquid fractions, while elemental mercury equilibrates amid gas/liquid fractions and inorganic mercury compounds segregate to water. A schematic showing mercury partitioning into the different phases can be seen in Fig. 2.2.

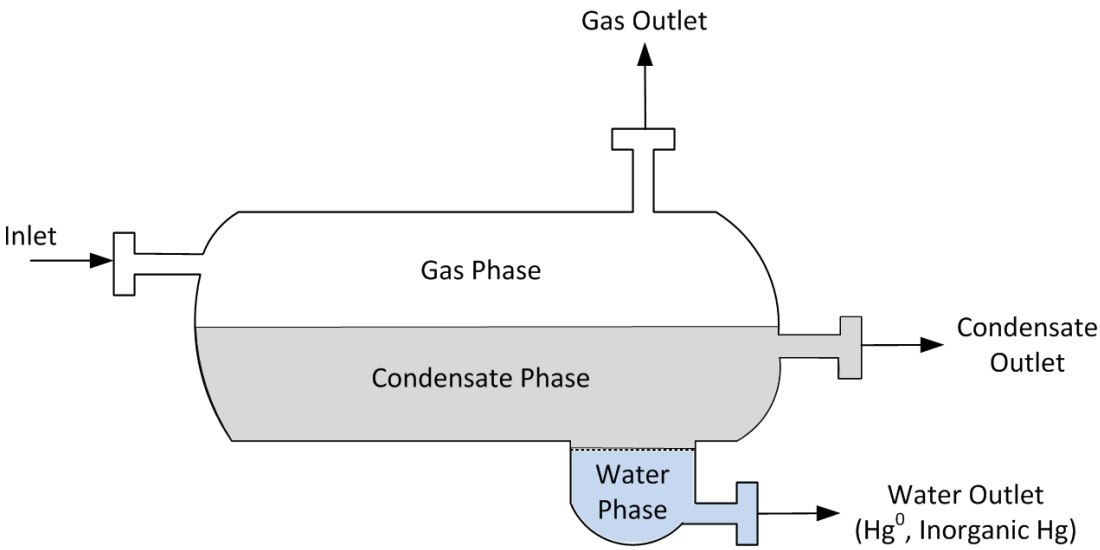

Fig. 2.2 Mercury Partitioning in a Multi-Phase Environment at Slug Catcher

2.2.2.1 Mercury Speciation in Natural Gas

Several mercury species have been reported to be present in natural gas, however it is difficult to generalise its total concentrations and species distribution, as they are highly dependent on geological location (Table 2.1). Zettlitzer et al. [27] have reported concentration as high as 700-4400 $\mu g/m^3$ in the north German gas reservoirs, while recently Ezzeldin et al. [25] reported concentration of 1.25 $\mu g/m^3$ in the outlet gas of the primary separation unit in Egypt. A summary of the distribution of mercury species found in the natural gas has been provided in Table 2.2.

Table 2.2 Mercury Species in Natural Gas

Elemental Hg	Inorganic Hg	Organic Hg	Source
Hg^0	$HgCl_2$	$Hg(CH_3)_2$	[12]
Hg^0	-	-	[28]
Hg^0	-	R-Hg-X (X= sulphate, halide or -S-R), R-Hg-R	[27]
Hg^0	-	-	[29]
Hg^0	-	R-Hg-X and R-Hg-R	[30]
Hg^0	-	-	[20]
Hg^0	Inorganic Hg (not specified)	Organic Hg (not specified)	[31]
Hg^0	-	$Hg(CH_3)_2$	[18]

As seen in Table 2.2, numerous authors have claimed that the Hg^0 is the dominant species within the natural gas, having an abundance of over 50%. Wilhelm and Bloom [18] have reviewed the presence of dimethyl mercury; $Hg(CH_3)_2$ in natural gas although in very small abundance (<1%). It is highly likely that several other organic mercury species would be present in the natural gas due to their volatile nature.

Presence of inorganic mercury in natural gas has not been much discussed, with Wilhelm [12] reported presence of inorganic mercury to be rarely detected. Occurrence of inorganic mercury such as $HgCl_2$ in natural gas is however expected, having derived from Hg^0. It is well known that Hg^0 is unstable and easily converted to other species through oxidation and reduction processes [14]. In presence of inorganic such as chlorides, sulphates and other sulphur bound compounds, the oxidised Hg^0 will react to form a more stable compounds such as $HgCl_2$ and its other chloride ligands [32, 33] and other types of organic mercury with R-Hg-X structures [27].

2.2.2.2 Mercury Speciation in Water Phase

Several authors have reported presence of mercury in both the produced water stream from the primary separation unit and the waste water stream [16, 25, 34-36]. A summary of the species that are present in produced water streams have been listed in Table 2.3. Typical mercury concentration detected in several well-known gas fields are between <0.001-0.3 mg/L [27, 37, 38]. Mercury occur within the water phase in all forms, namely elemental, inorganic, organic and particulate form [34]. In this case, the more water soluble species which is the inorganic species; namely $HgCl_2$ has the highest abundance of 10-50% [12].

Results from Table 2.3 indeed show the presence of $HgCl_2$ in most cases except for the samples analysed by Zettlitzer et al. [27]. Zettlitzer et al. [27] results however, are only based on two samples, one in which all mercury species were detected below the instruments' detection limit of 0.1 mg/L. Similar to the mercury in natural gas, presence of sulphur and its compounds in the natural gas processes have resulted in the formation and detection of the mercury complexes such as C-S-Hg-S-C in the produced water streams.

Table 2.3 Mercury Species in Water Phase

Elemental Hg	Inorganic Hg	Organic Hg	Source
-	$HgCl_2$	-	[36]
Hg^0	$HgCl_2$, Hg_2Cl_2, HgS, HgO, C-S-Hg-S-C	$Hg(CH_3)_2$, CH_3HgCl	[16]
-	$HgCl_2$	$HgCH_3$	[27]
Hg^0	$HgCl_2$	-	[39]

2.2.2.3 Mercury Speciation in Gas Condensate

A summary of the mercury species detected in several gas condensates around the world is provided in Table 2.4.

As seen in Table 2.4, mercury in gas condensate phase also exist in multiple species. The ones that have been detected include Hg°, methyl mercury $HgCH_3$, ethyl mercury HgC_2H_5, dimethyl mercury $Hg(CH_3)_2$, diethyl mercury $Hg(C_2H_5)_2$, phenyl mercury HgC_6H_5, diphenyl mercury $Hg(C_6H_5)_2$, $HgCl_2$, CH_3HgCl and suspended HgS and Hg_2Cl_2. Although present in multiple species, a lot of suspended mercury (HgS) was found to be present in the condensate phase. Abundance of HgS was found to be ~60%, as reported by Zettlitzer et al. Having said that, inorganic mercury such as $HgCl_2$ have been found to be the abundant species that is dissolved in the solution. Tao et al. [39] detected presence of $HgCl_2$ within the range of 53 – 97% of the total dissolved mercury in several condensate samples. Similarly, 58 – 85% of the total mercury in gas condensates detected by Zettlitzer et al. [27] was found to be $HgCl_2$.

Table 2.4 Mercury Species in Gas Condensates

Elemental Hg	Inorganic Hg	Organic Hg	Source
Hg^0	Ionic inorganic Hg (Hg^+, Hg^{2+})	$HgCH_3$, $Hg(CH_3)_2$, HgC_2H_5, $Hg(C_2H_5)_2$	[31]
Hg^0	$HgCl_2$	$Hg(CH_3)_2$, HgC_3H_8, $Hg(C_2H_5)_2$	[39]
Hg^0	$HgCl_2$, Hg_2Cl_2, HgS	$Hg(C_6H_5)_2$, CH_3HgCl, $HgCH_3$, $Hg(CH_3)_2$	[29]
Hg^0	Hg^{2+}	-	[40]
Hg^0	Inorganic Hg (Not specified)	$HgCH_3$	[25]
Hg^0	$HgCl_2$, Hg_2Cl_2	-	[31]
Volatile Hg	Ionic Hg (Hg^+, Hg^{2+})	Non-ionic organic Hg (Not specified)	[41]
Hg^0	Hg^{2+}, HgS	$HgCH_3$, HgC_2H_5, HgC_6H_5	[27]

The occurrence of other forms of organic mercury is still on debate, as organic mercury has the tendency to undergo species interconversion and photolysis to form Hg^0, which might explain the abundance of Hg^0 in the condensate detected [42-44]. A work by Schickling and Broekaert [29] has also observed reactions between $Hg(C_6H_5)_2$ with $HgCl_2$ and CH_3HgCl respectively to form other types of organic mercury. Furthermore, Gaulier et al. [41] did not specify the actual non-ionic organic mercury detected in their samples. However, their analysis was based on the standards of Hg^0, $Hg(C_6H_5)_2$, $HgCl_2$, mercury (II) pentyl, thiolate, octyl and tetradecyl. This might also suggest presence of those mercury samples in the samples analysed.

The likelihood of abundance of organic mercury within condensate is higher due to the fact that it is more soluble in organic solutions in comparison to water [45]. Several authors also discussed that partitioning of mercury into the gas condensate is generally related to the boiling point of gas condensate itself [23, 46]. Table 2.5 presents possible mercury species that may be present based on their boiling points [45]. As gas condensates are made up of several straight chain alkanes (C2 – C6+) with different boiling points, it is suspected that organic mercury will partition into those hydrocarbon phase as they condense from the gas phase

Table 2.5 Boiling Point of Various Volatile Mercury Species

Mercury Species	Boiling Point (K)
Elemental Mercury; Hg^0	630
Mercuric Chloride; $HgCl_2$	577
Di-isopropyl mercury; $Hg(iC_3H_7)_2$	443
Dipropyl mercury; $Hg(C_3H_7)_2$	463
Dimethyl Mercury; $HgCH_3$	366
Diethyl mercury; $Hg(C_2H_5)_2$	432
Dibutyl mercury; $Hg(C_4H_9)_2$	496
Diphenyl mercury; $Hg(C_6H_5)_2$	477

2.2.3 Transportation and Fate of Mercury

As mentioned in section 2.2.2.1 and 2.2.2.3, transport of mercury within the different parts of the oil and gas processes depend primarily on its chemical and physical forms and several factors play into part that will determine the fate of mercury.

Mercury present in the gas phase has been known to increase in concentration following its progression within the process, Ezzeldin et al. [25] pointed that this enrichment is likely to occur during the gas sweetening step. One of the challenges

with prediction of mercury speciation and distribution is due to the fact that mercury and its species readily reacts with each other and compounds present, transforming into other mercury compounds. One example is the oxidation of Hg^0 in crude oil which leads to formation of water-soluble inorganic mercury compounds and complexes. Another example would be the conversion of suspended HgS by anaerobic bacteria into a water soluble organic form, which eventually partition into the water stream [34, 47]. Additionally, Hg^0 and inorganic mercury are known to be very reactive with sulfur, forming HgS particles that have the tendency to accumulate in production equipment [12]. Possible chemical reactions that cause mercury species conversion within the oil and gas conditions are discussed in detail in section 2.4.

Transfer of mercury into both effluent and product streams from other parts of the process also occur when they come into contact. This tendency to partition between different phases is highly influenced by its solubility [46]. Solubility of several mercury species in different solutions are given in Table 2.6 [32, 45, 47-51].

Table 2.6 Solubility of Several Mercury Species in Different Solutions

Mercury Compound	**Water (mol/L)**	**Toluene (mol/L)**	**Alcohol (mol/L)**
Hg^0	2.84×10^{-7}	12.70×10^{-6}	Glycol: 9.95×10^{-7}
$HgCl_2$	0.27	2.21×10^{-3}	Methanol: 2
$Hg(C_6H_5)_2$	2.80×10^{-5}	-	Ethanol: Soluble
HgS	“insoluble”	“insoluble”	“insoluble”

2.2.4 Impact of Mercury within the Oil and Gas Industry and Environment

Mercury is a heavy metal that is persistent in the environment. Mercury cannot be destroyed, combusted and it does not degrade, hence it has the tendency to stay in the environment for a long time once introduced (Hg^0 has a lifetime of 1 year in the atmosphere). Once in the environment, mercury can be transformed into CH_3Hg by bacteria activities. This form of mercury is known to bio-accumulate in living organisms and ecosystem building up in the food chain over time. Its mechanism in which mercury bio-accumulate and transformed in the environment remains vague. Within the environment, mercury circulates between air, land and water where eventually it will leave the system and remain trapped within stable mineral compounds at the bottom of lake and sea sediments. This circulation of mercury is commonly known as the “global mercury cycle” [52], presented in Fig. 2.3. Within

this “global mercury cycle”, mercury is redistributed and transferred across different parts of the world as it changes to other forms when mercury meets other compounds in the environment. One common example is the oxidation of Hg^0 into a water-soluble Hg (II) by the O_3 in the atmosphere [53]. This Hg (II) would then be absorbed by the water vapours and enter the water streams as rain drops. Presence of contaminants such as chlorides and sulphur in the water streams will promote conversion of mercury into other inorganic ligands.

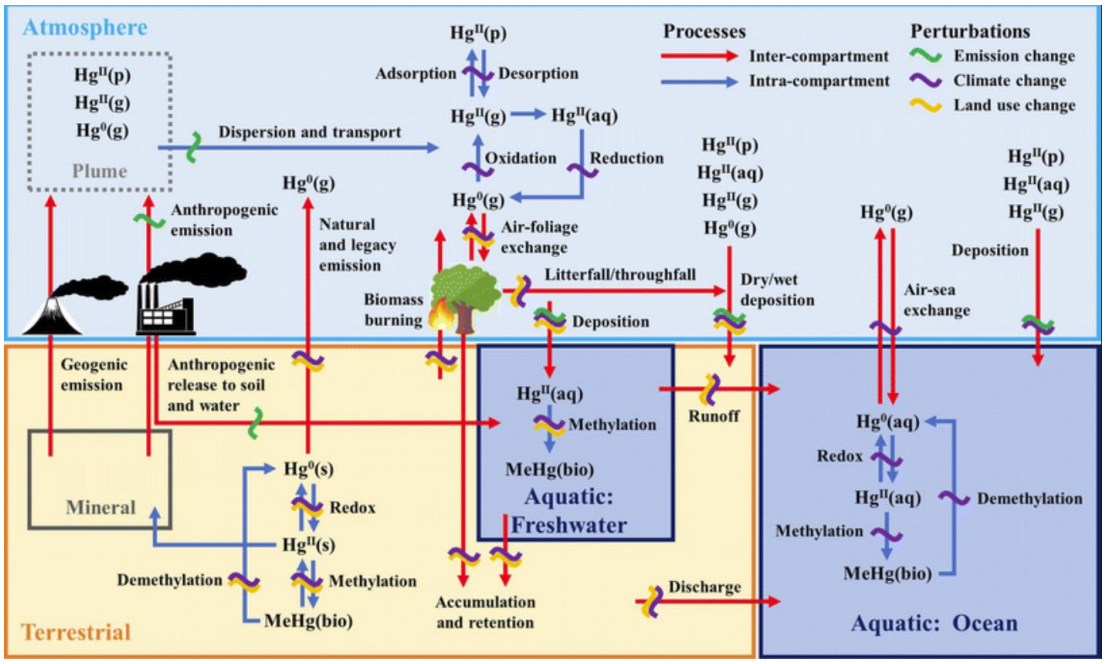

Fig. 2.3 Global Mercury Cycle [52]

All forms of mercury are highly toxic and exhibit different health effects in humans and animals. Most humans and animals are exposed to low levels of mercury which is quite harmless. However, in long term, exposure to constant low-levels mercury may lead to many harmful effects due to its tendency to accumulate inside living organisms. Exposure within chronic level will result in psychological anomalies (i.e. excitability, memory loss, insomnia and depression) and physical symptoms (i.e. weakness, fatigue, anorexia and weight loss) [18, 26]. In some acute high dose cases, tremors, kidney failure and gastrointestinal tract were also observed [54].

Mercury possesses several detrimental impacts within the refinery industries and gas processing plants, which may jeopardize the health and safety of personnel, and failure to comply with environmental regulations. Generally, the main pathway of occupational exposure is via inhalation of vapour and regular biological monitoring is required to detect the level of mercury in blood, urine and hair. Exposure needs to be

controlled to ensure blood, urine and hair concentration are below 1-8 µg/L, 4-5µg/L (equivalent to ~0.25 µmol/L) and 2 µg/g respectively. The occupational exposure standards as per WorkSafe Australia [55] for different mercury compounds are shown in Table 2.7.

Table 2.7 Occupational exposure standard for mercury according to WorkSafe Australia

Mercury Species	Exposure Standard (mg/m^3)
Elemental vapour	0.05
Alkyl	0.01
Aryl and inorganic	0.1

In terms of the integrity of production, mercury poisons precious metals catalysts and contributes in toxic waste generation that get discharged to the environment. Furthermore, having mercury in the feeds of a gas processing plant can cause equipment degradation [18, 26] production of toxic sludge deposit in separators and heat exchangers and fouling of cryogenic equipment [56]. Such impact can be seen dated back in 1973, during the catastrophic failure of aluminium heat exchangers in Skikda natural gas refinery in Algeria [18, 57, 58].

Mercury present in natural gas and process streams are prone to accumulation on the surface of the process equipment and pipelines by means of adsorption, chemical reaction, dissolution in sludge and condensation [56]. Mercury reacts chemically with metallic surfaces, namely adsorption (reversible bonds) and chemisorption (irreversible chemical bond). Adsorption mainly occurs for stainless steel surfaces while chemisorption applies for carbon steel surfaces. Moreover, Hg^0 being the major mercury species detected within the oil and gas processes may accumulate on surfaces of metals (such as silver, gold, copper, zinc and aluminium) via formation of amalgams [18, 32, 59]. Condensation of gaseous mercury takes place during changes to temperature and pressure; vapour pressure of mercury exceeds the limiting condensation partial pressure. Liquid mercury has been reported to precipitate in multiple locations within the system at lower temperature condition. The process equipment and pipeline that has been contaminated with mercury will pose serious health hazards to workers as they may be exposed to mercury vapours during routine inspection and maintenance. An extensive safety and decommissioning plan to deal with these contaminated materials will need to be considered within the project lifetime.

Attempts by the industry (mass balance studies, mercury mapping studies and long-term monitoring programs) [18, 19, 25, 56] still relies heavily on the observations from routine inspections of the deposited liquid mercury and the amount of mercury detected in several section of the waste streams. In addition, most of the published data of the total Hg concentrations in hydrocarbon matrices do not provide full information on the sampling, analytical procedures and other factors. For these reasons, some of the data reported may not take into consideration, any suspended forms and species conversion due to oxidation of Hg0 which ultimately result in inaccuracy in the speciation of mercury. Furthermore, the conditions in which the various mercury species form are not clearly understood in terms of their behaviour and reaction mechanisms with the surroundings.

Nevertheless, an accurate mercury mass balance is still unable to be performed due to the lack of understanding of the non-equilibrium condition of mercury partitioning and the chemical reactions involved. The lack of information has also led to less effective mercury removal process for the condensate and water phase. Information on the dynamic solubility of the different mercury species is hence very important to enable predictions of mercury behaviour when in contact with the different materials and liquids in the oil and gas processes.

2.3 Mercury Removal Technique in the Oil and Gas Industry

The importance of controlling and treating mercury within the oil and gas supply chain have been increasing in recent times. This is due to increasing stricter mercury discharge regulation and the importance in protecting personnel and equipment from toxic exposures. Mercury species exists in three different forms (Hg^0, organic and inorganic), meanwhile current generic removal methods are designed with Hg^0 in mind. In addition, mercury species are present in different phases (gas, condensate and water). This makes it even more of a challenge to design an effective mercury removal process.

Consequently, several alternative methods would be required to achieve effective mercury removal from the process stream. This can be done by installing different

mercury removal unit preferably upstream of the process stream as preventing accumulation of mercury will reduce possible damages to process equipment downstream.

2.3.1 Removal of Mercury in the Gas Phase

Several methods that have been utilised to remove mercury from the gas phase are summarised in Table 2.8. The most widely used technique for mercury control within the natural gas processing industry involves the use of fixed-bed scrubbers. The scrubber typically utilizes a solid adsorbent which conventionally removes mercury gas through three main mechanisms; adsorption, amalgamation, or oxidation prior to adsorption.

To date, the most commonly utilised adsorbents for removal of mercury is sulphur and metal-sulphide coated activated carbon or alumina [60, 61]. The mechanism of removal involves reaction of gaseous mercury (Hg^0 and $HgCl_2$) with the sulphur to form stable HgS. On the other hand, this removal technique comes with limitations such as being effective only for dry gas and relatively low concentration of hydrocarbons. Presence of moisture in the gas will cause sulphur dissolution and reduce the number of sulphur active sites for mercury adsorption [62].

The other common technique is using silver-coated molecular sieve. This removal technique focuses on absorption of Hg^0 by process of amalgamation with the silver (Ag) or other noble metals such as gold (Au) and platinum (Pt). One advantage of using this method is the fact that it can be regenerated by heating the adsorbents to release the mercury. Having said that, major drawbacks to using this technique include the high capital cost as well as their relatively low adsorption capacity [23].

Another type of mercury removal technique utilises oxidation of mercury species. The mechanism of oxidation of Hg^0 to Hg^{2+} and Hg^+ following capture by wet scrubbers have also been utilised [63]. This technique makes use of the high solubility Hg^{2+} and Hg^+ in solution for capture in the wet scrubber. Several more advanced oxidation methods that have been trialled include TiO_2 photocatalysis [64, 65], direct UV [66] and catalytic oxidation [67]. Unlike the use of molecular sieve, oxidation techniques do not allow for simple regeneration of the capture material.

A more recent and popular approach in mercury removal within the petroleum gas production industry involves the use of ionic liquids that is coated onto activated carbon [30] and silica [15]. The application of ionic liquids has been adapted from its successful removal of Hg^0 from flue gases [68-70].

Table 2.8 Mercury Removal Methods from Gas Phase

Method	Removed Mercury Species	Advantages	Disadvantages	Source
Sulphur/activated carbon	Hg^0, $HgCl_2$, organic Hg	Cheap, reasonable adsorption capacity (4500 µg/g) Commercial example: MERSORB® (Nucon International, Inc.), HGR-P (Calgon Carbon Corporation), Desorex HGD 2 S and HGS 4 S (Donau Carbon)	Effectivity reduced with presence of impurities in gas (moisture and hydrocarbons), capacity of adsorption depends on mercury species present (lower for organic Hg)	[60]
Metal sulphide/activated carbon. alumina	Hg^0, $HgCl_2$	Higher adsorption capacity (23000 µg/g for CuS) compared to just sulphur/activated carbon, less sensitive to moisture in gas, recyclable Commercial example: SELECT Hg-100 and SELECT Hg-110 (Schlumberger), $PURASPEC_{JM}$ 1157 (Johnson Matthey Catalysts)	Effectiveness of regenerated adsorbents is not worth the cost of regeneration	[61]
Metal/molecular sieve (Ag, Au, Pt)	Hg^0	Regenerable, Hg-free disposal Commercial example: $HgSIV^{TM}$ (UOP LLC)	Low adsorption capacity, high investment cost	[23]
Wet scrubber ($KMnO_4$, $NaClO_2$)	Hg^0, $HgCl_2$	Regenerable	Difficult to regenerate, system contamination	[63]
Adsorption on TiO_2 and photocatalysis	Hg^0	High adsorption capacity (30000 µg/g)	Oxidation is inhibited by presence of water and CO_2, high investment cost (complex system)	[64]

Direct UV/Adsorption on Quartz	Hg^0	Removal efficiency maintained with impurities present (moisture and acid gases)	Require presence of O_2, high investment cost (complex system), relatively high operating temperature (300 – 450 K), introduction of additional mercury species in the system (Hg_2SO_4 and HgO as oxidised mercury form)	[66]
Catalytic oxidation	Hg^0	Regenerable, removal efficiency maintained with impurities present (moisture and acid gases) Commercial example: ActiSorb GP400 (Clariant International Ltd)	Low adsorption capacity, high capital cost when using noble metals as catalysts, require high operating temperature (high operating cost)	[67]
Ionic liquids/carbon or silica	Hg^0	High adsorption capacity compared to sulphur/activated carbon (~3 times higher) Commercial example: HycaPure™ Hg (Clariant International Ltd)	Cannot be regenerated, high operating cost	[15, 30]

2.3.2 Removal of Mercury in Liquid Phase; Gas Condensate and Produced Water

Removal of mercury from gas condensate and produced water is very different to that of gas phase. The approach to the removal strategy slightly differs according to the media as well as the different species of mercury available. Table 2.9 summarizes the systems utilised to remove mercury from the gas condensates and the produced water phase.

As mentioned in section 2.2.2.2 and 2.2.2.3, mercury exists in all three species (elemental, organic and inorganic) within the water and condensate phase. The three species are available in both suspended and dissolved within both liquids within the LNG system. Presence of suspended inorganic mercury such as HgS are especially plenty within the condensate phase. Removal of suspended mercury is often done physically by means of filtration [71] and centrifuge [72].

For dissolved mercury, the use of adsorbents such as metal halide coated activated carbon, metal sulphide coated adsorbents (activated carbon or alumina) and metal coated molecular sieve can be applied to remove mercury from gas condensates. These methods are comparable to those employed for removal of mercury in natural gas (refer to section 2.3.1). Having said that, the use of sulphur coated activated carbon is not suitable for treatment of liquid phase as sulphur is known to be soluble in liquid hydrocarbon [73].

Alternative method to remove dissolved mercury would be through sulphide precipitation. Dissolved ionic mercury is often reacted with mercury precipitant to form water-insoluble compound such as HgS. This suspended HgS could then be remove by physical means as mentioned earlier. Mercury precipitant that is commonly used is comprised of sulphides group which are usually water soluble. Commercial precipitants are also available which is made out water-soluble polymers such as polydithiocarbamates [73].

Recently, techniques employing ion exchange and hollow fibre supported liquid membrane impregnated with different choice of extractants have been satisfactory in removing inorganic mercury from petroleum-produced water [36, 74-76], however success to remove organic mercury remain uncertain. On the other hand, Gallup [16]

claimed that these techniques will not be as effective for removal in produced waters due to presence of organics in petroleum-produced water. Common practise with contaminated water in the industry is to inject them back to the well. Several advantages of this method include displacement of more oil to the well along with supporting the pressure of the reservoir by replacing the void. In places where this is not practised, common practise is to employ the use of adsorbents mentioned earlier.

Majority of these removal techniques mainly focus on removing mercury through adsorption process, however adsorption does not work effectively on all mercury species that are present within both condensate and water phase. Study by Shafawi et al. [77] aimed to evaluate the performance of different types of mercury removal systems, demonstrated that majority were able to effectively adsorb Hg^0 but not for organic mercury compounds. The reliability of adsorbents as primary means of mercury removal is concerning as organic and inorganic mercury species are more prevalent in hydrocarbon liquids. Removal method that has been developed to address this issue involves a two-step process [78, 79]. The first step comprises of the conversion of organic mercury (tested on dialkyl mercury) to Hg^0 by using metal catalyst and hydrogen gas. Finally, the Hg^0 could be scavenged by using the conventional metal sulphide adsorbents mentioned earlier.

Table 2.9 Mercury Removal Methods from Condensate and Water Phase

Method	Removed Mercury Species	Advantages	Disadvantages	Source
Filtration and Centrifuge	Suspended Hg (HgS, HgO, Hg_2Cl_2)	Less chance for system contamination as process is physical in nature	Only limited to removal of non-soluble mercury species, require frequent clean ups and change of filter	[71, 72]
Metal halide/activated carbon (I, Br, Cl)	Hg^0, $HgCl_2$, organic Hg	Equivalent for removal of mercury from gas phase, most used, cheap Commercial example: HGR LH (Calgon Carbon Corporation)	Non-regenerable (contribute to increased mercury waste)	[80]
Metal sulphide/activated carbon or alumina	Hg^0, $HgCl_2$	Equivalent for removal of mercury from gas phase, less sensitive to liquid hydrocarbons and water Commercial example: PURASPEC$_{JM}$ 5159, 5169 (Johnson Matthey Catalysts)	Non-regenerable (contribute to increased mercury waste	[81]
Metal/Molecular Sieve (Ag)	Hg^0	Equivalent for removal of mercury from gas phase, regenerable Commercial example: HgSIV^{TM} (UOP LLC)	Low adsorption capacity, high investment cost	[82]
Catalyst with presence of hydrogen	Dialkyl Hg	Ensure thorough removal of organic mercury species by conversion to readily removed Hg^0	Cannot be a stand-alone treatment, require additional removal system to remove Hg^0,	[78, 79]

Sulphide precipitation	Ionic Hg (Hg^+, Hg^{2+}), $HgCl_2$	Effective removal of dissolved ionic Hg by precipitation Commercial example: METCLEAR™ 2405 (Betz-Dearborn Inc.), NALMET™ (Nalco Inc.)	Require installation of a filtration or centrifuge system to remove suspended Hg, system contamination	[34]
Hollow fibre/liquid membrane	Ionic Hg (Hg^+, Hg^{2+})	Effective in treating water streams, low capital and operation cost, low energy consumption, large surface area for mass transfer Commercial extractant: Aliquat 336 (Cognis Ltd), Cyanex 471 (Cytec Canada Inc.)	Regeneration problem, system contamination, removal is mercury species specific; dependent on types of extractants used	[36, 76]
Produced water re-injection	All mercury	Increase amount of oils extracted, effective to minimise mercury waste generated	Complicated process	[83]

2.4 Reactions of Mercury

Section 2.2.3 briefly discussed that the mercury distribution occurs through multiple reactions involving several mercury species and the various compounds available within the different parts of the oil and gas process. Summary of several reactions that might be responsible for the transformation and fate of mercury are provided for both inorganic ($HgCl_2$) and organic ($Hg(C_6H_5)_2$) mercury. Reactions between different types of mercury species and their interconversions that are available in literature are also reviewed.

2.4.1 Reactions of Inorganic Mercury; $HgCl_2$

Inorganic mercury; $HgCl_2$ is one of the more soluble and stable Hg compound in water, having solubility value of 73 g/L at 298 K [48]. When dissolved in water, Kozin and Hansen [32] reported that $HgCl_2$ has the tendency to remain un-dissociated as its equilibrium constant of dissociation reaction K is very small.

In aqueous conditions, $HgCl_2$ is known to easily form bonds with different types of ligands to form metal complexes with a general formula $[Hg(L)nCl_2]$ (L = ligand). Due to its polarity, $HgCl_2$ has the tendency to favour covalent bonds over ionic bonds [84, 85], with stronger affinity for S-, N- and P- type ligands, especially S- type. With the case with inorganic ligands such as chloride and hydroxide ions, distribution of the mercury complexes is reliant on pH, salinity and concentration of the ligand [85-87].

A summary of several mercury complexes formed from $HgCl_2$ with various ligands that have been reported are given in Table 2.10. Further information on stability constants of mercury complexes with their ligands have been compiled by several authors [88-91].

One of the main reactions involving $HgCl_2$ would be its reaction with NaCl to form stable $Na_2[HgCl_4]$ complexes;

$$\mathrm{HgCl_2 + 2NaCl \rightarrow Na_2HgCl_4}$$

This reaction is very important and is very likely to occur due to the high NaCl content in the water phase within the oil and gas processes.

Table 2.10 Complex Formation with Different Types of Ligands

Ligand	Complex	Reference
Alcohols; Methanol	$HgCl_2[CH_3OH]$	[84, 92]
Triethylene glycol (TEG)	$(HgCl_2)_3[TEG]$	[93]
Pentaethylene glycol (PEG)	$HgCl_2[PEG]$	[93]
Dissolved organic matter (DOM)	Hg[DOM]	[88]
Ammonia	$Hg(NH_3)_2Cl_2$, $Hg(NH_2)Cl$, Hg_2NHCl	[92, 94]
Halide ions (X = Cl^-, Br^-, I^-)	HgX^+, HgX_3^-, HgX_4^{2-},	[85, 95-97]
Hydroxide ions	$Hg(OH^+)$, $Hg(OH)_2$, $Hg(OH)_3^-$	[88]

In addition to reactions by complex formation, $HgCl_2$ may react with compounds present within the oil and gas processes such as H_2S and organic acids (mainly acetic acid), transforming to other species. The presence of insoluble mercury, HgS detected in sour gas reservoirs [16] might be attributed from the reaction between $HgCl_2$ with H_2S [98];

$$HgCl_2 + H_2S \rightarrow HgS + 2HCl$$

Several have reported the presence of acetic acid; CH_3COOH in gas condensate and its detrimental effect to carbon steel corrosions [99, 100]. $HgCl_2$ may react with acetic acid to form $(CH_3COO)_2Hg$ (mercury acetate) [84];

$$HgCl_2 + 2CH_3COOH \rightarrow (CH_3COO)_2Hg + 2HCl$$

Mercury (II) halide in general has been widely used to synthesise organic mercury by reactions with various compounds, therefore, transformation within the oil and gas processes to form various organic mercury is most likely to occur. Several possible reactions of formation of organic mercury from $HgCl_2$ are listed in Table 2.11 [44]. Note that the reactions are applicable to other mercury (II) halides.

Table 2.11 Formation of Organic Mercury from $HgCl_2$

	Reaction
Mercuration with C-H bonds	$R - H + HgCl_2 \rightarrow RHgCl + HCl$ (R = arenes, cyclopentadienyls, alkynes carbonyl and nitrile compounds)
Mercuration with alkenes (C=C)	$C = C + HgCl_2 + HY \rightarrow YC - CHgCl + HCl$ (Y = OH,OR, O_2H,NR_2, N_3, etc)
Transmetallation with other organometallic species	$R - M + HgCl_2 \rightarrow RHgCl + MCl$ $2R - M + HgCl_2 \rightarrow RHgCl + MCl$ (M = Metal)

2.4.2 Reactions of Organic Mercury; $Hg(C_6H_5)_2$

Organic mercury, such as Ph_2Hg; $Hg(C_6H_5)_2$ has limited solubility in water while on the other hand, soluble in various organic solvents and hydrocarbons [42, 101, 102]. $Hg(C_6H_5)_2$ is made up of strong Hg-C bond, allowing the compound to be stable in the presence of oxygen, water and alcohols [101]. On the contrary, $Hg(C_6H_5)_2$ is not stable and undergoes decomposition in the presence of heat and light [103] to form Hg^0;

$$Hg(C_6H_5)_2 \rightarrow Hg^0 + \text{phenyl radicals}$$

Like $HgCl_2$, $Hg(C_6H_5)_2$ has the tendency to react with compounds present within the oil and gas processes to form different mercury species. $Hg(C_6H_5)_2$ has been reported to react with H_2S to form HgS [102].

$$Hg(C_6H_5)_2 + H_2S \rightarrow HgS + 2C_6H_6$$

Consequently, McAuliffe [44] mentioned that there is possibility of complex formation with suitable anionic and/or neutral ligand to form mercury complex with general formula of $(C_6H_5)_2HgL$ and $(C_6H_5)\ HgX.L_2$ (X = halogen; Cl, etc). The suitable ligands however have not been discussed in detail.

Although a stable compound, presence of acids such as acetic acid will break down $Hg(C_6H_5)_2$ to produce organo-mercury halide compound through the reaction known as protodemercuration or acidolysis [103]. This transformation to other organic mercury species will affect speciation and distribution due to differing solubility nature [104]. Corwin and Naylor [105] and McCuthan and Kobe [102] have reported that $Hg(C_6H_5)_2$ readily reacts with acetic acid to form phenylmercuric acetate and the reaction is first order;

$$Hg(C_6H_5)_2 + CH_3COOH \rightarrow (C_6H_5)Hg(CH_3COO) + C_6H_6$$

Other common route of transformation of $Hg(C_6H_5)_2$ include transmetallation and symmetrisation reactions which resulted in organo-mercury halide as well as $HgCl_2$. Details of the reactions are included in Table 2.12 [101, 106].

Table 2.12 Formation of Other Mercury Species from Organic Mercury; $Hg(C_6H_5)_2$

	Reaction
Transmetallation with other organometallic species	$HgR_2 + R' - M \rightarrow RHgR' + R - M$ $HgR_2 + 2M \rightarrow Hg + 2R - M$ $HgR_2 + MCl \rightarrow RHgCl + R - M$ $HgR_2 + MCl \rightarrow Hg + R - Cl + R - M$
Symmetrisation	$RHgCl + RHgCl \rightleftharpoons HgR_2 + HgCl_2$

2.4.3 Reactions between Mercury Species

In addition to reactions with other compounds presence within the production and waste streams, occurring mercury species are also known to react among each other to contribute to the current speciation issues.

Presence of $HgCl_2$ in the water streams is known to absorb Hg^0 in the overhead gas to form Hg_2Cl_2 (calomel) which is less soluble in water. The reactions have been studied by several authors [33, 107, 108] and applied to control Hg^0 in flue gases. Mat et al. [33] have observed that the reactions are further enhanced at lower pH and at Cl^-:$HgCl_2$ molar ratio of 200:1. Excess amount of Cl^- will encourage formation of $HgCl_4^{2-}$ complexes which will discourage the absorption process. Summary of the $Hg^0/HgCl_2$ absorption reactions is as follows:

$$HgCl_2 + (n-2)Cl^- \rightleftharpoons HgCl_n{}^{2-n}; (2 \leq n \leq 4)$$

$$Hg^0 + HgCl_2 \rightarrow Hg_2Cl_2$$

$$Hg^0 + HgCl_3{}^- \rightarrow Hg_2Cl_3{}^- \rightarrow Hg_2Cl_2$$

As mentioned in section 2.2.2.3, the presence of dialkyl mercury, especially $Hg(C_6H_5)_2$ within the oil and gas processes is still debatable due to rare and low detection [39, 40, 42]. One of the leading suspects for the issues in detection is species interconversion. Although being labelled as one of the more stable organic mercury compounds, $Hg(C_6H_5)_2$ is known to react with $HgCl_2$ and CH_3HgCl to form phenyl mercuric salts through electrophilic substitution reaction [29, 42-44].

$$Hg(C_6H_5)_2 + HgCl_2 \rightarrow 2(C_6H_5)HgCl$$

$$Hg(C_6H_5)_2 + CH_3Hg^*Cl \rightarrow CH_3HgCl + Hg^*(C_6H_5)_2$$

$Hg(C_6H_5)_2$ may also react with Hg^0 by the following reaction with the presence of organic solvents [109];

$$Hg(C_6H_5)_2 + Hg^0 \rightarrow Hg + Hg^*(C_6H_5)_2$$

2.4.4 Mercury in Aquatic Environment

Mercury that is present in the LNG processing facilities may enter the aquatic environment in the form gas and water from different section of waste streams. Released waste waters and gas containing mercury from LNG processing facilities may be introduced into the aquatic environment via cycling of sea and fresh water sources. However, deposition from atmospheric mercury has been reported to be the main entry point into the aquatic environment [110]. Once present in the environment, mercury undergoes several reactions to convert to more bio-persistent species. Mercury behaviour within aquatic environment is illustrated in Fig. 2.4.

$HgCl_2$ being the major species detected in the waste waters, will undergo two main reactions, namely reduction to re-emit Hg^0 into the atmosphere and methylation to form soluble CH_3Hg [111]. These reactions occur by means of bacterial activity present in water bodies. CH_3Hg is soluble in water and is very persistent in environment due to its tendency to bio-accumulate in organisms [112].

In saltwater environment, deposition of $HgCl_2$ from the atmosphere is expected due to the formation of stable mercury-chloro complexes (as discussed in section 2.4.1). Moreover, deposition of Hg^0 is expected to increase as the produced mercury-chloro complexes can stabilise and promote the oxidation process to Hg(II) [113].

Organic mercury that is present in atmosphere will most likely be decomposed to Hg^0 prior to direct deposition into the water bodies via photochemical dissociation. Organic mercury released from LNG processes will most likely enter the aquatic environment through the waste water stream. Due to its high lipid absorption, organic mercury will be easily taken up by organisms and organic matter to bio-accumulate along with CH_3Hg [114].

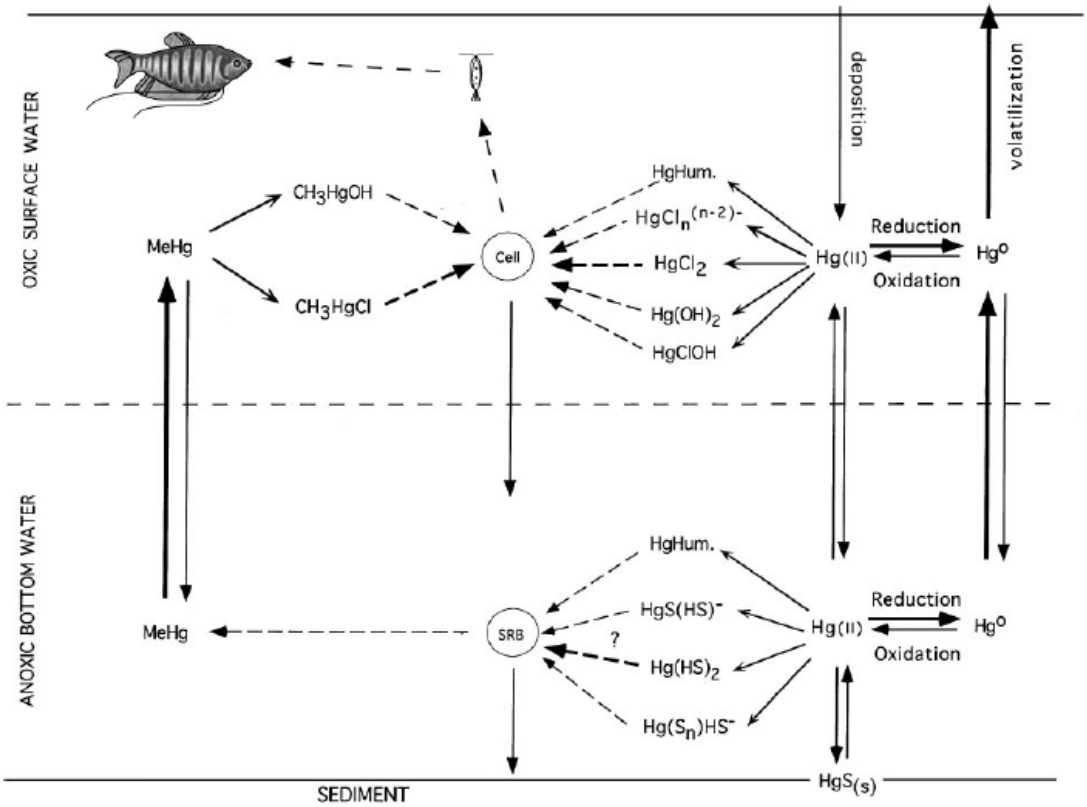

Fig. 2.4 Mercury Reaction Pathways within Aquatic Environment [89]

2.5 Mercury Solubility Kinetics Study

2.5.1 Opportunities of Mercury Solubility Kinetics Study

Very few studies have been published on solubility kinetics that may represent mercury behaviour within the oil and gas processes. Most studies are limited to the equilibrium/saturated condition and interpretations of field data by speciation, then the possible reaction pathways are proposed [25, 46, 48, 115-117].

Solubility kinetics study of Hg^0 into different solvents have been conducted by several authors and results have been used to model its atmospheric deposition as discussed in section 2.5.4.4. Review and findings of some dynamic solubility studies involving Hg^0 have been summarized in Table 2.13.

As seen in Table 2.13, solubility kinetics study of Hg^0 have been conducted in several types of reactor, namely batch and semi-batch stirred cell, bubble column and wetted column reactors. For system with continuous flow of reactants, it is more common to use bubble/wetted column reactors to study the absorption and kinetic processes. Although absorption studies could be shortened due to increased surface area of

contact, determination of the exact surface area is often difficult and having to rely on correlation equations. Moreover, these types of reactor will not be suitable to study the absorption of soluble gases. Equilibrium will be achieved almost instantaneously, making it a challenge to monitor and study the transient state. Finally, bubbling induces vaporization of the absorbing liquid phase, hence absorption at higher temperature and more volatile liquids will result in inaccuracies due to large volume loss. These limitations discourage long term absorption studies from being conducted. Based on the issues identified, the use of a stirred-tank semi-batch reactor should be considered when designing experimental set-up. Successful application of such type of reactor has been proven by Zhao [118] to study the absorption of Hg^0 into various solutions. Surface area of mass transfer is easily well-defined and controlled. Due to relatively smaller surface area of contact, pro-longed test could be conducted as equilibrium state takes longer to be achieved.

Another piece of finding from the review shown in Table 2.13 would be uncertainties with regards to the mercury balance and behaviour within the processes studied. Many of the current solubility kinetics studied often only analyse the outlet stream and compare them to the inlet stream. Quantifying the mercury content within the absorbing liquid and performing a thorough mass balance is crucial as this would ensure that the absorption system is functioning well. Furthermore, more information regarding the behaviour of the compounds would be understood as some mercury loss might occur from accumulation and condensation within a process system (as discussed in previous sections). Finally, kinetic parameters such as reaction order and constant should be evaluated carefully. Chemical reactions involving mercury are complicated due to its stability and many are not known.

Table 2.13 Hg^0 Dynamic Solubility Studies

Purpose	Experimental Set-up	Liquid Phase	Analysis Method	Results	Comment	Source
Evaluate removal efficiency of Hg^0 gas by potassium persulfate and silver nitrate solution	Bubble column glass reactor, constant Hg^0 gas bubbled in reactor	$K_2S_2O_8$/ $AgNO_3$	CV-AAS (Liquid samples)	Reaction mechanism of between Hg^0 and $K_2S_2O_8$ in the presence of Ag^+ was proposed.	• % of Hg^0 removed was calculated based on the ratio of Hg^0 collected at the outlet and inlet of the reactor. The $K_2S_2O_8$/$AgNO_3$ solution was only analysed for sulphate content and not Hg^0 • Equilibrium was almost achieved within 10 minutes of contact time. Although Hg^0 concentration profile was reported up to 210 minutes, the changes are quite minimal • Kinetic and absorption parameters were not evaluated	[119]
Solubility of metallic Hg^0 in water under oxidising and reducing condition	Batch and semi-batch bubble reactor, metallic Hg^0 placed inside reactor. Argon (Ar) gas bubbled to remove O_2 in semi-batch reactor	Water under 3 different conditions: presence of O_2, absence of O_2 (Ar) and reducing conditions ($NaBH_4$)	AAS; Total Hg and Hg^0 collected on gold substrate by amalgamation	• Quantity of oxidised mercury continue to increase in O_2 and Ar condition. This indicate oxidation of Hg^0 to a more soluble form. • Under $NaBH_4$ condition, maximum	• Equilibrium was not reached for solubility in water at O_2 and Ar conditions after 10 – 13 days of contact time. No means of mixing mentioned except bubbling of Ar gas. Unsure whether Hg sample taken is well-mixed • The Hg^0 concentration detected in water is much lower than commonly reported; 50 ppb. $NaBH_4$ is a stronger reduction	[120]

				concentration reached is very low; 2.75ppb at 306 K	agent than $SnCl_2$ used in CV-AAS method. The low Hg^0 concentration detected just indicate the effectiveness of such reducing agent. • Solubility kinetics results were not evaluated for absorption parameters information	
Evaluate mechanism of Hg^0 absorption into different liquids for removal from gas phase	Semi-batch stirred cell reactor, constant Hg^0 gas passed over the liquid surface	$KMnO_4$, NaOCl, H_2O_2/HNO_3, $K_2Cr_2O_7$, HNO_3, H_2SO_4, HCl, NaOH, NaCl, $MnSO_4$, $FeCl_3$, $MgCl_2$, $CaCl_2$	CV-AAS (Gas samples)	• Absorption parameters; mass transfer coefficients were determined using surface renewal theory • Reaction order and constants were determined for reaction between Hg^0 gas and multiple compounds	• Relationship (Arrhenius equation) between reaction and temperature was determined and extrapolated from two temperatures, 298 and 328 K. Reliability of relationship employed is questionable for other temperatures • Determination of reaction order were assumed to be proportional to the number of reactants. Justification of assumptions and determination of mercury kinetics are unclear	[118]

Evaluate absorption rate of Hg^0 and Cl_2 using sulphite solutions	Wetted-wall column reactor, constant Hg^0 gas passed over liquid surface	Aqueous sulphite and bisulphite (S(IV)), NaCl, $HgCl_2$ and NaOCl	CV-AAS (Gas samples); reactor outlet gas was bubbled into $SnCl_2$/NaOH solution and ice bath to remove excess moisture, Cl_2 and evolve Hg^0 for analysis	• Absorption model: mass transfer with fast irreversible chemical reaction in the boundary layer • Constant for the reaction studied were not determined, already well studied	• Not all mercury that is present in the reactor outlet might reach the CV-AAS detection • Some mercury might get absorbed and remain in the $SnCl_2$/NaOH solution. Condensation of Hg along with the water vapour at the ice bath might also occur, compromising the overall mass balance of the process. • It is unclear whether the author analysed the associating liquids other than the gas phase.	[121]
Study oxidative dissolution of Hg^0 in aqueous NaOCl	Batch stirred cell reactor, liquid Hg^0 placed inside reactor	NaOCl/HCl	CV-AAS (Liquid samples)	• Constant for reaction studied were expressed using power law kinetic equation • Reaction follows pseudo-first order reaction with respect to NaOCl	• Reaction between Hg^0 and NaOCl expressed as heterogenous reaction, as both are in liquid form • Author mentioned that addition of HCl was needed to dissolve the product HgO. However, reaction order with respect to concentration of HCl were not evaluated	[122]

There are significantly less information on absorption characteristics and kinetics data present in the literature for both inorganic and organic mercury as their contribution to mercury problem in the oil and gas is often neglected due to their small presence (refer to section 2.2.2.1). Nevertheless, although occurring in trace amount, mercury is notoriously known to cause problems in the long run due to its tendency to accumulate in different parts of the process and environment [89, 123].

Several works have been done to bridge the knowledge gap with regards to $HgCl_2$ and $Hg(C_6H_5)_2$ behaviour such as the saturated solubility in different solvents [45, 48, 49, 114, 124], distribution between gas and liquid system, henry coefficient and stability constant [90, 125, 126]. Information related to $HgCl_2$ kinetics are usually inferred from adsorption and control techniques developed for removal from flue gas [125, 127-129]. Attempts have been made to predict kinetics mechanisms and distribution under different conditions, however they are based on the currently existing equilibrium parameters. Based on the literature review, the solubility information on $HgCl_2$ and $Hg(C_6H_5)_2$ are currently limited to either saturated or equilibrium condition (Table 2.6) and no information available for its absorption kinetics. Much less information is available on $Hg(C_6H_5)_2$.

Given that solubility kinetic data for both inorganic and organic mercury in natural water is very limited, development of a kinetic model would be considered as a preliminary pathway or guide to the experiments required to bridge current knowledge gaps. Understanding the absorption behaviour of both $HgCl_2$ and $Hg(C_6H_5)_2$ as well as identification of their kinetics parameter will provide further insight on solving the problem with partitioning and speciation issue that have been outlined in section 2.2.2 and 2.2.3. Consequently, the knowledge gained will enable improvement of current models for mercury mapping within different sections of the process, the downstream products and environmental releases. Ultimately, effective strategies could be established for corrosion mitigation and mercury disposal plan as pollution control.

2.5.2 Challenges with Working with Mercury

In order to conduct accurate and reliable solubility kinetics study, handling and treatment of mercury samples should executed properly.

2.5.2.1 Stability of Compound

Selection of Storage Material

Due to the reactive nature of mercury and its tendency for species interconversion leading to sample loss, minute details such as selection of container materials itself is a challenge. Mercury samples should never be stored in polyethylene containers [130-133]. Occurring mercury both in solution and atmosphere can permeate and interact with polyethylene functional groups in container walls and be adsorbed from solution. Other poorly performing containers include metal, polyvinyl chloride (PVC), linear polyethylene (LPE) and polypropylene (PP) [134-137]. The use of Teflon have been demonstrated by several authors to have minimal reaction with mercury and is able to contain the sample for long period of time of a few months [131, 133]. Glass containers have also been reported to perform well in the storage and handling of different mercury species [130, 131].

Preservation Method

Several authors working with mercury have reported difficulties in keeping the integrity of the mercury samples prior to analysis associated with mercury loss through adsorption onto container walls and volatilisation [136-140]. It has been reported that Hg(II) in water samples are generally stable, especially $HgCl_2$ [141], however loss still observed over time [138]. Parker and Bloom have reported that methylmercury solution is only stable up to 1 week without any preservation, although being contained in relatively inert container [131]. To combat issues with mercury stability in samples, preservation is often required as well as to select suitable condition for storage.

It has been observed that addition of acids help preserve mercury in liquid samples by minimising wall adsorption [133, 136]. This is further supported by Rich [141], who found that presence of acid increase the solubility of Hg^{2+} and Hg^{+}, which makes them stay in solutions better. Recent work done by Sabri et al. [142] noted precipitation

occurring in mercury samples of higher pH (pH = 9) but immediately reduced upon addition of HCl.

Nitric acid (HNO_3) is usually the preferred choice of acid for preservation of trace elements due to its oxidising ability to keep them in solutions. However, HNO_3 is not suitable for preservation of organic mercury due to its tendency to cause decomposition and release of Hg^0 [131, 136, 139]. Loss of mercury from samples within a span of 8 hours was also reported by Parikh et al. [143] although preserved using 5% HNO_3. Another acid that has been widely used for mercury preservation is hydrochloric acid (HCl) and many have found it suitable to preserve mercury samples of varying species. Addition of HCl to samples works by preventing volatilisation of soluble mercury ions into Hg^0 by formation of stable Hg-chloro complexes [$HgCl_4^{2-}$] [91], keeping total mercury in solution. Addition of gold in the form of auric ions; Au^{3+} will also further enhance the stability of the sample as it readily oxidize mercury to its ionic state; Hg^{2+} [144]. When dealing with liquid sample with high salinity (i.e. salt water, etc), addition of H_2SO_4 has shown promising results to minimise mercury loss from samples [130, 131].

Following acid preservation, many argue that mercury samples should be stored in a refrigerator at temperature of between 1-4°C with minimal light exposure. Preservation of organic mercury in particular requires darkness as possibility of photodecomposition reported [131, 145]. On the contrary, Leermakers et al. [136] have experienced minimal effect of light on storage of inorganic and methylmercury when samples have been preserved with acids. Effect of temperature seemed to be contributing to stability issue as Lansens et al. [146] noticed significant amount of mercury loss in samples stored at room temperature over refrigerated condition.

2.5.2.2 Mercury Gas Generation Technique

In order to carry out the mercury solubility kinetics study, a reliable source of mercury gas is crucial. Generally, the generation of controlled test gas employ 2 methods, namely using a static and dynamic systems, the latter is usually preferred for common laboratory applications. Preparation of static system requires placement of a known weight of the compound of interest into a container of fixed size, whereby the compound is left to equilibrate at a certain pressure and temperature to produce vapour of specific concentration in a closed system. Since the volume of gas produced is

limited to the container, this method is usually preferred to yield gas for instrument calibrations [147]. Purchasing a certified commercial $HgCl_2$ test gas cylinder is not an option due to the unstable nature of mercury and its tendency to adsorb onto the vessel wall.

Dynamic method for generation of test gas make use of a continuous stream of gas to carry the equilibrated/saturated vapour generated from the compound of interest. This method is often preferred over the static method as problems with wall adsorption is eliminated as fresh stream of pure gas is continuously carrying the vapour produced. This feature also allows for large volume of gas to be generated for extended period of time, thus offering a wider range of test application. Common use of dynamic gas generation method includes adsorption, absorption, catalytic and kinetic measurements and test where direct monitoring of gas phase is required. The concentration of generated gas can be controlled by modifying temperature, dimensions of vessel and carrier gas flow rate [148].

Several authors have utilised the dynamic gas method for generation of various gaseous mercury species with different test applications. The types of dynamic gas generation system are shown in Table 2.14 with range of generated concentration error reported from 1% to 23%.

Table 2.14 Dynamic Gas System to Generate Various Mercury Gas

Type of Dynamic Generation System	Mercury Species	Reference
Vaporisation using saturation vessel	$HgCl_2$	[127, 149, 150]
	Various organic Hg	[151]
Evaporation	Hg^0	[147, 152]
	$(C_4H_9)_2Hg$	[153]
	CH_3HgCl	[154]
Diffusion using diffusion cell	Hg^0	[155]
	$HgCl_2$	[156-159]
	CH_3HgCl	[156]
Permeation using permeation tube	Hg^0	[118, 142, 160-163]
	$HgCl_2$	[118, 160, 161]

2.5.3 Analysis Technique for Trace Mercury Determination

Detection method for mercury in water has evolved along with a multitude of several very sensitive detecting equipment; up to parts per trillion (ppt) [164]. Essentially,

these quantitative analysis methods are valid for detecting various mercury species such as inorganic, organic, particulate and elemental mercury in liquid and gas phase.

Gas Phase

Detection of mercury present in gaseous samples is normally done using two methods, namely direct measurement (at a certain wavelength) and other by capturing the gas in a suitable trap. The latter require additional processing to be able to release and quantify the mercury captured.

For direct measurement, detection wavelengths for mercury gas via UV atomic absorbance are 185 and 253.7 nm [165]. 253.7 nm is utilised in most modern mercury detection system since wavelength at 185nm is prone to interference from other species, producing numerous peaks which will contribute in systematic error from measurement [42]. Having said that, performing direct measurement is challenging as mercury typically co-exist with other gases (hydrocarbons [12], SO_2, NO_2, NO_x [66]) that will interfere with the detection at wavelength of 253.7 nm.

In order to eliminate the problem with these interferences, mercury containing gas is usually captured by means of either solid or liquid trap. A common material of choice for solid trap is noble metals (gold, platinum, silver, etc), especially gold. Gold has been proven and successfully utilised by several authors for trapping and determination of gaseous concentration of mercury species such as $HgCl_2$, Hg^0 and organic Hg [125, 158, 166-170] via means of amalgamation. The solid trap will then require heating to decompose the amalgamated mercury, releasing them as Hg^0 for detection. The use of gold trap is able to trap organic mercury, however longer residence time would be required since the amalgamation process takes longer [12, 156]. Although many has deemed the use of gold solid trap as a reliable form of mercury gas capture, several limitations do exist such as low capacity and the decrease in adsorption capacity due to presence of other contaminants [171]. Another promising solid trap utilises denuders that is coated with different compounds for detection of specific mercury species. One such successful example is the use of KCl-coated denuders to selectively capture $HgCl_2$ gas in the presence of Hg^0 [156, 172].

A prevalent liquid trap method used to capture mercury in gas form is via bubbling the gas through a series suitable solution, typically potassium permanganate; $KMnO_4$. The principle of this method is via oxidation, whereby all the gaseous mercury species are

converted into mercury ions (Hg^{2+}, Hg^{+}). Following the capture, the liquid samples can then be analysed using commonly used analysis techniques for quantification. The use of $KMnO_4$ have been utilised by many researchers to capture and accurately identify various species of mercury such as elemental mercury (Hg°), inorganic mercury ($HgCl_2$), organic mercury ($(CH_3)_2Hg$) [148, 156, 159, 166, 169, 173-175]. In the presence of highly stable mercury species (longer chains organic mercury), use of stronger oxidant solutions such as $HNO_3/K_2S_2O_8$ is reported to absorb >99% total mercury [148, 175]. A few advantages of using this method over the solid trap are the higher capture capacity along with ease of preparation. Aspect of speciation can also be achieved using such trap as demonstrated by a few authors, whereby solutions of 0.1 M HCl is used to trap only $HgCl_2$ in a gas mixture [156, 175]. This is possible as $HgCl_2$ is many times more soluble in HCl in comparison to Hg^0, resulting in >99% capture.

Liquid Phase

Cold-Vapour - Atomic Absorption Spectrometry (CV-AAS)

One of the commonly used analysis methods for determination of trace levels of mercury is the use of CV-AAS. Since first introduced by Hatch and Ott in 1968, CV-AAS is often the preferred method for analysis of mercury samples due to its simplicity, sensitivity (pg to sub-g absolute detection limit), wide availability and low cost [42, 164, 176]. The concept behind CV-AAS method is via harsh oxidation of sample to destroy any organic matter. Commonly used oxidating agents include potassium permanganate [174], potassium persulfate [177], bromine chloride [137] and potassium dichromate [29]. The sample follows a reduction step, whereby mercuric ion (Hg^{2+}, Hg^{+}) is reduced to Hg^0. Hg^0 is then sent either directly to a detector via inert gas stream or collected on a trap which will be thermally evolved into an inert gas stream for detection. The CV-AAS method is also favoured since the sample matrix can be analysed directly, without the use of an atomizer unit (favouring accuracy and sample throughput) [164].

Two commonly used reduction agents are stannous chloride ($SnCl_2$) [164], sodium borohydride ($NaBH_4$) [29] and some utilise pyrolysis to vaporise the sample to release Hg^0 [178]. It is reported by Yamamoto et al. [179] that the use of $NaBH_4$ results in 2.5% precision and 4.9% for $SnCl_2$. An advantage of using $NaBH_4$ is reported by

Toffaletti and Savory[180] and Rooney[181], where a 10-fold increase in signal is observed when analysis was conducted. Study by Weltz and Schubert-Jacobs [167] also indicate that $NaBH_4$ performs on par or even better than $SnCl_2$. However, it should be noted that $NaBH_4$ solution must be used within 1 hour of preparation, making sample preparation rather tedious since solutions needed to be prepared at all time. Hence the reducing agent preferred is still $SnCl_2$ being a more efficient and robust choice (i.e. longer shelf life and less reactive in nature) [164].

In the recent years, a flow injection analysis system (FIAS) has been coupled with the CV-AAS system. This combination allows rapid analysis as well as contributing to improved precision and sensitivity of results [182-184]. Furthermore, contamination and splashing hazards are greatly reduced as the analysis is performed in a closed system.

Inductively coupled plasma – mass spectrometry (ICP-MS)

The use of inductively coupled plasma – mass spectrometry (ICP-MS) has been gaining popularities to analyse trace elements since it was first introduced in the 1980s. Its values include its capability of performing analysis of several element simultaneously with very low detection limit in parts per billion (ppb) and often in ppt level.

Analysis using ICP-MS can be separated into four parts, namely sample introduction, the inductively coupled plasma torch, interface and finally mass spectrometer for detection [185]. At the sample introduction phase, often samples for ICP-MS are in liquid phase, however they must be converted into either gas or aerosol phase by means of a nebulizer and a spray chamber to be introduced into the plasma torch. The aerosol created is then injected into the torch where it will be atomized and ionized by the plasma which is generated when continuous stream of argon gas is heated 6000°C. The resulting ions from the plasma then enters the interface where it comprises of a sampler and skimmer cone. The interface allow rapid cooling and de-pressurising of the hot plasma gas to the appropriate condition before the gas is sent to the final stage for detection. Following the interface, the ions are focussed into a beam by a single lens for transmission into the MS. The MS is commonly in the form of a quadrupole [186], consisting of 4 parallel rods that act as electrodes. The quadrupole separates the

ions based on their mass to charge ratio prior to entering the detector where a measurable pulse is detected.

An important aspect of analysis method using ICP-MS, is the fact that detection and quantification of elements occur as a total, not compound specific. This aspect can be regarded as both pros and cons for determination and speciation of mercury. In terms of total mercury determination, analysis using ICP-MS eliminates the pre-treatment step of samples which is required for CV-AAS as all occurring mercury species will be ionised upon contact with the plasma. This also reduces the uncertainty that comes from improper sample preparation. In terms of mercury speciation, other separation techniques such as gas chromatography (GC) [39, 40, 187], liquid chromatography (LC) [188] and high-performance liquid chromatography (HPLC) [189, 190] to be incorporated to the existing ICP-MS system. As these chromatography techniques utilised a column to separate the samples in both liquid and gas phase, the latter can be directly introduced into the ICP-MS torch. With liquid eluents, sample introduction follows that of normal liquid samples.

Although ICP-MS possesses many benefits over the conventional CV-AAS, the instrument is vulnerable to instrumental drift, which can be minimised by means of suitable internal standards [191]. Mercury is known to possess a very high first ionization potential; 10.44 eV, thus signals are often suppressed when high concentration of other elements of low ionization energy are present in the sample matrix [142, 192]. Furthermore, selection of acids in matrix preparation is also crucial as H_2SO_4 and H_3PO_4 have shown significant signal suppression during analysis [192]. Challenges with dealing with mercury samples with complicated matrix have been reported by several authors [142, 170].

2.5.4 Gas-Liquid Mass Transfer Theory

Gas-liquid absorption process occurs when component of a gas phase is transferred into a liquid phase when they come into contact with each other. This absorption process often occurs via mass transfer only, in which the process is described as purely physical absorption. In several cases, this mass transfer is enhanced when the gas and liquid phase undergo a chemical reaction simultaneous to the mass transfer process. The study of this process is very useful in developing an understanding with regards

to reactions kinetics. Influencing parameters on the process include concentration, presence of chemical reaction and temperature of absorption.

There are several factors that directly influence the rate of absorption, namely physicochemical and hydrodynamic. Physicochemical factors relate to the solubility and diffusivity of the gas in liquid, while hydrodynamic factors are affected by the physical properties of the liquid (viscosity, density, surface tension and flowrate) and the geometry of contact.

In order to understand and predict absorption processes, many models have been developed to determine parameters that govern these processes; such as overall mass transfer coefficient and kinetics parameter. A summary of the theoretical models commonly used for dynamic solubility studies is presented in Table 2.15. They are namely the film theory [193], penetration theory [194, 195] and surface renewal theory [196]. Despite film theory being the simplest method out of the three methods, Froment and Bischoff [197] have reported negligible difference (average of 1% and 2% for penetration and surface renewal respectively) for the prediction of pseudo-first order reaction. This finding explains why film theory remain one of the most widely used theory to model various gas/liquid absorption processes.

Table 2.15 Comparison of Gas/Liquid Mass Transfer Theories

Mass Transfer Theory	Basis	Mass Transfer Parameter	Comment
Film	• Mass transfer occurs in a stagnant film (of thickness δ) at the interface • Absorption flux is steady state across the film • No convection in the film, mass transfer is governed by molecular diffusion	$k = \frac{D}{\delta}$	Simple, most commonly used for gas/liquid modelling, film thickness is unknown
Penetration	• Clusters of gas molecules stay at the liquid surface for a constant time and penetrate the liquid bulk • Mass transfer governed by the exposure time • Unsteady mass transfer • Equilibrium exists at gas/liquid interface	$k = 2\sqrt{\frac{D}{\pi t_s}}$	Provide a more realistic model, exposure time is usually unknown
Surface Renewal	• Rate of absorption at liquid surface is an average of the absorption of each molecule • The liquid molecules at the interface are being randomly exchanged by fresh molecules from the bulk liquid • Rate of absorption of each molecule is governed by the exchange rate of bulk liquid surface (surface renewal rate) • Unsteady state mass transfer at interface	$k = \sqrt{D/t_s}$	Similar concept to penetration theory, surface renewal rate is unknown

2.5.4.1 Two-Film Theory

A number of different models have been used to describe the gas-liquid absorption. One of the most commonly used theory is the two-film theory which was first introduced by Whitman in 1923 [198]. The fundamental of the theory can be described by the diagram shown in Fig. 2.5.

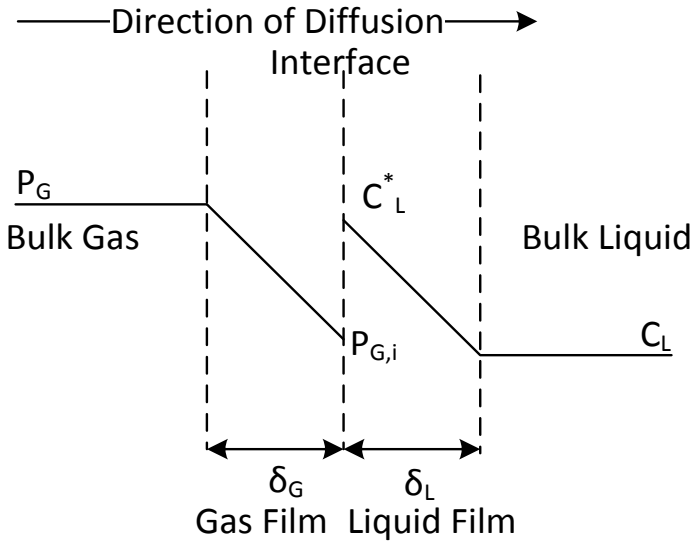

Fig. 2.5 Diagram of Two-Film Theory

As shown in Fig. 2.5, the two-film theory assumes a stagnant film with definite thickness (δ) that exists at the interface both at gas and liquid phase. Each stagnant film is assumed to provide the resistance to mass transfer. At the interface, the concentration of contacting gas and the liquid is assumed to be at equilibrium, where this relationship follows the Henry law ($P_{G,i}/H = C^*_L$). In most cases, there is no convection in the film and the rate of absorption is controlled by rate of diffusion (molecular diffusivity) through the film at the gas-liquid boundary.

The general mass transfer equation for mass transfer of gas A to liquid B can be described by Fick's law:

$$J = \frac{D_{AB}}{\delta}\left(C^*_{A,L} - C_{A,L}\right) \qquad (1)$$

The $\frac{D_{AB}}{\delta}$ in the equation can often be replaced by the overall liquid mass transfer coefficient,

$$J = K_L\left(C^*_{A,L} - C_{A,L}\right) \qquad (2)$$

The overall liquid mass transfer coefficient K_L is the characteristic parameter of an absorption process and can be determined by equation (3),

$$\frac{1}{K_L} = \frac{1}{k_L} + \frac{1}{\mathrm{H}\, k_G} \qquad (3)$$

Henry coefficient; H is a constant that described the phase distribution of compound between gas and liquid. H is a function of temperature and the values for various gases and water system has been published elsewhere [199]. General equation for H is described by equation (4).

$$\mathrm{H} = \frac{\mathrm{P_G}}{\mathrm{C_L}} \qquad (4)$$

2.5.4.2 Chemical Reaction Enhanced Absorption

Often gas-liquid absorption rate see enhancement when a chemical reaction is involved during the absorption process.

The enhancement effect in relation to chemical reaction can be represented by an enhancement factor; E. E factor is hence defined as the ratio of mass flux of component A with chemical reaction to the mass flux without chemical reaction. The ratio is represented by equation (5).

$$\mathrm{E} = \frac{\mathrm{J_{A,with\ reaction}}}{\mathrm{J_{A,without\ reaction}}} \qquad (5)$$

There are many factors affecting the rate of chemical enhanced absorption, namely stoichiometry of the reaction, concentration of the reactants, temperature and the mass transfer parameter of the system itself. Particularly, knowing kinetics parameter such as order of reaction and kinetic constant is crucial to model the absorption process. A particular chemical reaction can be described by their order of reaction (zero, first, pseudo-first, second, etc), their irreversibility and also how fast or slow the reaction occurs. These kinetics parameters will need to be taken into consideration and the overall absorption equation changes accordingly.

2.5.4.3 Absorption Characteristics of Gas in Liquids

Regardless of whether the absorption process is physical or chemically enhanced, often information such as H can help determine whether the gas or liquid phase resistance

are dominating. Information on H of several mercury compounds have been summarised in Table 2.16 [199]. For slightly soluble gases such as Hg^0, He is generally very large as the gas has a tendency to stay in the gas phase. By substituting this into equation (3), it can be seen that the term (1/ $H.k_G$) becomes very small, thus the resistance of mass transfer lies in the liquid phase. This is a reverse for highly soluble gases. This effect of gas solubility has also been demonstrated early on by Whitman [200] and has been used as a general clue to model various gas-liquid systems.

Table 2.16 Henry Coefficient of Different Mercury Compounds

Mercury	He at 298 K ($Pa.m^3/mol$)
Hg^0	769.23
$HgCl_2$	7.14×10^{-5}
HgO	3.13×10^{-5}
C_2H_6Hg	769.23
$C_4H_{10}Hg$	1000
$C_6H_{14}Hg$	1785.71

2.5.4.4 Application of Two-Film Theory in the Absorption of Mercury

Two-film theory still remain to date, the most commonly used theory as basis to a lot of gas-liquid absorption processes due to its simple approach yet still very reliable. Since it was first introduced, many authors have applied two-film theory to model absorption of mercury into liquids.

Liss and Slater [201] first utilised two-film theory to model the fluxes of pollutant gases, including mercury across the air-sea interface. Since then, several more authors employed the idea and model the rate of volatilization of Hg^0 from aqueous phase [202, 203]. More recently, effect of chemical reactions were included and evaluated to understand and model its behaviour within conditions with flue gas [119, 122] and Hg^0 emission and deposition in the environment [113, 204-207].

Review of recent modelling work on mercury suggest the lack of insight into inorganic and organic mercury as majority of the works published focusses on Hg^0. Nevertheless, work applying two-film theory on absorption processes involving mercury have been well documented, proposing the suitability of two-film theory to model other species of mercury under different conditions and practises.

2.6 Conclusions

The adverse effects of mercury on the health of personnel, environment and process equipment within the oil and gas industries are well documented, however understanding of the source and cause of mercury deposition in different parts of the processes are limited. Dealing with mercury possess many challenges and precautions need to be considered when preparing the samples and work set-up to ensure success of studies.

Review of available literatures on the solubility kinetics of inorganic and organic mercury suggest the lack of information and understanding of the absorption behaviour. There is also a lack of data such as transient absorption rate and reaction kinetics to conclude and predict behaviour of Hg upon extraction from the gas reservoirs up to disposal and production.

To the best of the Author's knowledge, the solubility kinetics information on $HgCl_2$ and $Hg(C_6H_5)_2$ are currently limited to either saturated or equilibrium condition and no information available for its absorption kinetics at transient condition. Additional studies need to be conducted to study the absorption behaviour of the selected mercury species when in contact with aqueous solutions that are available within the oil and gas processes. Evaluation of reaction kinetics of the selected mercury species with the readily available impurities is necessary to improve current mercury removal and mitigation plan. Consequently, the information investigated will improve understanding of the mechanism of mercury species interconversion issues.

2.7 Reference

[1] Registry, US Government Agency for Toxic Substances and Disease. *ATSDR's Substance Priority List*. Agency for Toxic Substances and Disease Registry 2017. Available from https://www.atsdr.cdc.gov/spl/index.html#modalIdString_myTable2017.

[2] UNEP. 2013. Global Mercury Assessment - Sources, Emissions, Releases and Environmental Transport.

[3] Services, US Department of Health and Human. 1999. Toxicological profile for mercury. edited by Department of Health and Human Services. Atlanta, Georgia

[4] Rice, Kevin M., Jr Ernest M. Walker, Miaozong Wu, Chris Gillette, and Eric R. Blough. 2014. "Environmental Mercury and Its Toxic Effects." *Journal of Preventitive Medicine & Public Health* no. 47 (2):74-83. doi: 10.3961/jpmph.2014.47.2.74.

[5] Pacyna, Jozef M., Oleg Travnikov, Francesco De Simone, Ian M. Hedgecock, Kyrre Sundseth, Elisabeth G. Pacyna, Frits Steenhuisen, Nicola Pirrone, John Munthe, and Karin Kindbom. 2016. "Current and future levels of mercury atmospheric pollution on a global scale." *Atmospheric Chemistry and Physics* no. 16:12495–12511. doi: 10.5194/acp-16-12495-2016.

[6] BP. 2017. BP Statistical Review of World Energy June 2017. https://www.bp.com/content/dam/bp/en/corporate/pdf/energy-economics/statistical-review-2017/bp-statistical-review-of-world-energy-2017-full-report.pdf.

[7] AMAP/UNEP. 2013. Technical Background Report for the Global Mercury Assessment 2013. *Arctic Monitoring and Assessment Programme*: 263 pp.

[8] EIA, U.S. 2017. Annual Energy Outlook 2017 with projections to 2050.

[9] Gworek, Barbara, Wojciech Dmuchowski, Aneta H. Baczewska, Paulina Brągoszewska, Olga Bemowska-Kałabun, and Justyna Wrzosek-Jakubowska. 2017. "Air Contamination by Mercury, Emissions and Transformations—a Review." *Water, Air and Soil Pollution* no. 228 (123). doi: 10.1007/s11270-017-3311-y.

[10] Wilhelm, S. Mark. 2001. "Estimate of Mercury Emissions to the Atmosphere from Petroleum " *Environmental Science & Technology* no. 35 (24):4704-4710. doi: 10.1021/es001804h.

[11] Mason, Robert. 2008. Geomicrobiology of Mercury. In *Geomicrobiology*, edited by Henry Lutz Ehrlich and Dianne K. Newman. Boca Raton: CRC Press.

[12] Wilhelm, S. Mark. 2001. Mercury in Petroleum and Natural Gas: Estimation of Emissions from Production, Processing, and Combustion. Tomball, Texas.

[13] Lang, David, Murray Gardner, and John Holmes. 2012. Mercury arising from oil and gas production in the United Kingdom and UK continental shelf. University of Oxford.

[14] Yan, Qituan, Zhongxi Han, and Shuying Wang. 2017. Geochemical Characteristics of Mercury in Oil and Gas In *2017 International Conference on Environmental and Energy Engineering (IC3E 2017)*: Earth and Environmental Science.

[15] Abai, Mahpuzah, Martin P. Atkins, Amiruddin Hassan, John D. Holbrey, Yongcheun Kuah, Peter Nockemann, Alexander A. Oliferenko, Natalia V. Plechkova, Syamzari Rafeen, Adam A. Rahman, Rafin Ramli, Shahidah M. Shariff, Kenneth R. Seddon, Geetha Srinivasan, and Yiran Zou. 2015. "An

ionic liquid process for mercury removal from natural gas." *Dalton Transations* no. 44 (18):8617-8624 doi: 10.1039/C4DT03273J.

[16] Gallup, Darrell L. 2014. Removal of mercury from water in the petroleum industry. Paper read at 21st International Petroleum Environmental Conference

[17] Filby, Royston H. 1994. "Origin and nature of trace element species in crude oils, bitumens and kerogens: implications for correlation and other geochemical studies." *Geological Society, London, Special Publications* no. 78:203-219. doi: 10.1144/GSL.SP.1994.078.01.15.

[18] Wilhelm, S. Mark, and Nicholas Bloom. 2000. "Mercury in Petroleum." *Fuel Processing Technology* no. 63 (2000):1-27.

[19] Ryzhov, Vladimir V., Nikolai R. Mashyanov, Nina A. Ozerova, and Sergey E. Pogarev. 2003. "Regular variations of the mercury concentration in natural gas." *Science of The Total Environment* no. 304 (1-3):145-152. doi: 10.1016/S0048-9697(02)00564-8.

[20] Mussig, S., and B. Rothmann. 1997. Mercury in Natural Gas - Problems and Technical Solutions for its Removal Paper read at SPE Asia Pacific Oil and Gas Conference and Exhibition, 14-16 April 1997, at Kuala Lumpur, Malaysia.

[21] Liu, QuanYou. 2013. "Mercury concentration in natural gas and its distribution in the Tarim Basin." *Science China Earth Science* no. 56 (8):1371-1379. doi: 10.1007/s11430-013-4609-2.

[22] Wilhelm, S. Mark, Lian Liang, Deborah Cussen, and David A. Kirchgessner. 2007. "Mercury in Crude Oil Processed in the United States (2004)." *Environmental Science & Technology* no. 41 (13):4509-4514. doi: 10.1021/es062742j.

[23] Shafawi, Azman Bin. 1999. *Mercury Species in Natural Gas Condensate* Department of Environmental Sciences, University of Plymouth Plymouth

[24] Woodside. 2014. Browse FLNG Development Draft Environmental Impact Statement EPBC 2013/7079. http://www.woodside.com.au/Our-Business/Developing/Browse/Documents/Environmental%20Impact%20Statement/Browse%20FLNG%20Development%20Draft%20EIS.PDF.

[25] Ezzeldin, Mohamed F., Zuzana Gajdosechova, Mohamed B. Masod, Tamer Zaki, Jörg Feldmann, and Eva M. Krupp. 2016. "Mercury Speciation and Distribution in an Egyptian Natural Gas Processing Plant." *Energy & Fuels* no. 30 (12):10236-10243. doi: 10.1021/acs.energyfuels.6b02035.

[26] Wilhelm, S. Mark. 1999. "Avoiding Exposure to Mercury During Inspection and Maintenance Operations in Oil and Gas Processing." *Process Safety Progress* no. 18 (3):178-188.

[27] Zettlitzer, M., R. Scholer, and R. Falter. 1997. Determination of elemental, inorganic and organic mercury in North German gas condesates and formation brines. In *SPE International Symposium on Oilfiled Chemistry*. Houston, Texas: Society of Petroleum Engineers, Inc. .

[28] Bingham, Mark D. 1990. "Field Detection and Implications of Mercury in Natural Gas." *Society of Petroleum Engineers Production Engineering*:120-124.

[29] Schickling, C., and J. A. C. Broekaert. 1995. "Determination of mercury species in gas condensates by on-line coupled High-performance liquid Chromatography and Cold-vapor atomic absorption spectrometry." *Applied Organometallic Chemistry* no. 9:29-36.

[30] Abbas, Tauqeer, Girma Gonfa, Kallidanthiyil Chellappan Lethesh, M.I. Abdul Mutalib, Mahpuzah bt Abai, Kuah Yong Cheun, and Eakalak Khan. 2016.

"Mercury capture from natural gas by carbon supported ionic liquids: Synthesis, evaluation and molecular mechanism." *Fuel* no. 177:296-303. doi: 10.1016/j.fuel.2016.03.032.

[31] Frech, Wolfgang, Douglas C. Baxter, Berit Bakke, James Snell, and Yngvar Thomassen. 1996. "Determination and Speciation of Mercury in Natural Gases and Gas Condensates." *Analytical Communications* no. 33:7H-9H.

[32] Kozin, Leonid F, and Steve Hansen. 2013. "Mercury Handbook: Chemistry, Applications and Environmental Impact." In: Royal Society of Chemistry.

[33] Ma, Yongpeng, Haomiao Xu, Zan Qu, Naiqiang Yan, and Wenhua Wang. 2014. "Absorption characteristics of elemental mercury in mercury chloride solutions." *Journal of Environmental Sciences* no. 26 (11):2257-2265. doi: 10.1016/j.jes.2014.09.011.

[34] Gustafsson, Meredith B., Bal K. Kaul, Brian S. Fox, David A. Masciola, and Bowornsak Wanichkul. 2007. Wastewater mercury removal process. edited by ExxonMobil Research and Engineering Co.

[35] Corvini, Giacomo, Julie Stiltner, and Keith Clark. 2016. Mercury removal from natural gas and liquid streams https://www.uop.com/?document=mercury-removal-from-natural-gas-and-liquid-streams&download=1.

[36] Lothongkum, Anchaleeporn Waritswat, Sira Suren, Srestha Chaturabul, Nopphawat Thamphiphit, and Ura Pancharoen. 2011. "Simultaneous removal of arsenic and mercury from natural-gas-co-produced water from the Gulf of Thailand using synergistic extractant via HFSLM." *Journal of Membrane Science* no. 369 (1-2):350-358. doi: 10.1016/j.memsci.2010.12.013.

[37] Ahmadun, Fakhru'l-Razi, AlirezaPendashteh, Luqman Chuah Abdullah, Dayang Radiah Awang Biak, Sayed Siavash Madaeni, and Zurina Zainal Abidin. 2009. "Review of technologies for oil and gas produced water treatment." *Journal of Hazardous Materials* no. 170 (2-3):530-551. doi: 10.1016/j.jhazmat.2009.05.044.

[38] Gallup, Darrell L., and James B. Strong. 2007. Removal of Mercury and Arsenic from Produced Water http://citeseerx.ist.psu.edu/viewdoc/download?doi=10.1.1.626.7356&rep=rep1&type=pdf.

[39] Tao, Hiroaki, Tadahiko Murakami, Mamoru Tominaga, and Akira Miyazaki. 1998. "Mercury speciation in natural gas condensate by gas chromatography-inductively coupled plasma mass spectrometry." *Journal of Analytical Atomic Spectrometry* no. 13 (1998):1086-1093.

[40] Bouyssiere, Brice, Franck Baco, Laurent Savary, and Ryszard Lobinski. 2002. "Speciation analysis for mercury in gas condensates by capillary gas chromatography with inductively coupled plasma mass spectrometric detection." *Journal of Chromatography A* no. 976 (2002):431-439.

[41] Gaulier, Florine, Alexandre Gibert, David Walls, Michael Langford, Stuart Baker, Arnaud Baudot, Fabien Porcheron, and Charles-Philippe Lienemann. 2015. "Mercury speciation in liquid petroleum product : comparison between on-site approach and lab measurement using size exclusion chromatography with high resolution inductively coupled plasma mass spectrometric detection (SEC-ICP-HR MS)." *Fuel Processing Technology* no. 131:254-261. doi: 10.1016/j.fuproc.2014.10.024.

[42] Bouyssiere, B., F. Baco, L. Savary, and R. Lobinski. 2000. "Analytical methods for speciation of mercury in gas condensates." *Oil & Gas Science and Technology* no. 55 (6):639-648.

[43] Dessy, Raymond E., and Y. K. Lee. 1960. "The Mechanism of the Reaction of Mercuric Halides with Dialkyl and Diarylmercury Compounds." *Journal of the Americal Chemical Society* no. 82 (3):689-693. doi: 0.1021/ja01488a047.

[44] McAuliffe, C. A. 1977. *The Chemistry of Mercury* London The Macmillan Press Ltd.

[45] Haynes, William M. Internet Version 2017. "CRC Handbook of Chemistry and Physics." In: CRC Press/Taylor & Francis, Boca Raton, FL.

[46] Edmonds, B., R. A. S. Moorwood, and R. Szczepanski. 1996. Mercury Partitioning in Natural Gases and Condensates. In *GPA European Chapter Meeting*. London.

[47] Chen, Ying, Yongguang Yin, Jianbo Shi, Guangliang Liu, Ligang Hu, Jingfu Liu, Yong Cai, and Guibin Jiang. 2017. "Analytical methods, formation, and dissolution of cinnabar and its impact on environmental cycle of mercury." *Critical Reviews in Environmental Science and Technology* no. 47 (24):2415-2447. doi: 10.1080/10643389.2018.1429764.

[48] Clever, H. Lawrence, Susan A. Johnson, and M. Elizabeth Derrick. 1985. "The Solubility of Mercury and Some Sparingly Soluble Mercury Salts in Water and Aqueous Electrolyte Solutions." *Journal of Physical and Chemical Reference Data* no. 14 (3).

[49] Okamoto, G., and M. Nagayama. 1952. "Physiochemical properties of aqueous solutions of mercury compounds." *Japan Journal of Pharmacy and Chemistry* no. 24:358-362.

[50] Gallup, Darrell L., Dennis J. O'Rear, and Ron Radford. 2017. "The behavior of mercury in water, alcohols, monoethylene glycol and triethylene glycol." *Fuel* no. 196:179-184. doi: 10.1016/j.fuel.2017.01.100.

[51] Marsh, Kenneth N., John W. Bevan, James C. Holste, David L. McFarlane, Michael Eliades, and William J. Rogers. 2016. "Solubility of Mercury in Liquid Hydrocarbons and Hydrocarbon Mixtures." *Journal of Chemical and Engineering Data* no. 61 (8):2805-2817. doi: 10.1021/acs.jced.6b00173.

[52] Obrist, Daniel, Jane L. Kirk, Lei Zhang, Elsie M. Sunderland, Martin Jiskra, and Noelle E. Selin. 2018. "A review of global environmental mercury processes in response to human and natural perturbations: Changes of emissions, climate, and land use." *Ambio* no. 47 (2):116-140. doi: 10.1007/s13280-017-1004-9.

[53] Pala, Biswajit, and Parisa A. Ariya. 2004. "Studies of ozone initiated reactions of gaseous mercury: kinetics, product studies, and atmospheric implications." *Physical Chemistry Chemical Physics* no. 6 (3):572-279. doi: 10.1039/B311150D.

[54] Organization, World Health. 2014. *Fact Sheet No. 361* 2013 [cited 1 August 2014]. Available from http://www.who.int/mediacentre/factsheets/fs361/en/.

[55] Australia, SafeWork. 1995. Adopted National Exposure Standards for Atmospheric Contaminants in the Occupational Environment http://www.safeworkaustralia.gov.au/sites/SWA/about/Publications/Documents/237/AdoptedNationalExposureStandardsAtmosphericContaminants_NOHSC1003-1995_PDF.pdf.

[56] Radford, Ron. 2013. "Lessons Learned in Mercury Management." *Hart Energy*, 1 November 2013.

[57] Bingham, Mark D. 1990. "Field Detection and Implications of Mercury in Natural Gas." *Society of Petroleum Engineers Production Engineering*:1220-124.

[58] Nengkoda, Ardian, Hendrikus Reerink, Zaher Hinai, PDO, Supranto, Imam Prasetyo, and Suryo Purwono. 2009. Understanding of Mercury Corrosion Attach on Stainless Steel Material and Gas Well: Case Study. In *International Petroleum Technology Conference*. Doha, Qatar.

[59] LLC, CRC Press. 2014. "Handbook of Chemistry and Physics." In *Properties of the Elements and Inorganic Compounds*, ed W. M. Haynes: Boca Raton, FL: CRC Press LLC. http://www.hbcpnetbase.com.dbgw.lis.curtin.edu.au/ (accessed 25 August 2014).

[60] Hsi, Hsing-Cheng, Mark J. Rood, M.ASCE, Massoud Rostam-Abadi, Shiaoguo Chen, and Ramsay Chang. 2002. "Mercury Adsorption Properties of Sulfur-Impregnated Adsorbents." *Journal of environmental Engineering* no. 128 (11):1080-1089. doi: 10.1061/~ASCE!0733-9372~2002!128:11~1080!

[61] Reddy, K. Suresh Kumar, Ahmed Al Shoaibi, and C. Srinivasakannan. 2018. "Mercury removal using metal sulfide porous carbon complex." *Process Safety and Environmental Protection* no. 114 (153-158). doi: 10.1016/j.psep.2017.12.022.

[62] Mokhatab, Saeid, William Poe, and James Speight. 2006. "Handbook of Natural Gas Transmission and Processing." In: Gulf Professional Publishing.

[63] Hutson, Nick D., Renata Krzyzynska, and Ravi K. Srivastava. 2008. "Simultaneous Removal of SO2, NOX, and Hg from Coal Flue Gas Using a NaClO2-Enhanced Wet Scrubber." *Industrial & Engineering Chemistry Research* no. 47 (16):5825-5831. doi: 10.1021/ie800339p.

[64] Pitoniak, Erik, Chang-Yu Wu, David W. Mazyck, Kevin W. Powers, and Wolfgang Sigmund. 2005. "Adsorption Enhancement Mechanisms of Silica-Titania Nanocomposites for Elemental Mercury Vapor Removal." *Environmental Science & Technology* no. 39 (5):1269-1274. doi: 10.1021/es049202b.

[65] Liu, Yangxian, and Yusuf G. Adewuyi. 2016. "A review on removal of elemental mercury from flue gas using advanced oxidation process: Chemistry and process." *Chemical Engineering Research and Design* no. 112:199-250. doi: 10.1016/j.cherd.2016.06.024.

[66] Granite, Evan J., and Henry W. Pennline. 2002. "Photochemical Removal of Mercury from Flue Gas." *Industrial & Engineering Chemistry Research* no. 41 (22):5470-5476. doi: 10.1021/ie020251b.

[67] Gao, Yanshan, Zhang Zhang, Jingwen Wu, Linhai Duan, Ahmad Umar, Luyi Sun, Zhanhu Guo, and Qiang Wang. 2013. "A Critical Review on the Heterogeneous Catalytic Oxidation of Elemental Mercury in Flue Gases." *Environmental Science & Technology* no. 47 (19):10813-10823. doi: 10.1021/es402495h.

[68] Mancini, Maria Vincenza, Nicoletta Spreti, Pietro Di Profio, and Raimondo Germani. 2013. "Understanding mercury extraction mechanism in ionic liquids." *Separation and Purification Technology* no. 116:294-299. doi: 10.1016/j.seppur.2013.06.006.

[69] Li, Xiaoshan, Liqi Zhang, Dong Zhou, Wenqian Liu, Xinyang Zhu, Yongqing Xu, Ying Zheng, and Chuguang Zheng. 2017. "Elemental Mercury Capture from Flue Gas by a Supported Ionic Liquid Phase Adsorbent." *Energy & Fuels* no. 31 (1):714-723. doi: 10.1021/acs.energyfuels.6b01956.

[70] Cheng, Guangwen, Bofeng Bai, Qiang Zhang, and Ming Cai. 2014. "Hg^0 removal from flue gas by ionic liquid/H_2O_2." *Journal of Hazardous Materials* no. 280:767-773. doi: 10.1016/j.jhazmat.2014.09.007.

[71] Wilhelm, S. Mark. 1999. "Generation and Disposal of Petroleum Processing Waste That Contains Mercury." *Environmental Progress* no. 18 (2):130-143.
[72] Manelius, Tom, and Imane Aguedach. 2018. Efficient Condensate Mercury Removal Offshore. Paper read at Offshore Technology Conference, 30 April - 3 May at Houston, Texas, USA.
[73] Eckersley, N. 2010. "Advanced Mercury Removal Technologies " *Hydrocarbon Processing* 29-35.
[74] Sharma, Abhi, Anmol Sharma, and Raj Kumar Arya. 2015. "Removal of Mercury(II) from Aqueous Solution: A Review of Recent Work." *Separation Science and Technology* no. 50 (9):1310-1320. doi: g/10.1080/01496395.2014.968261.
[75] Pancharoen, Ura, Sawatpop Somboonpanya, Srestha Chaturabul, and Anchaleeporn Waritswat Lothongkum. 2010. "Selective removal of mercury as HgCl42− from natural gas well produced water by TOA via HFSLM." *Journal of Alloys and Compounds* no. 489 (1):72-79. doi: 10.1016/j.jallcom.2009.08.145.
[76] Chaturabul, Srestha, Wanchalerm Srirachat, Thanaporn Wannachod, Prakorn Ramakul, Ura Pancharoen, and Soorathep Kheawhom. 2015. "Separation of mercury(II) from petroleum produced water via hollow fiber supported liquid membrane and mass transfer modeling." *Chemical Engineering Journal* no. 265:34-46. doi: 10.1016/j.cej.2014.12.034.
[77] Shafawi, Azman, Les Ebdon, Mike Foulkes, Peter Stockwell, and Warren Corns. 2000. "Preliminary evaluation of adsorbent-based mercury removal systems for gas condensate." *Analytica Chimica Acta* no. 415 (1-2):21-32. doi: 10.1016/S0003-2670(00)00838-2.
[78] Roussel, Michel, Philippe Courty, Jean-Paul Boitiaux, and Jean Cosyns. 1990. Process for elimination of mercury and possibly arsenic in hydrocarbons. IFP Energies Nouvelles
[79] Cameron, Charles, Philippe Courty, Jean-Paul Boitiaux, Philipe Varin, and Gerard Leger. 1993. Method of eliminating mercury or arsenic from a fluid in the presence of a mercury and/or arsenic recovery mass. IFP Energies Nouvelles.
[80] McNamara, James D. 1994. Product/process/application for removal of mercury from liquid hydrocarbon. Calgon Carbon Corporation
[81] Yan, Tsoung Y. 1996. "Mercury Removal from Oil by Reactive Adsorption." *Industrial & Engineering Chemistry Research* no. 35 (10):3697-3701. doi: 10.1021/ie950630n.
[82] Markovs, John, Richard T. Maurer, Andrew S. Zarchy, and Ervine S. Holmes. 1994. Removal of mercury from process streams. Honeywell UOP LLC
[83] Ochi, Jalel, Dominique Dexheimer, and Vincent Corpel. 2013. Produced Water Re-Injection Design and Uncertainties Assessment In *SPE European Formation Damage Conference & Exhibition*. Noordwijk, The Netherlands.
[84] Balyatinskaya, L N. 1979. "The Solvation of Mercury Ions and the Formation of Their Complexes in Water and Non-aqueous Solvents." *Russian Chemical Reviews* no. 48 (4):418-429.
[85] Coulibaly, Mariame, Drissa Bamba, N'Guessan Alfred Yao, Elogne Guessan Zoro, and Mama El Rhazi. 2016. "Some aspects of speciation and reactivity of mercury in various matrices." *Comptes Rendus Chimie* no. 19:832-840. doi: 10.1016/j.crci.2016.02.005.

[86] Turner, D.R, M Whitfield, and A. G Dickson. 1981. "The equilibrium speciation of dissolved components in freshwater and sea water at 25°C and 1 atm pressure." *Geochimica et Cosmochimica Acta* no. 45 (6):855-881. doi: doi.org/10.1016/0016-7037(81)90115-0.

[87] Omwoma, Solomon, Silah C. Lagat, Joseph O. Lalah, Philip O. Owuor, and Karl-Werner Schramm. 2017. "Recent Advances on Mercury Speciation in Aquatic Ecosystems, Health Effects and Analytical Techniques." *British Journal of Applied Science & Technology* no. 19 (1):1-37. doi: 10.9734/BJAST/2017/31635

[88] Ravichandran, Mahalingam. 2004. "Interactions between mercury and dissolved organic matter—a review." *Chemosphere* no. 55 (3):319-331. doi: 10.1016/j.chemosphere.2003.11.011.

[89] Morel, Francois M. M., Anne M. L. Kraepiel, and Marc Amyot. 1998. "The Chemical Cycle and Bioaccumulation of Mercury." *Annual Review Ecology and Systematics* no. 29:543-566.

[90] Sillen, Lars Gunnar, and Arthur E. Martell. 1971. *Stability constants of metal-ion complexes [with] supplement no.1* 2nd edition, Special publication no. 25 ed. London Chemical Society.

[91] Ciavatta, Liberato, and Maria Grimaldi. 1968. "Equililbrium Constants of Mercury (II) Chloride Complexes." *Journal of Inorganic Nuclear Chemistry* no. 30:197-205.

[92] Bebout, Deborah C. 2006. "Mercury: Inorganic & Coordination Chemistry." *Encyclopedia of Inorganic Chemistry*. doi: 10.1002/0470862106.ia131.

[93] Rogers, Robin D., Andrew H. Bond, and Janice L. Wolff. 2006. "Structural Studies of Polyether Coordination to Mercury (II) Halides: Crown Ether Versus Polyethylene Glycol Complexation " *Journal of Coordination Chemistry* no. 29 (4):187-207. doi: 10.1080/00958979308037425.

[94] Jacobson, C. A. 1951. *Encyclopedia of chemical reactions*. Vol. Volume 4. New York, USA: Reinhold Publishing Corp. .

[95] Sandström, Magnus, and Georg Johansson. 1977. "An X-Ray Diffraction Study of Iodide and Bromide Complexes of Mercury(II) in Aqueous Solution." *Acta Chemica Scandinavica* no. 31a:132-140. doi: 10.3891/acta.chem.scand.31a-0132.

[96] Powell, Kipton J., Paul L. Brown, Robert H. Byrne, Tamas Gajda, Glenn Hefter, Staffan Sjoberg, and Hans Wanner. 2005. "Chemical Speciation of Environmentally Significant Heavy Metals with Inorganic Ligands Part1: The Hg2+-Cl-, OH-, CO32-, SO42- and PO43- Aqueous Systems " *Pure Appl. Chem* no. 77 (4):739-800. doi: 10.1351/pac200577040739.

[97] Sillén, Lars Gunnar. 1949. "Electrometic Investigation of Equilibria between Mercury and Halogen Ions. VIII. Survey and Conclusions." *Acta Chemica Scandinavica* no. 3:554-559. doi: 10.3891/acta.chem.scand.03-0554.

[98] Ralston, A. W., and J. A. Wilkinson. 1928. "Reactions in liquid hydrogen sulfide. III Thiohydrolysis of chlorides[1]." *Journal of the American Chemical Society* no. 50 (2):258-264. doi: 10.1021/ja01389a002.

[99] Joosten, Michael W., Juri Kolts, Justin W. Hembree, and Mohsen Achour. 2002. Organic Acid Corrosion In Oil And Gas Production. Paper read at CORROSION 2002, 7-11 April 2002, at Denver, Colorado.

[100] Okafor, P. C., and S. Nesic. 2007. "Effect of Acetic Acid on CO2 Corrosion of Carbon Steel in Vapor-Water Two-Phase Horizontal Flow." *Chemical*

Engineering Communications no. 194:141-157. doi: 10.1080/00986440600642975.
[101] Lobana, Tarlok S. 2006. Organometallics. In *Inorganic Chemistry*. Amritsar 143005 Guru Nanak Dev University
[102] McCutchan, Roy T., and Kenneth A. Kobe. 1954. "Diphenylmercury Synthesis." *Industrial & Engineering Chemistry* no. 46 (4):675-680. doi: 10.1021/ie50532a027.
[103] Bamford, C.H., and C.F.H. Tipper. 1972. *Reactions of Aromatic Compounds*. Vol. 13, *Comprehensive Chemical Kinetics*.
[104] Seidell, Atherton, and William F. Linke. 1940. "Solubilities of inorganic and metal organic compounds: a compilation of quantitative solubility data from the periodical literature." In, ed D. Van Nostrand Co. New York: The American Chemical Society.
[105] Corwin, Alsoph H., and Marcus A. Naylor Jr. 1947. "Aromatic Substitution. The Cleavage of Diphenylmercury." *Journal of the American Chemical Society* no. 69 (5):1004-1009. doi: 10.1021/ja01197a008.
[106] Rausch, Marvin D., and John R. Van Wazer. 1964. "Exchange Reactions and Nuclear Magnetic Resonance Analysis of Some Organomercury Compounds." *Inorganic Chemistry* no. 3 (5):761-766. doi: 10.1021/ic50015a034.
[107] Hylander, Lars D., and Roger B. Herbert. 2008. "Global Emission and Production of Mercury during the Pyrometallurgical Extraction of Nonferrous Sulfide Ores." *Environmental Science & Technology* no. 42 (16):5971-5977. doi: 10.1021/es800495g.
[108] Zhao, Lynn L., and Gary T. Rochelle. 1998. "Mercury Absorption in Aqueous Oxidants Catalyzed by Mercury(II)." *Industrial & Engineering Chemistry Research* no. 37 (2):381-387. doi: 10.1021/ie970155o.
[109] Pollard, D. R., and J. V. Westwood. 1965. "Kinetic Studies of Exchange between Metallic Mercury and Mercury Compounds in Solution. I." *Journal of the American Chemical Society* no. 87 (13):2809-2815. doi: 10.1021/ja01091a006.
[110] Driscoll, Charles T., Robert P. Mason, Hing Man Chan, Daniel J. Jacob, and Nicola Pirrone. 2013. "Mercury as a Global Pollutant: Sources, Pathways, and Effects." *Environmental Science & Technology* no. 47 (10):4967-4983. doi: 10.1021/es305071v.
[111] Clarkson, Thomas W., and Laszlo Magos. 2006. "The Toxicology of Mercury and Its Chemical Compounds." *Critical Reviews in Toxicology* no. 36 (8):609-662. doi: 10.1080/10408440600845619.
[112] Benoit, J. M., C. C. Gilmour, A. Heyes, R. P. Mason, and C. L. Miller. 2002. Geochemical and Biological Controls over Methylmercury Production and Degradation in Aquatic Ecosystems. In *Biogeochemistry of Environmentally Important Trace Elements*.
[113] Zhu, Wei, Che-Jen Lin, Xun Wang, Jonas Sommar, Xuewu Fu, and Xinbin Feng. 2016. "Global observations and modeling of atmosphere–surface exchange of elemental mercury: a critical review." *Atmospheric Chemistry and Physics* no. 16:4451-4480. doi: 10.5194/acp-16-4451-2016.
[114] (ECHA), European Chemicals Agency. 2011. Background document to the Opinions on the Annex XV dossier proposing restrictions on five Phenylmercury compounds. https://echa.europa.eu/documents/10162/4a71bea0-31f0-406d-8a85-59e4bf2409da.

[115] Onat, E. 1974. "Solubility studies of metallic mercury in pure water at various temperatures." *Journal of Inorganic Nuclear Chemistry* no. 36 (1974):2029-2032.

[116] Mroczek, E. K. 1994. The Solubility of Elemental Mercury in Water Between 30 and 210°C. Paper read at 19th Workshop on Geothermal Reservoir Engineering, 18-20 January 1994, at Stanford, California.

[117] Hagelberg, Erik. n. d. . The Matrix Dependent Solubility and Speciation of Mercury.

[118] Zhao, Lingbing. 1997. *Mercury Absorption in Aqueous Solutions* The University of Texas, Austin.

[119] Chang, John C. S., and S. Behrooz Ghorishi. 2003. "Simulation and Evaluation of Elemental Mercury Concentration Increase in Flue Gas Across a Wet Scrubber." *Environmental Science & Technology* no. 37 (24):5763-5766. doi: 10.1021/es034352s.

[120] Alekhin, Y. V., N. R. Zagrtdenov, R. V. Mukhamadiyarova, and A. S. Smirnova. 2011. "Experimental study of metallic mercury solubility in water." *Vestnik Otdelenia nauk o Zemle RAN* no. 3 (NZ6006). doi: 10.2205/2011NZ000136.

[121] Roy, Sharmistha, and Gary T. Rochelle. 2004. "Simultaneous absorption of mercury and chlorine in sulfite solutions." *Chemical Engineering Science* no. 59 (6):1309-1323. doi: 10.1016/j.ces.2003.10.021.

[122] Bandyopadhyay, S., S. Chakraborty, D. B. Zaini, and S. Bhattacharjee. 2016. "Kinetic Studies on Oxidative Dissolution of Elemental Mercury in Aqueous Sodium Hypochlorite." *International Journal of Environmental Science and Development* no. 7 (7):516-519. doi: 10.18178/ijesd.2016.7.7.831.

[123] IPIECA. 2014. Mercury management in petroleum refining. *An IPIECA Good Practice Guide*.

[124] Sloot, H. A. van der, C. Blomberg, and H. A. Das. 1974. "Solubility and adsorption of some organo-mercury compounds " *Reactor Centrum Nederland*.

[125] Sommar, Jonas, Oliver Lindqvist, and Dan Strömberg. 2000. "Distribution Equilibrium of Mercury (II) Chloride between Water and Air Applied to Flue Gas Scrubbing." *Journal of the Air & Waste Management Association* no. 50 (9):1663-1666. doi: 10.1080/10473289.2000.10464192.

[126] Bernard, L., K. Awitor, J. Badaud, O. Bonnin, B. Coupat, J. Fournier, and P. Verdier. 1997. "D´etermination de la pression de vapeur de HgCl2 par la m´ethode d'effusion de Knudsen." *Journal de Physique III* no. 7 (2):311-319. doi: 10.1051/jp3:1997124.

[127] Lancia, A., D. Musmarra, F. Pepe, and G. Volpicelli. 1993. "Adsorption of Mercuric Chloride Vapours from Incinerator Flue Gases on Calcium Hydroxide Particles." *Combustion Science and Technology* no. 93 (1):277-289. doi: 10.1080/00102209308935293.

[128] Wilcox, Jennifer, Joe Robles, David C. J. Marsden, and Paul Blowers. 2003. "Theoretically Predicted Rate Constants for Mercury Oxidation by Hydrogen Chloride in Coal Combustion Flue Gases." In *Environmental Science & Technology*.

[129] Lee, Tai-Gyu. 1999. *Study of Mercury Kinetics and Control Methodologies in Simulated Combustion Flue Gases*, Department of Civil and Environmental Engineering University of Cincinnati.

[130] Feldman, Cyrus. 1974. "Preservation of Dilute Mercury Solutions." *Analytical Chemistry* no. 46 (1):99-102.
[131] Parker, Jennifer L., and Nicolas S. Bloom. 2005. "Preservation and storage techniques for low-level aqueous mercury speciation." *Science of the Total Environment* no. 337:253-263.
[132] Bothner, Micheal H., and D. E. Robertson. 1975. "Mercury contamination of sea water samples stored in polyethylene containers." *Analytical Chemistry* no. 47 (3):592-595. doi: 10.1021/ac60353a012.
[133] Yu, Li-Ping, and Xiu-Ping Yan. 2003. "Factors affecting the stability of inorganic and methylmercury during sample storage." *Trends in Analytical Chemistry* no. 22 (4):245-253. doi: 10.1016/S0165-9936(03)00407-2.
[134] Rosain, R. M., and C. M. Wai. 1973. "The rate of loss of mercury from aqueous solution when stored in various containers." *Analytica Chimica Acta* no. 65 (2):279-284. doi: 10.1016/S0003-2670(01)82493-4.
[135] Krivan, V., and H. F. Haas. 1988. "Prevention of loss of mercury(II) during storage of dilute solutions in various containers." *Fresenius' Zeitschrift für analytische Chemie* no. 322 (1):1-6. doi: 10.1007/BF00487020.
[136] Leermakers, M., P. Lansens, and W. Baeyens. 1991. "Storage and stability of inorganic and methylmercury solutions." *Fresenius' Journal of Analytical Chemistry* no. 336 (8):655-662. doi: 10.1007/BF00331410.
[137] Bloom, N. S. 2000. "Analysis and stability of mercury speciation in petroleum hydrocarbons." *Fresenius J Anal Chem* no. 366:438-443.
[138] Snell, James, Jin Qian, Magnus Johansson, Kees Smit, and Woflgang Frech. 1998. "Stability and reactions of mercury species in organic solution." *Analyst* no. 123.
[139] Harvey, Sarah Elyse. 2015. *Stability of Monomethymercury in Water* Department of Earth and Environmental Sciences, Wright State University
[140] Sommer, Yuliya L., Cynthia D. Ward, Yi Pan, Kathleen L. Caldwell, and Robert L. Jones. 2016. "Long-Term Stability of Inorganic, Methyl and Ethyl Mercury in Whole Blood: Effects of Storage Temperature and Time." *Journal of Analytical Toxicology* no. 40 (3):222-228. doi: 10.1093/jat/bkw007.
[141] Rich, Ronald. 2007. Inorganic Reactions in Water. Springer-Verlag Berlin Heidelberg.
[142] Sabri, Y.M., S.J. Ippolito, J. Tardio, P.D. Morrison, and S.K. Bhargava. 2015. "Studying mercury partition in monoethylene glycol (MEG) used in gas facilities." *Fuel* no. 159:917-924. doi: 10.1016/j.fuel.2015.07.047.
[143] Parikh, Yogesh, Samantha Mahmoud, James Lallo, and Huifang Lang. 2015. "Sample Preparation Method for Mercury Analysis in Reagent Chemicals by ICP-OES." *Spectroscopy* no. 30 (s11):8-17.
[144] Lo, J. M., and C. M. Wai. 1975. "Mercury Loss from Water during Storage: Mechanisms and Prevention." *Analytical Chemistry* no. 47 (11):1869-1870. doi: 10.1021/ac60361a003.
[145] Tsui, Martin Tsz Ki, Joel D. Blum, Jacques C. Finlay, Steven J. Balogh, Sae Yun Kwon, and Yabing H. Nollet. 2013. "Photodegradation of methylmercury in stream ecosystems." *Limnology and Oceanography* no. 58 (1):13-22. doi: 10.4319/lo.2013.58.1.0013.
[146] Lansens, Patrick, Carine Meuleman, and Willy Baeyens. 1990. "Long-term stability of methylmercury standard solutions in distilled, deionized water." *Analytica Chimica Acta* no. 229:281-285. doi: 10.1016/S0003-2670(00)85140-5.

[147] Nelson, Gary O. 1971. *Controlled Test Atmospheres - Principles and Techniques* United States of America Ann Arbor Science Publishers, Inc. .

[148] Larjava, Kari T., T. Laitinen, T. Vahlman, S. Artmann, V. Siemens, J. A. C. Broekaert, and D. Klockow. 1992. "Measurement and control of mercury species in flue gases from liquid waste incineration." *International Journal of Environment Analytical Chemistry* no. 149 (1-2):73-85. doi: 10.1080/03067319208028128.

[149] Karatza, D., A. Lancia, D. Musmarra, F. Pepe, and G. Volpicelli. 1996. "Kinetics of Adsorption of Mercuric Chloride Vapors on Sulfur Impregnated Activated Carbon." *Combustion Science and Technology* no. 112 (1):163-174. doi: 10.1080/00102209608951954.

[150] Lin, Hsun-Yu, Chung-Shin Yuan, Chun-Hsin Wu, and Chung-Hsuang Hung. 2012. "The Adsorptive Capacity of Vapor-Phase Mercury Chloride onto Powdered Activated Carbon Derived from Waste Tires." *Journal of the Air & Waste Management Association* no. 56 (11):1558-1566. doi: 10.1080/10473289.2006.10464562.

[151] Phillips, G. F., B. E. Dixon, and R. G. Lidzey. 1959. "The volatility of organo-mercury compounds." *Journal of the Science of Food and Agriculture* no. 10 (11):604-610. doi: 10.1002/jsfa.2740101105.

[152] Scheide, E. P., R. Alvarez, B. Greifer, E. E. Hughes, and J. K. Taylor. 1973. A mercury vapor generation and dilution system. Nationall Bureau of Standards, Department of Commerce

[153] Quino, E. A. 1962. "Determination of dibutyl mercury vapors in air." *American Industrial Hygiene Association Journal* no. 23 (3):231-234. doi: 10.1080/00028896209342859.

[154] Iverfeldt, Åke, and Oliver Lindqvist. 1982. "Distribution equilibrium of methyl mercury chloride between water and air." *Atmospheric Environment* no. 16 (12):2917-2925. doi: 10.1016/0004-6981(82)90042-7.

[155] Hugo Ent, Inge van Andel, Maurice Heemskerk, Peter van Otterloo, Wijnand Bavius, Annarita Baldan, Milena Horvat, Richard J C Brown, and Christophe R Quétel. 2014. "A gravimetric approach to providing SI traceability for concentration measurement results of mercury vapor at ambient air levels." *Measurement Science and technology* no. 25 (11). doi: 10.1088/0957-0233/25/11/115801.

[156] Xiao, Z., J. Sommar, S. Wei, and O. Lindqvist. 1997. "Sampling and determination of gas phase divalent mercury in the air using a KCl coated denuder." *Fresenius Journal of Analytical Chemistry* no. 358 (3):386-391. doi: 10.1007/s002160050434.

[157] Larjava, K., T. Laitinen, T. Kiviranta, V. Siemens, and D. Klockow. 1993. "Application Of The Diffusion Screen Technique To The Determination Of Gaseous Mercury And Mercury (II) Chloride In Flue Gases." *International Journal of Environmental Analytical Chemistry* no. 52 (1-4):65-73. doi: 10.1080/03067319308042849.

[158] Feng, Xinbin, Julia Y. Lu, Yingjie Hao, Cathy Banic, and William H. Schroeder. 2003. "Evaluation and applications of a gaseous mercuric chloride source." *Analytical and Bioanalytical Chemistry* no. 376:1137-1140. doi: 10.1007/s00216-003-2034-7.

[159] Wang, J., Z. Xiao, and O. Lindqvist. 1995. "On-line measurement of mercury in simulated flue gas " *Water, Air and Soil Pollution* no. 80:1217-1226.

[160] Mibeck, Blaise A.F., Edwin S. Olson, and Stanley J. Miller. 2009. "$HgCl_2$ sorption on lignite activated carbon: Analysis of fixed-bed results." *Fuel Processing Technology* no. 90 (11):1364-1371. doi: 10.1016/j.fuproc.2009.08.004.

[161] Norton, Glenn A., David E. Eckels, and Colin D. Chriswell. 2001. Development of Mercury and Hydrogen Chloride Emission Monitors for Coal Gasifiers. United States Ames Laboratory

[162] Ye, Qun-feng, Cheng-yun Wang, Da-hui Wang, Guan Sun, and Xin-hua Xu. 2006. "Hg0 absorption in potassium persulfate solution." *Journal of Zhejiang University Science B* no. 7 (5):404-410. doi: 10.1631/jzus.2006.B0404.

[163] Larsson, Tom. 2007. *Instrumental and methodological developments for isotope dilution analysis of gaseous mercury species* Department of Chemistry, Umeå University, Canada.

[164] Clevenger, W. L., B. W. Smith, and J. D. Winefordner. 1997. "Trace Determination of Mercury : A Review." *Critical Reviews in Analytical Chemistry* no. 27 (1):1-26.

[165] Slavin, Morris. 1978. *Atomic Absorption Spectroscopy*. 2 ed. New York, USA: John Wiley & Sons.

[166] Chang, Michael J., Reta L. McDaniel, John D. Naworal, and David A. Self. 2002. "A rapid method for the determination of mercury in mainstream cigarette smoke by two-stage amalgamation cold vapor atomic absorption spectrometry " *Journal of Analytical Atomic Spectrometry* no. 17:710-715.

[167] Welz, Bernhard, and Marianne Schubert-Jacobs. 1988. "Cold vapor atomic absorption spectrometric determination of mercury using sodium tetrahydroborate reduction and collection on gold." *Fresenius' Zeitschrift für analytische Chemie* no. 331 (3-4):324-329.

[168] KOPYSC, Edyta, Krystyna PYRZYNSKA, Slawomir GARBOS, and Ewa BULSKA. 2000. "Determination of Mercury by Cold-Vapor Atomic Absorption Spectrometry with Preconcentration on a Gold-Trap." *Analytical Sciences* no. 16:1309-1312. doi: 10.2116/analsci.16.1309.

[169] Frech, Wolfgang, Douglas C. Baxter, Geir Dyvik, and Bjorn Dybdahl. 1995. "On the determination of total mercury in natural gases using the amalgamation technique and cold vapour atomic absorption spectrometry " *Journal of Analytical Atomic Spectrometry* no. 10.

[170] Snell, James P., Wolfgang Frech, and Yngvar Thomassen. 1996. "Performance improvements in the determination of mercury species in natural gas condensate using an on-line amalgamation trap for solid-phase micro-extraction with capillary gas chromatography-microwave-induced plasma atomic emission spectrometry." *Analyst* no. 121 (August 1996):1055-1060.

[171] Wang, Chao, and Chenxu Yu. 2012. "Detection of chemical pollutants in water using gold nanoparticles as sensors: a review." *Reviews in Analytical Chemistry* no. 32 (1):1-14. doi: 10.1515/revac-2012-0023.

[172] Feng, Xinbin, Jonas Sommar, Katarina Gardfeldt, and Oliver Lindqvist. 2000. "Improved determination of gaseous divalent mercury in ambient air using KCl coated denuders " *Fresenius J Anal Chem* no. 366:423-428.

[173] Keeler, Gerald J., and Matthew S. Landis. 1994. Standard Operating Procedure for Analysis of Vapor Phase Mercury. University of Michigan.

[174] Hara, Noboru. 1975. "Capture of mercury vapor in air with potassium permanganate solution." *Industrial Health* no. 13:243-251.

[175] Metzger, M., and H. Braun. 1987. "In-situ mercury speciation in flue gas by liquid and solid sorption systems " *Chemosphere* no. 16 (4):821-832.
[176] Suvarapu, Lakshmi Narayana, and Sung-Ok Baek. 2015. "Recent Developments in the Speciation and Determination of Mercury Using Various Analytical Techniques." *Journal of Analytical Methods in Chemistry* no. 2015:Article ID 372459, 18 pages. doi: 10.1155/2015/372459.
[177] EPA, U.S. 1974. Method 245.2: Mercury (Automated Cold Vapor Technique) by Atomic Absorption edited by United States Environmental Protection Agency.
[178] Shafawi, Azman Bin. 1999. *Mercury Species in Natural Gas Condensate*, Department of Environmental Sciences, University of Plymouth.
[179] Yamamoto, Yuroku, Takahiro Kumamaru, and Atsuo Shiraki. 1978. "Comparative Study of Sodium Borohydride Tablet and Tin(II) Chloride Reducing Systems in the Determination of Mercury by Atomic-Absoprtion Spectrophotometry." *Fresenius' Zeitschrift für analytische Chemie* no. 292 (4):273-277.
[180] Toffaletti, John, and John Savory. 1975. "Use of sodium borohydride for determination of total mercury in urine by atomic absorption spectrometry." *Fresenius' Zeitschrift für analytische Chemie* no. 47 (13):2091-2095. doi: 10.1021/ac60363a001.
[181] Rooney, R. C. 1976. "Use of Sodium Borohydride for Cold-Vapour Atomic Absorption Determination of Trace Amounts of Inorganic Mercury." *Analyst* no. 101:679-682. doi: 10.1039/AN9760100678.
[182] Murphy, James, Phil Jones, and Steve J. Hill. 1996. "Determination of total mercury in environmental and biological samples by flow injection cold vapour atomic absorption spectrometry." *Spectrochimica Acta Part B: Atomic Spectroscopy* no. 51 (14):1867-1873. doi: 10.1016/S0584-8547(96)01571-6.
[183] Saraswati, Rajananda, Charles M. Beck, and Michael S. Epstein. 1993. "Determination of mercury in zinc ore concentrate reference materials using flow injection and cold-vapor atomic absorption spectrometry." *Talanta* no. 40 (10):1477-1480. doi: 10.1016/0039-9140(93)80356-V.
[184] Hanna, Christopher P., Julian F. Tyson, and Susan McIntosh. 1993. "Determination of total mercury in waters and urine by flow injection atomic absorption spectrometry procedures involving on- and off-line oxidation of organomercury species." *Analytical Chemistry* no. 65 (5):653-656. doi: 10.1021/ac00053a029.
[185] Bazilio, Arianne, and Jacob Weinrich. 2012. Inductively Coupled Plasma - Mass Spectrometry (ICP-MS) College of Engineering, University of Massachusetts Amherst.
[186] Skoog, Douglas A., F. James Holler, and Stanley R. Crouch. 2007. *Principles of Instrumental Analysis*. 6th Edition ed: Thomson Brooks/Cole.
[187] Nevado, J.J. Berzas, R.C. Rodríguez Martín-Doimeadios, E.M. Krupp, F.J. Guzmán Bernardo, N. Rodríguez Fariñas, M. Jiménez Moreno, D. Wallace, and M.J. Patiño Ropero. 2011. "Comparison of gas chromatographic hyphenated techniques for mercury speciation analysis." *Journal of Chromatography A* no. 1218 (28):4545-4551. doi: 10.1016/j.chroma.2011.05.036.
[188] Koplík, Richard, Iva Klimešová, Kateřina Mališová, and Oto Mestek. 2014. "Determination of Mercury Species in Foodstuffs using LC-ICP-MS: the

Applicability and Limitations of the Method." *Czech Journal of Food Sciences* no. 32 (3):249-259.

[189] Vidler, Daniel S., Richard O. Jenkins, John F. Hall, and Chris F. Harrington. 2006. "The determination of methylmercury in biological samples by HPLC coupled to ICP‐MS detection." *Speciation Analysis and Environment* no. 21 (5):303-310. doi: 10.1002/aoc.1173

[190] Moreno, F., T. García-Barrera, and J. L. Gómez-Ariza. 2013. "Simultaneous speciation and preconcentration of ultra trace concentrations of mercury and selenium species in environmental and biological samples by hollow fiber liquid phase microextraction prior to high performance liquid chromatography coupled to inductively coupled plasma mass spectrometry." *Journal of Chromatography A* no. 1300:43-50. doi: 10.1016/j.chroma.2013.02.083.

[191] Pyhtilä, Heidi, Matti Niemelä, Paavo Perämäki, Juha Piispanen, and Liisa Ukonmaanaho. 2013. "The use of a dual mode sample introduction system for internal standardization in the determination of Hg at the ng L−1 level by cold vapor ICP-MS." *Analytical Methods* no. 5:3082-3088. doi: 10.1039/c3ay40275d.

[192] Jian, L., W. Goessler, and K. J. Irgolic. 2000. "Mercury determination with ICP-MS: signal suppression by acids." *Fresenius' Journal of Analytical Chemistry* no. 366 (1):48-53. doi: 10.1007/s002160050010.

[193] Whitman, Walter G. 1962. "A Preliminary Experimental Confirmation of The Two-Film Theory of Gas Absorption." *Journal of Heat Mass Transfer* no. 5:429-433.

[194] Elk, Edwin Pieter van. 2001. *Gas-Liquid reactions - Influence of bulk and mass transfer on process performance*, Twente University, Enschede.

[195] Elk, E. P. van, P.C. Borman, J. A. M. Kuipers, and G. F. Versteeg. 2000. "Modelling of gas–liquid reactors — implementation of the penetration model in dynamic modelling of gas–liquid processes with the presence of a liquid bulk." *Chemical Engineering Journal* no. 76:223-237.

[196] Danckwerts, P. V., and A. M. Kennedy. 1954. "Kinetics of Liquid-Film Process in Gas Absorption. Part I: Models of the Absorption Process." *Trans IChemE* no. 75:S101-S104.

[197] Froment, Gilbert F., and Kenneth B. Bischoff. 1990. *Chemical reactor analysis and design*: New York : Wiley

[198] Whitman, Walter G. 1923. "The two-film theory of gas absorption." *International Journal of Heat and Mass Transfer* no. 5 (5):429-433. doi: 10.1016/0017-9310(62)90032-7.

[199] Sander, R. 2015. "Compilation of Henry's law constants (version 4.0) for water as solvent." *Atmospheric Chemistry and Physics* no. 15:4399-4981. doi: 10.5194/acp-15-4399-2015.

[200] Whitman, Walter G., and D. S. Davis. 1924. "Comparative Absorption Rates for Various Gases." *Industrial & Engineering Chemistry* no. 16 (12):1233-1237. doi: 10.1021/ie50180a008.

[201] Liss, P. S., and P. G. Slater. 1974. "Flux of Gases across the Air-Sea Interface." *Nature* no. 247:181-184. doi: 10.1038/247181a0.

[202] Okouchi, Shoichi, and Sokichi Sasaki. 1984. "Volatility of mercury in water " *Journal of Hazardous Materials* no. 8 (4):341-348. doi: 10.1016/0304-3894(84)87030-2.

[203] Schroeder, William, Oliver Lindqvist, John Munthe, and Zifan Xiao. 1992. "Volatilization of mercury from lake surfaces." *The Science of the Total Environment* no. 125 (7):47-66. doi: 10.1016/0048-9697(92)90382-3.

[204] Singhasuk, Pattaraporn. 2012. *Development of surface exchange models for estimating mercury evasion and deposition* The Faculty of the College of Graduate Studies, Lamar University.

[205] Kuss, Joachim, Siegfried Krüger, Johann Ruickoldt, and Klaus-Peter Wlost. 2018. "High-resolution measurements of elemental mercury in surface water for an improved quantitative understanding of the Baltic Sea as a source of atmospheric mercury." *Atmospheric Chemistry and Physics* no. 18 (4361-4376). doi: 10.5194/acp-18-4361-2018.

[206] Fantozzi, L., G. Manca, and F. Sprovieri. 2013. A comparison of recent methods for modelling mercury fluxes at the airwater interface. Paper read at 16th International Conference on Heavy Metals in the Environment, 23 April 2013.

[207] Gustin, M. S., H. M. Amos, J. Huang, M. B. Miller, and K. Heidecorn. 2015. "Measuring and modeling mercury in the atmosphere: a critical review." *Atmospheric Chemistry and Physics* no. 15:5697-5713. doi: 10.5194/acp-15-5697-2015.

CHAPTER 3:
RESEARCH METHODOLOGY AND ANALYTICAL TECHNIQUES

3.1 Introduction

This chapter provides the overall research methodology employed to meet the thesis objectives in Chapter 1. The experimental and analytical procedures are discussed in detail in the succeeding sections.

3.2 Gaseous Mercury Feed Source

There is no certified commercial mercury test gas cylinder available in the market, therefore the test gas needs to be freshly generated for all test in this study of the solubility kinetics of mercury gas in water. Two gas generations methods have been tested to generate mercury gas for different applications, namely vaporization from liquid and solid phase. The two methods were tested to determine their suitability for solubility kinetics study and the results are presented.

3.2.1 Liquid Vaporization Method

Generation of mercury gas from liquid vaporization is based on the principle of Henry's law. Henry's law states that at a certain temperature, a body of liquid has a direct proportion with the partial pressure of the overhead gas at equilibrium condition (Eqn 1).

$$P_{Hg} = H\, C_{Hg} \qquad (1)$$

Consequently, for a given mercury concentration in liquid, the gas vaporized from the solution should be able to be calculated from the known He coefficient available [1]. Moreover, this concept would provide an advantage of ease of variating the generated mercury gas concentration by simply adjusting the concentration of the solution itself. To test this concept, a bubbling set-up was prepared and can be seen in Fig. 3.1.

As seen in Fig. 3.1, three bubbling bottles were each filled with 10 ppm $HgCl_2$ solutions. N_2 gas was introduced to the bubbling set-up (via the inlet of bubbling bottle 1) and solutions are subjected to bubbling for 24 hours. Vaporization was conducted

by bubbling through a series of solutions to maintain gas/liquid equilibrium, ensuring a controlled P_{HgCl2} leaving the bubbling set-up at all times. $HgCl_2$ was selected for this test due to its high solubility in water, thus should generate a fairly high partial pressure.

The bubbling set-up were not connected to the reactor and constant flow of N_2 (500 ml/min) were supplied to the bubbling set-up (sinter porosity grade 3), supplying fresh carrier gas at all time. The test was carried out at room temperature; ~298 K. Throughout the purging period, several aliquots (5 ml) from each bottle were taken and analysed for their mercury content to map out mercury distribution as well as stability of the mercury solution.

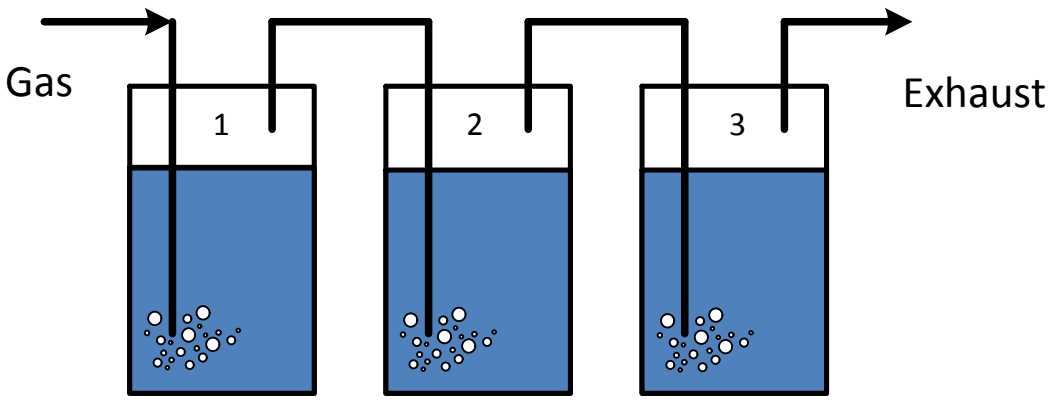

Fig. 3.1 Liquid Vaporization Test Set-Up

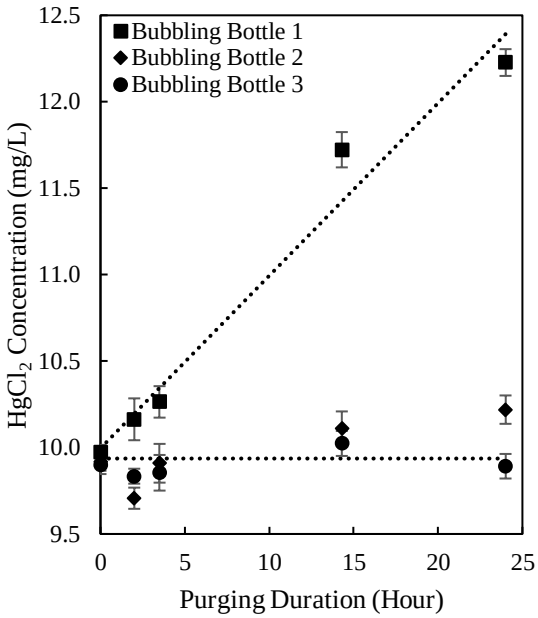

Fig. 3.2 $HgCl_2$ Concentration in Solutions after Being Subjected to Bubbling

Fig. 3.2 shows the $HgCl_2$ concentration profile of the bubbling solutions when subjected to bubbling. As seen in Fig. 3.2, the $HgCl_2$ concentration in bubbling bottle

1 increases up to 22% while the concentration in bubbling bottle 2 and 3 remain constant. It was to be noted that the level of liquid inside bubbling bottle 1 was relatively lower than the liquid level in bubbling bottle 2 and 3 at the end of the test. Vapour pressure of water is much higher than $HgCl_2$, thus water has the tendency to vaporise quickly. Therefore, volume of bubbling solution 1 was reduced as the water phase was carried out by the dry N_2 inlet gas. On the other hand, $HgCl_2$ is very water soluble (73 g/L at 298 K), thus it has the tendency to stay in the solution (Henry coefficient = 1.4×10^4 mol/m^3.Pa at 298 K). Hence, the concentration of the bubbling solution 1 increases as the total volume of the solution decreases. Error bars were calculated after 3 independent tests. Higher variations were observed in the samples obtained from bubbling bottle 1. Higher error is suspected to be contributed from the loss of liquids observed.

The liquid volume at bubbling solution 2 and 3 remained constant as the gas phase at the outlet of bubbling solution 1 is saturated with water. Hence, the water in bubbling solution 2 and 3 cannot vaporize. Result from Fig. 3.2 show that $HgCl_2$ concentration also remained constant for the period of bubbling. The constant $HgCl_2$ concentration indicate that very little $HgCl_2$ was being carried over by the water saturated carrier gas.

Based on the results from this set-up, the gas phase generated from the bubble set-up will be saturated in water vapour with minimal concentration of mercury. The presence of water vapour will have a strong influence on the absorption process especially in the case of very soluble mercury compound; such as $HgCl_2$ as possible absorption along the gas line may occur. In terms of running a long-term absorption test, a lot of water will be carried over from the liquid vaporizer to the absorption reactor. Not only will this change the reaction volume, chances of water droplets forming along the gas line as well as on the reactor wall will increase. The system will then require very precise and uniform heating to avoid condensation from forming at cold spots. Therefore, it was inferred that mercury gas generation using liquid vaporization method was not suitable for solubility kinetics in this work. Another more suitable gas generation method needed to be explored and tested.

3.2.2 Solid Vaporization Method

Generation of mercury gas from solid vaporization is based on the physical property of a pure substance, namely its vapour phase. A pure solid substance of a given surface area will vaporize when its vaporization energy is reached. Vaporization energy in this case is related to temperature at which the substance transition from solid to gas phase. When an inert gas is passed over the solid surface, the vaporized molecules will be carried, resulting in production of test gases at a certain concentration. This method of gas generation using a constant flow of carrier gas is referred to as temperature-controlled dynamic generation.

Generation of constant source of mercury gas using such method has been successfully utilised to produce constant mercury gas concentration for different research objectives.

Larjava et al. [2] implemented this method in 1992 to generate $HgCl_2$ and Hg^0 gas to simulate mercury in flue gases from liquid waste incineration. This was achieved by placing pure $HgCl_2$ and Hg^0 in a temperature-controlled diffusion tube. The vaporized mercury gas then travelled through the capillary of the diffusion tube and will be swept away by a carrier gas; in this case N_2. Schematic of mercury gas generation using a diffusion tube used by Larjava et al. [2] can be seen in Fig. 3.3. The generated gas concentration could be varied by modifying the vaporization temperature, flow rate of carrier gas and dimensions (length and diameter) of the capillary of the diffusion tube. Since then, various authors [3-5] have utilised this set-up to generate mercury gases of different concentration with error reported ranging from 1-23%. Limitation of using a diffusion tube would be the generation of high mercury gas concentration. As the vaporized mercury needs to diffuse through the capillary of the diffusion tube, this limits the number of mercury molecules that can be carried by the carrier gas. The system needs to be operating at a fairly high temperature (>363 K) to achieve higher mercury content in the gas phase.

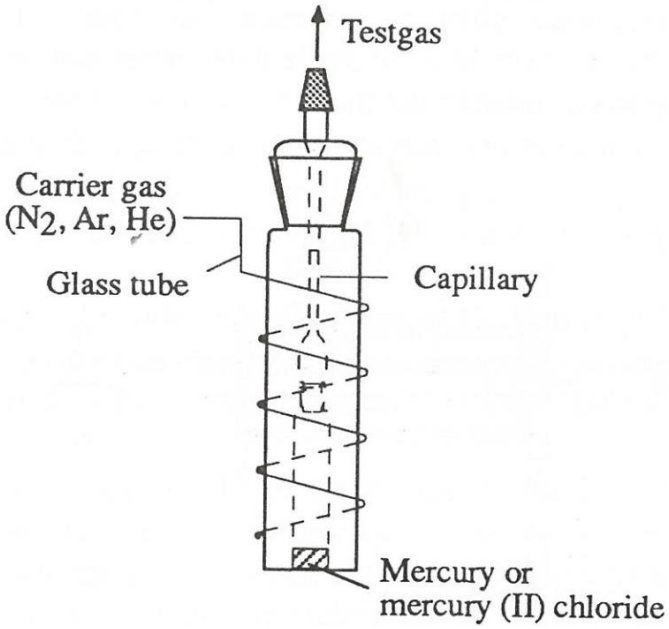

Fig. 3.3 Diffusion Tube for Mercury Gas Generation [2]

Another more common and recently commercialised mercury gas generation employs the use of a permeation tube. A pure substance (solid or liquid) at equilibrium with its gas phase was placed inside an inert material tube and sealed with either glass beads or PTFE plugs. At a certain temperature, the gas phase escapes the tube from the permeable portion of the device at a constant rate. The desired test gas could then be achieved by passing carrier gas over the tube to carry the escaped gas molecules. The permeation rate was relative to the tube length and has a logarithmic relationship with the reciprocal of temperature. A schematic of a permeation device using PTFE is shown in Fig. 3.4 [6]. Mercury gas concentration could be controlled by varying the length of the permeation tube, temperature of permeation and flow rate of carrier gas.

The use of mercury permeation tubes to generate mercury gas (mostly Hg^0 and $HgCl_2$) seemed to gain popularity over diffusion tubes since its commercialisation by VICI Metronics, USA [7-10]. Although commercialised and commonly used, there are several s limitations to using this method to generate Hg^0 and $HgCl_2$ test gas.

Firstly, there is an issue with stability. With generation of Hg^0 gas, Norton et al. [9] reported error of 25 – 50% with the gas generated despite being 'certified'. In terms of generation of $HgCl_2$ gas, the issue is more major. Norton et al. [9] observed that the mercury gas generated from the $HgCl_2$ permeation tube was contaminated with 15% of Hg^0. It was suspected that the conversion of $HgCl_2$ to Hg^0 occurred from prolonged storage of the tube. The issues with stability could be minimised by continued use of

the permeation tube. Having said that, the stabilization process of the permeation tube may require a number of days [9] which lead to wastage of carrier gas. Secondly, limitation to generate high mercury concentration is also applicable for this method, due to the indirect contact of carrier gas with the vaporized solid along with the permeation rate restricted by the material of choice.

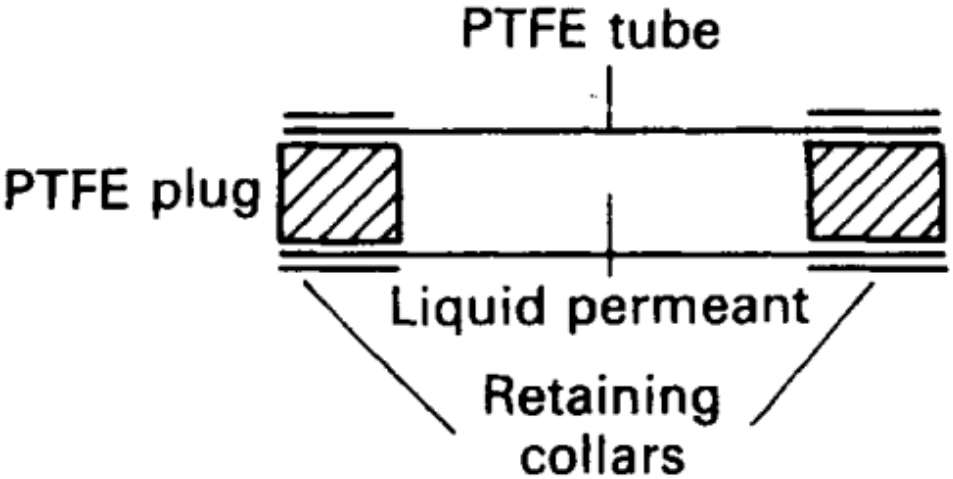

Fig. 3.4 Permeation Tube for Generating Test Gas [6]

A mercury gas vaporizer was devised in this work learning from the limitations of the other methods discussed earlier. In this work, a required mercury amount (Hg^0: 100% Univar, $HgCl_2$: ≥99.5% Sigma Aldrich and Ph_2Hg: 99% Alfa Aesar) was placed inside a glass/quartz vessel and left to vaporize at a controlled temperature. The configurations and placement of mercury inside the vaporizer slightly differs depending on the nature of the mercury species. A summary of the configuration of vaporizer used to generate various mercury gases in this work is included in Table 3.1.

Prior to the test, the vaporization vessel was placed in a temperature-controlled water bath at least 3 days to ensure no temperature gradient exists in the vaporizer. This is done in which the carrier gas (UHP N_2, 99.999% purchased from BOC) is sent to the bottom of the vaporizer and distributed by a fritted quartz disk. The introduction of carrier gas was selected to maximise the contact with vaporized solids. The flow rate of the carrier gas was set at 500 ml/min for all the test in this work and controlled by a mass flow controller (MFC) to ensure constant supply of mercury gas concentration throughout the test. The mercury contaminated gas then leaves the vaporizer at the top of the vessel.

Table 3.1 Configuration of Mercury Vaporization Vessel

Mercury Species	Vaporizer Vessel	Distribution of Mercury
Hg^0	125 ml cylindrical glass vessel (ID: 40mm, Height: 155mm) MF 29/3/125 Quickfit Drechsel bottle	Placed directly in the vessel
$HgCl_2$	125 ml cylindrical glass vessel (ID: 40mm, Height: 155mm) MF 29/3/125 Quickfit Drechsel bottle	Distributed in the middle of a quartz wool bed
Ph_2Hg	Quartz U-Tube (OD: 13.5mm, Height: 100mm)	Distributed in the middle of a quartz wool bed

Vaporizer configuration of Hg^0 and $HgCl_2$ involved their placement inside a 125 ml cylindrical glass vessel (ID: 40mm, Height: 155mm) MF 29/3/125 Quickfit Drechsel bottle. For $HgCl_2$, the solid phase was distributed in the middle of a quartz wool as a fixed bed to keep mercury solid surface area of vaporization constant. This distribution of $HgCl_2$ crystals was necessary as it has a lower vapour pressure compared to Hg^0. It is well known that Hg^0 is volatile at room temperature, hence even at lower surface area of contact, the system was able to generate relatively high concentration of Hg^0 gas. In terms of Ph_2Hg gas generation, a different configuration was utilised as Ph_2Hg has the lowest vapour pressure amongst the mercury species used in this work. Similar to the $HgCl_2$ vaporizer, Ph_2Hg solid particles were packed and distributed in between a quartz wool bed to increase surface area of vaporization. A U-tube configuration was selected for Ph_2Hg to maximise contact of the carrier gas with the solid particles. Furthermore, as the diameter of the U-tube is smaller compared to the glass vessel, a higher velocity of carrier gas would be achieved, increasing the concentration of Ph_2Hg gas leaving the vaporizer vessel.

Similar to the other gas generation methods mentioned earlier, the mercury concentration in the gas phase can be varied by modifying the vaporization temperature, flow rate of carrier gas, weight of mercury and dimensions of the vaporizer [2]. UHP N_2 is used instead of air to avoid possible oxidation reaction of mercury with O_2 [11]. The system devised for this work has an advantage whereby it is much easier to increase and re-distribute the mercury crystals in the vaporizer due to its accessibility. This advantage further increases the flexibility of the mercury vaporizer system to generate a higher variation of mercury gas concentration.

Prior to each experiment, the system was allowed to run with N_2 at a set flow rate for at least 2 hours. This was necessary as it is well known that issues stability of mercury concentration in the test gas may occur if the vaporization system was not treated properly [2, 9, 10]. For further assurance of the stability and quality control of the test gas, the gas phase before and after the test were analysed in triplicates by using different techniques. At the end of each test, the mercury mass balance was performed to ensure the measured data are correct and reliable. For all tests, the mercury balance was within an acceptable error range between 5 and 9%. The analysis results of the gas phase analysis are given in Table 3.6. The mercury in the gas phase analysis is described in detail in section 3.4 below.

The mercury vaporizer was able to produce higher mercury gas concentration in comparison with other set-ups discussed [2, 12] using diffusion cells and permeation tubes to generate test gas. This is because of the larger mercury bed used in this work, allowing higher surface area of vaporization to be achieved while minimising the vaporization temperature condition at 323 K. Furthermore, the carrier gas was in direct contact with solid, hence enabling to carry more of the vaporized solid out of the mercury vaporizer. This set up was also capable for generation of desired mercury gas concentration from $HgCl_2$ solid for the tests in this work although its vapour pressure is very low [13, 14]. The result of the mercury gas concentration generated using this vaporization method is detailed in the following sections.

3.2.2.1 Effect of Vaporization Temperature on Gas Concentration

Table 3.2 Effect of Vaporisation Temperature on $HgCl_2$ Gas Phase Generated

Temperature of Vaporiser (K)	Flow Rate of Carrier Gas (ml/min)	Measured Gas Concentration (ng Hg/L gas)
323	500	458±30
333	500	1150±50

Table 3.2 shows the effect of varying vaporisation temperature on the $HgCl_2$ gas phase concentration generated from the set up. It can be seen that an increase of 10° in vaporisation temperature, for the same flow rate of carrier gas of 500 ml/min, caused the concentration of the gas phase generated to increase by a factor of 2.5.

The observed result shows that the vaporisation process of $HgCl_2$ is very sensitive with the temperature. The result agrees with the research finding of Bernard, L. , et al. who reported that the relationship between $HgCl_2$ concentration in the gas phase and vaporisation temperature follows an exponential relationship [15]. The result suggest that the mercury gas vaporiser system is capable to produce a gas phase with desired $HgCl_2$ concentration by varying the vaporisation temperature. Furthermore, the vaporisation process can be used for different mercury species, which have different vaporisation properties. From this work, the $HgCl_2$ test gas was created using 1 gram(s) of $HgCl_2$ crystals at N_2 carrier gas flowrate of 500 ml/min and vaporisation temperature of 333 K.

For the generation of Hg^0 test gas, 5 grams of Hg^0 was distributed in the vaporisation vessel at 298 K with the N_2 carrier gas flow rate of 100 ml/min. The system was stable after 24 hours. As Hg^0 is a volatile compound, the Hg^0 concentration in the gas phase reached saturated concentration of 21.15×10^3 ng Hg/L [14] and was constant during the tests in this work.

3.2.2.2 Effect of Temperature of Gas Line on the $HgCl_2$ Gas Concentration

Possibility of condensation is of concern as the temperature of vaporization need to be kept higher than room temperature to generate higher concentration mercury gases for some test conditions. When condensation occur in the system, aspect of maintaining constant mercury gas generated will be challenging as possible loss can occur while being transported through the gas line. Although Metzger and Braun [16] have confirmed that Hg^0 do not condense in the gas line, several authors have reported the need to maintain a heated gas line for $HgCl_2$ due to its tendency to condense [12, 17, 18].

To confirm this possible issue, a test configuration shown in Fig. 3.5 was used to determine the effect of gas line temperature on the delivery of generated mercury (specifically $HgCl_2$) gas from the vaporizer. The vaporization condition was maintained at temperature of 333 K and constant carrier flow rate of 500 ml/min for all tests. Two gas lines were set-up, one wrapped with heating tape and temperature kept 5°C higher than the vaporization vessel (338-340 K) while the other was kept at

room temperature. Two liquid traps consisting of 5 w/v% $KMnO_4$/0.5N H_2SO_4 were placed in series at the end of both gas line to ensure all gas were captured. The result of the confirmation test is summarised in Table 3.3.

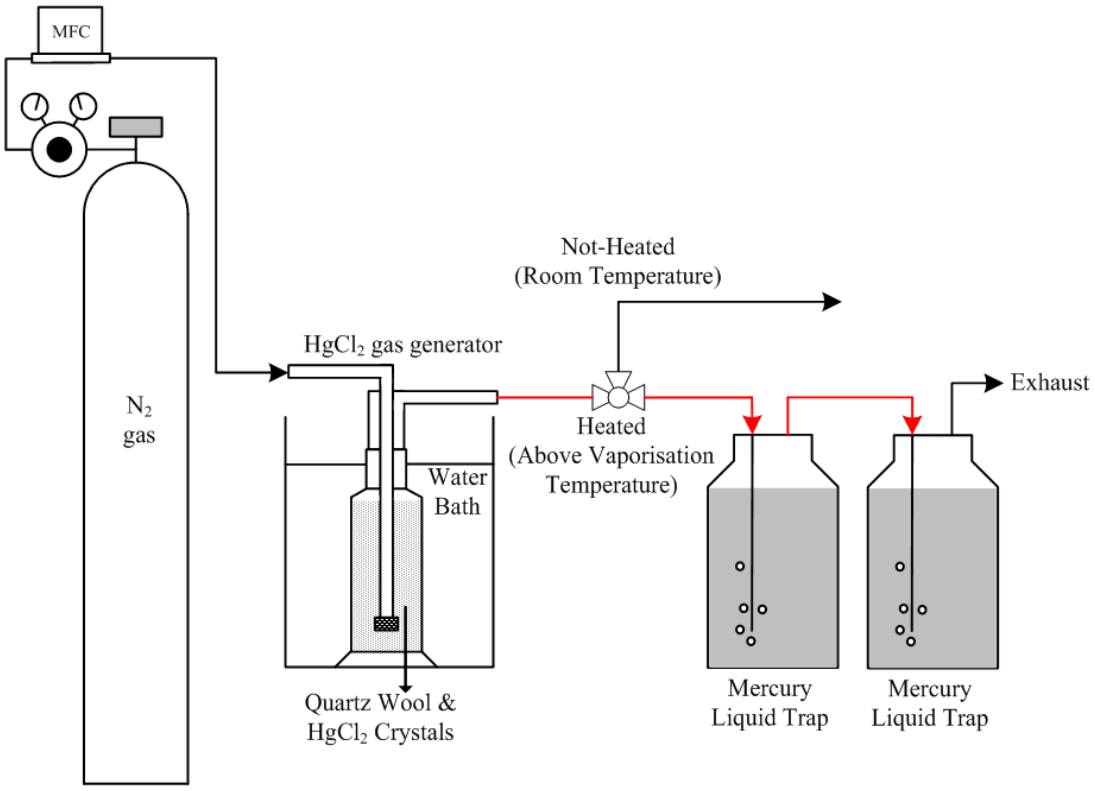

Fig. 3.5 Heated Gas Line Set-Up for $HgCl_2$

Table 3.3 Effect of Temperature of Gas Line on Gas Measurement. Measurement Using $KMnO_4/H_2SO_4$ Liquid Trap at Vaporizer Temperature: 333 K, Mass of $HgCl_2$ Solid: 3.234 gram(s) and Carrier Gas Flow Rate: 500 ml/min.

Temperature of Gas Line	**Measured Gas (ng Hg /L gas) (mean ± SD)**
Heated (338-340 K)	2400 ± 216 (n=5)
Non-heated (Room temperature ~298K)	473 ± 187 (n=6)

The results in Table 3.3 show that $HgCl_2$ gas concentration measured at the outlet of the non-heated line is much lower than that of using the heated line. The lower gas concentration measured from the non-heated gas line show that condensation did occur during transport of $HgCl_2$ gas, therefore resulting in the loss of mercury observed. Furthermore, the measured gas concentration shows a larger fluctuation in comparison with the heated line; 39.5% and 9.0% respectively. From the findings of this test, it can be concluded that the gas lines connecting the vaporizer to the reactor need to be maintained at a similar temperature to the vaporizer to avoid mercury loss and to perform an accurate mercury balance. This is especially true when $HgCl_2$ gas involved.

3.2.2.3 Amount of Loaded Mercury

Several vaporizers were prepared by weighing and loading several different masses of $HgCl_2$ crystal to study its effect on the generated mercury gas concentration. Effect of varying amount of solid mercury loaded into the mercury vaporizer was studied at a constant carrier flow rate of 500 ml/min and at constant vaporization temperature of 333 K. The effect of increasing the amount of loaded $HgCl_2$ on the concentration of gas generated from the solid vaporization set-up is shown in Fig. 3.6.

The results in Fig. 3.6 show that increase in amount of $HgCl_2$ inside the vaporizer directly correspond to the increase in gas concentration generated. As more $HgCl_2$ were distributed among the quartz wool inside the vaporizer, this will increase both the surface of area of vaporization as well as contact when the carrier gas pass through the vessel, carrying more vaporized $HgCl_2$ molecules. This aspect of the vaporizer will enable larger range of working conditions for this work in terms of generation of various mercury gas concentrations.

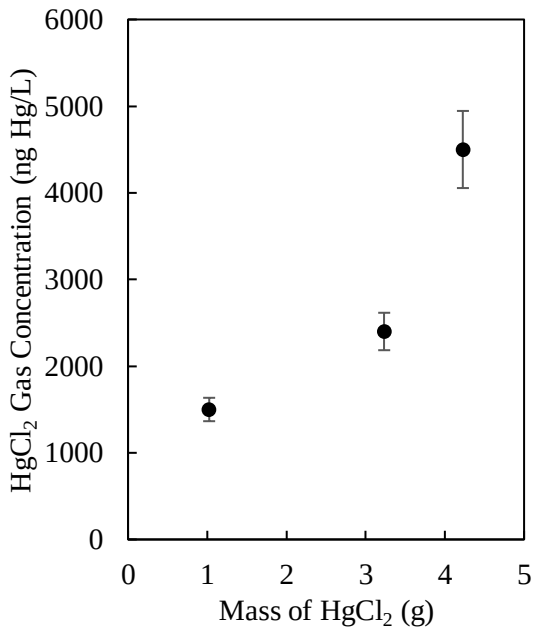

Fig. 3.6 Effect of Mass of $HgCl_2$ on Generated Gas Concentration

3.3 Reactor Set-up

All absorption experiments were conducted using a semi-batch type reactor (ID: 100 mm, Height: 200 mm, Capacity: 900 ml) with a multi-port cap and water jacket. The

experimental set-up is illustrated in Fig. 3.7. The use of a semi-batch reactor system for mercury absorption studies have been reviewed in detail in Chapter 2, section 2.5.1.

A continuous flow at 500 ml/min of nitrogen gas was directed through the mercury vaporiser, introducing the mercury test gas to the reactor. The vaporizer and the reactor were connected by PTFE tubing and kept at ~5°C higher than the vaporizer water bath by means of heating tape to avoid possible condensation in the tubing [12]. The reactor cap was also wrapped with heating tape and its temperature kept at 5-10°C higher than the operating reactor temperature to prevent possible water condensing on the reactor overhead. The temperature of absorption liquid and reactor overhead were controlled by the reactor jacket and a water bath. A thermometer was installed in the reactor overhead for temperature monitoring purpose.

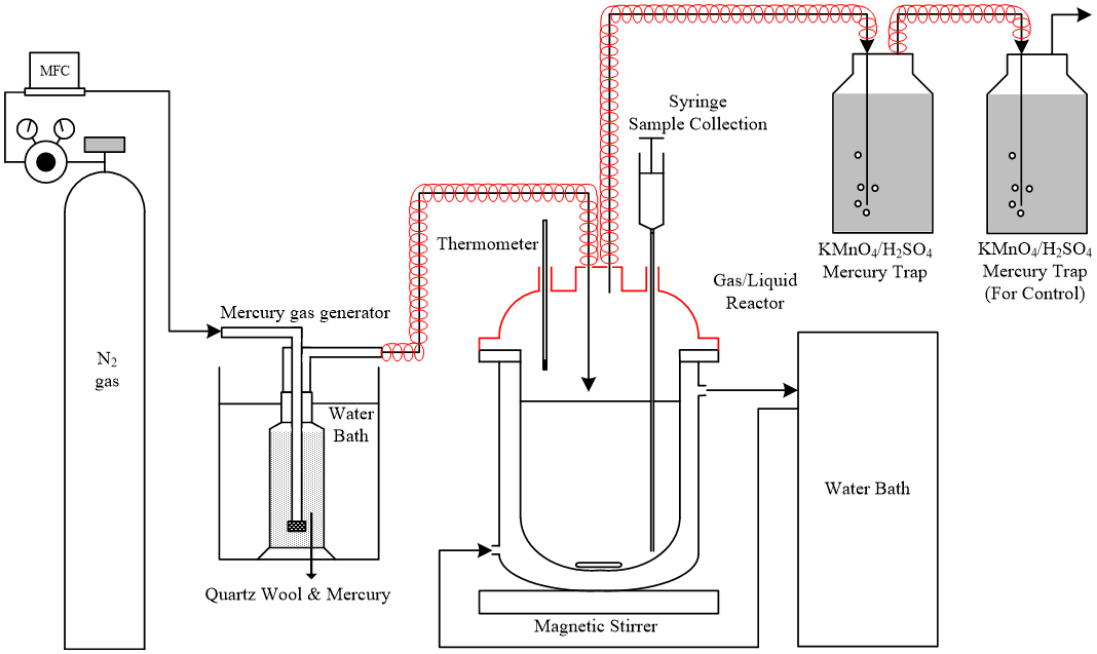

Fig. 3.7 Experimental Set-Up for Absorption Kinetics Study

The mercury test gas was allowed to pass over the surface of the water inside the reactor for dynamic solubility study. For all experiment, the water body was agitated using a PTFE magnetic stirrer at the same rotation speed per minute (260rpm) to ensure the same hydrodynamic condition and uniform concentration in the water body. At this rotation condition, the surface of the liquid remains smooth and unchanged during the test. Due to the small reactor head volume and high-test gas flow rate used in this work, the gas residence time is short (30 seconds). For each experiment, about 10 water samples (10 ml/sample) were collected within 50 test hours via a sample collection

glass syringe. The range of experimental conditions used in this work are described in Table 3.4. Prior to each test, the system was purged with the nitrogen gas to eliminate dissolved O_2 and any other impurities. All glassware was acid washed and rinsed with Milli-Q water before use to avoid any traces of mercury in the system.

Table 3.4 Range of Experimental Conditions for Mercury Absorption Kinetics Study

Experimental Condition	
Temperature (K)	298-333
Solution Volume (ml)	700
Mercury Gas Flowrate (ml/min)	500
Total Absorption Time (Hour)	48-51
Total Sample(s) Collected	10

3.4 Gas Phase Mercury Analysis

3.4.1 Inorganic Gaseous Mercury Analysis

3.4.1.1 Gold/Platinum solid trap

Gold trap has been proven and successfully utilised by a several authors for trapping and determination of gaseous concentration of Hg species such as $HgCl_2$ and Hg^0 [4, 19]. In this work, the Au/Pt cartridge trap used for the quantitative analysis of $HgCl_2$ in gas phase was in a gauze form, nestled inside a quartz cylindrical tube. The Au/Pt trap came with the PerkinElmer amalgam system and for the analysis, the amalgam system was connected to the spectrometer in the Perkin-Elmer, FIMS 400 Flow Injection System for detection.

Before each measurement, the Au/Pt trap was heated a couple of times at 873 K under carrier gas flow until the base line was stable. Gaseous $HgCl_2$ generated from the $HgCl_2$ vaporizer was directed to the Au/Pt trap for loading at the set gas flow rate (500 ml/min) for 20 seconds at room temperature. The Au/Pt trap loaded with mercury was then placed back into the amalgam system and heated to 873 K using halogen lamps. At this temperature, the trapped $HgCl_2$ in the Au/Pt trap underwent thermal decomposition to form Hg° [20], which was carried by the carrier gas (300 ml/min of UHP N_2) to the FIMS for detection at a specific wavelength of 253.7 nm. Following the analysis, a stream of compressed air was directed to the heated trap to cool it down to ambient temperature. A summary of the analysis process is illustrated in Fig. 3.8.

The settings of the analysis process using the amalgam/FIMS system are listed in Table 3.5. In the prefill and in step 1, the mercury loaded Au/Pt trap was flushed with the carrier gas to purge any impurities that may be present during sample collection. In step 2, the trapped mercury was released from the Au/Pt trap and determined in the detector. In this step, the Au/Pt trap was heated to thermally release the trapped mercury. The detector was also set to 'Read' mode to record the absorption peak of mercury. Step 3 provides a cool-down time for the Au/Pt prior to the capture of the next sample. 60 seconds were selected to bring the temperature of the Au/Pt close to ambient temperature. For all the steps, speed of pump 1 and pump 2 were set to 0 as the analysis did not require the introduction of carrier and reductant solution. FI valve position was also set to 'Fill' to only use the amalgam accessory without the liquids introduction.

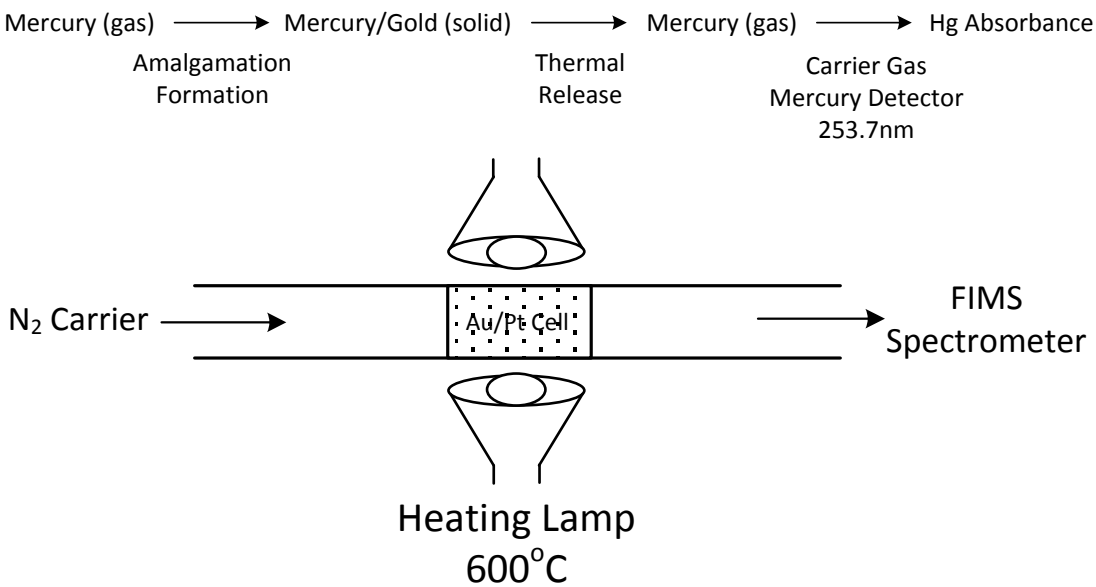

Fig. 3.8 Solid Trap Analysis Process

Table 3.5 FIMS Settings For Gas Analysis Using Amalgam Accessory

Step	Time (s)	Pump 1 Speed	Pump 2 Speed	Valve	Heat	Cool	Carrier
Prefill	10	0	0	Fill	Off	On	On
1	20	0	0	Fill	Off	Off	On
2*	20	0	0	Fill	On	Off	On
3	60	0	0	Fill	Off	On	On

*Read Step

The evolved Hg was calibrated against the absorbance peak area instead of absorbance for better representation of the total Hg detected by the spectrometer. Constant volume (500 µl sample loop) of mercury standard solutions were injected into the FIMS

whereby the solutions are reduced by $SnCl_2$ to evolve all mercury into its elemental gaseous form. The evolved Hg was then carried by UHP nitrogen gas to the Au/Pt trap for loading. Preparation of mercury standard solutions follow the analysis for liquid samples outlined in section 3.5. Calibration curve for the analysis was generated from known mercury standard solutions; typical calibration curve is shown in Fig. 3.9.

The calibration curve in Fig. 3.9 show a linear relationship between peak area and mercury in the gas phase. This result suggests that the process parameters for trapping of mercury gas using the Au/Pt trap was functioning properly. The trap used was able to effectively trap 0 – 30 ng of mercury without overloading. If overloading were to occur, there would be a sudden jump in the peak area recorded by the instrument. Furthermore, the mercury detected by the UV-detector is still within the instrument's detection limit. If detection limit were surpassed, the calibration curve would show a flat line despite the increase in amount of mercury available in the gas phase. Finally, the heating time selected in Table 3.5 for Au/Pt trap was effective to release all the trapped mercury, providing a consistently linear curve.

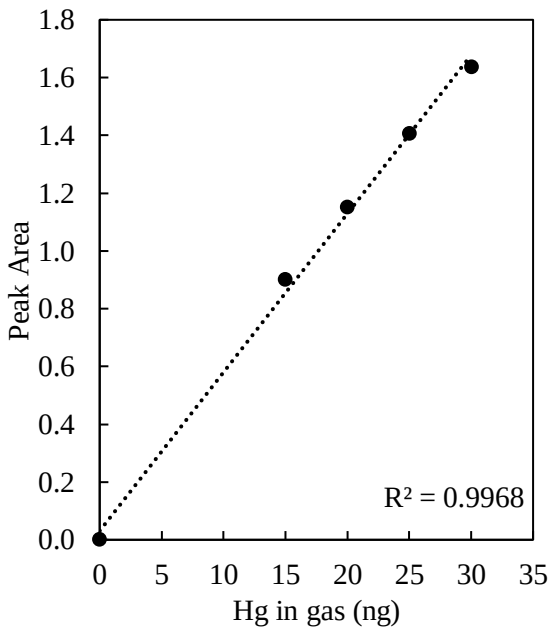

Fig. 3.9 Typical Calibration Curve for Au/Pt Trap

3.4.1.2 $KMnO_4$ Liquid Trap

The liquid trap (5 w/v % $KMnO_4$, 0.5N H_2SO_4) has been proven and used successfully by many researchers to capture various species of mercury such as elemental mercury (Hg°) and inorganic mercury ($HgCl_2$) for their research purposes [2, 3, 12, 16, 21-24].

The liquid trap was prepared by dilution of $KMnO_4$ solid (50 g in 1000 mL solution) and concentrated H_2SO_4 (98%, Sigma Aldrich) solution (14 mL in 1000 mL solution); 200 ml of the liquid trap was placed inside a gas washing bottle with frits for gas dispersion to ensure all $HgCl_2$ gas were trapped. Gaseous mercury was captured by the liquid trap by bubbling the gas through the trap solution for a period of 2 hours at the set gas flow rate. The trap solution was then diluted and analysed following the analysis and calibration procedure for liquid samples in section 3.5.

Table 3.6 Comparison of Gaseous Mercury Measurement Using Au/Pt and $KMnO_4/H_2SO_4$ Liquid Trap (Vaporizer Temperature: 323 K, Mass of $HgCl_2$ solid: 1 gram(s), Carrier Gas Flow Rate: 500 ml/min).

Gas Measurement Method	Measured Gas (ng Hg /L gas) (mean ± SD)
Au/Pt Trap	429.8 ± 22.5 (n=7)
Liquid $KMnO_4/H_2SO_4$ Trap	486.1 ± 34.9 (n=4)

At the same $HgCl_2$ vaporizer conditions described above, the gas measurement results obtained from using solid trap (Au/Pt) and liquid trap (5 w/v % $KMnO_4$, 0.5N H_2SO_4) are given in Table 3.6 for comparison and discussion purposes.

According to Table 3.6, for the mentioned vaporization conditions, the average gas concentration was measured to be 458 ng Hg/L±8.8%. Based on the results, the concentration measured using the two mentioned methods agree with each other proving their suitability to measure the concentration of gaseous mercury.

However, when comparing the two gas measurement methods, the use of Au/Pt trap method is prone to overloading when the test gas concentration is at high mercury level. This would then require dilution of the test gas for analysis. However, having said that, the use Au/Pt trap would be more suitable for measuring lower concentration of mercury in gas phase. In contrast, the liquid $KMnO_4/H_2SO_4$ trap capacity is flexible and can be increased by using a larger liquid volume in the trap, thus this method is selected to measure the $HgCl_2$ concentration in the test gas in this work.

3.4.1.3 HCl Liquid Trap

The use of other liquid trap containing chlorides such as HCl has also been used by several authors to aid in simple mercury speciation, Hg^0 and $HgCl_2$. This is due to the increased solubility of the latter in chloride solutions [16, 25]. A simple test was conducted to evaluate the suitability of HCl solution to trap $HgCl_2$ gas by comparison

with $KMnO_4$. The HCl liquid trap was prepared by dilution of appropriate concentrated HCl (32% AR Reagent, Univar) to make up concentration of 2 v/v% in Milli-Q water. The preparation of $KMnO_4$ trap follows the procedure described in section 3.4.1.2

Table 3.7 Comparison of Gaseous Mercury Measurement Using Different Liquid Traps; $KMnO_4/H_2SO_4$ and HCl Liquid Trap (Vaporizer Temperature: 333 K, Mass of $HgCl_2$ Solid: 1.024 gram(s), Carrier Gas Flow Rate: 500 ml/min).

Liquid Trap	Measured Gas (ng Hg /L gas) (mean ± SD)
5 w/v% $KMnO_4$/0.5 N H_2SO_4	1477 ± 124 (n=3)
2 v/v% HCl (pH 1)	1533 ± 76 (n=3)

At the same $HgCl_2$ vaporizer conditions described, the gas measurement results obtained from using different liquid trap, namely 5 w/v % $KMnO_4$/0.5N H_2SO_4 and 2 v/v% HCl are given in Table 3.7. According to Table 3.7, for the mentioned vaporization conditions, the average gas concentration was measured to be 1505 ng Hg/L ± 6.4%. Based on the results, the concentration measured using the two mentioned methods agree with each other, proving the suitability of HCl to capture $HgCl_2$ gas for analysis. Nonetheless, it is to be noted that the use of HCl as a liquid trap is only valid to capture $HgCl_2$ and not suitable for trapping Hg^0 gas [16]. Trapping mercury gas using $KMnO_4/H_2SO_4$ will still be required to confirm the total amount of mercury in gas as other gaseous species of mercury require strong oxidants to convert them into a more soluble form to stay in liquid.

3.4.2 Organic Gaseous Mercury Analysis

Most of the gaseous mercury analysis method focuses mainly on Hg^0 and $HgCl_2$ and not a lot of documentation available on organic gaseous mercury. Common methods analysing organic gaseous mercury involve the use of different types of solid traps such as Supelco Carbotrap and direct elution of the captured mercury into the GC-MS for detection [26, 27].

There is currently a very limited amount of information on suitable liquid trap for capturing organic gaseous mercury. Work done by Quino [28] reported ~95% efficiency of trapping dibutyl mercury by using isopropyl alcohol. Organic mercury such as dibutyl mercury, Ph_2Hg and the more commonly found DMM are known to be very soluble in organic solvents compared to water [25]. To take advantage of this solubility property, a simple test was conducted using several well-known liquid

mercury traps ($KMnO_4$ and HCl) and alcohol to compare their suitability in capturing Ph_2Hg gas generated in this work. The alcohol of choice in this work is ethanol (99.9%, Sigma Aldrich) as Ph_2Hg is reported to be soluble in this solvent [25]. The setup of the test follows that as shown in Fig. 3.10.

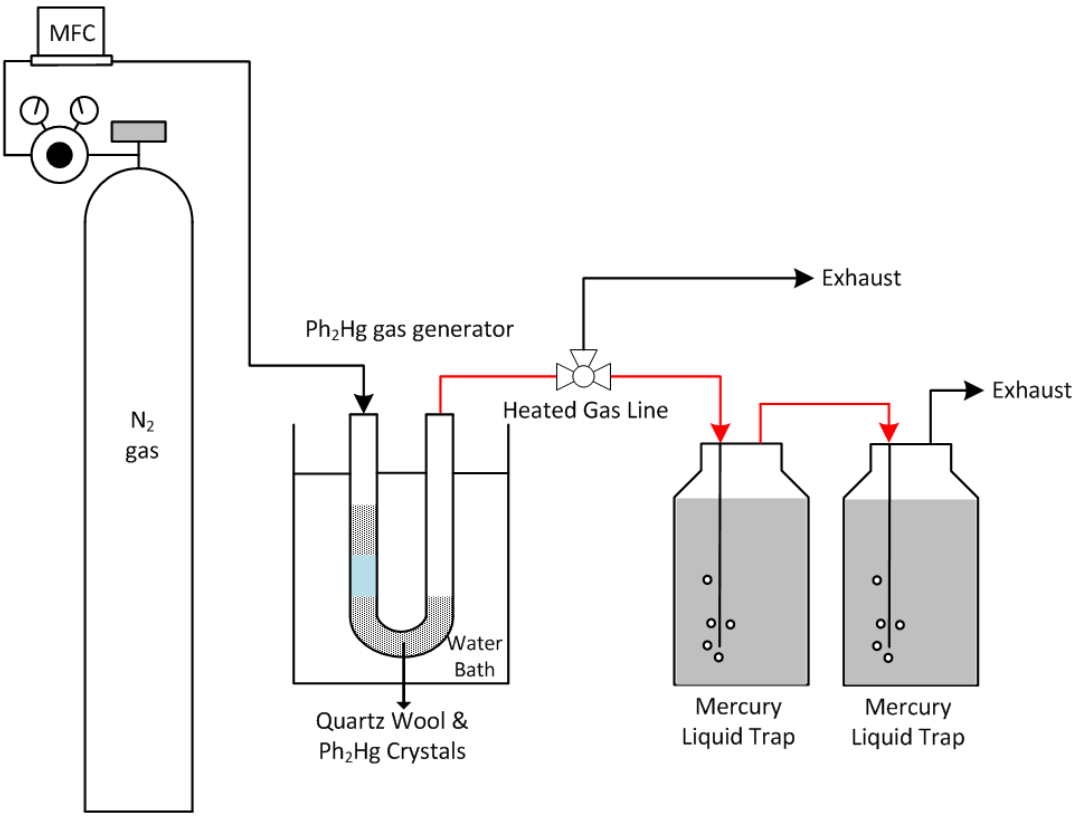

Fig. 3.10 Heated Gas Line Set-Up for Ph_2Hg

Two trap solutions are placed in series at the end of the gas line to ensure all Ph_2Hg gas were collected. The liquid traps were then analysed following the method outlined in section 3.5 to quantify the amount of Ph_2Hg captured. The results of the Ph_2Hg gas analysis are presented in Table 3.8.

Table 3.8 Comparison of Gaseous Organic Mercury Measurement Using Different Liquid Traps, 2 In Series (Vaporizer Temperature: 333 K, Mass of Ph_2Hg Solid: 0.145 gram(s), Carrier Gas Flow Rate: 500 ml/min, Trapping Time: 2 hours).

Liquid Trap	**Average Hg Captured (ng Hg)**		**Measured Gas (ng Hg /L gas) (mean ± SD)**
	Trap 1	**Trap 2**	
5 w/v% $KMnO_4$/ 0.5 N H_2SO_4	179	172	6 ± 1 (n=3)
2 v/v% HCl (pH 1)	1990	853	47 ± 3 (n=3)
99.9% Ethanol	28103	1649	501±41 (n=5)

The results from Table 3.8 show that $KMnO_4/H_2SO_4$ and HCl were not very effective at capturing Ph_2Hg gas with 49% and 30% of the measured gas found in the second trap respectively. This high percentage of breakthrough suggest that high amount of Ph_2Hg were probably lost and that a few more solutions in series would be required to capture all Ph_2Hg generated. $KMnO_4/H_2SO_4$ is proven to be excellent at trapping Hg^0 due to its oxidising property, however the very stable Hg-C bond present in Ph_2Hg requires a much stronger oxidant to oxidise the compound to a more soluble form [29]. While HCl was able to capture more Ph_2Hg in comparison to $KMnO_4/H_2SO_4$, majority of Ph_2Hg was lost at the outlet of trap 2.

As expected, the use of ethanol seemed to be excellent at capturing Ph_2Hg gas [25]. It can be seen from Table 3.8 that the total amount of mercury captured in each trap were much higher (80 and 10 times higher) than that found in $KMnO_4/H_2SO_4$ and HCl. This further suggest their poor capability in trapping Ph_2Hg gas. Moreover, the first trap was able to capture 95% of the total gaseous Ph_2Hg. The observed trapping efficiency is comparable with that reported by Quino [28]. It is to be noted that although 5% of mercury was supposed to be found in trap 2, negligible amount of mercury was able to be detected due to the relatively low gas concentration generated. Having said that, it can be assumed that no mercury was lost for the condition of this work. The use of a second mercury trap is still recommended to assure a mass balanced process.

From the findings of this test, ethanol is used as liquid trap to quantify Ph_2Hg gas generated in this work. Having said that, ethanol is known to be volatile in nature. With that knowledge considered, the ethanol solutions used in this work were replaced after a couple of hours for long term gas sampling. This was done to prevent large amount of liquid lost via vaporization.

3.5 Liquid Phase Mercury Analysis

Two instruments are utilised to effectively quantify the total amount of dissolved mercury in this work namely FIMS and ICP-MS. Detail of the analysis process and optimisation tests are discussed further.

3.5.1 FIMS

The dissolved mercury in the liquid samples were determined by PerkinElmer, FIMS 400 instrument using the following steps: flow injection – cold vapour – atomic absorption spectrometry method (CV-AAS). This instrument allows continuous constant flow rate of the oxidant, reductant, carrier solution and carrier gas as well as having consistent volume of liquid sample to the purging chamber for the analysis. This feature ensures accurate readings to be made as the analysis conditions are controlled precisely by a computer program. The analysis method for liquid samples using FIMS enable to minimise the sample size as the actual analysis only requires 2 ml (loading and unloading into the injection loop) per replicate, in comparison of 100-200 ml per analysis if a conventional CV-AAS was utilised [30]. This aspect of the instrument allows for more samples to be obtained for long time (50 hours) dynamic solubility study without having the need to have a very large volume of liquid for each experiment and also minimises sample preparation time.

A 1000 mg/l dissolved mercury standard (high purity standard, Thermo Fischer) was utilised as a stock solution for instrument calibration. All standards and 1.1 w/v % $SnCl_2$ (98%, Scharlau) in 3 v/v % HCl reducing solution were prepared daily by appropriate dilution of the stock solution. The relationship between Hg standard concentration and the measured absorbance follows a linear relationship within the measured mercury concentration range in this work. Precision of measurement between each replicate was also reliable as RSD values recorded were below 2% for this work.

Samples collected from the reactor were acidified with HCl to preserve the samples. Presence of chloride in the solution helps to stabilise the mercury to stay in the solution for up to 50 days [31, 32]. Analysis of the samples in this work is done within 3 days, thus ensuring measured mercury concentration represents the total mercury absorbed during the experiment. Prior to analysis, samples were diluted and oxidised using 5 w/v % $KMnO_4$ (>99.0%, Chem-Supply) to stabilise the mercury in the solution. Samples were then introduced into the sample loop by means of a continuous stream of carrier solution (3 v/v % HCl solution) and injected into a mixing chamber where ionic Hg was reduced to Hg^0 by a continuous stream of $SnCl_2$. The Hg° evolved from the mixing chamber was then carried to the spectrometer for detection by means of

UHP nitrogen carrier gas. The important parameters for dissolved mercury analysis using FIMS 400 instrument are as follows: flow rates of carrier gas, carrier and reductant solutions were 50 ml/min, 10 ml/min and 6 ml/min respectively. For each sample, analysis was programmed for 3 replicates with injected sample volume of 500 µl per replicate [33].

3.5.2 ICP-MS Optimisation

The dissolved mercury in the liquid samples were also determined successfully using ICP-MS; NexION 350D from Perkin Elmer. Multiple factors could influence the reliability and accuracy of the ICP-MS analysis. Several challenges could occur for analysing sample matrices with organics present (MEG, Ph_2Hg) in this work as they may cause significant suppression of Hg signals during analysis (refer to Chapter 2, section 2.6.2). Moreover, mercury is known to have a very high first ionization energy 10.44 eV [34] and only around 4% of the samples could be ionised in the argon plasma. Several ICP-MS optimisation tests were conducted using prepared standards to establish the optimum acid matrix and internal standard that would yield precise and accurate readings. The general parameter of the ICP-MS operation is summarised in Table 3.9. The operational conditions used for all mercury analysis comes default from the equipment except for the RF power. RF power of 1500 W were optimised to increase degree of ionization of mercury and improve resolution of readings. Further increment to a maximum value of 1600 W would result in rapid equipment degradation.

Table 3.9 Operational Conditions and Parameters of ICP-MS

Instrument Condition and Operation Parameter	
RF Power	1500 W
Nebulizer Gas Flow	0.96 L/min
Scanning Mode	Peak Hopping
Replicates	3
Sweeps	200
Integration Time	1 sec/mass
Mode	Standard (STD) and Helium (KED)

3.5.2.1 Stable Acid Matrix Selection

Two commonly used acids, namely HNO_3 and HCl were tested for their suitability for ICP-MS analysis in the presence of organic compound in the matrix. Mercury standards were prepared by dilution of appropriate volumes of a mercury stock solution to form concentrations of 1, 10, 20 and 50 µg/L. For this test, all the standards consist of 2 v/v% MEG within 2 v/v% HNO_3 or 2 v/v% HCl. It is important to investigate the presence of MEG within the sample matrix to ensure accurate and reliable sample analysis for the following work undertaken. This information would also be beneficial to the industry as several have reported presence of mercury in the recirculated MEG phase within the pipeline. The results of the calibration curves produced by using 2 v/v% HNO_3 and 2 v/v% HCl to prepare the standards are shown in Fig. 3.11 and Fig. 3.12 respectively.

200 ppb of Bismuth (Bi^{209}) was selected to be the internal standard for the optimisation test due to its similar molecular weight to mercury. Both the internal standard and carrier solution used in this test were in accordance to the acid used in the prepared mercury standards.

The calibration curves produced from the ICP-MS readings should show a linear correlation as definite quantities of mercury were added to each standard solution. As seen in Fig. 3.11 (a), the calibration curve produced from using HNO_3 to prepare the sample matrix are not perfectly linear with R^2 values of 0.9598 and 0.9597 in both STD and KED mode. For a suitable calibration, the R^2 value should be very close to 1.0 as it gives an indication on how closely the curve fits the data. R^2 value of 1.0 would indicate that the calibration curve is perfectly linear, with the minimum accepted value being 0.9995 for a reliable analysis. Hence, the set of results from run 1 were not acceptable.

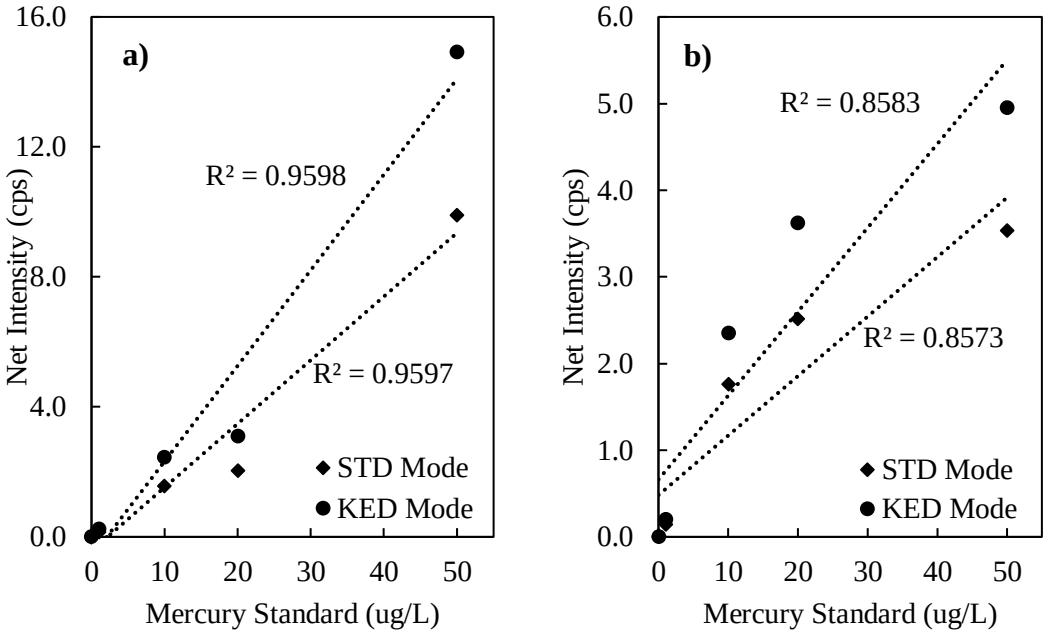

Fig. 3.11 ICP-MS Calibration Curve Using Mercury Standards Prepared in 2 v/v% MEG and 2v/v% HNO_3 (a) Run 1 (b) Run 2

To further confirm the effect of HNO_3, the same set of standards were analysed again within the next hour to check the reproducibility of the calibration curve. The calibration curve generated from run 2 is shown in Fig. 3.11 (b). It can be seen from Fig. 3.11 (b) that the net intensity of the same standards reduced quite significantly within the span of 45 minutes. This reduction in net intensity suggest that the HNO_3 matrix may be causing mercury content to degrade over time. Although HNO_3 is a powerful oxidising acid, it is known to cause a violent reaction with many organic materials [35]. Based on the nature of this acid, HNO_3 might be causing some interference with the matrix by reacting with the MEG present and in turn, decreasing the overall mercury concentration detected. Moreover, due to the instability of the net intensity detected, this also causes further reduction of the linearity of the calibration curve. From the results observed, it is strongly recommended that HNO_3 should not be used to prepare mercury samples containing organic compounds.

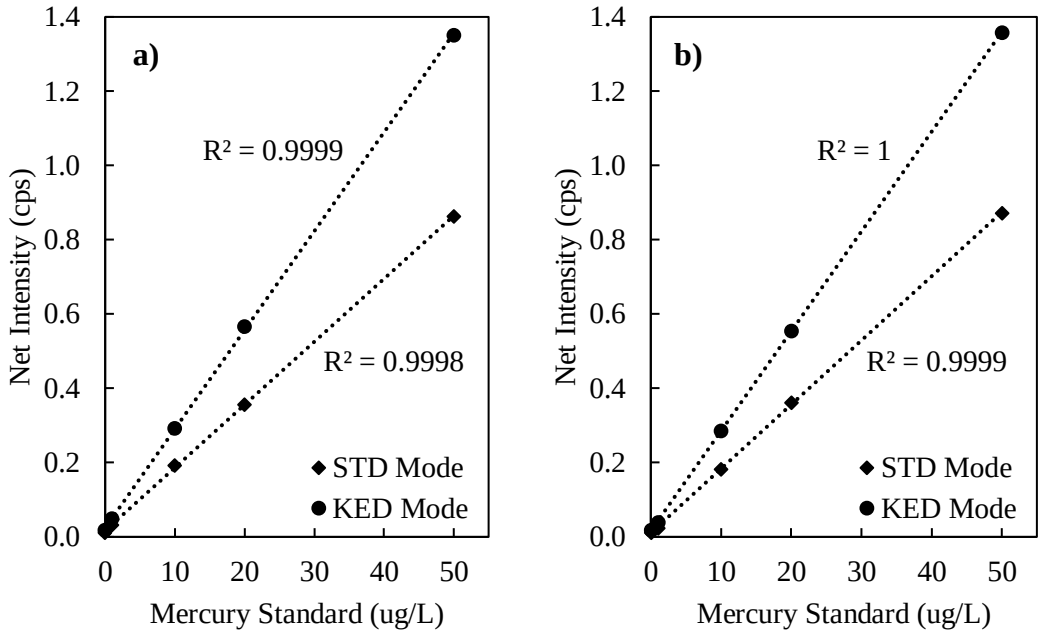

Fig. 3.12 ICP-MS Calibration Curve Using Mercury Standards Prepared in 2 v/v% MEG and 2v/v% HCl (a) Run 1 (b) Run 2

Due to HNO_3 being inappropriate choice of acid, another set mercury standard was prepared in 2v/v% MEG and 2 v/v% HCl. The calibration curve produced is shown in Fig. 3.12 (a). As seen in Fig. 3.12 (a), the R^2 values for both STD and KED mode show great linearity and above the acceptance level of 0.9995. To further confirm the suitability of HCl as acid matrix, the same set of standards were analysed again within the next hour to check the reproducibility of the calibration curve. The calibration curve of run 2 is shown in Fig. 3.12 (b). Comparison of Fig. 3.12 (a) and (b) show that the calibration curve of mercury using HCl matrix is reproducible. It has been widely known that addition of HCl (presence of Cl^-) into mercury samples is excellent to keep mercury stable in solution by formation of stable complex $[HgCl_4]^{2-}$ [13]. Furthermore, it is a much better choice of matrix for samples containing organic compound it doesn't have the strong oxidising properties like HNO_3.

In comparison to the calibration curves using HNO_3, the overall net intensity of the readings is lower in value. The KED mode results show higher overall net intensity with better R^2 value. As the generated calibration curve by using HCl show the best linearity, it was decided that HCl would be the optimal acid matrix for mercury samples containing organic compound.

3.5.2.2 Internal Standard Selection

The use of internal standards is very crucial in analysis using ICP-MS to correct the instrumental drift caused by the nebuliser and plasma signal effects. Presence of an appropriate internal standards will also ensure a more reliable and accurate mercury reading when the sample matrix is quite variable. Selection of internal standard should have a similar molecular weight to the desired element [36]. Selection of internal standard should be approached cautiously as presence in the samples would affect the accuracy of the readings. The percentage of recovery should be consistent with values close to 100% for each standard to ensure the instrumentation condition is stable during analysis. There are many elements which can be used as a suitable choice of internal standards. For this optimisation test, Bismuth (Bi^{209}) and Uranium (U^{238}) were tested for their suitability in mercury analysis. The two elements of choice were selected due to their similar molecular weight to mercury (Hg^{202}). Both internal standard solutions were prepared in 2 v/v% HCl matrix and each contained 200 ppb of the respective elements. The internal standards recoveries of Bi^{209} and U^{238} during calibration in KED mode were illustrated in Fig. 3.13.

Fig. 3.13 shows consistent recovery of Bi^{209} with a minimum of 99% and maximum of 103.3% after analysing a total of 9 samples. On the other hand, the recovery of U^{238} was quite stable for the first 5 samples. This however started to go down, reaching a minimum of 78% recovery and fluctuates between 78-90% recovery after sample no. 5. The fluctuations seen for U^{238} indicate the instability of the plasma when U^{238} was introduced during the analysis process.

Based on the findings, Bi^{209} is a more stable internal standard and thus selected to be the internal standard of choice to analyse mercury samples using ICP-MS.

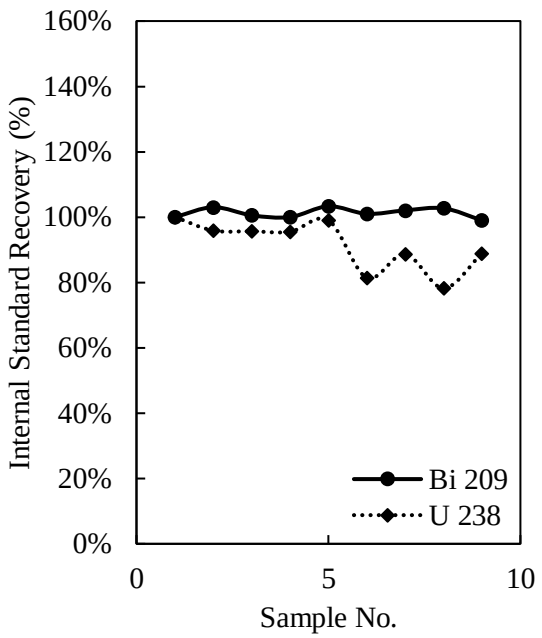

Fig. 3.13 Recovery of Internal Standards for Mercury Analysis

3.5.3 Characterization of Liquid Samples

Qualitative analysis of the liquid samples obtained from the absorption studies were conducted using several optical methods, namely Fourier transform infrared spectroscopy (FTIR) and Raman spectroscopy. These techniques were applied to determine the chemical compounds present in the liquid samples by detection of functional groups within energy range of 200 – 4000 cm^{-1} [37].

FTIR analysis makes use of infrared radiation on the samples, which causes excitation of the molecules to a higher vibrational state. The absorption and transmission results of the infrared radiation will give us the corresponding functional groups present. Functional groups are a combination of two or three atoms that were bonded through the infrared absorption.

Raman spectroscopy makes use of the Raman scattering effect. Scattering occurred when a photon beam (from a laser; visible, infrared and UV range) hits a molecule and cause its excitation to a higher vibrational state. In this technique, the photon energy that was not absorbed were scattered and provides information regarding the vibrational modes of the molecules. Raman spectroscopy is a more sensitive optical technique compared to FTIR due to its sensitivity to homo-nuclear and non-polar bonds such as C-C and C=C. FTIR in general is more sensitive to hetero-nuclear and polar bonds such as O-H and C-H [38].

Both FTIR and Raman provide very quick analysis with no sample preparation required. Both methods have been widely established for analysis of various organic and inorganic functional groups due to their sensitivity and reliability to analyse low sample concentrations. Most importantly, unlike the conventional mercury analysis involving CV-AAS and ICP-MS, the sample will not be destroyed when analysed using FTIR and Raman. This provides a big advantage as mercury species in the samples were able to be qualitatively identified and provide key information for mercury speciation issues.

FTIR and Raman have been used to effectively detect peaks of several different mercury species. The FTIR and Raman spectra of several organic and inorganic mercury compounds have been compiled by Nyquist et al. [39].

3.6 Proof of Concept - Absorption of Hg^0 Gas in Water

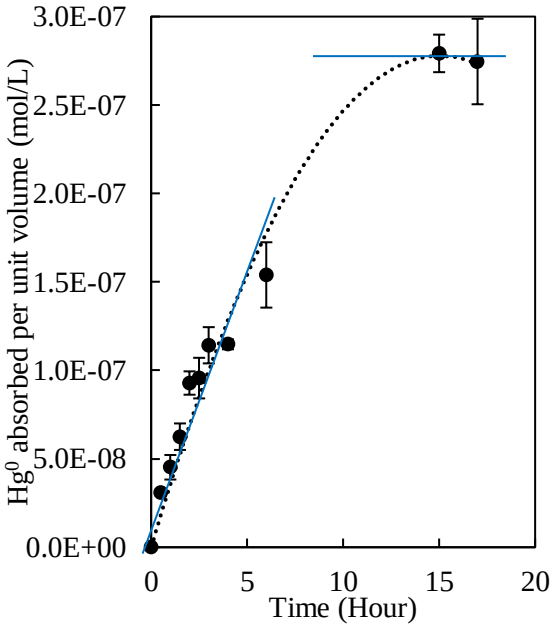

Fig. 3.14 Measured Concentration of Absorbed Hg^0 in Liquid at Gas Concentration of 21.15×10^3 ng Hg/L, Gas Flow Rate of 100 ml/min, Absorbing Liquid of 100 ml Milli-Q Water and Temperature of 298 K. Error Bars Were Calculated After 3-5 Independent Experiments.

Absorption study of Hg^0 was conducted as a proof of concept test using the experimental set-up discussed in the previous sections. The proof of concept test was conducted at gas flow rate of 100 ml/min (UHP N_2), 100 ml of Milli-Q water and temperature of 298 K. Fig. 3.14 shows the concentration of Hg^0 in liquid phase as a function of absorption time.

The results shown in Fig. 3.14 show a linear relationship between Hg^0 concentration in the liquid phase and the absorption time for the first 6 hours. The concentration time curve started to bend after 6 hours to approach gas-liquid equilibrium condition. The last samples recorded the concentration of Hg^0 in water to be 2.8 and 2.7 mol/L (56 and 55.1 µg/L respectively) at absorption time of 15 and 17 hours respectively and these results suggest that the gas/liquid system has reached the equilibrium condition.

In order to confirm the test results, the published Henry coefficient in the literature was used to calculate the Hg^0 concentration in the gas (P_{Hg^0}) and liquid (C_{Hg^0}) phase at equilibrium condition at 298 K [1, 40].

$$P_{Hg^0} = H \times C_{Hg^0} \qquad (2)$$

$$H = 769.23 \frac{Pa.m^3}{mol}$$

On one hand, the expected equilibrium liquid concentration was calculated to be 66.39 µg/L, the result is about 15% higher than the measured value after 17 hours. It is noteworthy to mention that the Hg^0 vaporization process is very sensitive with the vaporization temperature [41], so a small temperature fluctuation of the vaporization water bath (± 1°) may lead to the change of gas phase concentration and caused possible errors of the measured data in this work. On the other hand, the reported maximum solubility of Hg^0 in water at 298 K is 57.4 µg/L [42]. This value agrees with the measured value after 17 hours in this work. The above results confirm the Hg^0 absorption at 298 K has reached equilibrium condition after 15 hours of absorption time.

The two-film theory has been applied to model the absorption and desorption of Hg° with liquid phase by several authors [43, 44], thus the same will be applied to calculate the overall liquid mass transfer coefficient K_L for Hg^0 absorption in water. From Chapter 4, the absorption flux of gas into liquid can be calculated using equation (3)

$$J = K_L\left(C_L^{\ *} - C_L\right) \quad (3)$$

Gas-liquid equilibrium occurs at the interface, thus

$$C_L^{\ *} = {P_G^{\ *}}/{H} \quad (4)$$

The Henry constant as a function of temperature for Hg^0 and water system can be calculated by using equation (5) [1].

$$H_T = H_{298K} \times \exp[2700 \times \left(\frac{1}{T} - \frac{1}{298\ K}\right)] \quad (5)$$

The overall liquid mass transfer coefficient K_L is the characteristic parameter of an absorption process and can be determined by equation (6).

$$\frac{1}{K_L} = \frac{1}{k_L} + \frac{1}{H\,k_G} \quad (6)$$

Unlike the highly soluble gas $HgCl_2$, Hg^0 is known as a slightly soluble gas, whereby the resistance of mass transfer from gas to liquid is dominated by the liquid phase resistance. This is further supported by its high H constant (H = 769.23 Pa.m^3/mol, at 298 K). Substituting this value into equation (6), causing the term (1/H.k_G) to become very small, hence K_L is equivalent to the liquid phase resistance; k_L. Equation (3) can then be rearranged into an integrated form to include a time constant,

$$J = \frac{N}{A} = k_L\left(C_L^{\ *} - C_L\right) \quad (7)$$

Integrating equation (7) from concentration 0 – C and time 0 – t;

$$\ln \frac{C_L^{\ *}}{C_L^{\ *} - C_L} = k_L a\ t \quad (8)$$

$k_L a$ can be determined from the slope of a linear plot of ln [(C_L^*-C_L)/ C_L^*] against absorption time t as shown in Fig. 3.15. Value of a can be determined from the ratio of absorption area with volume of liquid, which both are known. Calculated value of k_L for Hg^0 at 298 K is 7.34×10^{-7} m/s for this work.

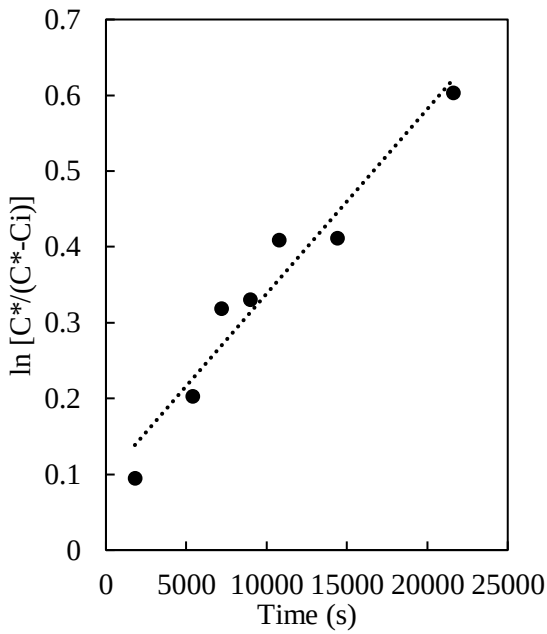

Fig. 3.15 Measurement of k_La of Hg^0 at 298 K

As $K_L \approx k_L$, the k_L value calculated in this work is compared with some of the estimated overall mass transfer coefficient for Hg^0 reported by other authors at temperature range 293-300 K. The list is given in Table 3.10. As seen in Table 3.10, the measured K_L for this work is lower in comparison to the K_L reported by other authors that worked at similar temperature range. It is known that as velocity of gas increased, enhancement of K_L can be observed [45] for systems involving mercury. The low K_L observed may resulted from the relatively low gas flow rate used in this work; 100 ml/min. For the other systems, flow rate of gas can go as high as 5 L/min. Consequently, mass transfer is often represented by K_La values in systems such as bubbling gas-liquid contactors when interfacial area is often unknown. K_La is dependent on the hydrodynamic condition of the absorption process. Hence, the K_La value reported by Okouchi and Sakaki [44] shown in Table 3.10 is quite high in comparison to this work as mass transfer was promoted by the increase surface of contact in a bubbling system. The effect of different types of gas-liquid contactors (stirred tank and bubbler) have also been observed by several authors [46, 47] whereby under similar power consumption, mass transfer coefficients can vary by a factor of 10. This difference further increased in a linear manner when gas velocities are greater.

Table 3.10 Comparison of Estimated K_L of Hg^0 at Temperature Range 293-300 K

K_L (m/s)	Conditions	Reference
$0.81\text{-}5.79\times10^{-2*}$	Semi-batch reactor, volatilization from water, bubbled, flow rate = 1-5 L/min, liquid volume = 200 ml	[44]
$1.98\text{-}3.28\times10^{-5}$	Sea-air exchange, Sc = 600	[48]
2.60×10^{-5}	Semi-batch reactor, agitated, flow rate =1000 ml/min	[49]
2.50×10^{-5}	Volatilization from lake, wind speed = 0.3-8 m/s	[43]
$1.97\text{-}47.3\times10^{-6}$	Surface waters, wind speed =3.1-6.4 m/s	[50]
1.64×10^{-6}	Lake surface, wind speed = ~1-10 m/s	[51]
7.34×10^{-7}, $2.44\times10^{-5*}$	Semi-batch reactor, flow rate = 100 ml/min	This Work

*K_La (1/s)

3.7 Reference

[1] Sander, R. 2015. "Compilation of Henry's law constants (version 4.0) for water as solvent." *Atmospheric Chemistry and Physics* no. 15:4399-4981. doi: 10.5194/acp-15-4399-2015.

[2] Larjava, Kari T., T. Laitinen, T. Vahlman, S. Artmann, V. Siemens, J. A. C. Broekaert, and D. Klockow. 1992. "Measurement and control of mercury species in flue gases from liquid waste incineration." *International Journal of Environment Analytical Chemistry* no. 149 (1-2):73-85. doi: 10.1080/03067319208028128.

[3] Xiao, Z., J. Sommar, S. Wei, and O. Lindqvist. 1997. "Sampling and determination of gas phase divalent mercury in the air using a KCl coated denuder." *Fresenius Journal of Analytical Chemistry* no. 358 (3):386-391. doi: 10.1007/s002160050434.

[4] Feng, Xinbin, Julia Y. Lu, Yingjie Hao, Cathy Banic, and William H. Schroeder. 2003. "Evaluation and applications of a gaseous mercuric chloride source." *Analytical and Bioanalytical Chemistry* no. 376:1137-1140. doi: 10.1007/s00216-003-2034-7.

[5] Feng, Xinbin, Jonas Sommar, Katarina Gardfeldt, and Oliver Lindqvist. 2000. "Improved determination of gaseous divalent mercury in ambient air using KCl coated denuders " *Fresenius J Anal Chem* no. 366:423-428.

[6] Barratt, R. S. 1981. "The preparation of standard gas mixtures. A review." *Analyst* no. 106 (1265):817-849 doi: 10.1039/AN9810600817.

[7] Chen, Wei-Chin, Hsun-Yu Lin, Chung-Shin Yuan, and Chung-Hsuang Hung. 2009. "Kinetic Modeling on the Adsorption of VaporPhase Mercury Chloride on Activated Carbon by Thermogravimetric Analysis." *Journal of the Air & Waste Management Association* no. 59 (2):227-235. doi: 10.3155/1047-3289.59.2.227.

[8] Lyman, Seth N., Daniel A. Jaffe, and Mae S. Gustin. 2010. "Release of mercury halides from KCl denuders in the presence of ozone." *Atmospheric Chemistry and Physics* no. 10:8197-8204. doi: 10.5194/acp-10-8197-2010.

[9] Norton, Glenn A., David E. Eckels, and Colin D. Chriswell. 2001. Development of Mercury and Hydrogen Chloride Emission Monitors for Coal Gasifiers. United States Ames Laboratory

[10] Mibeck, Blaise A.F., Edwin S. Olson, and Stanley J. Miller. 2009. "$HgCl_2$ sorption on lignite activated carbon: Analysis of fixed-bed results." *Fuel Processing Technology* no. 90 (11):1364-1371. doi: 10.1016/j.fuproc.2009.08.004.

[11] Magalhães, Maria Elizabeth Afonso de, and Matthieu Tubino. 1995. "A possible path for mercury in biological systems: the oxidation of metallic mercury by molecular oxygen in aqueous solutions." *The Science of the Total Environment* no. 170 (3):229-239. doi: 10.1016/0048-9697(95)04711-5.

[12] Wang, J., Z. Xiao, and O. Lindqvist. 1995. "On-line measurement of mercury in simulated flue gas " *Water, Air and Soil Pollution* no. 80:1217-1226.

[13] Kozin, Leonid F, and Steve Hansen. 2013. "Mercury Handbook: Chemistry, Applications and Environmental Impact." In: Royal Society of Chemistry.

[14] Huber, Marcia L., Arno Laesecke, and Daniel G. Friend. 2006. "Correlation for the Vapor Pressure of Mercury." *Industrial & Engineering Chemistry Research* no. 45 (21):7351-7361. doi: 10.1021/ie060560s.

[15] Bernard, L., K. Awitor, J. Badaud, O. Bonnin, B. Coupat, J. Fournier, and P. Verdier. 1997. "D´etermination de la pression de vapeur de HgCl2 par la m´ethode d'effusion de Knudsen." *Journal de Physique III* no. 7 (2):311-319. doi: 10.1051/jp3:1997124.

[16] Metzger, M., and H. Braun. 1987. "In-situ mercury speciation in flue gas by liquid and solid sorption systems " *Chemosphere* no. 16 (4):821-832.

[17] Lancia, A., D. Musmarra, F. Pepe, and G. Volpicelli. 1993. "Adsorption of Mercuric Chloride Vapours from Incinerator Flue Gases on Calcium Hydroxide Particles." *Combustion Science and Technology* no. 93 (1):277-289. doi: 10.1080/00102209308935293.

[18] Larjava, K., T. Laitinen, T. Kiviranta, V. Siemens, and D. Klockow. 1993. "Application Of The Diffusion Screen Technique To The Determination Of Gaseous Mercury And Mercury (II) Chloride In Flue Gases." *International Journal of Environmental Analytical Chemistry* no. 52 (1-4):65-73. doi: 10.1080/03067319308042849.

[19] Sommar, Jonas, Oliver Lindqvist, and Dan Strömberg. 2000. "Distribution Equilibrium of Mercury (II) Chloride between Water and Air Applied to Flue Gas Scrubbing." *Journal of the Air & Waste Management Association* no. 50 (9):1663-1666. doi: 10.1080/10473289.2000.10464192.

[20] Shafawi, Azman Bin. 1999. *Mercury Species in Natural Gas Condensate* Department of Environmental Sciences, University of Plymouth Plymouth

[21] Frech, Wolfgang, Douglas C. Baxter, Geir Dyvik, and Bjorn Dybdahl. 1995. "On the determination of total mercury in natural gases using the amalgamation technique and cold vapour atomic absorption spectrometry " *Journal of Analytical Atomic Spectrometry* no. 10.

[22] Keeler, Gerald J., and Matthew S. Landis. 1994. Standard Operating Procedure for Analysis of Vapor Phase Mercury. University of Michigan.

[23] Chang, Michael J., Reta L. McDaniel, John D. Naworal, and David A. Self. 2002. "A rapid method for the determination of mercury in mainstream cigarette smoke by two-stage amalgamation cold vapor atomic absorption spectrometry " *Journal of Analytical Atomic Spectrometry* no. 17:710-715.

[24] Hara, Noboru. 1975. "Capture of mercury vapor in air with potassium permanganate solution." *Industrial Health* no. 13:243-251.

[25] Seidell, Atherton, and William F. Linke. 1940. "Solubilities of inorganic and metal organic compounds: a compilation of quantitative solubility data from the periodical literature." In, ed D. Van Nostrand Co. New York: The American Chemical Society.

[26] Prestbo, Eric, Lucas Hawkins, Deb Cussen, and Christabel Fowler. 2003. Determination of Total and Dimethyl Mercury in Raw Landfill Gas with Site Screening for Elemental Mercury at Eight Washington State Landfills for the Washington State Department of Ecology Frontier Geosciences Inc. .

[27] Ballantine, David S., and Willian H. Zoller. 1984. "Collection and determination of volatile organic mercury compounds in the atmosphere by gas chromatography with microwave plasma detection " *Analytical Chemistry* no. 56 (8):1288-1293. doi: 10.1021/ac00272a022.

[28] Quino, E. A. 1962. "Determination of dibutyl mercury vapors in air." *American Industrial Hygiene Association Journal* no. 23 (3):231-234. doi: 10.1080/00028896209342859.

[29] EPA, U.S. 1974. Method 245.2: Mercury (Automated Cold Vapor Technique) by Atomic Absorption edited by United States Environmental Protection Agency.

[30] Kopp, John F., Mary C. Longbottom, and Larry B. Lobring. 1972. ""Cold Vapor" Method for Determining Mercury." *Journal American Water Works Association* no. 64 (1):20-25.

[31] Louie, Honway, Choon Wong, Yi Jian Huang, and Susan Fredrickson. 2012. "A study of techniques for the preservation of mercury and other trace elements in water for analysis by inductively coupled plasma mass spectrometry (ICP-MS)." *Analytical Methods* no. 4:522-529.

[32] Parker, Jennifer L., and Nicolas S. Bloom. 2005. "Preservation and storage techniques for low-level aqueous mercury speciation." *Science of the Total Environment* no. 337:253-263.

[33] PerkinElmer, Inc. . 2007. *FIMS Flow Injection Mercury System Hardware Guide*.

[34] Linstrom, P. J., and W. G. Mallard. 2005. NIST Chemistry WebBook, NIST Standard Reference Database Number 69.

[35] Urben, Peter. 2017. "Bretherick's Handbook of Reactive Chemical Hazards " In, ed Peter Urben: Elsevier Ltd. .

[36] Vanhaecke, F., H. Vanhoe, R. Dams, and C. Vandecasteele. 1992. "The use of internal standards in ICP-MS." *Talanta* no. 39 (7):737-742. doi: 10.1016/0039-9140(92)80088-U.

[37] Larkin, Peter. 2011. "Infrared and Raman Spectroscopy: Principles and Spectral Interpretation." In.

[38] Colthup, Norman B., Lawrence H. Daly, and Stephen E. Wiberley. 1964. *Introduction to Infrared and Raman Spectroscopy*: Academic Press.

[39] Nyquist, Richard A., Curtis L. Putzig, Anne M. Leugers, and Ronald O. Kage. 1997. *Handbook of Infrared and Raman Spectra of Inorganic Compounds and Organic Salts*: San Diego : Academic Press.

[40] Andersson, Maria E., Katarina Gårdfeldt, Ingvar Wängberg, and Dan Strömberg. 2008. "Determination of Henry's law constant for elemental mercury." *Chemosphere* no. 73 (4):587-592. doi: 10.1016/j.chemosphere.2008.05.067.

[41] Nelson, Gary O. 1971. *Controlled Test Atmospheres - Principles and Techniques* United States of America Ann Arbor Science Publishers, Inc. .

[42] Gallup, Darrell L., Dennis J. O'Rear, and Ron Radford. 2017. "The behavior of mercury in water, alcohols, monoethylene glycol and triethylene glycol." *Fuel* no. 196:179-184. doi: 10.1016/j.fuel.2017.01.100.

[43] Schroeder, William, Oliver Lindqvist, John Munthe, and Zifan Xiao. 1992. "Volatilization of mercury from lake surfaces." *The Science of the Total Environment* no. 125 (7):47-66. doi: 10.1016/0048-9697(92)90382-3.

[44] Okouchi, Shoichi, and Sokichi Sasaki. 1984. "Volatility of mercury in water " *Journal of Hazardous Materials* no. 8 (4):341-348. doi: 10.1016/0304-3894(84)87030-2.

[45] Loux, Nicholas T. 2004. "A critical assessment of elemental mercury air/water exchange parameters." *Chemical Speciation & Bioavailability* no. 16 (4):127-138. doi: 10.3184/095422904782775018.

[46] Gaddis, E. S. 1999. "Mass Transfer in Gas-Liquid Contactors " *Chemical Engineering and Processing* no. 38 (4-6):503-510. doi: 10.1016/S0255-2701(99)00046-X.

[47] Bouaifi, Mounir, Gilles Hebrard, Dominique Bastoul, and Michel Roustan. 2001. "A comparative study of gas hold-up, bubble size, interfacial area and mass transfer coefficients in stirred gas–liquid reactors and bubble columns." *Chemical Engineering and Processing: Process Intensification* no. 40 (2):97-111. doi: 10.1016/S0255-2701(00)00129-X.

[48] Kuss, Joachim, Siegfried Krüger, Johann Ruickoldt, and Klaus-Peter Wlost. 2018. "High-resolution measurements of elemental mercury in surface water for an improved quantitative understanding of the Baltic Sea as a source of atmospheric mercury." *Atmospheric Chemistry and Physics* no. 18 (4361-4376). doi: 10.5194/acp-18-4361-2018.

[49] Zhao, Lingbing. 1997. *Mercury Absorption in Aqueous Solutions* The University of Texas, Austin.

[50] Rolfhus, Kristofer R., and William F. Fitzgerald. 2001. "The evasion and spatial/temporal distribution of mercury species in Long Island Sound, CT-NY." *Geochimica et Cosmochimica Acta* no. 65 (3):407-418.

[51] Frost, Thomas, and Robert C. Upstill-Goddard. 2002. "Meteorological controls of gas exchange at a small English lake." *Limnology and Oceanography* no. 47 (4):1165-1174. doi: 10.4319/lo.2002.47.4.1165.

CHAPTER 4:
DYNAMIC SOLUBILITY OF INORGANIC MERCURY IN WATER

4.1 Introduction

$HgCl_2$ is found to be the main mercury species detected in the water phase of the slug catcher (refer to Chapter 2, section 2.2.2.2) and often untreated water phase is released from natural gas process and this becomes one of the major way of mercury enter the environment [1]. Mercury accumulation in the process also raises some concerns as MEG used to prevent hydrate formation, is typically recycled after use due to its large volume injected in these processes; typical range between 30-60% to successfully depress the hydrate temperature [2, 3] Consequently, it is highly likely that Hg^0 and $HgCl_2$ that are present in natural gas can partition into the MEG solutions, accumulate and potentially contaminate the system as MEG continue to be circulated back into the process.

Additional source of mercury accumulated in the environment includes $HgCl_2$ released in exhaust gas from burning coal and heavy oil. Absorption into water by means of gas-liquid contactor has been developed and can be an effective way to remove $HgCl_2$ from flue gas [4].

Being the major species found in the fossil fuels and environment, Hg° is very well studied [5, 6], however there is a lack of information about organic and inorganic mercury available. With the current mercury problems and knowledge standpoint, the information with regards to the kinetics of absorption of each mercury species, especially $HgCl_2$ is needed urgently to enable the prediction of the dynamics of mercury accumulation in oil and gas processing equipment and mercury behaviours in flue gas treatment process using absorption technique at any given time.

Several work has been done to close the knowledge gap with regards to $HgCl_2$ behaviour such as the saturated solubility in different solvents [7], distribution between gas and liquid system and henry coefficient [8, 9]. To the best of our knowledge, the solubility information on $HgCl_2$ are currently limited to either saturated or equilibrium condition, and no information available for its absorption kinetics.

With regards to the interaction between mercury and MEG, several authors have recently studied the partitioning of mercury during the MEG regeneration process [10, 11] and its solubility in several different glycols solutions [12, 13]. Their research findings have represented important advancement in the understanding of MEG-mercury system, however information is limited to conclude reaction mechanisms and whether reactions even occurred when the mercury species investigated came upon contact with MEG. $HgCl_2$ having reported to have higher solubility in water and solvents [14] is the major species detected in the recirculated MEG stream [10]. Furthermore, to our knowledge, there are no information available regarding the absorption characteristics, transient conditions and to whether there is a chemical reaction between $HgCl_2$ and MEG.

The main objective of this chapter is thus to study the absorption kinetics of $HgCl_2$ gas into water, aqueous NaCl solutions at different temperatures (283-333 K) and NaCl concentrations (0.5-3.5 wt.%) and MEG solutions at different temperature (283-333 K) and MEG concentrations (2-30 v/v%) using a bench scale semi-batch reactor system described in Chapter 3, section 3.2.1. The reaction mechanism for the reaction between $HgCl_2$ (g) and NaCl (aq) is proposed and the Two-Film theory will be used to model the reaction and calculate the reaction kinetics constant. Consequently, the reaction between $HgCl_2$ (g) and MEG will also be investigated and evaluated.

4.2 Effect of Temperature on Dynamic Solubility of $HgCl_2$ in Fresh Water

The effect of temperature on the absorption kinetics of $HgCl_2$ in water was investigated under constant $HgCl_2$ gas concentration (550 ± 49 ng Hg/L) and within a wide range of temperature (298-333 K) for a period of 50 test hours. The experimental set-up and procedure are explained in detail in Chapter 3. Although the absorption experiments were conducted at the temperature between 298 K and 333 K, equal or lower than the gas phase temperature at the reactor inlet, it can be assumed that the condensation of $HgCl_2$ cannot occur in the reactor head space, as the $HgCl_2$ partial pressure used in this work (7.50×10^{-8} atm at 333 K) was far below the saturation level (6.37×10^{-6} atm) [15]. With a known gas/liquid interface area in the reactor, the measured $HgCl_2$ absorbed concentration in the water and calculated $HgCl_2$ absorbed per gas/liquid interface area as a function of absorption time is given in Fig. 4.1 (a) and (b) respectively. As

expected, the results in Fig. 4.1 (a) and (b) show a linear relationship between dissolved $HgCl_2$ and a long period of absorption time. This is due to the $HgCl_2$ concentration in water phase in this work was far below the equilibrium level (28.9 g/l at 298 K) for the gas concentration used in this work [8]. The slope of the curves in Fig. 4.1 (b) represents the absorption flux of $HgCl_2$ in water. The absorption flux as a function of absorption temperature was calculated and the results are given in the Fig. 4.1 (c).

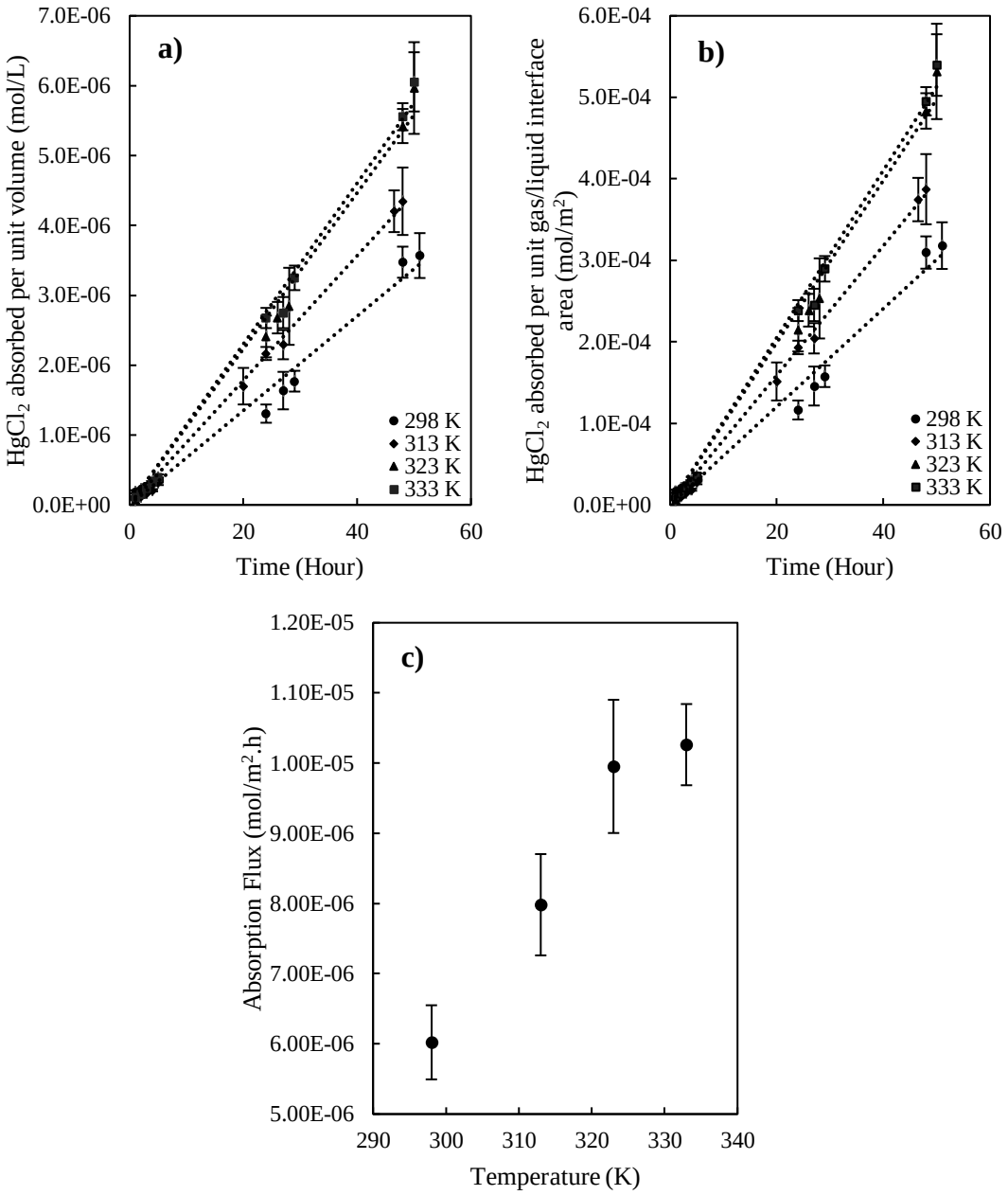

Fig. 4.1 (a) Measured Concentration Of Absorbed $HgCl_2$ in Liquid (b) Calculated Absorbed $HgCl_2$ in Liquid Per Unit Gas/Liquid Interface Unit Area (c) Calculated Absorption Flux at Gas Concentration of 550 ± 49 ng Hg/L, Gas Flow Rate of 500

ml/min, Absorbing Liquid of 700 ml Milli-Q Water And Temperature Range Between 298 and 333 K. Error Bars Were Calculated After 3-5 Independent Experiments.

The results in Fig. 4.1 (c) show that the absorption flux increases significantly with increasing temperature at the low temperature range (298 to 323 K). Above this temperature range, the absorption flux is not very sensitive with the temperature. Gas absorption is a complicated process, as it is affected by a number of parameters such as physical and chemical properties of the solute and solvent, and the hydrodynamic conditions of the system. Several different theories to describe gas absorption processes were proposed, such as film theory, two-film theory, penetration theory and surface renewable theory [16-19]. Among them, the two-film theory is the most common and frequently applied to model different gas absorption processes due to its simplicity and delivery of results [20] comparable to much more complicated theories.

According to the Two-film theory, the absorption flux of gas into liquid is calculated using equation (1)

$$J = K_L\left(C_L^{\ *} - C_L\right) \qquad (1)$$

The overall liquid mass transfer coefficient K_L is the characteristic parameter of an absorption process and can be determined by equation (2),

$$\frac{1}{K_L} = \frac{1}{k_L} + \frac{1}{H\,k_G} \qquad (2)$$

The Henry constant as a function of temperature for $HgCl_2$ and water system can be calculated by using equation (3) [21].

$$H_T = H_{298K} \times \exp[5300 \times \left(\frac{1}{T} - \frac{1}{298\ K}\right)] \qquad (3)$$

In the case of highly soluble gas such as $HgCl_2$ [22], the gas phase resistance is dominant in the mass transfer from gas to liquid, due to very small Henry constant (H = 7.14×10^{-5} Pa.m^3/mol, at 298 K). As a result, the term ($1/H.k_G$) in equation (2) is much larger than ($1/k_L$), which can be ignored. In other word, the absorption of $HgCl_2$ into water is controlled by the gas phase diffusion resistance. By substituting K_L into equation (1), the mass transfer coefficient k_G can be calculated by equation (4). The calculated k_G at different temperatures are given in Table 4.1 and Fig. 4.2.

$$k_G = \frac{J}{H\,(C_L^{*} - C_L)} \qquad (4)$$

Table 4.1. Calculated k_G for the Absorption System at Different Temperatures.

Temperature (K)	**k_G (mol/Pa.m^2.s)**
298	$(2.20 \pm 0.12)\times10^{-7}$
313	$(2.92 \pm 0.27)\times10^{-7}$
323	$(3.64 \pm 0.23)\times10^{-7}$
333	$(3.75 \pm 0.07)\times10^{-7}$

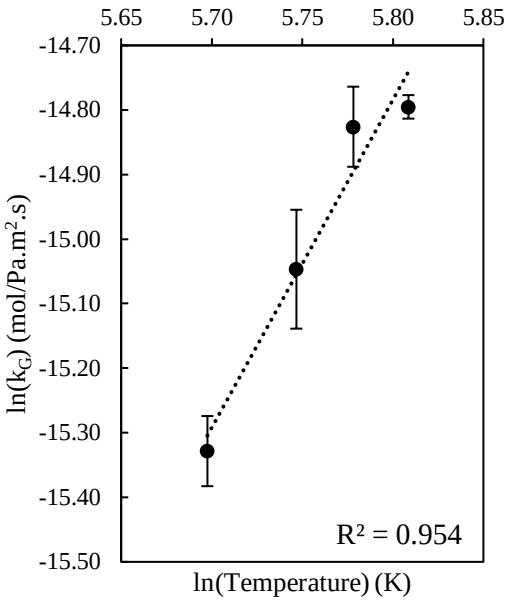

Fig. 4.2. Relationship Between k_G with Temperature. Error Bars Were Calculated After 3-5 Independent Experiments.

Under the same hydrodynamic conditions, the mass transfer coefficient k_G increases with increasing temperature. This can be explained as according to the film theory, the mass transfer coefficient k_G is represented by the ratio between diffusion coefficient and film thickness. At the same fluid dynamic condition, the film thickness is unchanged while the diffusion coefficient increases with increasing temperature [23]. The relationship between k_G and absorption temperature of the system was determined and can be described by equation (5).

$$\ln(k_G)\left({}^{\mathrm{mol}}/_{\mathrm{Pa.\,m^2.\,s}}\right) = 5.078\ln(\mathrm{T})\ (\mathrm{K}) - 44.238 \qquad (5)$$

4.3 Effect of $HgCl_2$ Gas Concentration on k_G

In order to investigate the effect of the $HgCl_2$ concentration in the gas phase on the mass transfer coefficient, three experiments were carried out at 293 K at the same gas flow rate and different $HgCl_2$ gas concentration (550 ± 49, 2400 ± 216 and 4500 ± 445 ng Hg/L). The measured results are given in Fig. 4.3, which shows that k_G increases very slightly within a wide range of $HgCl_2$ gas concentration. This result agrees with the reported results in the literature as k_G is mainly dependent on the hydrodynamic condition of the system, such as agitation and flow rate of the gas side [24, 25].

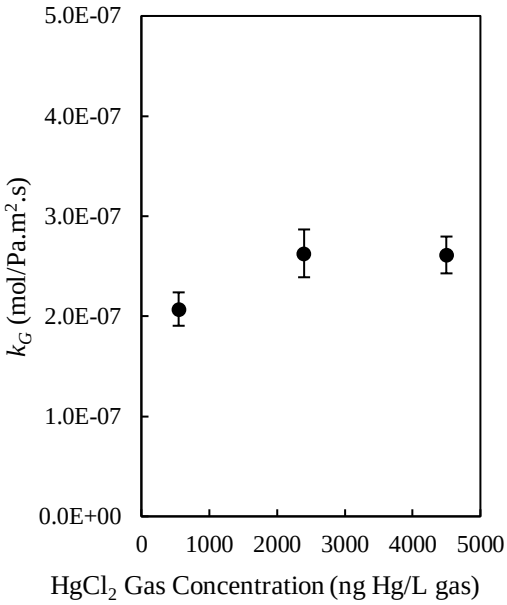

Fig. 4.3. Effect of $HgCl_2$ Gas Concentration on k_G at 293 K. Error Bars Were Calculated After 3-5 Independent Experiments.

4.4 Absorption of $HgCl_2$ in NaCl Solutions

The dynamic solubility of $HgCl_2$ in NaCl solution was investigated under constant temperature (313 K), $HgCl_2$ gas concentration (1500 ± 135 ng Hg/L) and varying NaCl concentration (0.5, 1.5 and 3.5 wt. %). The NaCl solutions were prepared by diluting appropriate mass of NaCl solid (>99.0%, Univar) in Milli-Q water.

As expected, the physical properties of the NaCl solution will change with increasing NaCl concentrations in water such as the elevation in boiling point and dynamic viscosity of the solution. A summary of the physical properties of solution containing different NaCl concentration is given in Table 4.2. The results in Table 4.2 show that

the change in physical properties of the solution with NaCl concentration up to 3.5 wt. % is minimal, so that it will not affect the rate of the studied reaction.

Table 4.2. Physical Properties of Water and NaCl Solutions

At 313 K	Water	0.5 wt.% NaCl	3.5 wt.% NaCl
Dynamic Viscosity (centipoise) [26]	0.65	0.65	0.73
Diffusivity of $HgCl_2$ (cm^2/s)*	1.48×10^{-5}	1.22×10^{-5}	1.09×10^{-5}
Boiling Point Elevation (K) [27]	273.07	273.21	273.52

*Diffusivity values of $HgCl_2$ into the respective solutions are calculated using correlations from Wilke & Chang [23]

4.4.1 Reaction Mechanism of $HgCl_2$ and NaCl

The product of the reaction between $HgCl_2$ and NaCl has been identified by several authors [15, 28, 29] to be $Na_2[HgCl_4]$ and its reaction is as shown in Rxn. 1.:

$$2NaCl + HgCl_2 \rightarrow Na_2[HgCl_4]$$
Rxn. 1

$HgCl_4^{2-}$ is well known as a stable complex especially in the present of Cl- in water phase [15, 28, 29]. It was reported in the literature that $HgCl_2$ is practically un-dissociated in water as the equilibrium constant of Rxn. 2 was reported by Kozin and Hansen to be extremely small ($K = 7.1 \times 10^{-15}$ M) [15].

$$HgCl_2 \rightleftharpoons Hg^{2+} + 2Cl^-$$
Rxn. 2

Thus, reaction Rxn. 1 can be divided into four steps as follows:

$$2NaCl \rightarrow 2Na^+ + 2Cl^- \quad (1)$$
$$HgCl_2 + Cl^- \rightarrow HgCl_3^- \quad (2)$$
$$HgCl_3^- + Cl^- \rightarrow HgCl_4^{2-} \quad (3)$$
$$HgCl_4^{2-} + 2Na^+ \rightarrow Na_2[HgCl_4] \quad (4)$$
$$2\,NaCl + HgCl_2 \rightarrow Na_2[HgCl_4]$$

Based on the research results published, $HgCl_3^-$ is not stable and its formation constant is lower in comparison to other Hg-Cl ion complexes [15, 30, 31], meaning that step (2) is the rate control step of the studied reaction. With the findings above, the rate of reaction Rxn. 1 can be determined by the step $HgCl_3^-$formation. Eigen and Wilkins reported that the kinetics of the formation of metal-halogen complexes from bivalent transition metal Hg ions follows a second order reaction, first order with respect to $HgCl_2$ and Cl^- [32], therefore the formation rate of the $HgCl_3^-$ can be written as:

$$r_{HgCl_3^-} = k_2[HgCl_2][Cl^-] \quad (6)$$

Consequently, the reaction rate of reaction Rxn. 1 can be written as:

$$-r_{HgCl_2} = r_{HgCl_3^-} = k_2[HgCl_2][Cl^-] \quad (7)$$

4.4.2 Effect of NaCl Aqueous Concentrations at 313 K

Three absorption tests for three NaCl solutions (0.5, 1.5 and 3.5 wt. %) were carried out at the same absorption temperature and the measured results are given in Fig. 4.4 below. Fig. 4.4(a) and (b) show the measured absorbed concentration of $HgCl_2$ in liquid and calculated $HgCl_2$ absorbed per unit gas/liquid interface area as a function of absorption time at 313 K.

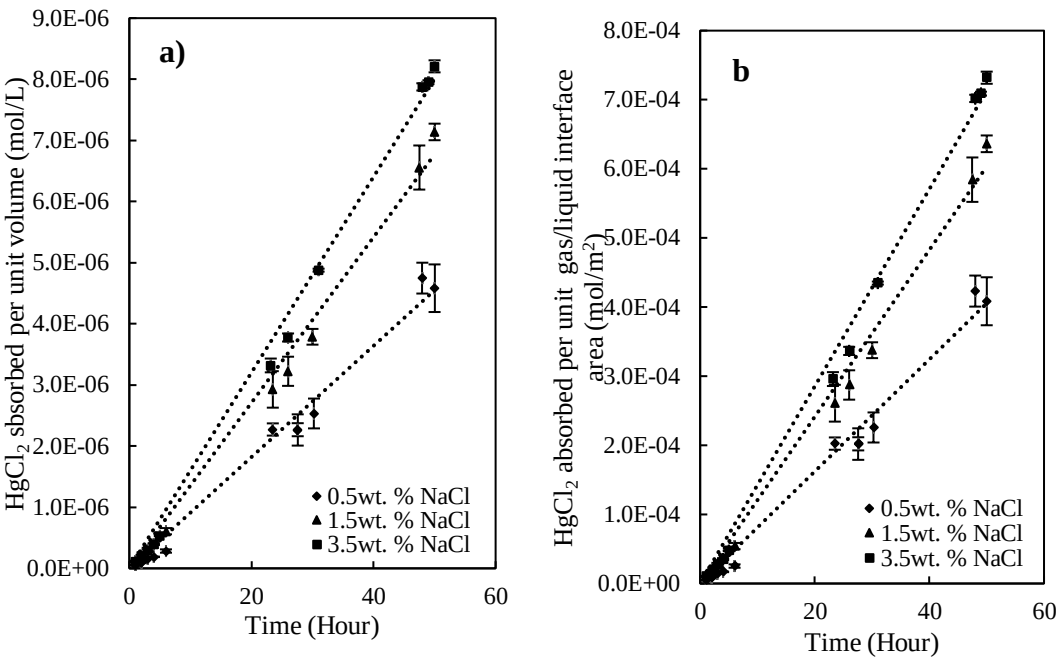

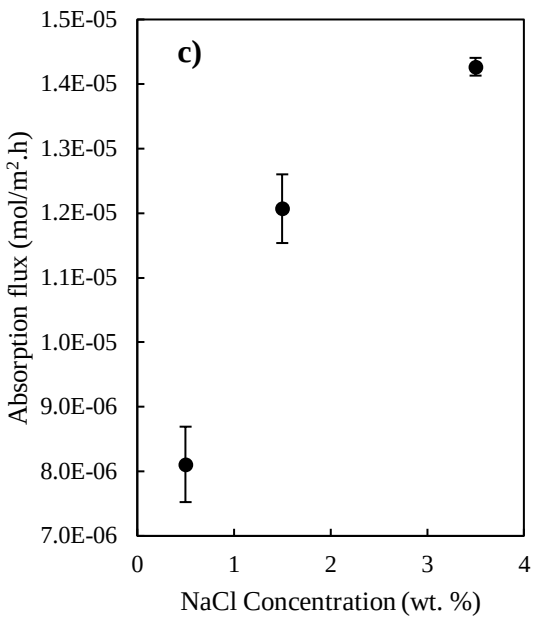

Fig. 4.4. (a) Measured concentration of $HgCl_2$ in Liquid Absorbed Overtime (b) Calculated $HgCl_2$ in Liquid Absorbed per Unit Gas/Liquid Interface Area (c) Calculated Absorption Flux at Gas Concentration of 1500 ± 135 ng Hg/L, gas Flow Rate of 500 ml/min, Absorbing Liquid of 700 ml NaCl Solutions (0.5, 1.5, 3.5 wt. %), and Temperature of 313 K. Error Bars Were Calculated After 3-5 Independent Experiments.

The results in Fig. 4.4(a) show that for all the NaCl concentrations, at constant temperature of 313 K, the absorbed concentration of $HgCl_2$ increases with the absorption time linearly within the test duration of 50 hours. The absorption flux as a function of NaCl concentration was calculated as explained above and the results are given in Fig. 4.4(c). The results in Fig. 4.4(c) show that the absorption flux increases slightly with the increasing NaCl concentration in the solution. The saturated solubility of $HgCl_2$ in aqueous NaCl solution was investigated very early by Homeyer and Ritsert and Herz and Paul [33, 34]. The authors reported saturated solubility of $HgCl_2$ increases slightly with the NaCl concentration in the water phase [35]. The results suggest that the absorption of $HgCl_2$ into aqueous NaCl solution is enhanced by chemical reaction Rxn. 1. The absorption kinetics of the investigated process is further discussed below.

4.4.3 Effect of Temperature in 3.5 wt% NaCl Solution

The effect of temperature on the absorption of $HgCl_2$ gas in water was investigated under constant NaCl concentration (3.5 wt. %), gas flow rate (500 ml/min) and gas concentration of 1500 ng Hg/L at varying temperatures (283-333 K) of the absorbing

solutions. Fig. 4.5(a) and (b) show the measured concentration of absorbed $HgCl_2$ in liquid and the calculated $HgCl_2$ absorbed per unit gas/liquid interface area as a function of absorption at different temperatures.

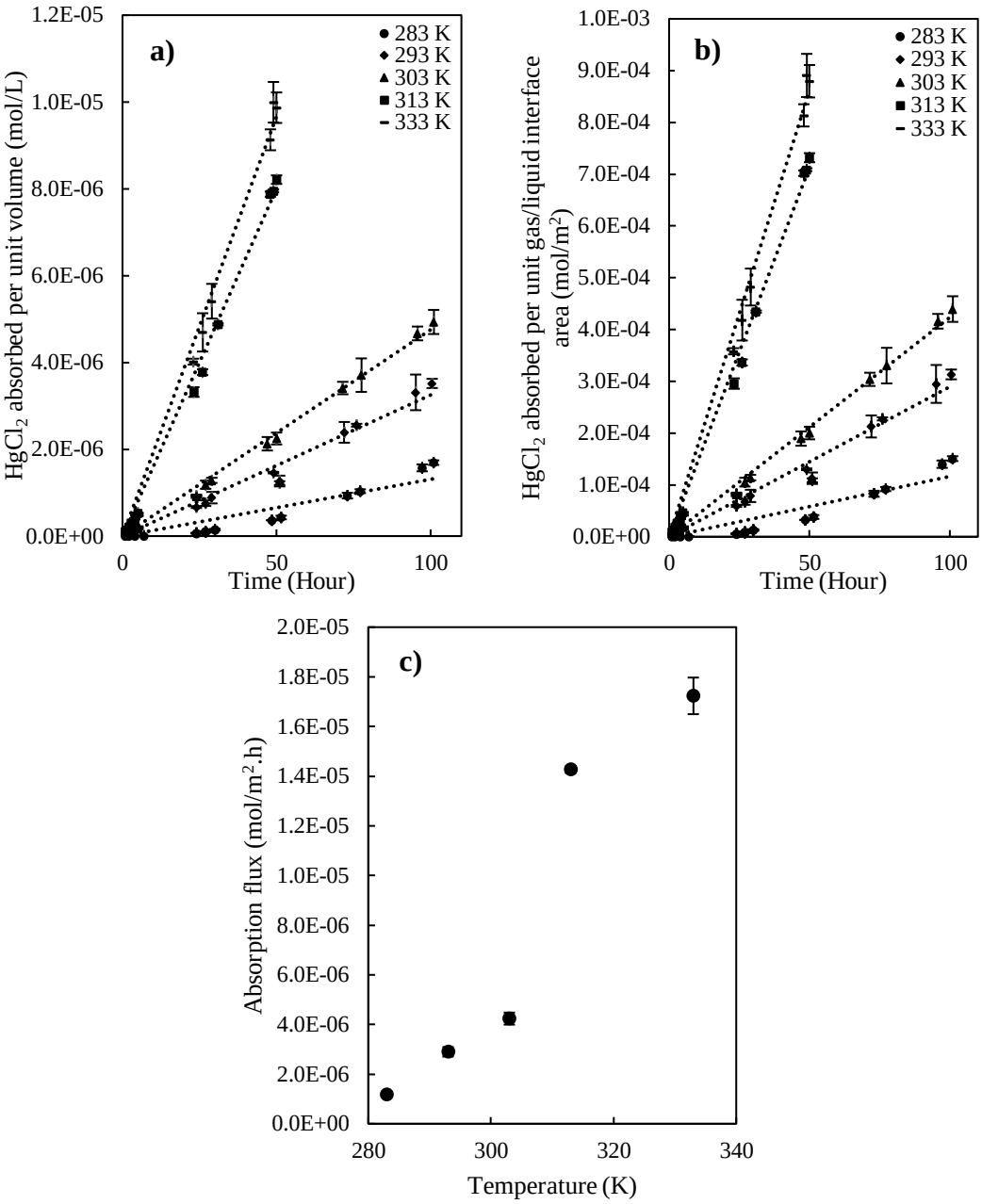

Fig. 4.5. (a) Measured Concentration of $HgCl_2$ in Liquid Absorbed Overtime (b) $HgCl_2$ in Liquid Absorbed per Unit Gas/Liquid Interface Area (c) Calculated Absorption Flux at Gas Concentration of 1500 ± 135 ng Hg/L, Gas Flow Rate of 500 ml /min, Absorbing Liquid of 700 ml of 3.5 wt. % NaCl Solutions and Temperature of 283-333 K. Error Bars Were Calculated After 3-5 Independent Experiments.

The effect of temperature on the absorption of $HgCl_2$ into 3.5 wt. % NaCl solution show a consistent trend with the $HgCl_2$ absorption in water shown in Fig. 4.1 (a) and (b), whereby the absorption rate increases with the increasing absorption temperature,

the effect is less pronounced compared with that of absorption at lower temperature range (283-303 K). Using the same calculation method discussed above, the absorption flux of $HgCl_2$ in aqueous NaCl solution at different temperature is calculated and given in Fig. 4.5(c).

The enhancement factor; E is a dimensionless parameter that describes the effect of a chemical reaction on the rate of absorption. Based on the experimental data obtained, E value for the reaction between $HgCl_2$ and NaCl can be estimated by taking the ratio of absorption flux with and without chemical reaction at the same temperature. Despite the absorption flux with chemical reaction having higher gas concentration, the calculated E at 313 and 333 K was found to be low at 1.79 and 1.68 respectively, The low value of E (less than 2) indicate that the reaction studied is very slow [36]. To further support these findings, the reaction rate constant was determined and discussed further in section 4.4.4

4.4.4 Determination of Reaction Rate Constant

According to the Two-Film theory and the above findings, the absorption kinetics of $HgCl_2$ into NaCl solution is controlled by the gas film and the second order reaction resistance. The reaction occurs in the liquid body as the reaction rate is controlled by a very slow reaction $HgCl_2 + Cl^- \rightarrow HgCl_3^-$ (Rxn. 1 (step 2)). For this absorption process, the absorption rate can be calculated by using equation (8) [37]

$$-r''''_{HgCl_2} = \frac{1}{\frac{1}{k_G a} + \frac{He}{k_2 C_{Cl^-} f_l}} P_{HgCl_2,g} \qquad (8)$$

Although NaCl is almost fully dissociated at low concentration, the dissociation constant for NaCl is taken into consideration to calculate C_{Cl^-} to improve the accuracy of the determination of k_2 [38]. With the measured k_G, absorption rate and well-known parameters of the used reactor system, the reaction constant k_2 of reaction Rxn. 1 at different NaCl concentration and absorption temperature can be calculated, and the results are given in Fig. 4.6(a) and (b) respectively.

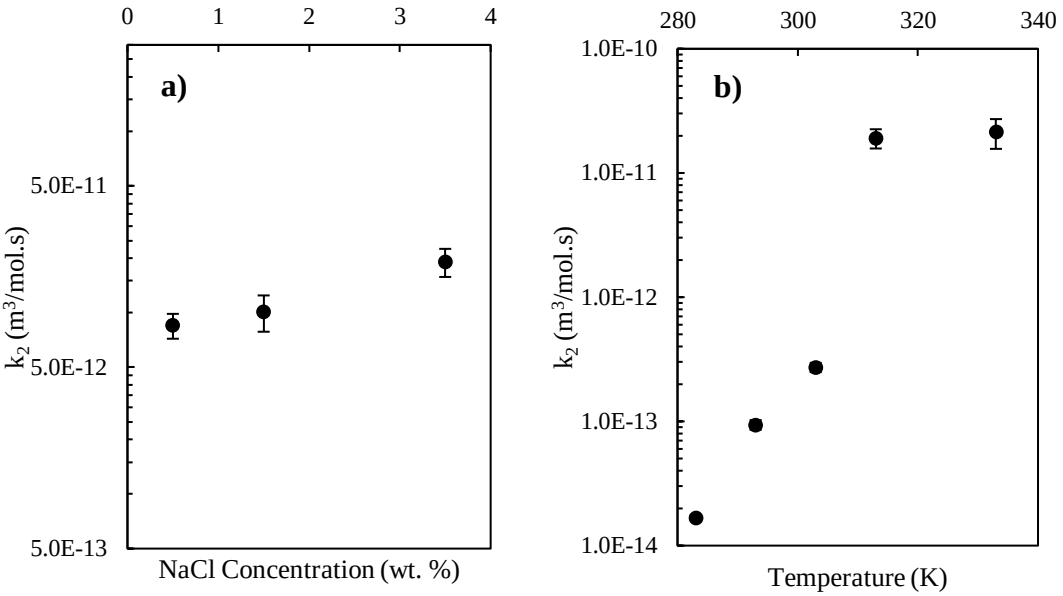

Fig. 4.6. (a) k_2 Values at 313 K (b) Dependence of k_2 with Temperature. Error Bars Were Calculated After 3-5 Independent Experiments.

As shown in Fig. 4.6(a), at 313 K, the k_2 calculated show a very small magnitude within the range of 0.9 -1.9 × 10^{-11} m^3/mol.s, indicating that the reaction between $HgCl_2$ and NaCl is indeed very slow. This finding is further supported by the measured absorption rate and E factor as discussed in section 4.4.2 and 4.4.3. With the measured reaction constant k_2 at different temperature, the activation energy, E_a of reaction Rxn. 1 can be calculated by using the Arrhenius equation as shown in Fig. 4.7.

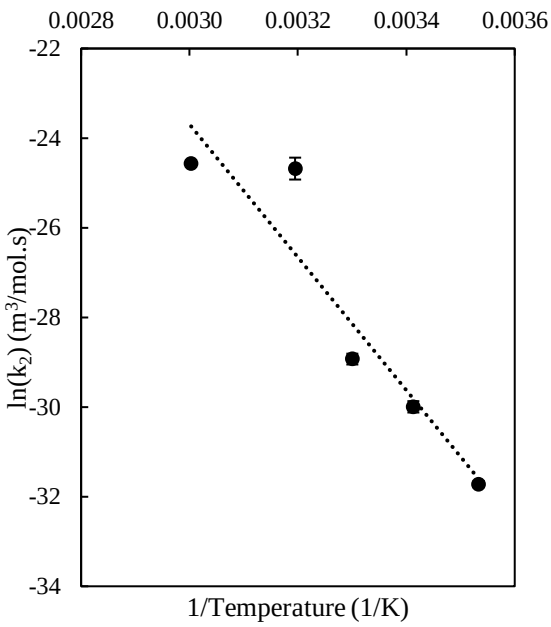

Fig. 4.7. Arrhenius Plot of k_2. Error Bars Were Calculated After 3-5 Independent Experiments.

As a result, the reaction constant k_2 is represented by the following expressions;

$$k_2 = 1.09 \times 10^9 \exp(\frac{-123.32\ \text{kJ/mol}}{RT}) \quad (9)$$

As stated in the introduction, up to date, the data for the absorption kinetics of $HgCl_2$ in NaCl solution have not been studied, therefore it is not possible to compare the results of this work with others. However, the reaction rate constant of second order reaction between elemental mercury and other compounds are listed in Table 4.3 for comparison purposes.

Table 4.3. Reaction Rate Constant and Activation Energy of Second Order Reaction between Mercury Species and Other Compounds

Reaction	Ea (kJ/mol)	k_2(@298K) (m^3/mol.s)	k_2(@333K) (m^3/mol.s)	Source
Hg and $KMnO_4$	56	1.58×10^{4}	1.70×10^{5}	[39]
Mercury Chloride and HCl	131	3.91×10^{-18}	9.98×10^{-16}	[40]
Hg and Cl_2	151	1.80×10^{-19}	1.07×10^{-16}	[40]
Hg and I_2	159	$1.99\times10^{-21*}$	1.11×10^{-18}	[41]
Hg and Br_2	169	$4.15\times10^{-23*}$	3.83×10^{-20}	[41]
Hg and Cl_2	190	$1.09\times10^{-26*}$	2.38×10^{-23}	[41]
Hg and HCl	334	8.46×10^{-50}	1.20×10^{-43}	[40]
$HgCl_2$ and NaCl	123.32	$(1.12\pm0.18)\times10^{-13\ddagger}$	$(4.91\pm2.77)\times10^{-11}$	This Work

*k_2 at 300K
‡k_2 at 293 K

The results in Table 4.3 show that the reaction constant of most listed reactions is very sensitive with the temperature and this may be contributed by their high activation energy.

4.5 Absorption of $HgCl_2$ in MEG Solutions

In order to determine the dynamic solubility of $HgCl_2$ in MEG solutions, physical properties of MEG/Water would need to be investigated in advance. It is well-known that the physical properties of MEG solution will change with increasing concentration of MEG in the solution, especially the viscosity of the solution [42]. Diffusivity of $HgCl_2$ gas into varying MEG solutions has also been estimated from the commonly used Wilke & Chang correlation [23]. A summary of both the dynamic viscosity of solution with varying MEG concentration and diffusivity are given in Table 4.4. The results in Table 4.4 show that dynamic viscosity of the solution increases quite significantly (increase by 2.34 times from 0 – 30v/v% MEG), which in turn has a significant negative effect on the diffusivity of $HgCl_2$ gas into the MEG solution. This

change in physical properties might affect the rate of the studied gas absorption as viscosity has an inverse relationship to the mass transfer coefficients [43].

Table 4.4 Physical Properties of MEG Solutions

At 293K	Water	2 v/v% MEG	10 v/v% MEG	30 v/v% MEG
Dynamic Viscosity (centipoise)	1	1.05	1.26	2.34
Diffusivity of $HgCl_2$ (cm^2/s)*	7.40×10^{-6}	7.07×10^{-6}	5.88×10^{-6}	3.16×10^{-6}

*Diffusivity values of $HgCl_2$ into the respective solutions are calculated using correlations from Wilke & Chang [23]

Another important point to note is whether the interactions within the MEG/water solution will affect the dynamic solubility study. Unlike NaCl where it dissociates in water, MEG is known to be miscible in water, interacting with each other through formation of hydrogen bonding between the –OH group of MEG and water [44]. Several authors have reported that aqueous MEG solutions have possibility to degrade to form oxalic, glycolic and formic acids that can cause corrosions in equipment [45, 46]. The acids formed from degradation of MEG solutions are weak acids and are partially dissociated. This information is crucial as these dissociated acids may react with $HgCl_2$ upon contact. However, having said that, it was also studied that MEG solutions stayed stable at condition of N_2 aeration and at temperature of 293 – 348 K, which is within the test parameters conducted in this work. This confirms that if any reaction were to occur in the system, MEG will not dissociate in the solution and stay as MEG when contacted with $HgCl_2$ under the selected test conditions.

MEG can act as a ligand with divalent metal halides to form metal complexes with the general formula $[M(L)nX_2]$, where M = Divalent metals (Co, Ni, Cu), L= Ligand (MEG), X = Cl, Br, NO_3, $\frac{1}{2}SO_4$ and n = 2, 3 or 4 [47-49], by coordination of the oxygen atoms of the ligand with the metal ion. This reaction of complex formation also occurs for $HgCl_2$ with polyethylene glycols such as triethylene glycol [EO3], and pentaethylene glycol [EO5], yielding $[(HgCl_2)_3[EO3]]$ and $[HgCl_2[EO5]]$ metal complexes respectively [50]. The structure of the EO3 and EO5 metal complexes are similar to the MEG metal complex whereby oxygen are coordinated with the mercury atom. Tests were conducted by utilising the difference in analytical techniques and the results discussed further in section 4.5.3 to check for formation of organic-Hg (Hg-C) species during the absorption processes.

4.5.1 Effect of MEG Concentrations

In order to investigate the absorption enhancement caused by MEG, the absorption of $HgCl_2$ at the same condition were performed for two different ranges of MEG concentration. Absorption tests at lower range were conducted at 0 and 2 v/v% MEG and at $HgCl_2$ gas concentration of 2400 ± 216 ng Hg/L with the measured results given in Fig. 4.8. Absorption tests were also performed at higher range at 0, 10 and 30 v/v% MEG and $HgCl_2$ gas concentration of 4500 ± 445 ng Hg/L with the measured results given in Fig. 4.9. The tests at both ranges were conducted at absorption temperature of 293 K and at the same gas flow rate.

4.5.1.1 Lower Range

As discussed above, addition of high amount of MEG drastically increases the dynamic viscosity of the solution (Table 4.4). Therefore, it is important to start the test at a lower range to minimise the effect of physical properties on the absorption process. Absorption in 2 v/v% MEG would be a suitable starting point as its effect on dynamic viscosity is minimal, while concentration of MEG is relatively high, sufficient for the reaction to occur.

Fig. 4.8 (a) and (b) show the measured absorbed concentration of $HgCl_2$ in liquid and calculated $HgCl_2$ absorbed per unit gas/liquid interface area as a function of absorption time at 293 K. The results in Fig. 4.8 (a) and (b) show that at 2 v/v% MEG concentrations, temperature of 293 K, the absorbed concentration of $HgCl_2$ increased with absorption time linearly. The result follows the same trend as those in water and NaCl solutions in section 4.2 and 4.4.2 respectively. The absorption flux in pure water and 2v/v% MEG solution were calculated as explained in section 4.2 and the results are given in Fig. 4.8 (c). The results in Fig. 4.8 (c) show that the absorption flux of $HgCl_2$ in water is slightly (8%) higher than in 2 v/v% MEG solution. The calculated enhanced factor E using the measured data shows a low value of 0.91. As value of E is expected to be ≥ 1, the discrepancy can be contributed from experimental errors and/or effect of physical properties change in the liquid phase. The results in Table 4.4, show that changes in viscosity and diffusivity of the used liquids were less than 5%. These results suggest that experimental errors and the change of physical properties of the liquid phase were responsible for the unexpected result (E = 0.91).

Having said that, the estimated value shows that E is very close to 1, indicating that chemical reaction enhanced effect of MEG on absorption of $HgCl_2$ unable to be detected for the lower range tests.

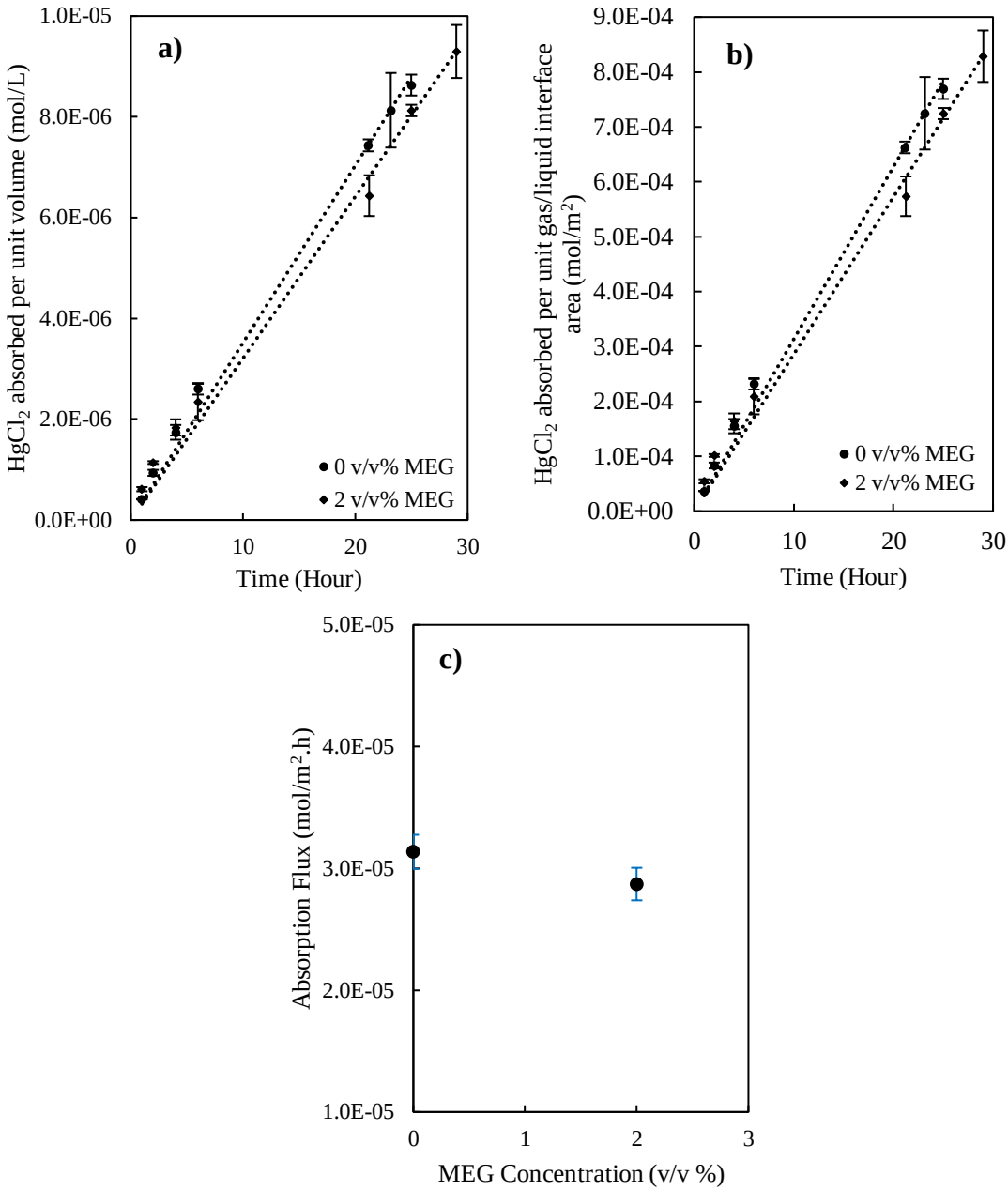

Fig. 4.8 (a) Measured Concentration of $HgCl_2$ in Liquid Absorbed Overtime (b) $HgCl_2$ in Liquid Absorbed per Unit Gas/Liquid Interface Area (c) Calculated absorption flux at Gas Concentration of 2400 ± 216 ng Hg/L, gas flow rate of 500 ml /min, Absorbing

Liquid of 700 ml of MEG Solutions (0 and 2 v/v%) and Temperature of 293 K. Error Bars Were Calculated After 3-5 Independent Experiments.

4.5.1.2 Higher Range

It is expected that at higher $HgCl_2$ and MEG concentration, the reaction between the two compounds will be more significant, resulting in larger E value. This expectation should occur if the reaction between $HgCl_2$ and MEG follows first or higher order. Should the reaction follow zero-order, the enhancement of reaction will be independent of the concentrations of $HgCl_2$ and MEG. In order to increase the likelihood of chemical reaction enhanced absorption to occur, the concentration of both MEG and $HgCl_2$ gas were increased to 10 and 30 v/v% and 4500 ± 445 ng Hg/L respectively to study the effect of MEG on $HgCl_2$ absorption.

Fig. 4.9 (a) and (b) show the measured absorbed concentration of $HgCl_2$ in liquid and calculated $HgCl_2$ absorbed per unit gas/liquid interface area as a function of absorption time at 293 K. The results shown in Fig. 4.9 (a) and (b) show linear increment of $HgCl_2$ absorbed in 2 different MEG concentrations with absorption time, which is consistent with the results presented in previous sections in this chapter. The absorption flux as a function of MEG concentrations was calculated following the previous sections and the results are given in Fig. 4.9 (c).

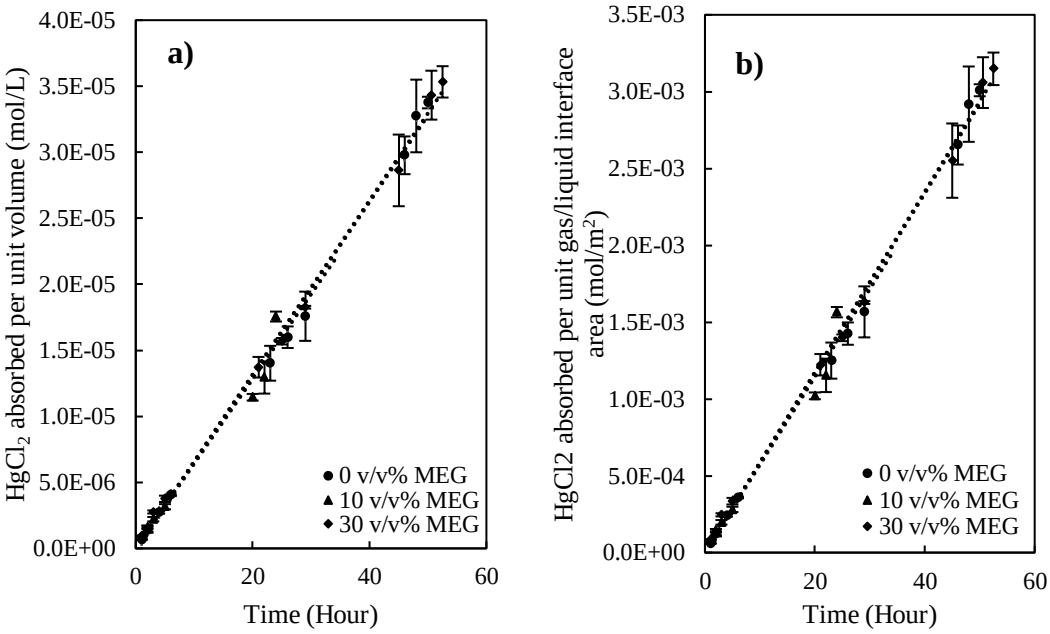

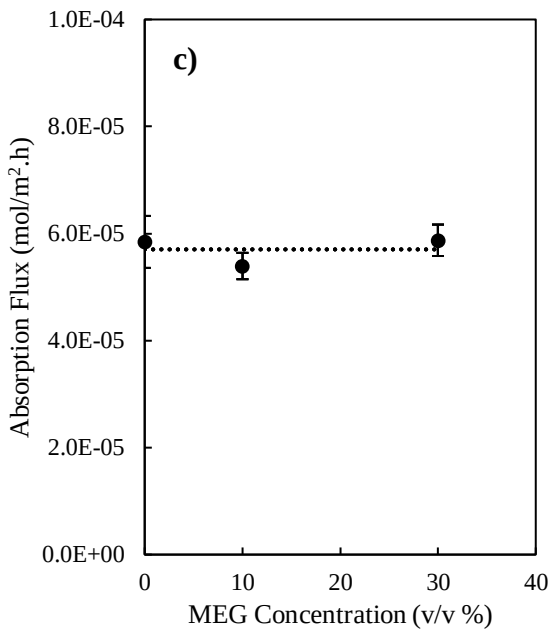

Fig. 4.9 (a) Measured Concentration of $HgCl_2$ in Liquid Absorbed Overtime (b) Calculated $HgCl_2$ in Liquid Absorbed per Unit Gas/Liquid Interface Area (c) Calculated Absorption Flux at Gas Concentration of 4500 ± 445 ng Hg/L, Gas Flow Rate of 500 ml/min, Absorbing Liquid of 700 ml MEG Solutions (0, 10 and 30 v/v %), and Temperature of 293 K. Error Bars Were Calculated After 3-5 Independent Experiments.

Despite performing the test at higher chemical concentrations, the results from Fig. 4.9 (c) show similar absorption flux of $HgCl_2$ in both water and in 10 and 30 v/v% MEG solution (agreement to within 4.7%). A possible reason for this could be due to the concentration of MEG introduced to the system. It has been widely studied that liquid viscosity has an impact on the overall gas-liquid mass transfer through its effect on the hydrodynamic condition of the reactor. Viscosity has a direct correlation to the thickness of the liquid film (according to the Two Film theory), thus affecting the turbulence in the liquid phase as well as diffusivity at the gas-liquid interface [51, 52]. As viscosity of the liquid increases, boundary layer becomes thicker, increasing the mass transfer resistance at the liquid film and making it harder for the gas to penetrate to the liquid body. However, as the liquid viscosity remain considerably the same (refer to Table 4.4) when 2 v/v% MEG was added, its effect on the overall absorption flux of $HgCl_2$ in water cannot be seen.

As explained above, the increase in liquid phase viscosity has an impact on lowering the mass transfer rate, but the results from Fig. 4.9 (c) suggest otherwise. There is however a special case, for when absorption is controlled by gas film (which is true for $HgCl_2$-Water system, section 4.2), it has been reported by several authors that no effect on absorption rate were observed when liquid viscosity was increased within the range of 1 to 4 cP [53-55]. If viscosities were increased further, a reduction in absorption rate will be noticed [53]. This effect was attributed by the increased effect of liquid diffusivity, making the absorption to be controlled by the liquid film instead. The MEG concentration used in this work increased the viscosity up to 2.34 times (Table 4.4); the condition in which the absorption is still heavily controlled by the gas film resistance. The effect noticed hence suggest that the absorption of $HgCl_2$ into solution of 30 v/v% MEG in water is governed by gas film-controlled absorption and not enhanced by chemical reaction.

Other than viscosity, another physical parameter that has been reported to affect the absorption process is surface tension as when viscosity of solution increases, its surface tension decreases instead [42]. In both spray and bubble contactor, surface tension has been reported to have a positive effect on absorption rates of several gases in water of increasing viscosity [55, 56]. This phenomenon was caused by an increase in surface area of contact as the size liquid droplets and bubbles decreased correspondingly with surface tension. However, as the reactor system used in this test is a flat surface with constant surface area, this enhancement effect should be minimal.

Table 4.5 Effect of Gas Concentration and MEG Concentration on Absorption Flux of $HgCl_2$ in Water

MEG Concentration (v/v %)	**$HgCl_2$ Gas Concentration (ng Hg/L gas)**	**Absorption Flux ($mol/m^2.h$)**	**E Factor**
0	2400	3.14×10^{-5}	-
2	2400	2.87×10^{-5}	0.91
0	4500	5.84×10^{-5}	-
10	4500	5.39×10^{-5}	0.92
30	4500	5.87×10^{-5}	1.01

Table 4.5 shows the results from both ranges of concentration from Fig. 4.8 (c) and Fig. 4.9 (c) compiled and E factor calculated. The data from Table 4.5 reveals that the overall absorption flux of $HgCl_2$ into liquid was increased when the concentration of the feed gas was increased from 2400 to 4500 ng Hg/L gas. This result is as expected

as higher concentration gradient will promote mass transfer from the gas to the liquid side. Furthermore, $HgCl_2$ is classified to be a very soluble gas, as the absorption rate is sensitive with the changes in the gas side [25]. In addition, from Table 4.5, the measured E factor for 2, 10 and 30 v/v% MEG show value of 0.91, 0.92 and 1.01 respectively, which further indicate the very minimal to no chemical reaction enhancement absorption of $HgCl_2$ in MEG solution.

4.5.2 Effect of Temperature

The effect of temperature on the absorption of $HgCl_2$ gas in water was investigated under constant MEG concentration (30 v/v %), gas flow rate (500 ml/min) and gas concentration of 4500 ng Hg/L at varying temperatures (283-333 K) of the absorbing solutions. Fig. 4.10 (a) and (b) show the measured concentration of absorbed $HgCl_2$ in liquid and the calculated $HgCl_2$ absorbed per unit gas/liquid interface area as a function of absorption at different temperatures.

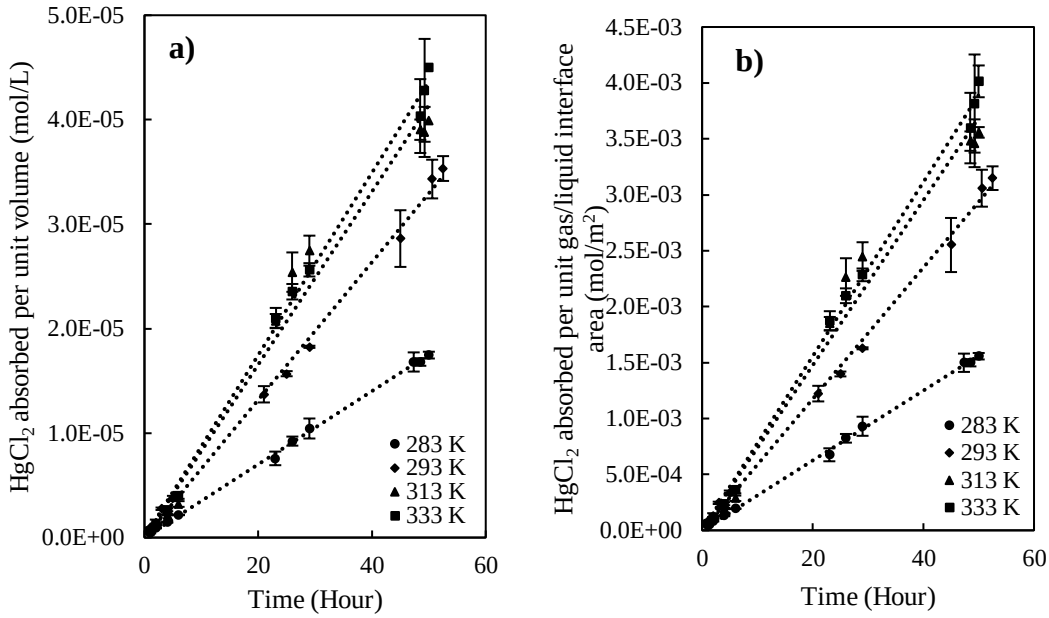

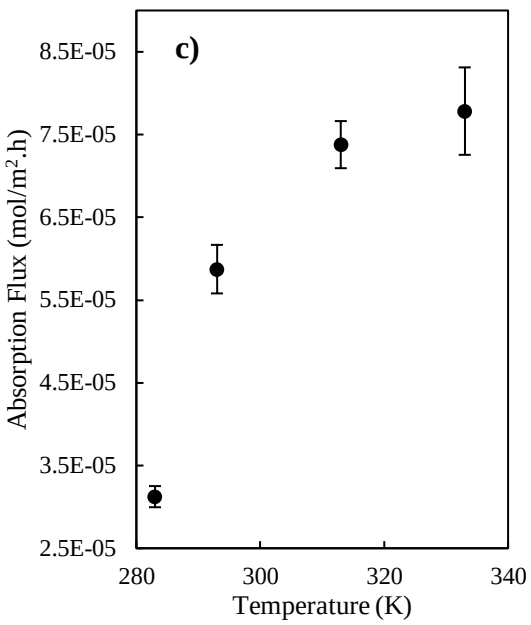

Fig. 4.10 (a) Measured Concentration of $HgCl_2$ in Liquid Absorbed Overtime (b) $HgCl_2$ in Liquid Absorbed per Unit Gas/Liquid Interface Area (c) Calculated Absorption Flux at Gas Concentration of 4500 ± 445 ng Hg/L, Gas Flow Rate of 500 ml /min, Absorbing Liquid of 700 ml of 30 v/v% MEG Solutions and Temperature of 283-333 K. Error Bars Were Calculated After 3-5 Independent Experiments.

The effect of temperature on the absorption of $HgCl_2$ into 30 v/v% MEG solution show a consistent trend with the $HgCl_2$ absorption in water and 3.5 wt. % NaCl solution shown in Fig. 4.1 and Fig. 4.5 respectively, whereby the absorption rate increases with the increasing absorption temperature, the effect is less pronounced compared with that of absorption at lower temperature range (283-313 K). Using the same calculation method discussed above, the absorption flux of $HgCl_2$ in aqueous MEG solution at different temperature is calculated and given in Fig. 4.5(c).

4.5.3 Investigation of Reaction between $HgCl_2$ and MEG

4.5.3.1 ICP-MS and FIMS Method

Investigation was conducted to confirm the possibility of organic-Hg compounds in liquid, formed from the reaction between $HgCl_2$ and MEG. The liquid samples after 50 hours of absorption were analysed using two different analysis methods and compared. The two analysis methods were FIMS and ICP-MS, which the use of latter has been increasing in the past years for its ability to detect trace amount of mercury down to sub parts per billion and parts per trillion level [57-59]. The MEG

concentration selected for this comparison study is of lower concentration, 2 v/v % to minimise signal interferences due to effect of sample matrix [11]. To further ensure matrix effect is diminished during sample analysis, the mercury calibration standards were prepared with similar matrix as the samples (MEG and acid concentrations). Details of the procedure are further explained in Chapter 3, section 3.5

ICP-MS quantify the total amount of mercury in the sample by dissociating mercury molecules then ionizing the sample with inductively couple plasma at a temperature of around 6273 K before directing into a mass spectrometer for detection. This analysis method means that regardless of mercury species present in the sample, measurements obtained from the instrument would quantify the total dissolved Hg in the sample. In comparison with FIMS, which is based on CV-AAS method, the analysis requires addition of oxidants and acids as a pre-treatment step to ensure both organic and inorganic mercury species are fully oxidised to its ionic form (Hg^{+} and Hg^{2+}). In the case with organic mercury, the bond dissociation energy between Hg-C such as Hg^{+}-CH_3, H_3C-$HgCH_3$, H_5C_6-HgC_6H_5 (285±3, 239±6.3 and 285 kJ/mol respectively) [60, 61] are much higher in comparison with Hg-Cl, Hg-Hg and Hg^{+}-Hg (92±0.92, 8.10±0.18 and 134 kJ/mol respectively) [60, 61]. This difference in bond energy hence explains why organic mercury analysis require addition of strong oxidants and acids to completely break the Hg-C bonds [62]. Following the pre-treatment step, addition of a reducing agent will evolve all ionic forms as gaseous Hg^{0} for detection.

This aspect of FIMS would yield lower results if organic mercury are present in the sample as the Hg-C bond will be retained and less Hg^{0} would be detected if addition of strong oxidants pre-treatment step is omitted [63]. Taking advantage of the different mechanism of the two analysis techniques, elimination of the oxidation step prior to analysis using FIMS and comparing the results to the total dissolved Hg obtained from ICP-MS would give information to whether there are any organic bound mercury present in the samples from the absorption study.

Comparison of the total dissolved Hg and free ionic Hg present in the samples from $HgCl_2$ absorption into 2 v/v % MEG solution from ICP-MS and FIMS respectively are given in Fig. 4.11. It can be seen in Fig. 4.11 that the data points obtained from the sample analysis using ICP-MS and FIMS are very close to each other. If chemical reactions producing organic Hg were to occur in the system, the FIMS readings would

be lower in comparison to the ICP-MS readings as some $HgCl_2$ would be consumed to produce an organic mercury compound. This would also mean that there would be additional mercury detected by the ICP-MS. Based on the results from Fig. 4.11, it is clear that the total dissolved Hg in the sample is made up mostly of free ionic Hg. This means that no organic bound mercury present in the product from $HgCl_2$ and MEG if chemical reaction were to occur.

The result observed is also in agreement with those discussed in section 4.5. This suggest the likelihood of metal complexes formation reaction between $HgCl_2$ and MEG which have an absence of Hg-C bonding within their structure [47, 50]. Having said that, the result in this section cannot fully conclude the presence of these metal complexes as ICP-MS and FIMS are unable to detect these metal complexes.

Although it is quite likely that $HgCl_2$ will react with MEG to form metal complexes, the E value calculated in section 4.5.1.1 and 4.5.1.2 is 1. The reaction described in section 4.5 is suspected to be very slow to enhance the absorption process for the test condition used in this work. The small concentration of $HgCl_2$ in gas relative to the MEG concentration might be the cause of the minimal enhancement calculated in section 4.5.1.1 and 4.5.1.2. The small concentration of Hg detected in the liquid body (< 2 ppm) might also play a contributing factor to the small enhancement observed.

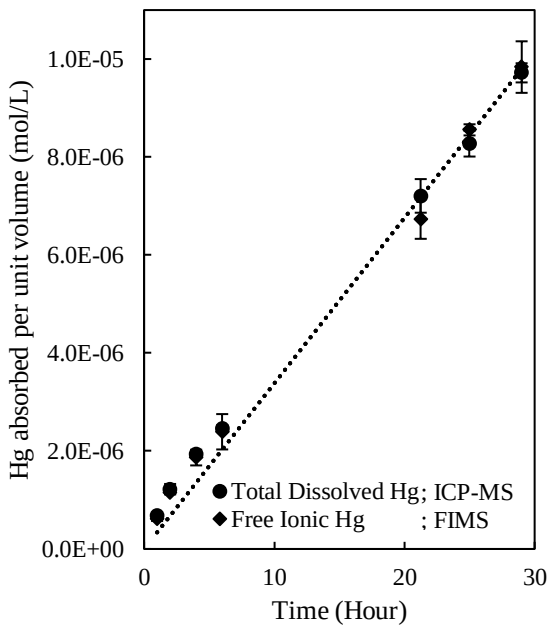

Fig. 4.11 Comparison of Amount of Total Dissolved and Free Ionic Hg from Absorption of $HgCl_2$ Gas into 2 v/v% MEG Solution at Gas Concentration of 2400 ± 216 ng Hg/L, Gas Flow Rate of 500 ml /min, Absorbing Liquid of 700 ml of 2 v/v%

MEG Solution and Temperature of 293 K. Error Bars Were Calculated After 3-5 Independent Experiments.

4.5.3.2 Optical Analysis Method

FTIR

To further rectify the uncertainty of $HgCl_2$ and MEG reaction, solutions of 100 ppb $HgCl_2$ in 2 and 30 v/v% MEG were prepared and heated to 40°C for 5 hours to promote the reaction. The solutions containing 100 ppb $HgCl_2$ in 2 and 30 v/v% MEG respectively were analysed using FTIR to characterize the functional groups present in the solutions (detailed procedure as described in Chapter 3). Solutions of 2 and 30 v/v% MEG without $HgCl_2$ were also analysed to identify any new functional groups that might have formed when $HgCl_2$ is present. The results of the FTIR spectrum can be seen in Fig. 4.12 (a) and (b) for 2 v/v% and 30 v/v% MEG respectively.

The spectrum shown in Fig. 4.12 (a) and (b) depict a typical MEG spectrum reported [64]. The peak at 3200-3600 cm^{-1} (I at Fig. 4.12 (a) and (b)) in both spectrums represents the O-H functional group. As MEG concentration increased from 2 to 30 v/v%, peaks at 2850-300 cm^{-1} (II at Fig. 4.12 (a) and (b)) and 1041-1044 cm^{-1} (III at Fig. 4.12 (a) and (b)) becomes more prominent. These peaks represent the C-H and C-O functional groups respectively. Comparison of the spectrum of samples containing $HgCl_2$ in 2 v/v% and 30 v/v% MEG show no additional functional groups that are formed during the absorption process. A summary of the detected functional groups based on the peaks identified in Fig. 4.12 (a) and (b) are detailed in Table 4.6.

The results from Fig. 4.12 (a) and (b) are not very conclusive in identifying the possible product formed from reaction of $HgCl_2$ and MEG. This could be a possibility that a complex containing the same functional group as MEG was formed, thus the use of FTIR was not able to detect this product formed.

Table 4.6 Functional Groups Identified in Samples Containing 100 ppb $HgCl_2$ and 2-30 v/v% MEG

Peak Wavelength (cm^{-1})	Functional Group
3200-3600	O-H
2850-3000	C-H
1041-1044	C-O

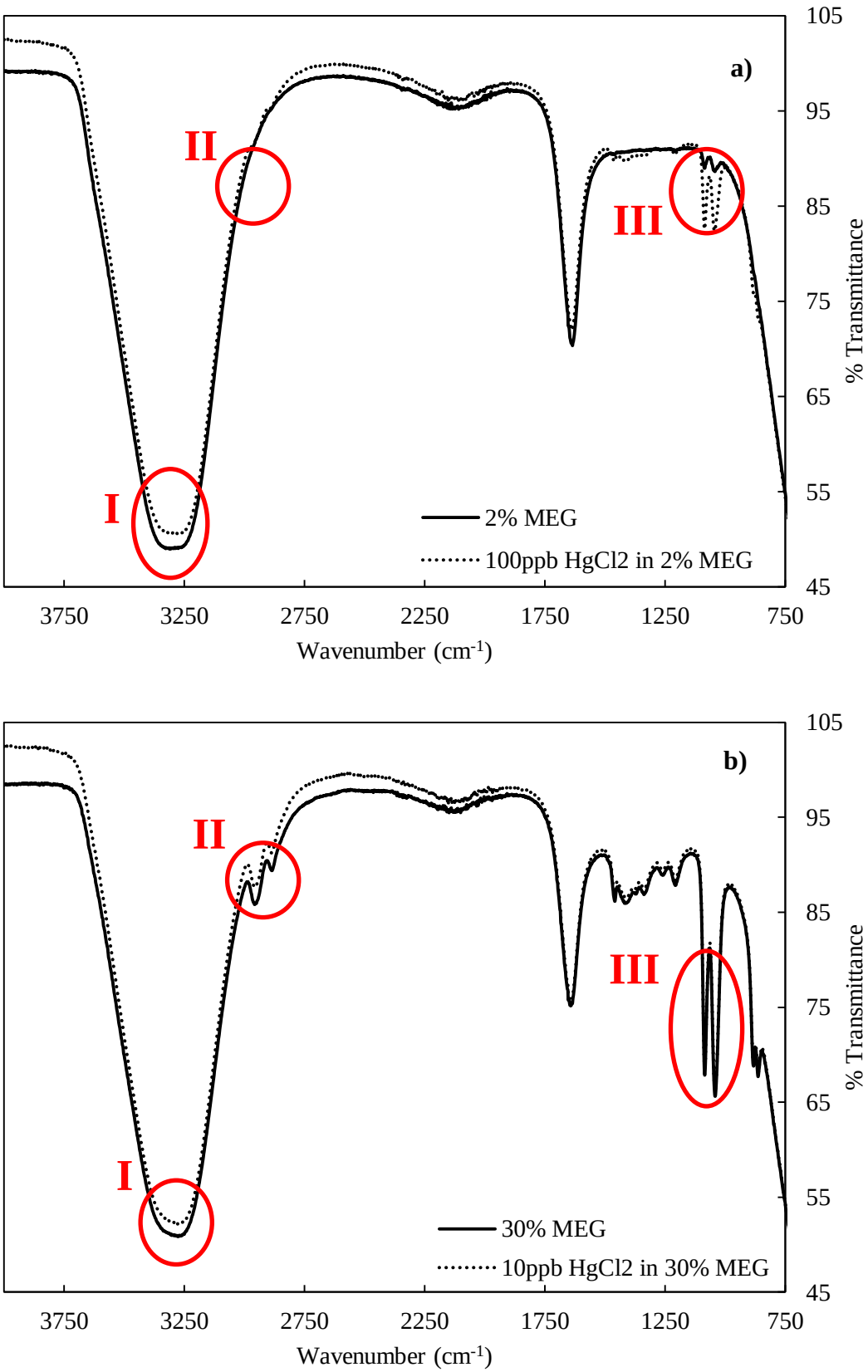

Fig. 4.12 Comparison of FTIR Spectrum of Diluted MEG Solution with 100 ppm $HgCl_2$ at (a) 2% MEG (b) 30% MEG Concentration

Raman Spectroscopy

Since FTIR was not able to detect any additional peaks, samples containing 0.1 wt% $HgCl_2$ in 50 v/v% MEG solution was analysed using Raman spectroscopy. Raman spectroscopy is a more sensitive optical technique compared to FTIR and it has been proven to be able to detect peaks of $HgCl_2$ and MEG in solutions [65, 66]. Higher concentrations of $HgCl_2$ and MEG were prepared for this analysis to improve the likelihood of identifying the additional peak from the reaction between $HgCl_2$ and MEG. To identify the extent of product formation using the effect of temperature on the reaction, the prepared solution was divided into two. After mixing $HgCl_2$ with MEG, one of the samples was placed in the fridge immediately at 275-278 K to slow down any reactions. At the same time, the second solution was heated to 50°C and left overnight to emulate the absorption study and promote the reactions. Summary of the sample conditions and treatment is provided in Table 4.7.

Table 4.7 Treatment of Samples Containing 0.1 wt. % $HgCl_2$ and 50 v/v% MEG

Sample	Treatment
1	Mixed and placed in fridge immediately (275-278 K)
2	Mixed and heated at 50°C overnight

The results of the Raman spectrum of the two samples are represented in Fig. 4.13 (a) and (b). The functional groups that are corresponding to the peaks in Fig. 4.13 (a) and (b) have been summarised in Table 4.8. Results from Table 4.8 show that majority of the functional group peaks present in both spectra are very similar to the peaks of 50 v/v% MEG available in the work by Krishnan and Krishnan [65]. It is to be noted that peak at 348 cm^{-1} that exists in both Sample 1 and Sample 2 were not present in the spectrum of 50 v/v% MEG. The peak at 348 cm^{-1} is however, present in the spectrum of 100% MEG solution, corresponding to C – C – O group. As the concentration of MEG further is reduced in solution, this peak becomes non-existent in the over spectrum [65].

One possibility could be that the peak at 348 cm^{-1} could represent $HgCl_2$. K. V. Krishna Rao studied the Raman spectrum of $HgCl_2$ in several states (dissolved, molten, gas and crystal) and has reported $HgCl_2$ peak to be between the range of 312-381 cm^{-1} [66]. Since the peak observed in the samples is within the range, it is quite likely to be $HgCl_2$. The small peak height might be due to the small concentration of $HgCl_2$ being present in the samples.

The results obtained from the Raman spectrum show only the peaks of MEG and $HgCl_2$ to be present in Sample 1 and 2. No additional peaks that might represent the product formed could be seen. Therefore, based on the characterization results using Raman and FTIR, the reactions between $HgCl_2$ and MEG was not present within the given experimental condition used in this work. Henceforth, this further explains the no enhancement effect of MEG observed during the absorption process.

Table 4.8 Functional Groups Identified in Samples Containing 0.1 wt. % $HgCl_2$ and 50 v/v% MEG

Peak Wavenumber (cm^{-1})	**Functional Group**
96 - 118	Hydrogen bonding
480	C – C – O
521	C – C – O
865	C – C
1049	C – O
1085	C – O
1275	CH_2
1462	CH_2
2885	C – H
2939	C – H

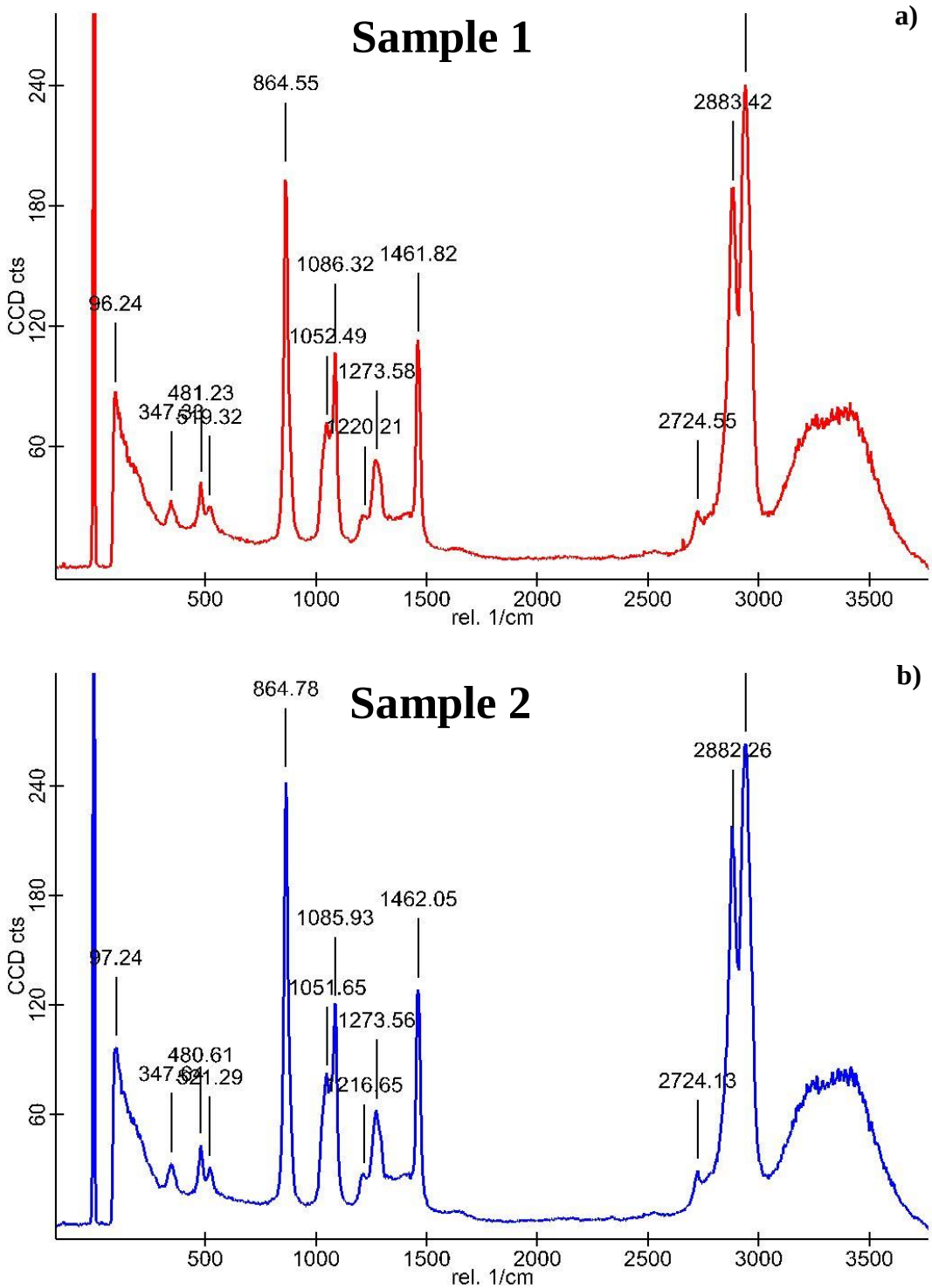

Fig. 4.13 Raman Spectrum of Solutions of 0.1 wt.% $HgCl_2$ in 50 v/v% MEG in (a) Sample 1 (b) Sample 2

4.6 Summary

This work evaluated the absorption kinetics of $HgCl_2$ gas in water, aqueous NaCl solutions and MEG solutions. From the results presented, the following conclusions can be drawn:

- Two-film theory can be used to explain the studied absorption process. Absorption of $HgCl_2$ into water is controlled by the gas phase resistance. The mass transfer coefficient k_G increases with increasing absorption temperature significantly but not sensitive with the $HgCl_2$ concentration in the gas phase.
- The mechanism of the studied reaction is proposed and the rate of reaction between $HgCl_2$ and NaCl is controlled by the formation rate of the $HgCl_3^-$ ion, which is formed from $HgCl_2$ and Cl^-. The rate law of this reaction follows second order whereby it is first order with respect to each reactant, namely $HgCl_2$ and Cl^-.
- Using two-film theory, the reaction rate constant k_2 is found and can be represented as:

$$k_2 = 1.09 \times 10^9 \exp\left(\frac{-123.32\ \mathrm{kJ/mol}}{RT}\right)$$

- Absorption of $HgCl_2$ into water in the presence of MEG (2 – 30 v/v %) are comparable to the absorption in water and has no significant enhancement effect to the absorption flux. The absorption process shows no effect when viscosity was increased due to the addition of MEG but was more sensitive with regards to the $HgCl_2$ feed gas concentration. The absorption process depicts characteristic of physical absorption controlled by the gas film.
- E factor calculated for absorption of $HgCl_2$ in 2 – 30 v/v% yield a value of 1, indicating no chemical reaction enhanced absorption can be found under the experimental condition in this work.
- Organic-Hg species were not detectable after 30 hours of absorption, suggesting that $HgCl_2$ react with MEG to form non-organically bound metal complexes. This reaction however, cannot be detected within the experimental conditions used in this study.

4.7 Reference

[1] Gallup, Darrell L. 2014. Removal of mercury from water in the petroleum industry. Paper read at 21st International Petroleum Environmental Conference

[2] V.Hemmingsen, Pål, RoderickBurgass, Karen Schou Pedersen, Keijo Kinnari, and Henrik Sørensen. 2011. "Hydrate temperature depression of MEG solutions at concentrations up to 60 wt%. Experimental data and simulation results." *Fluid Phase Equilibria* no. 307 (2):175-179. doi: 10.1016/j.fluid.2011.05.010.

[3] Cha, Minjun, Kyuchul Shin, Juneyoung Kim, Daejun Chang, Yutaek Seo, Huen Lee, and Seong-Pil Kang. 2013. "Thermodynamic and kinetic hydrate inhibition performance of aqueous ethylene glycol solutions for natural gas." *Chemical Engineering Science* no. 99:184-190. doi: 10.1016/j.ces.2013.05.060.

[4] Takeuchi, Yasuhiromi, Yoshio Nakayama, Satoru Sugita, Susumu Okino, and Shintaro Honjo. 2007. System and method for removing mercury in exhaust gas edited by Mitsubishi Heavy Industries Ltd.

[5] Zhao, Lingbing. 1997. *Mercury Absorption in Aqueous Solutions* The University of Texas, Austin.

[6] Iverfeldt, Åke, and Oliver Lindqvist. 1984. "The Transfer of Mercury at the Air/Water Interface." In *Gas Transfer at Water Surfaces*, 533-538. Springer Netherlands.

[7] Clever, H. Lawrence, Susan A. Johnson, and M. Elizabeth Derrick. 1985. "The Solubility of Mercury and Some Sparingly Soluble Mercury Salts in Water and Aqueous Electrolyte Solutions." *Journal of Physical and Chemical Reference Data* no. 14 (3).

[8] Sommar, Jonas, Oliver Lindqvist, and Dan Strömberg. 2000. "Distribution Equilibrium of Mercury (II) Chloride between Water and Air Applied to Flue Gas Scrubbing." *Journal of the Air & Waste Management Association* no. 50 (9):1663-1666. doi: 10.1080/10473289.2000.10464192.

[9] Bernard, L., K. Awitor, J. Badaud, O. Bonnin, B. Coupat, J. Fournier, and P. Verdier. 1997. "D´etermination de la pression de vapeur de HgCl2 par la m´ethode d'effusion de Knudsen." *Journal de Physique III* no. 7 (2):311-319. doi: 10.1051/jp3:1997124.

[10] Sabri, Y. M., S. J. Ippolito, J. Tardio, S. Bee Abd Hamid, and S. K. Bhargava. 2015. "Mercury Migration and Speciation Study during Monoethylene Glycol Regeneration Processes." *Industrial & Engineering Chemistry Research* no. 54 (19):5349-5355. doi: 10.1021/acs.iecr.5b00492.

[11] Sabri, Y.M., S.J. Ippolito, J. Tardio, P.D. Morrison, and S.K. Bhargava. 2015. "Studying mercury partition in monoethylene glycol (MEG) used in gas facilities." *Fuel* no. 159:917-924. doi: 10.1016/j.fuel.2015.07.047.

[12] Gallup, Darrell L., Dennis J. O'Rear, and Ron Radford. 2017. "The behavior of mercury in water, alcohols, monoethylene glycol and triethylene glycol." *Fuel* no. 196:179-184. doi: 10.1016/j.fuel.2017.01.100.

[13] Khalifa, Mansour, and Leo Lue. 2017. "A group contribution method for predicting the solubility of mercury." *Fluid Phase Equilibria* no. 432:76-84. doi: doi.org/10.1016/j.fluid.2016.10.025.

[14] Gallup, Darrell L., and N. S. Bloom. 2010. On the Solubility of Mercury in Liquid Hydrocarbons. Paper read at AIChE Spring Meeting and Global Congress on Process Safety, 22 March 2010.

[15] Kozin, Leonid F, and Steve Hansen. 2013. "Mercury Handbook: Chemistry, Applications and Environmental Impact." In: Royal Society of Chemistry.

[16] Lewis, W. K., and W. G. Whitman. 1924. "Priciples of Gas Absorption " *Industrial & Engineering Chemistry* no. 16 (12):1215-1220. doi: 10.1021/ie50180a002.

[17] Whitman, Walter G. 1923. "The two-film theory of gas absorption." *International Journal of Heat and Mass Transfer* no. 5 (5):429-433. doi: 10.1016/0017-9310(62)90032-7.

[18] Danckwerts, Peter Victor. 1970. *Gas-liquid reactions*. New York: McGraw-Hill Book Co

[19] Elk, E. P. van, P.C. Borman, J. A. M. Kuipers, and G. F. Versteeg. 2000. "Modelling of gas–liquid reactors — implementation of the penetration model in dynamic modelling of gas–liquid processes with the presence of a liquid bulk." *Chemical Engineering Journal* no. 76:223-237.

[20] Froment, Gilbert F., and Kenneth B. Bischoff. 1990. *Chemical reactor analysis and design*: New York : Wiley

[21] Sander, R. 2015. "Compilation of Henry's law constants (version 4.0) for water as solvent." *Atmospheric Chemistry and Physics* no. 15:4399-4981. doi: 10.5194/acp-15-4399-2015.

[22] Edwards, Jack R., Ravi K. Srivastava, and James D. Kilgroe. 2011. "A Study of Gas-Phase Mercury Speciation Using Detailed Chemical Kinetics." *Journal of the Air & Waste Management Association* no. 51 (6):869-877. doi: 10.1080/10473289.2001.10464316.

[23] Wilke, C. R., and Pin Chang. 1955. "Correlation of diffusion coefficients in dilute solutions " *AIChE Journal* no. 1 (2):264-270.

[24] Levenspiel, Octave, and J.H. Godfrey. 1974. "A gradientless contactor for experimental study of interphase mass transfer with/without reaction." *Chemical Engineering Science* no. 29 (8):1723-1730. doi: 10.1016/0009-2509(74)87030-2.

[25] Ibusuki, Takashi, and Viney P. Aneja. 1984. "Mass Transfer of NH_3 into Water at Environmental Concentrations " *Chemical Engineering Science* no. 39 (7-8):1143-1155. doi: 10.1016/0009-2509(84)85076-9.

[26] Ozbek, H., J. A. Fair, and S. L. Phillips. 1971. "Viscosity of Aqueous Sodium Chloride Solutions from 0-150ºC." *American Chemical Society 29th Southeast Regional Meeting*

[27] Sharqawy, Mostafa H., John H. Lienhard V, and Syed M. Zubair. 2010. "Thermophysical properties of seawater: A review of existing correlations and data." *Desalination and Water Treatment* no. 16:354-380.

[28] Powell, Kipton J., Paul L. Brown, Robert H. Byrne, Tamas Gajda, Glenn Hefter, Staffan Sjoberg, and Hans Wanner. 2005. "Chemical Speciation of Environmentally Significant Heavy Metals with Inorganic Ligands Part1: The Hg2+-Cl-, OH-, CO32-, SO42- and PO43- Aqueous Systems " *Pure Appl. Chem* no. 77 (4):739-800. doi: 10.1351/pac200577040739.

[29] Ma, Yongpeng, Haomiao Xu, Zan Qu, Naiqiang Yan, and Wenhua Wang. 2014. "Absorption characteristics of elemental mercury in mercury chloride solutions." *Journal of Environmental Sciences* no. 26 (11):2257-2265. doi: 10.1016/j.jes.2014.09.011.

[30] Sjöberg, Staffan. 1977. "Metal Complexes with Mixed Ligands. 11. The Formation of Ternary Mononuclear and Polynuclear Mercury(II) Complexes in the System Hg2+ -- Cl- -- OH-. A Potentiometric Study in 3.0 M (Na)ClO4,

Cl Media." *Acta Chemica Scandinavica A* no. 31:705-717. doi: 10.3891/acta.chem.scand.31a-0705.

[31] Sjöberg, Staffan. 1977. "Metal Complexes with Mixed Ligands. 12. A Potentiometric Study of the Systems Hg2+ -- Imidazole, Hg2+ -- OH- -- Imidazole and Hg2+ -- Cl- -- Imidazole in 3.0 M (Na)ClO4, Cl Media." *Acta Chemica Scandinavica A*:718-728. doi: 10.3891/acta.chem.scand.31a-0718.

[32] Eigen, Manfred, and Ralph. G. Wilkins. 1965. "The Kinetics and Mechanism of Formation of Metal Complexes " *Advances in Chemistry Series* no. 49 (3):55-80. doi: 10.1021/ba-1965-0049.ch003.

[33] Homeyer, and Ritsert. 1888. "Ueber die Löslichkeit des Sublimats in Kochsalzlösungen." *Pharmazeutische Zeitung* no. 33:738.

[34] Herz, W., and W. Paul. 1913. "Die Löslichkeit der Quecksilberhaloide in Haloidsalzlösungen." *Zeitschrift für anorganische und allgemeine Chemie* no. 82 (1):431-437. doi: 10.1002/zaac.19130820135.

[35] Seidell, Atherton. 1919. "Solubilities of Inorganic And Organic Compounds." In. New York: D. Van Nostrand Company

[36] Kierzkowska-Pawlak, Hanna. 2012. "Determination of Kinetics in Gas-Liquid Reaction Systems. An Overview." *Ecological Chemistry and Engineering S* no. 19 (2):175-196. doi: 10.2478/v10216-011-0014-y

[37] Levenspiel, Octave. 1999. *Chemical Reaction Engineering*. New York John Wiley & Sons

[38] Heyrovska, Raji. 1997. "Equations for Densities and Dissociation Constant of NaCl(aq) at 25°C from “Zero to Saturation” Based on Partial Dissociation." *Journal of The Electrochemical Society* no. 144 (7):2380-2384. doi: 10.1149/1.1837822.

[39] Zhao, LingBing, and Gary T. Rochelle. 1996. "Hg Absorption in Aqueous Permanganate " *AIChE Journal* no. 42 (12):3559-3562.

[40] Krishnakumar, Balaji, and Joseph J. Helble. 2012. "Determination of transition state theory rate constants to describe mercury oxidation in combustion systems mediated by Cl, Cl2, HCl and HOCl." *Fuel Processing Technology* no. 94 (1):1-9. doi: 10.1016/j.fuproc.2011.09.015.

[41] Auzmendi-Murua, Itsaso, Álvaro Castillo, and Joseph W. Bozzelli. 2014. "Mercury Oxidation via Chlorine, Bromine, and Iodine under Atmospheric Conditions: Thermochemistry and Kinetics." *Journal of Physical Chemistry A* no. 118 (16):2959-2975. doi: 10.1021/jp412654s.

[42] Wang, Peiming, Jerzy J. Kosinski, Andrzej Anderko, Ronald D. Springer, Malgorzata M. Lencka, and Jiangping Liu. 2013. "Ethylene Glycol and Its Mixtures with Water and Electrolytes: Thermodynamic and Transport Properties." *Industrial & Engineering Chemistry Research* no. 52:15968-15987. doi: 10.1021/ie4019353.

[43] Haslam, R. T., R. L. Hershey, and R. H. Keen. 1924. "Effect of gas velocity and temperature on rate of absorption " *Industrial and Engineering Chemistry* no. 16 (12):1224-1230. doi: 10.1021/ie50180a004.

[44] Zhang, JianBin, PengYan Zhang, Kai Ma, GuoHua Chen, and XiongHui Wei. 2008. "Hydrogen bonding interactions between ethylene glycol and water: density, excess molar volume, and spectral study." *Science in China Series B: Chemistry* no. 51 (5):420-426. doi: 10.1007/s11426-008-0045-0.

[45] Clifton, James R., Walter J. Rossiter Jr, and Paul W. Brown. 1985. "Degraded Aqueous Glycol Solutions: pH Values and The Effects of Common Ions on Suppressing pH Decreases." *Solar Energy Materials* no. 12:77-86.

[46] Jr, Walter J. Rossiter, McClure Godette, Paul W. Brown, and Kevin G. Galuk. 1985. "An Investigation of the Degradation of Aqueous Ethylene Glycol and Propylene Glycol Solutions using Ion Chromatography." *Solar Energy materials* no. 11:455-467.

[47] Knetsch, D., and L. Groeneveld. 1973. "Alcohols as Ligands. III. Complexes of Ethylene Glycol with some Divalent Metal Halides." *Inorganica Chimica Acta* no. 7 (1):81-87.

[48] Dean, Phillip A. W. 2009. *Progress in Inorganic Chemistry*. Edited by Stephen J. Lippard. Vol. 24, *The Coordination Chemistry of the Mercuric Halides* John Wiley & Sons.

[49] Bebout, Deborah C. 2006. "Mercury: Inorganic & Coordination Chemistry." *Encyclopedia of Inorganic Chemistry*. doi: 10.1002/0470862106.ia131.

[50] Rogers, Robin D., Andrew H. Bond, and Janice L. Wolff. 2006. "STRUCTURAL STUDIES OF POLYETHER COORDINATION TO MERCURY(II) HALIDES: CROWN ETHER VERSUS POLYETHYLENE GLYCOL COMPLEXATION." *Journal of Coordination Chemistry* no. 29 (4):187-207. doi: 10.1080/00958979308037425.

[51] Song, Di, A. Frank Seibert, and Gary T. Rochelle. 2014. "Effect of liquid viscosity on the liquid phase mass transfer coefficient of packing." *Energy Procedia* no. 63:1268-1286. doi: 10.1016/j.egypro.2014.11.136.

[52] Kadic, Enec, and Theodore J. Heindel. 2010. Mixing Considerations in Stirred Tank Bioreactors When Using Fluid Property Altering Microorganisms. Paper read at ASME 2010 3rd Joint US-European Fluids Engineering Summer Meeting and 8th International Conference on Nanochannels, Microchannels, and Minichannels 1-5 August 2010, at Montreal, Canada

[53] Gerster, J. A. 1960. "Distillation—Theory and Fundamentals." *Industrial & Engineering Chemistry* no. 52 (8):645-653. doi: 10.1021/ie50608a021.

[54] Mehta, V. D., and M. M. Sharma. 1966. "Effect of diffusivity on gas-side mass transfer coefficient " *Chemical Engineering Scienc* no. 21:361-365.

[55] Griffith, Donald Edwin. 1956. *The Effect of Sodium Oleate on the Absorption of Ammonia by Water in a Spray Column* Georgia Institute of Technology

[56] Gómez-Díaz, Diego, and José M. Navaza. 2003. "Effect of Ethylene Glycol on the CO_2/Water Gas-Liquid Mass Transfer Process." *Chemical Engineering & Technology* no. 26 (1):75-80. doi: 10.1002/ceat.200390010.

[57] Pyhtilä, Heidi, Matti Niemelä, Paavo Perämäki, Juha Piispanen, and Liisa Ukonmaanaho. 2013. "The use of a dual mode sample introduction system for internal standardization in the determination of Hg at the ng L−1 level by cold vapor ICP-MS." *Analytical Methods* no. 5:3082-3088. doi: 10.1039/c3ay40275d.

[58] Powell, M. J., E. S. K. Quan, D. W. Boomer, and Daniel R. Wiederin. 1992. "Inductively Couple Plasma Mass Spectrometry with Direct Injection Nebulization for Mercury Analysis of Drinking Water " *Analytical Chemistry* no. 64:2253-2257.

[59] EPA, U.S. 2014. Method 6020B (SW-846): Inductively Coupled Plasma-Mass Spectrometry. (Revision 2).

[60] Dean, John A. 1999. "Lange's Handbook of Chemistry " In: McGraw-Hill, Inc.

[61] Luo, Yu-Ran. 2010. "Bond Dissociation Energies " In *Comprehensive Handbook of Chemical Bond Energies*. Boca Raton, FL: CRC Press.

[62] EPA, U.S. 1974. Method 245.2: Mercury (Automated Cold Vapor Technique) by Atomic Absorption edited by United States Environmental Protection Agency.
[63] El-Awady, Abbas A., Robert B. Miller, and Mark J. Carter. 1976. "Automated method for the determination of total and inorganic mercury in water and wastewater samples." *Analytical Chemistry* no. 48 (1):110-116. doi: 0.1021/ac60365a051.
[64] Linstrom, P. J., and W. G. Mallard. 2005. NIST Chemistry WebBook, NIST Standard Reference Database Number 69.
[65] Krishnan, K., and R. S. Krishnan. 1966. "Raman and infrared spectra of ethylene glycol." *Proceedings of the Indian Academy of Sciences - Section A* no. 64:111-122. doi: 10.1007/BF03047675.
[66] Rao, K. V. Krishna. 1941. "Raman spectrum of mercuric chloride in relation to its structure." *Proceedings of the Indian Academy of Sciences - Section A* no. 14 (5):521-528.

CHAPTER 5:
DYNAMIC SOLUBILITY OF ORGANIC MERCURY IN WATER

5.1 Introduction

In Chapter 4, the dynamic solubility of inorganic mercury; $HgCl_2$ was studied in water, aqueous NaCl and MEG solutions and it was observed that absorption was controlled by gas film due to its highly soluble nature in water. However, other than inorganic mercury, organic mercury has also been reported to be present in the different stages of the oil and gas processes [1-3]. This presence of organic mercury have raise many concerns for the health and safety for workers involved in both maintenance and inspection as well as product quality as organic mercury is known to be more toxic than its inorganic counterparts [2, 4] due to its lipid solubility. Furthermore, when present in the waste stream and released into the environment, organic mercury is known for its persistence in the ecosystem due to its tendency to bioaccumulate and biomagnify in the aquatic systems [5].

Several authors have identified monoalkyl mercury to be the most common species of organic mercury to be detected in gas, water and hydrocarbon phases [2, 5, 6]. Presence of the dialkyl mercury such as dimethyl mercury (DMM), diethyl mercury (DEM) and diphenyl mercury (Ph_2Hg) have been debatable as results obtained are not consistent with each other; some reported dialkyl mercury to be not present in various samples although detection limit of the analysis method was quite low [7-9].

Several authors [9-12] have reported the presence of several dialkyl mercury such as DMM and DEM but reported no Ph_2Hg in their samples. On the other hand, -speciation study by Schickling and Broekaert have found diphenyl mercury in gas condensate [11]. One of the main reasons for the detection problem in the samples, especially in the case of Ph_2Hg is caused by species interconversion. It is well known that Ph_2Hg reacts with $HgCl_2$ and MeHgCl to form phenyl mercuric salts through electrophilic substitution reaction [7, 13]. There is also a high tendency of species conversion in the presence of Hg^0 as the Hg in Ph_2Hg are exchanged with metallic mercury to form Ph_2Hg* and Hg in the presence of organic solvents [14]. Although Ph_2Hg is known to be a more stable organic mercury compound [15], it easily decomposes via photolysis

to form Hg^0 and phenyl radicals [16]. Based these findings, it is of paramount importance to investigate the absorption behaviour of Ph_2Hg into commonly present liquids in the oil and gas processes to further close the knowledge gap on the dynamics of mercury accumulation and distribution. Ph_2Hg being reactive with $HgCl_2$ and is soluble in various organic solvents and hydrocarbons [7, 15, 17], has a high potential of being present in the water and MEG recirculated stream.

Ph_2Hg has been historically known and studied as it is the product of biodegradation of Phenyl mercuric acetate, which was commonly used as a fungicide [18, 19]. Despite this, to the best of our knowledge, not a lot of information on its properties such as saturated solubility in different solvents and henry coefficient [17, 19-22] are available. Information on solubility of Ph_2Hg in water is even conflicting, where several have reported that the compound is insoluble [22].

The aim of this chapter is to study the absorption kinetics of the selected organic mercury gas; Ph_2Hg in water at different temperatures (283-323 K), aqueous NaCl solutions at different temperatures (283-313 K) and NaCl concentrations (0-3.5 wt. %). Furthermore, absorption in MEG solutions at varying temperatures and MEG concentrations (0-50 v/v %) will also be performed using the bench scale semi-batch reactor system used in Chapter 4. Due to inconsistency and lack of solubility of Ph_2Hg in aqueous solvent, an experiment was conducted to fill in the knowledge gap. Finally, occurrence of the reaction between Ph_2Hg with NaCl and MEG during the absorption process will be investigated and evaluated for the test conditions respectively.

5.2 Equilibrium Solubility of Ph_2Hg in Fresh Water

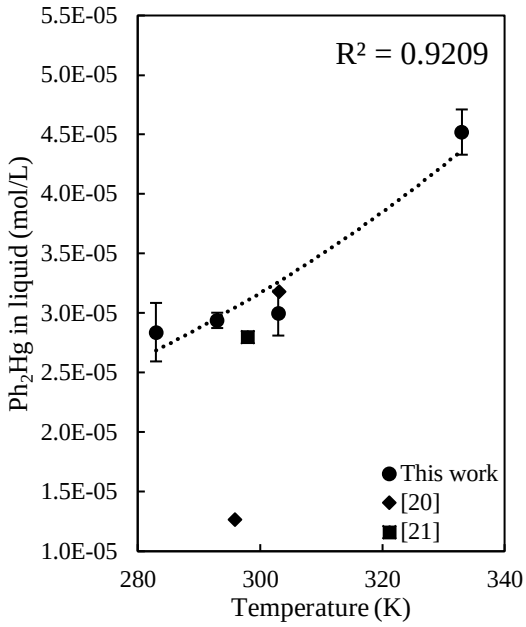

Fig. 5.1 Ph_2Hg Solubility in Milli-Q Water at Temperature of 283-333 K. Error Bars Were Calculated After 3-5 Independent Experiments.

The equilibrium solubility of Ph_2Hg in water is not very well known with information from several publications conflicting each other. It was published in the CRC Handbook of Chemistry and Physics that Ph_2Hg is insoluble in water [22], however several sources have reported otherwise. Ph_2Hg solubility in water has been reported to be 1.27×10^{-5} mol/L at 296 K and 3.18×10^{-5} mol/L at 303 K [20] and 2.8×10^{-5} mol/L at 298 K [21]. Due to the discrepancies found, an experiment was conducted to validate the solubility of Ph_2Hg in water at different temperatures.

To a volume of 700 ml Mili-Q water in the same reactor at set temperatures as described in Chapter 3, section 3.2.1, isolated from the gas line, several grams of Ph_2Hg crystals was placed in the solution and was stirred. After a period of 24 hours, an aliquot was taken and analysed using the method described in Chapter 3, section 3.2.4. It was assumed that the concentration of dissolved Ph_2Hg in water is at saturation as floating white crystals of Ph_2Hg was observed during the time of sample collection. To prevent overestimation of the analysis due to presence of Ph_2Hg crystals in the sample, the aliquots were centrifuged and only the clear liquid was analysed. The experiment was repeated at different temperatures and the results are shown in Fig. 5.1. For reference and comparative purposes, the solubility results from other sources were also included in Fig. 5.1.

The Ph_2Hg solubility results over a temperature range of 283-333 K shown in Fig. 5.1 follow an exponential relationship. The trend observed is similar with the trend of Hg^0 [23] and $HgCl_2$ [24] solubilities in several solutions as reported. Furthermore, the solubility data obtained from this work have a good agreement (within 10%) with those reported by Okamoto and Nagayama and Sloot et al. at 298 K and 303 K respectively [20, 21]. Having said that, the solubility data obtained by Sloot et al. at 296 K is lower in comparison to this work by a factor of 2.4.

5.3 Effects of Temperature on Dynamic Solubility of Ph_2Hg in Fresh Water

The effect of temperature on the absorption kinetics of Ph_2Hg in water was investigated under constant Ph_2Hg gas concentration (500 ± 33 ng Hg/L) and within a range of temperature (283-323 K) for a period of 50 test hours. The experimental set-up and procedure are explained in detail in Chapter 3. The measured Ph_2Hg absorbed concentration in water and the calculated Ph_2Hg absorbed per gas/liquid interface area as a function of absorption time is given in Fig. 5.2 (a) and (b) respectively. The results shown in Fig. 5.2 (a) and (b) show a linear relationship between dissolved Ph_2Hg and absorption time of 50 hours. This is as expected as the maximum concentration achieved at the end of the test (2.51×10^{-6} mol/L at 293 K) are still far below the maximum solubility of Ph_2Hg in water (2.94×10^{-5} mol/L at 293 K, Fig. 5.1). The slope of the curves in Fig. 5.2 (b) represents the absorption flux of Ph_2Hg in water. The absorption flux as a function of absorption temperature was calculated and the results are given in Fig. 5.2 (c).

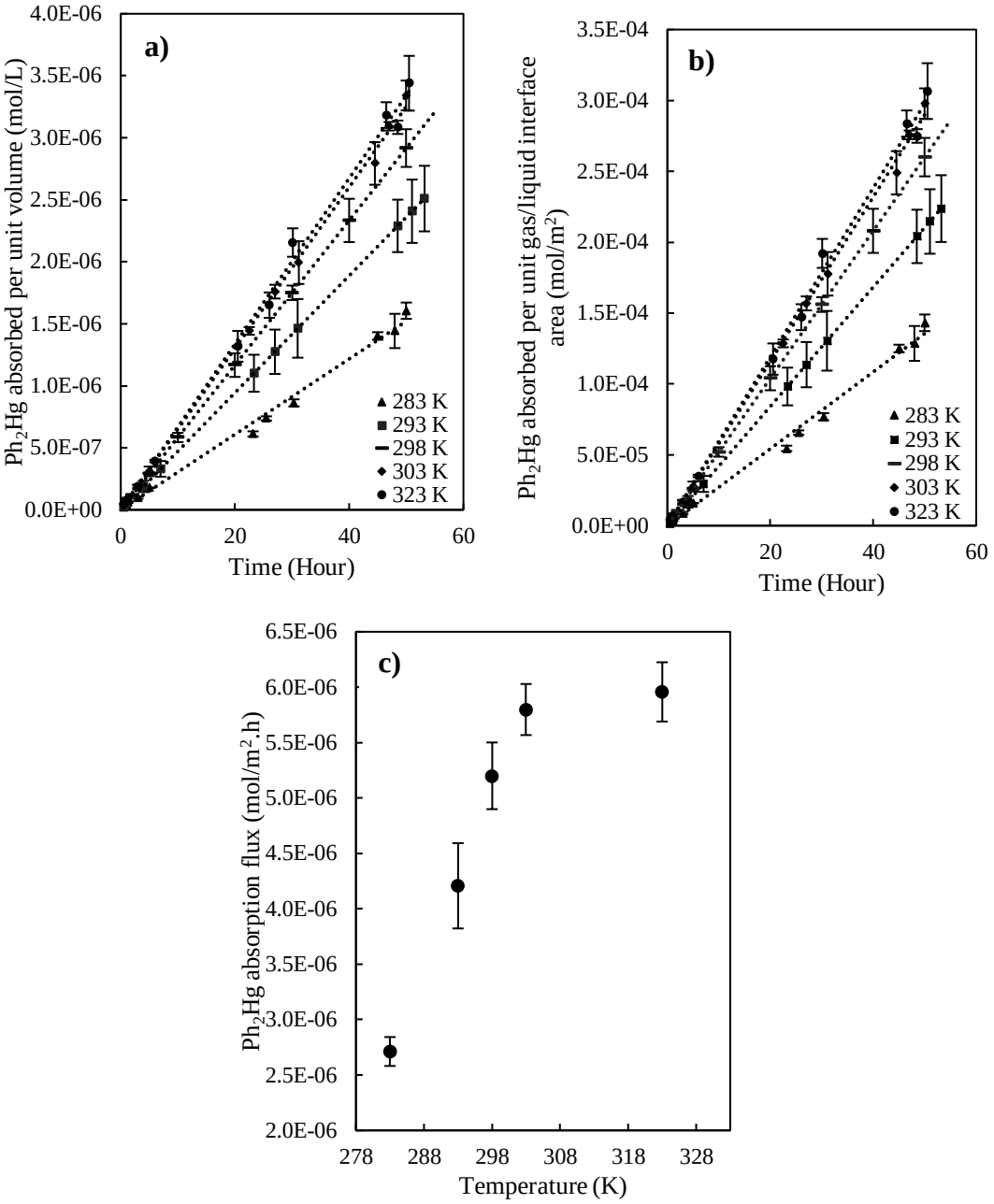

Fig. 5.2 (a) Measured Concentration of Absorbed Ph_2Hg in Liquid (b) Calculated Absorbed Ph_2Hg in Liquid per Unit Gas/Liquid Interface Unit Area (c) Calculated Absorption Flux at Gas Concentration of 500 ± 33 ng Hg/L, Gas Flow Rate of 500 ml/min, Absorbing Liquid of 700 ml Milli-Q Water and Temperature Range Between 283 and 323 K. Error Bars Were Calculated After 3-5 Independent Experiments.

The results in Fig. 5.2 (c) show significant increase in absorption flux with increasing temperature within the range of 283-303 K. The absorption flux above 303 K show a very slight increase, consistency with the absorption trends other mercury species in water.

Henry constant (H) is a very important parameter to determine absorption characteristics of gaseous Ph_2Hg. Currently to the best of our knowledge, no work has been done to determine He experimentally, hence a few authors have attempted to estimate this parameter by using different computational methods. At 298 K, two sources have reported H of Ph_2Hg to be 3.57×10^{-3} Pa.m^3/mol [25], 200.90 Pa.m^3/mol, 0.981 Pa.m^3/mol [19] using three different estimation methods.

The differences between the three H estimates are very large, estimates by ECHA [19] are 56 000 and 27 times larger than those estimated by Abraham et al. [25]. Although these methods pose as a good preliminary evaluation, the large uncertainties make it difficult to determine which value is more reliable due to the lack of a reference point; the experimental data. Hence, an evaluation process needs to be conducted to determine the correct value based on the physical and chemical properties of Ph_2Hg.

An evaluation process could be performed by comparison of the maximum solubility and equilibrium concentration (C*) expected from the gas phase used in this work. It is known that C* between gas and liquid should not exceed the maximum concentration in liquid. Therefore, based on this general guideline, the two H values can be assessed. At 298 K, the C* is calculated based on Ph_2Hg gas phase of 500 ng Hg/L gas and the maximum solubility of 3.11×10^{-5} mol/L (section 5.2). The result of the calculation is summarised in Table 5.1.

Comparison of the results in Table 5.1 suggest that the H estimated by Abraham is probably unsuitable to be used since C* is much higher (62 times higher) than the maximum solubility in water.

Table 5.1 Equilibrium Concentration of Ph_2Hg in Water at Gas Concentration of 500 ng Hg/L Gas and Temperature of 298 K

Method	H (Pa.m3/mol)	C* (mol/L)	Source
Linear Free Energy Relationships	3.57×10^{-3}	1.93×10^{-3}	[25]
Bond Contribution	0.981	7.04×10^{-6}	[19]
VP/WS	200.90	3.44×10^{-8}	[19]

The ratio of vapour pressure (VP) and water solubility (WS) is a simple way to help estimate H value of a compound. Having said that, in the work by ECHA [19], He of Ph_2Hg was estimated by using VP and WS of 8.04 Pa and 4×10^{-5} mol/L respectively. WP values used was quite high (28.6% higher) compared to those measured in section 5.2. Vapour pressure of pure Ph_2Hg crystals has been experimentally measured by

Carson et al. [26] dated in 1958, they reported value of 2.90×10^{-4} Pa at 298 K. Comparison of these values and those assumed by ECHA [19] would suggest that the authors have largely overestimated the VP values in their calculation, which has led to the over estimation seen in Table 5.1. Consequently, although calculated C* is below the maximum solubility, its value is much smaller than the concentration of Ph_2Hg reported in Fig. 5.2 (a). This is not possible since the absorption profile shown in Fig. 5.2 has not reached equilibrium even after absorption period of 50 hours. Based on this evaluation, the H value that is estimated using bond contribution method is the most suitable to represent the equilibrium distribution of Ph_2Hg and water.

As shown in section 5.2, Ph_2Hg is barely soluble in water. Therefore, based on this property, it is expected that its absorption into water is controlled by liquid film resistance (k_L). As discussed previously in Chapter 3, section 3.6, k_L can be calculated from the slope of ln $[C_L^*/(C_L^*-C_L)]$ against absorption time t, represented by equation (1).

$$\ln \frac{C_L^*}{C_L^* - C_L} = k_L a \, t \qquad (1)$$

Only k_L at 298 K could be calculated in this work as relationship of H with different temperatures is not available in the literatures. The k_L for absorption of Ph_2Hg in water at 298 K was calculated to be 8.83×10^{-8} m/s.

5.4 Absorption of Ph_2Hg in NaCl Solutions

The dynamic solubility of Ph_2Hg in NaCl solution was investigated under constant temperature of 293 K, Ph_2Hg gas concentration of 500 ± 33 ng Hg/L and varying NaCl concentration (1.5 and 3.5 wt. %). Preparations of NaCl solutions are similar to those outlined in Chapter 4, section 4.4.

Physical properties of solution with varying NaCl concentration were calculated and the results are summarised in Table 5.2. Results in Table 5.2 show that viscosity of the solution increases 10% with addition of 3.5 wt. % NaCl in the water. The addition of NaCl however reduced the diffusivity of Ph_2Hg into the solution by 9.4%. The effect of NaCl although affect the physical properties of the solution, the overall changes in both viscosity and diffusivity of the solvent are minimal to have a significant effect the absorption process. Diffusivity of Ph_2Hg into water and aqueous solutions of NaCl

are lower in comparison to $HgCl_2$ due to it being a larger molecule, it has a larger molar volume.

Table 5.2 Physical Properties of Water and NaCl Solutions

At 293K	Water	1.5 wt.% NaCl	3.5 wt.% NaCl
Dynamic Viscosity (centipoise)	1	1.04	1.10
Diffusivity of Ph_2Hg (cm^2/s)*	6.09×10^{-6}	5.83×10^{-6}	5.52×10^{-6}

*Diffusivity values of Ph_2Hg into the respective solutions are calculated using correlations from Wilke & Chang [27]

In Chapter 2 section 2.4.2, it has been found that Ph_2Hg may undergo transmetallation with metal halides such as NaCl to form organo-mercury halide; $(C_6H_5)HgCl$ and $(C_6H_5)Na$. This transmetallation process is a two-step process whereby it involves the cleavage of Ph_2Hg yielding $(C_6H_5)Hg^+$ and $(C_6H_5)^-$. This reaction is then followed by the combination of the organic mercury ions with the dissociated anions of the metal halides. The reaction has been reported to follow first order [28] and is shown below.

$$\mathrm{Hg(C_6H_5)_2 \rightarrow Hg(C_6H_5)^+ + (C_6H_5)^-} \qquad (1)$$

$$\mathrm{Hg(C_6H_5)_2 + NaCl \rightarrow (C_6H_5)HgCl + (C_6H_5)Na} \qquad (2)$$

It is to be noted that the formation of $(C_6H_5)HgCl$ described will only occur successively after the cleavage step of Ph_2Hg. This cleavage step will only occur in the presence of acids (such as perchloric, acetic and formic acid) [28, 29]. Kaufman and Corwin [29] have reported no reaction occurred between Ph_2Hg and NaCl even at saturation. As presence of acids is the determining condition, it is suggested that this reaction will not be observed as no acids will be added within the test conditions in this work.

5.4.1 Effect of NaCl Aqueous Concentrations at 293 K

Three absorption tests for 3 NaCl solutions (0, 1.5 and 3.5 wt. %) were carried out at the same absorption temperature and the measured results are given in Fig. 5.3 below. Fig. 5.3 (a) and (b) show the measured absorbed concentration of Ph_2Hg in liquid and calculated Ph_2Hg absorbed per unit gas/liquid interface area as a function of absorption time at 293 K.

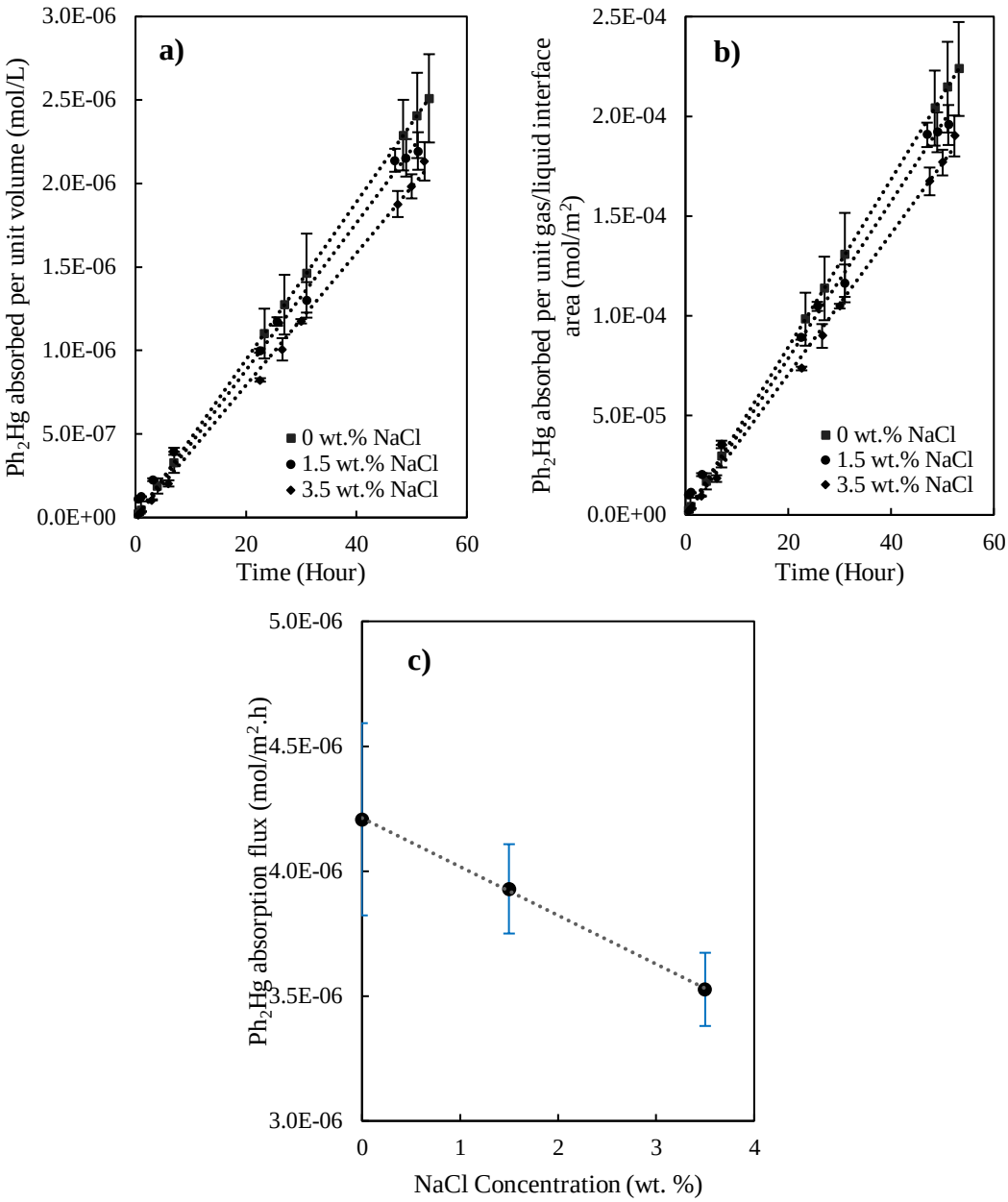

Fig. 5.3 (a) Measured Concentration of Ph_2Hg in Liquid Absorbed Overtime (b) Calculated Ph_2Hg in Liquid Absorbed per Unit Gas/Liquid Interface Area (c) Calculated Absorption Flux at Gas Concentration of 500 ± 33 ng Hg/L, Gas Flow Rate of 500 ml/min, Absorbing Liquid of 700 ml NaCl Solutions (0, 1.5, 3.5 wt. %), and Temperature of 293 K. Error Bars Were Calculated After 3-5 Independent Experiments.

The results shown in Fig. 5.3 (a) show that for NaCl concentrations of 1.5 and 3.5 wt. % NaCl, at a constant temperature of 293 K, the absorbed concentration of Ph_2Hg increases linearly with the absorption time. Using the same calculation method discussed above, the absorption flux of Ph_2Hg in different aqueous NaCl solution at 293 K are calculated and given in Fig. 5.3 (c). The results in Fig. 5.3 (c) show a decrease in absorption flux when NaCl concentration increased up to 3.5 wt. %. The

effect of salt has been investigated and it is well known that a decrease in aqueous solubility can occur, the effect commonly known as salting-out effect. Electrolytes present in water with small ionic size (associated with anions) is known to affect the structure of the water molecules, resulting in decreased solubility of the solute [30].

Presence of salt has been reported to have an influence on mass transfer between gas and liquid and on equilibrium distribution (H). Although physical properties of water changes around 10% (both viscosity and diffusivity), several have observed presence of salt in solution to have a much depressing effect on the overall mass transfer coefficient for absorption of several gasses in water [31-34]. In terms of equilibrium distribution, Iverfeldt and Lindqvist [35] have reported that for an organic mercury species; CH_3HgCl, presence of salt decreases the Henry constant while Xie et al. [36] have reviewed that salt has a negative effect on the solubility of organic compounds in water. As a common guideline, salting-out effect is reported to be enhanced when molecular size and polarizability (associated with aromatics) of the solute increases [37]. Due to this relationship, salting-out effect would be more commonly associated with organic mercury. This is because organic mercury has a much larger molecular size compared to inorganic mercury due to presence of carbon chains and benzene rings in their structure.

For compounds that are small and highly water soluble, such as the case with $HgCl_2$, it is expected to undergo weak salting-out [37]. If salting-out effect were to dominate the absorption system, presence of Cl^- is supposed to hinder the solubility of $HgCl_2$. Instead, this effect was not observed with $HgCl_2$ due to presence of a chemical reaction outlined in Chapter 4, section 4.4. It is suspected that the Cl^- that is involved in organising the water molecules has a higher likelihood to react with $HgCl_2$ to form a highly soluble Na_2HgCl_4, which increases its overall solubility in water. It could be assumed that the presence of chemical reaction greatly outweighs the molecular interactions that contributes to the salting-out effect.

Furthermore, salting-out effect is a process that occurs within the liquid phase. Since absorption of $HgCl_2$ is controlled by the gas film resistance, effect of the liquid phase should be minimal on the overall absorption rate. On the other hand, it has been discussed that Ph_2Hg absorption is controlled by the liquid film resistance in the previous section. Hence, the effect of salting-out will be significant on its absorption.

The results further verified the absorption model of $HgCl_2$ and Ph_2Hg using Two-film theory.

The findings suggest that absorption of Ph_2Hg into aqueous NaCl solution further suggest that it is not governed by a chemical reaction since the salting-out effect dominates.

5.4.2 Effect of Temperature in 3.5 wt. % NaCl Solution

The effect of temperature on the absorption of Ph_2Hg gas in water was investigated under constant NaCl concentration (3.5 wt. %), gas flow rate (500 ml/min) and gas concentration of 500 ± 33 ng Hg/L at varying temperatures (283-313 K) of the absorbing solution.

The absorption tests were conducted slightly different from the previous tests by running the test longer at continuous gas flow up to 80 hours. The absorption results obtained from the previous tests consistently show a linear relationship between Ph_2Hg absorbed and absorption time in a wide range of temperature (absorption in water for up to 323 K) and NaCl concentrations.

Based on these results, the temperature effect tests were decided to be performed differently to reduce the overall testing time to complete a data set. The overall time were reduced by decreasing the frequency of washing and setting up the reactor for each successive test. Moreover, having a continuous system would reduce the uncertainties such as fluctuating gas phase that might arise from dismantling the reactor system at the end of each test for cleaning purposes. The effect of temperature change can be seen by comparing the slope of the absorption curve. This is possible as absorption curve of Ph_2Hg in water still follows a linear relationship for long period of absorption time.

Fig. 5.4 (a) and (b) show the measured concentration of absorbed Ph_2Hg in liquid and the calculated Ph_2Hg absorbed per unit gas/liquid interface area as a function of absorption at different temperatures. Using the same calculation method discussed above, the absorption flux of Ph_2Hg in aqueous NaCl solution at different temperature is calculated and given in Fig. 5.4 (c).

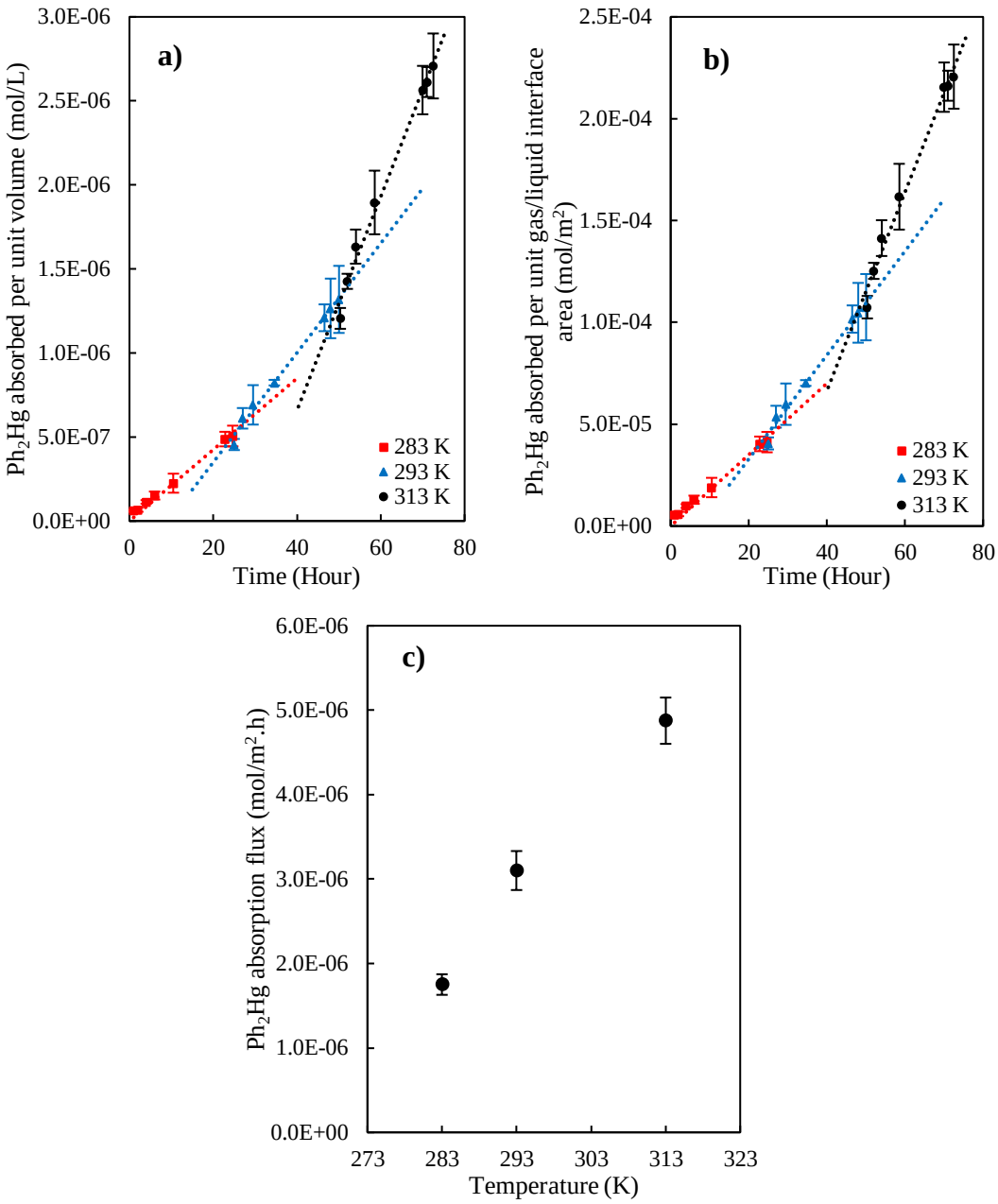

Fig. 5.4 (a) Measured Concentration of Ph_2Hg in Liquid Absorbed Overtime (b) Ph_2Hg in Liquid Absorbed per Unit Gas/Liquid Interface Area (c) Calculated Absorption Flux at Gas Concentration of 500 ± 33 ng Hg/L, Gas Flow Rate of 500 ml /min, Absorbing Liquid of 700 ml of 3.5 wt. % NaCl Solutions and Temperature of 283-313 K. Error Bars Were Calculated After 3-5 Independent Experiments.

The increasing effect of temperature on the absorption of Ph_2Hg into 3.5 wt. % NaCl solution show a consistent linear trend with the Ph_2Hg absorption in water shown in Fig. 5.2 (a) and (b). From Fig. 5.4 (a), the maximum recorded Ph_2Hg concentration at the end of the 80-hour run are still far below the saturation concentration studied in section 5.2. This result further supports the validity of the results obtained from this continuous test.

The enhancement factor; E was determined to see the effect of increasing temperature on the absorption of Ph_2Hg into 3.5 wt.% NaCl solution. E factors were calculated by taking the ratio of absorption flux with 3.5 wt. % NaCl and just water at the same temperature and the results are shown in Table 5.3. Results in Table 5.3 show an increase in E factor with increasing temperature. As temperature is increased, the viscosity of the liquid would decrease, at the same time, reducing the thickness of the boundary layer at the liquid side. This effect on the liquid film will lessen the mass transfer resistance and consequently promotes diffusion of Ph_2Hg into the liquid phase.

In addition, it is known that interactions between water molecules and salt ions are reduced when temperature is increased. This may have a negative impact on the salting-out effect in the system [38]. As salting out effect is reduced, the absorption flux of Ph_2Hg should in-turn be increased and may contribute to the increase in enhancement factor observed in Table 5.3.

Despite increasing the temperature up to 313 K, the E factor observed in Table 5.3 remained less than 1. E factor of less than 1 suggest that absorption flux of Ph_2Hg in 3.5 wt.% NaCl is lower in comparison to absorption in pure water. This reduction in absorption flux further supports the salting-out effect of NaCl observed in the previous section. The results obtained in this work point out that physical liquid properties have a high influence on the absorption of Ph_2Hg in 3.5 wt. % NaCl solution. The results suggest that chemical reactions between Ph_2Hg and NaCl may occur, but the reactions are not significant enough to overcome the salting-out effect under the test conditions in this work.

Table 5.3 Enhancement Factor of 3.5 wt. % NaCl at 293 K

Temperature (K)	Enhancement Factor; E
283	0.65
293	0.74
313	0.83

5.5 Absorption of Ph_2Hg in MEG Solutions

The dynamic solubility of Ph_2Hg in MEG solution was investigated under constant temperature of 293 K, Ph_2Hg gas concentration of 500 ± 33 ng Hg/L and varying MEG concentrations (10, 30 and 50 v/v%). Similar to the experiment procedure described in section 5.4.2, the dynamic solubility test was conducted under continuous manner for period 80 hours.

As discussed in Chapter 4 section 4.5, the physical properties of MEG solution changes with increasing concentration of MEG in the solution, namely the viscosity of the solution. Diffusivity of Ph_2Hg gas into varying MEG solutions has also been estimated from the commonly used Wilke & Chang correlation [27] and summary of both the dynamic viscosity of solution with varying MEG concentration and diffusivity are given in Table 5.4. As expected, the results in Table 5.4 show that dynamic viscosity of the solution increases significantly with increasing concentration of MEG (increase by 4.47 times from 0-50 v/v % MEG) and in turn, reduced the diffusivity of Ph_2Hg gas into MEG solution. The noted change in physical properties of the absorbing liquid might have an effect on the absorption flux of the studied gas absorption as increase in viscosity is known to result in decreasing mass transfer coefficients [39].

Table 5.4 Physical Properties of Water and MEG Solutions

At 293K	**Water**	**10 v/v% MEG**	**30 v/v% MEG**	**50 v/v% MEG**
Dynamic Viscosity (centipoise)	1	1.05	2.34	4.47
Diffusivity of Ph_2Hg (cm^2/s)*	6.09×10^{-6}	4.83×10^{-6}	2.60×10^{-6}	1.36×10^{-6}

*Diffusivity values of Ph_2Hg into the respective solutions are calculated using correlations from Wilke & Chang [27]

5.5.1 Equilibrium Solubility of Ph_2Hg in 50 v/v% MEG

It is a general knowledge that organic mercury such as Ph_2Hg should be more soluble in organic solutions in comparison to in water. However, information regarding the equilibrium solubility of Ph_2Hg in various organic solutions such as aqueous solutions of MEG is scarce. It has been reported in CRC Handbook of Chemistry and Physics that Ph_2Hg is soluble in ethanol, diethyl ether, benzene and chloroform [22]. Nevertheless, the extent of solubility in these reported organic solvents have not been quantified. It is noteworthy to investigate the solubility of Ph_2Hg as streams within the oil and gas processes contain complex matrix made up of hydrocarbons and organic phase. Furthermore, current mercury mapping strategies are based on the saturated solubility of mercury species in aqueous solutions to determine their partitioning behaviour. Hence, information on solubility of Ph_2Hg in process fluids present in the oil and gas processes is vital.

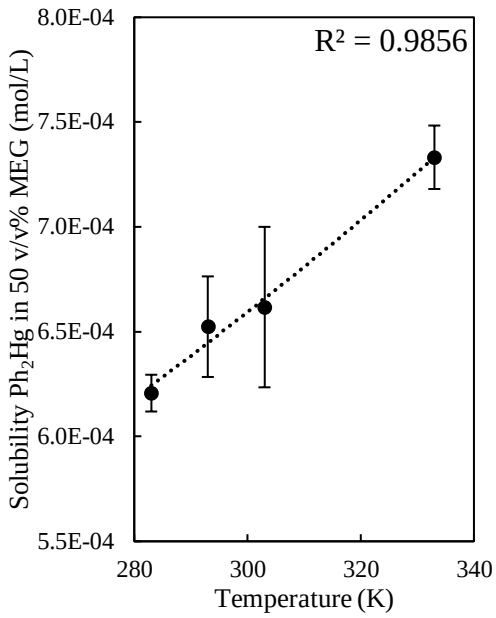

Fig. 5.5 Ph_2Hg Solubility in 50 v/v% MEG Solution at Temperature of 283-333 K. Error Bars Were Calculated After 3-5 Independent Experiments.

As discussed in previous sections, determination of the equilibrium solubility of Ph_2Hg especially in aqueous MEG solution is necessary. This information will aid in understanding the behaviour and partitioning tendencies of Ph_2Hg during transport in the pipeline and MEG regeneration units. The experiment conducted and discussed in section 5.2 was repeated using 50 v/v% MEG solution at temperatures of 283-333 K. This test was selected to see the effect of MEG on the equilibrium solubility of Ph_2Hg in water prior to studying its absorption kinetics. The result is shown in Fig. 5.5 and summarised in Table 5.5.

Table 5.5 Solubility of Ph_2Hg in 50 v/v% MEG Solution

Temperature (K)	**Ph_2Hg Solubility (mol/L)**
283	$(6.21\pm0.09) \times 10^{-4}$
293	$(6.52\pm0.24) \times 10^{-4}$
303	$(6.62\pm0.38) \times 10^{-4}$
333	$(7.33\pm0.47) \times 10^{-4}$

The results in Fig. 5.5 show consistent trend with solubility of Ph_2Hg and other mercury species in water as mentioned earlier. Comparison of Fig. 5.1 and Fig. 5.5 indicate that Ph_2Hg is approximately 20 times more soluble in solution containing 50 v/v% MEG (6.52×10^{-4} mol/L at 293 K). The effect of addition of MEG is somewhat expected as organic mercury is known to be more soluble in organic solvents in comparison to water [15]. Similar effect has been reported by Gallup et al. [23] whereby solubility of Hg^0 increased with increasing concentration of MEG in water.

The enhancement effect of MEG on solubility of Ph_2Hg is suspected to be related to the change in the polarity of the solution as oppose to enhancement by chemical reactions.

5.5.2 Effect of MEG Concentrations at 293 K

Absorption tests were conducted for three different MEG solutions (10, 30 and 50 v/v %) at the same absorption temperature and continuously for 80 hours straight. The effect of each concentration was monitored for a period of 24 hours before more MEG (AR Grade, Thermo Fischer) was injected into the reactor to make up the desired concentration in v/v %. The effect of MEG onto the absorption of Ph_2Hg into water at 293 K was studied by comparison of the gradient of the concentration time curve.

Fig. 5.6 (a) and (b) show the measured absorbed concentration of Ph_2Hg in liquid and calculated Ph_2Hg absorbed per unit gas/liquid interface area as a function of absorption time at 293 K. The results shown in Fig. 5.6 (a) and (b) show linear increment of Ph_2Hg absorbed in different MEG concentrations with absorption time, which is consistent with the results presented in previous sections in this chapter. The absorption flux as a function of MEG concentrations was calculated following the previous sections and the results are given in Fig. 5.6 (c).

The results shown in Fig. 5.6 (c) show no effect of MEG on the absorption of Ph_2Hg in water when MEG concentration was increased up to 30 v/v%. Although Ph_2Hg is 20 times more soluble in 50 v/v% MEG solutions compared to in water, Fig. 5.6 (c) show that there is a slight reduction in absorption flux for absorption of Ph_2Hg in 50 v/v % MEG. The resistance at the liquid film dominates the absorption process which was accounted by the significant increase in the viscosity of the absorbing solution at higher concentration of MEG (Table 5.4) [40, 41].

In order to see the effect of increasing MEG on the absorption flux of Ph_2Hg in water, E factors for absorption in 10 – 50 v/v% MEG solutions were calculated following the procedure in section 5.4.2. The results are summarised in Table 5.6. The results shown in Table 5.6 show that all E values within 1 although MEG concentration was increased up to 50 v/v%. Despite Ph_2Hg being more soluble in MEG solutions, the changes in physical properties of the liquid phase dominate the absorption process and

reduces the overall absorption flux into water. The results suggest that there is no effect of chemical reaction by MEG to overcome the physical properties effect for the experimental conditions used. The high influence of physical properties of the liquid phase suggest that absorption of Ph_2Hg into water and solution of MEG is controlled by the liquid film resistance.

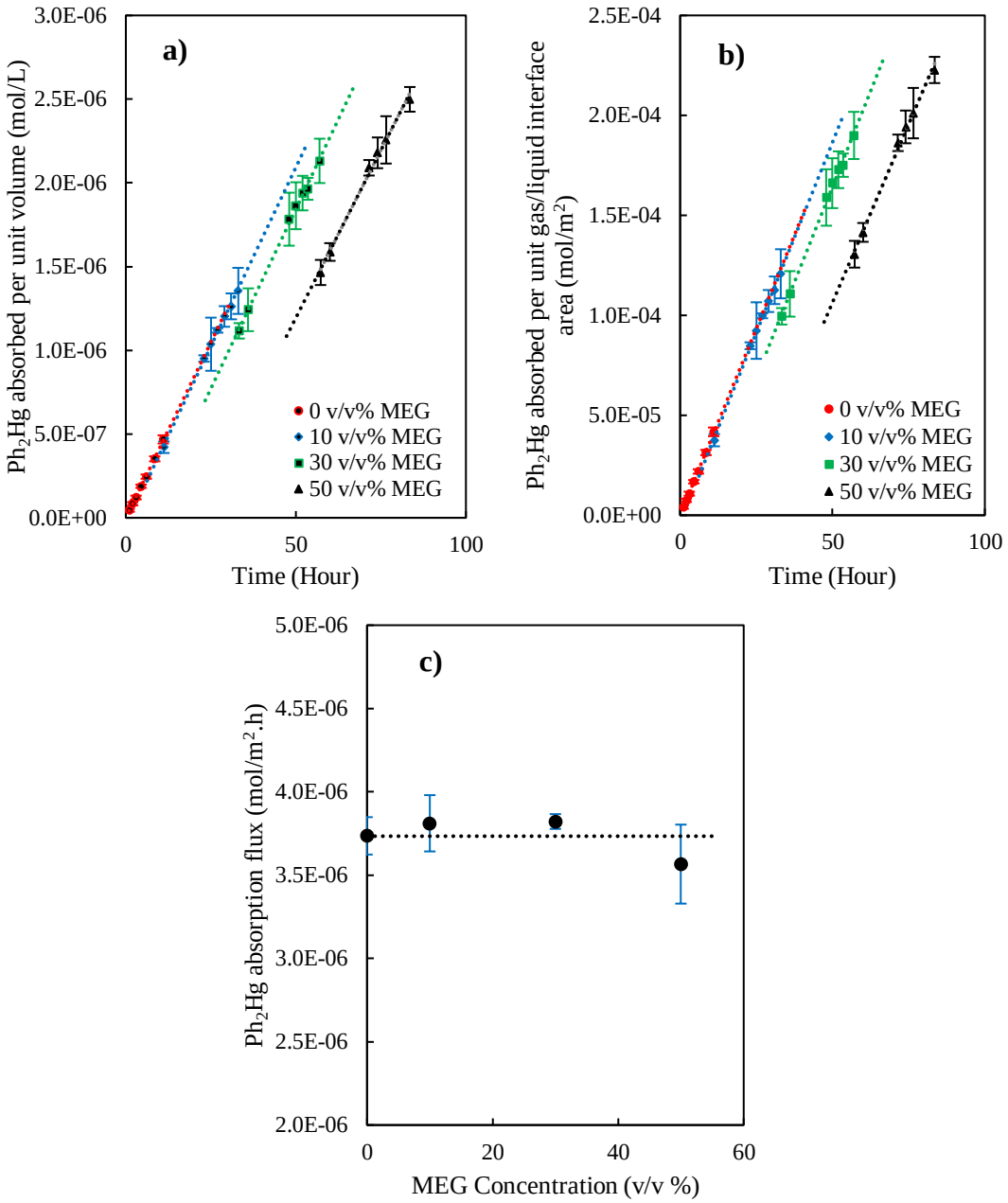

Fig. 5.6 (a) Measured Concentration of Ph_2Hg in Liquid Absorbed Overtime (b) Calculated Ph_2Hg in Liquid Absorbed per Unit Gas/Liquid Interface Area (c) Calculated Absorption Flux at Gas Concentration of 500 ± 33 ng Hg/L, Gas Flow Rate of 500 ml/min, Absorbing Liquid of 700 ml MEG Solutions (0, 10, 30 and 50 v/v %), and Temperature of 293 K. Error Bars Were Calculated After 3-5 Independent Experiments.

Table 5.6 Enhancement Factor of Varying MEG Concentrations at 293 K

MEG Concentration (v/v %)	Enhancement Factor; E
10	1.02
30	1.02
50	0.95

5.5.3 Effect of Temperature in 50 v/v% MEG Solution

The effect of temperature on the absorption of Ph_2Hg gas in water was investigated under constant MEG concentration (50 v/v %), gas flow rate (500 ml/min) and gas concentration of 500 ± 33 ng Hg/L at varying temperatures (283-313 K) of the absorbing solutions for a period of 80 hours. The absorption test was conducted following the same procedure as described in section 5.4.2 and effect of temperature was studied by comparing the change in the gradient of the absorption curve. Fig. 5.7 (a) and (b) show the measured concentration of absorbed Ph_2Hg in liquid and the calculated Ph_2Hg absorbed per unit gas/liquid interface area as a function of absorption at different temperatures.

The effect of temperature on the absorption of Ph_2Hg into 50 v/v% MEG solution as shown in Fig. 5.7 (a) and (b) show a consistent trend with the Ph_2Hg absorption in water and 3.5 wt. % NaCl solution shown in Fig. 5.2 and Fig. 5.4 respectively. The absorption rate increases with the increasing absorption temperature, the effect is less pronounced compared with that of absorption at lower temperature range (283-313 K). Using the same calculation method discussed above, the absorption flux of Ph_2Hg in 50 v/v% MEG solution at different temperature is calculated and given in Fig. 5.7 (c).

As outlined in Chapter 2, MEG is widely used within the LNG processing facilities and is injected in the pipeline for flow assurance purposes. MEG exists in different temperatures and concentrations at the different stages of the process and its concentration is highest at the outlet of the MEG regeneration process. The findings from this chapter suggest that absorption of non-ionic organic mercury such as Ph_2Hg within the pipeline and any state of MEG regeneration process would be affected by the process temperature only. This is because absorption rate of Ph_2Hg into water is not affected by MEG concentrations for up to 50 v/v%. Having said that, Ph_2Hg absorption would mainly occur at the distillation step of the MEG regeneration process. As ‘lean’ MEG solution is heated to evolve the water content, Ph_2Hg present

in the gas phase will likely partition into the MEG 'rich' solution and gets recirculated back into the pipeline.

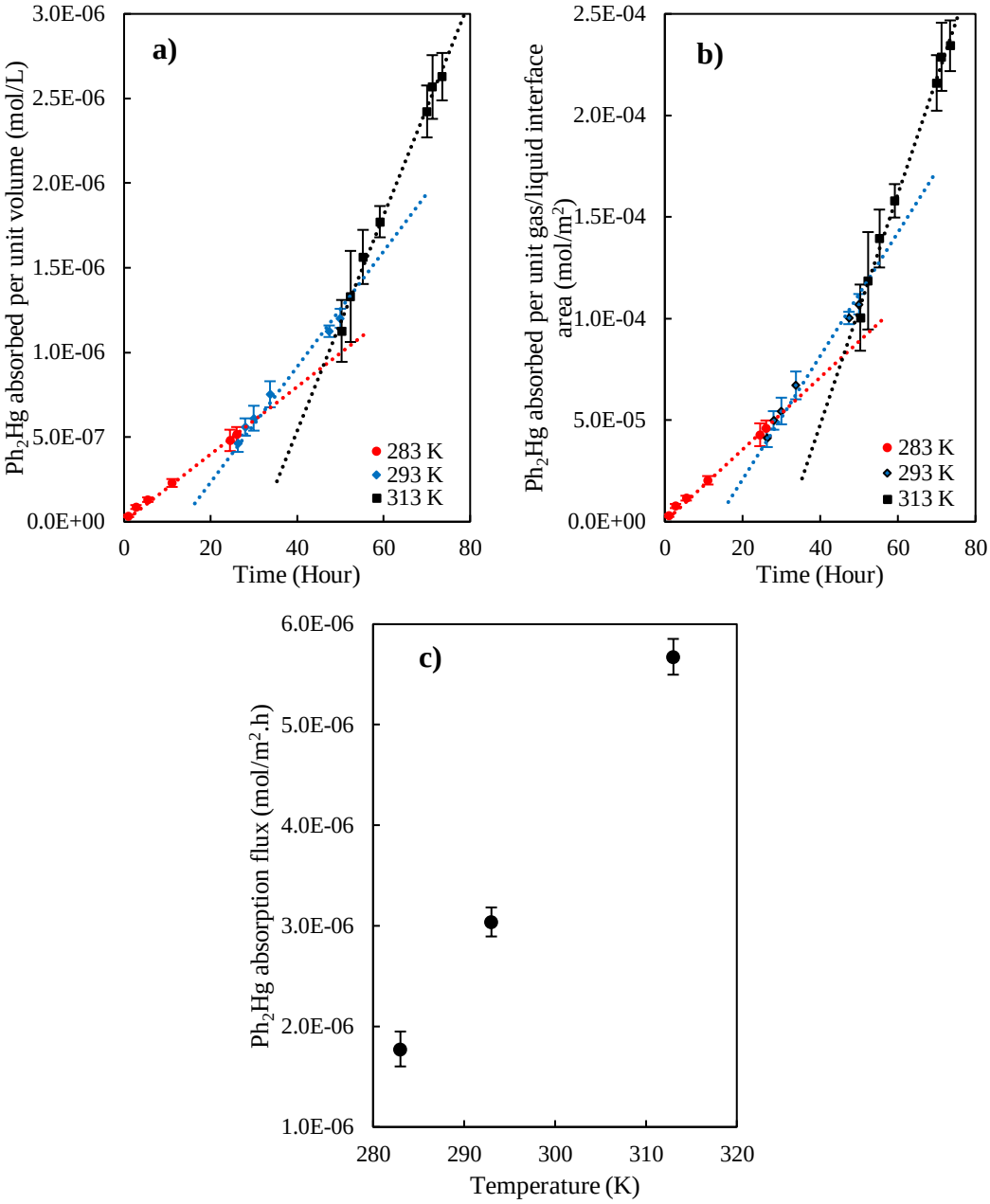

Fig. 5.7 (a) Measured Concentration of Ph_2Hg in Liquid Absorbed Overtime (b) Ph_2Hg in Liquid Absorbed per Unit Gas/Liquid Interface Area (c) Calculated Absorption Flux at Gas Concentration of 500 ± 33 ng Hg/L, Gas Flow Rate of 500 ml /min, Absorbing Liquid of 700 ml of 50 v/v% MEG Solutions and Temperature of 283-313 K. Error Bars Were Calculated After 3-5 Independent Experiments.

5.6 Comparison of Absorption Rates of Various Mercury Gases

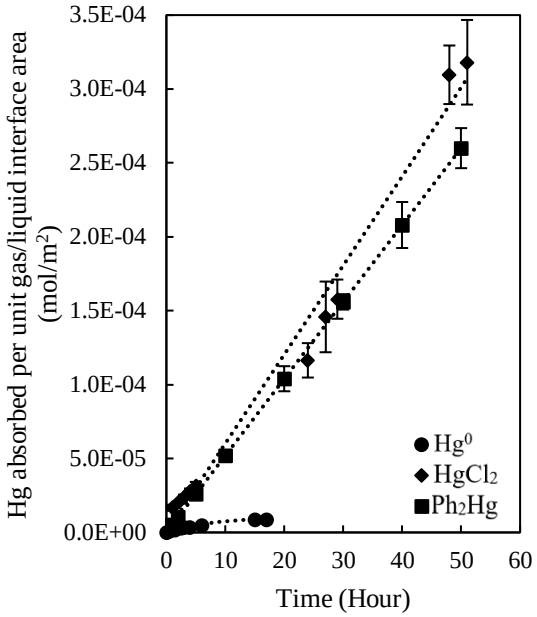

Fig. 5.8 Comparison of Absorbed Hg in Water per Unit Gas/Liquid Interface Area of Hg^0, $HgCl_2$ and Ph_2Hg at 298 K

The absorption results of Hg^0, $HgCl_2$ and Ph_2Hg in water were normalised to account for the gas/liquid interface area. The measured results from Fig. 3.14 in Chapter 3 were used to calculate the Hg absorbed per unit gas/liquid interface area at different absorption time for Hg^0. The results are then compared to absorption of $HgCl_2$ and Ph_2Hg taken from Fig. 4.1 in Chapter 4 and Fig. 5.2 from section 5.3. Comparison of the absorption of Hg^0, $HgCl_2$ and Ph_2Hg per unit gas/liquid interface in water at 298 K is given in Fig. 5.8.

Fig. 5.8 shows that unlike Hg^0 absorption observed, the relationship between $HgCl_2$ and Ph_2Hg concentration in liquid phase and absorption time follows a linear relationship for a long period of absorption time; 53 hours. This result suggests that the absorption test in this work was carried out at a condition far below equilibrium. It is known that $HgCl_2$ is a highly soluble compound in water; its maximum solubility in water at 298 K reaches 73 g /L [24] as reported in literature. Furthermore, the calculated C* for $HgCl_2$ at gas concentration of 550 ng Hg/L is 0.11 mol/L, which is 2.98×10^4 times higher than the highest value measured during the absorption test in this work. This is also valid for Ph_2Hg whereby its maximum solubility in water at 293 K is 0.010 g/L (section 5.2). The C* for Ph_2Hg concentration in water at 298 K at gas

concentration of 500 ng Hg/L is 7.04×10^{-6} mol/L which is around 2.4 times higher than the highest value measured at 50 hours.

Fig. 5.8 also demonstrates that Ph_2Hg and $HgCl_2$ absorption flux is higher than that of Hg^0 at temperature range of 293-298 K, although Ph_2Hg and $HgCl_2$ feed gas concentration was much lower than that of Hg^0 feed gas. It is clear to see the Hg^0 absorption flux reduces with absorption time when the process approaches the equilibrium condition. For comparison purposes, absorption flux of the various mercury species was calculated and listed in Table 5.7. For Hg^0, the maximum absorption flux of was used, which was calculated by using the data within the first 6 hours of absorption.

Table 5.7 Parameter of Hg^0, Ph_2Hg and $HgCl_2$ Absorption in Water

Mercury Species	**Mercury Gas Concentration (ng Hg/L gas)**	**Calculated Partial Pressure (Pa)**	**Absorption Temperature (K)**	**Absorption Flux (mol/m^2.h)**
Hg^0	21.15×10^3	0.261	298	0.76×10^{-6}
Ph_2Hg	500	0.007	298	5.20×10^{-6}
$HgCl_2$	550	0.008	298	6.02×10^{-6}

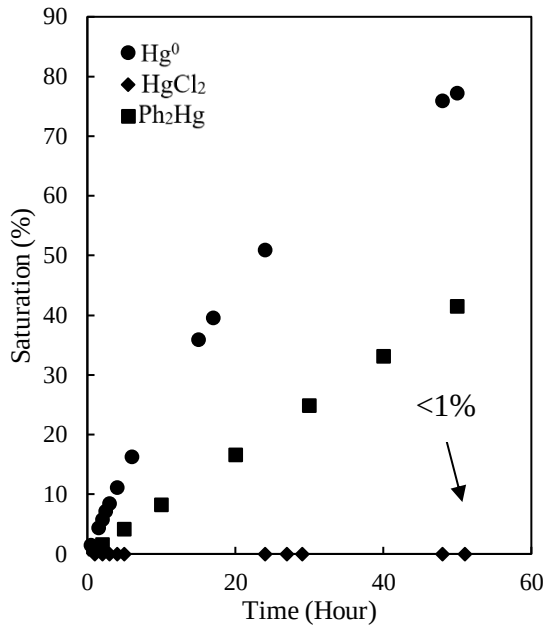

Fig. 5.9 Percent Saturation Curve as a Function of Absorption Time at 298 K. Absorption Results Adjusted to Gas Concentration of 500 ng Hg/L Gas, Contact Area of 0.008 m^2 and Liquid Volume of 0.7 L Water.

Comparison of the absorption of the three-mercury species can be shown in a different way as seen in Fig. 5.9. In Fig. 5.9, the percentage of saturation was plotted instead of the actual molar concentration over the absorption period. Percentage saturation in this

case refers to how far the liquid concentration is from the equilibrium concentration, C*. From the absorption parameters defined in Table 5.7, the conditions of the absorption are adjusted for mercury gas concentration of 500 ng Hg/L gas with area of absorption (A) of 0.008 m^2 and 0.7 L volume of water (V_L) for standardisation purposes. As the ratio of A/V_L is lower, percent saturation of Hg^0 also decreases and requires about twice as much time to reach a given percent saturation. This is expected as absorption process is highly dependent on the surface area of contact. Under the same A/V_L ratio, the percent saturation curve of Hg^0 is consistent although gas concentration was reduced to 500 ng Hg/L gas. The percent saturation curve for Ph2Hg is still within the linear stage of absorption, which is consistent with those seen in Fig. 5.2 (a). The percent saturation curve for $HgCl_2$ reaches less than 1% even after 50 hours of absorption time. This is because $HgCl_2$ being highly soluble in water, diffuses through the liquid film very rapidly, while on the other hand, they are unable to diffuse through the gas film quick enough to overcome the high resistance. Having said that, although <1% saturation is reached after 50 hours, more $HgCl_2$ are being absorbed per unit volume water compared to Hg^0 and Ph_2Hg.

The results obtained suggest that when the three-mercury species are present above a water body, Hg^0 will be the first one to reach saturation. It will not be odd to find higher concentration of $HgCl_2$ and Ph_2Hg in the water body as an overall due to their higher solubility in water. Having said that, it is quite unlikely for $HgCl_2$ to reach saturation as mercury gas concentration reported to date are lower than 500 ng Hg/L, except for the high value reported from China and North German (please refer to Chapter 2, section 2.2).

5.7 Summary

This work evaluated the absorption kinetics of Ph_2Hg gas in water, aqueous NaCl solutions and MEG solutions. From the results presented, the following conclusions can be drawn:

- Ph_2Hg is soluble in water and its solubility follows an exponential relationship of:

$$\text{Solubility of } Ph_2Hg \text{ (mol/L)} = 1.72 \times 10^{-6} e^{9.72\times10^{-3}\ T\ (K)}$$

- Effect of salting out was observed whereby addition of NaCl in water for concentration up to 3.5 wt. % depresses the absorption flux of Ph_2Hg into water. Enhancement factor for the effect of temperature was <1.
- Ph_2Hg is 20 times more soluble in solution containing 50 v/v% MEG compared to water alone. Ph_2Hg solubility follows an exponential relationship of:

$$\text{Solubility of } Ph_2Hg \text{ (mol/L)} = 2.51 \times 10^{-4} e^{3.21\times10^{-3}\ T\ (K)}$$

- Absorption flux of Ph_2Hg into MEG solutions (10 and 30 v/v %) are comparable with absorption in water with a slight reduction in flux for MEG concentration of 50 v/v %. The absorption process follows characteristics of physical absorption controlled by liquid film for MEG concentration of up to 30 v/v%. Further increasing MEG concentration to 50 v/v% would results in liquid film dominating the absorption process, hence decreasing the overall absorption flux. E factor calculated for MEG concentration of 10-50 v/v % yield a value of 1, indicating no enhancement effect of chemical reaction could be seen within the experimental conditions used.
- Comparison of the absorption of Hg^0, $HgCl_2$ and Ph_2 found that when the three species are present above water, Hg^0 will be the first one to reach equilibrium, followed by Ph_2Hg and $HgCl_2$. It is likely that $HgCl_2$ will take a very long time (a few months) before equilibrium could be reached. Although C* will take some time to be reached, it is expected to find much higher concentration of $HgCl_2$ in the water phase due to its very high solubility.

5.8 Reference

[1] Wilhelm, S. Mark. 2001. Mercury in Petroleum and Natural Gas: Estimation of Emissions from Production, Processing, and Combustion. Tomball, Texas.

[2] Wilhelm, S. Mark, and Nicholas Bloom. 2000. "Mercury in Petroleum." *Fuel Processing Technology* no. 63 (2000):1-27.

[3] Ezzeldin, Mohamed F., Zuzana Gajdosechova, Mohamed B. Masod, Tamer Zaki, Jörg Feldmann, and Eva M. Krupp. 2016. "Mercury Speciation and Distribution in an Egyptian Natural Gas Processing Plant." *Energy & Fuels* no. 30 (12):10236-10243. doi: 10.1021/acs.energyfuels.6b02035.

[4] Rice, Kevin M., Jr Ernest M. Walker, Miaozong Wu, Chris Gillette, and Eric R. Blough. 2014. "Environmental Mercury and Its Toxic Effects." *Journal of Preventitive Medicine & Public Health* no. 47 (2):74-83. doi: 10.3961/jpmph.2014.47.2.74.

[5] Gallup, Darrell L. 2014. Removal of mercury from water in the petroleum industry. Paper read at 21st International Petroleum Environmental Conference

[6] Lang, David, Murray Gardner, and John Holmes. 2012. Mercury arising from oil and gas production in the United Kingdom and UK continental shelf. University of Oxford.

[7] Bouyssiere, B., F. Baco, L. Savary, and R. Lobinski. 2000. "Analytical methods for speciation of mercury in gas condensates." *Oil & Gas Science and Technology* no. 55 (6):639-648.

[8] Bouyssiere, Brice, Franck Baco, Laurent Savary, and Ryszard Lobinski. 2002. "Speciation analysis for mercury in gas condensates by capillary gas chromatography with inductively coupled plasma mass spectrometric detection." *Journal of Chromatography A* no. 976 (2002):431-439.

[9] Tao, Hiroaki, Tadahiko Murakami, Mamoru Tominaga, and Akira Miyazaki. 1998. "Mercury speciation in natural gas condensate by gas chromatography-inductively coupled plasma mass spectrometry." *Journal of Analytical Atomic Spectrometry* no. 13 (1998):1086-1093.

[10] Frech, Wolfgang, Douglas C. Baxter, Berit Bakke, James Snell, and Yngvar Thomassen. 1996. "Determination and Speciation of Mercury in Natural Gases and Gas Condensates." *Analytical Communications* no. 33:7H-9H.

[11] Schickling, C., and J. A. C. Broekaert. 1995. "Determination of mercury species in gas condensates by on-line coupled High-performance liquid Chromatography and Cold-vapor atomic absorption spectrometry." *Applied Organometallic Chemistry* no. 9:29-36.

[12] Zettlitzer, M., R. Scholer, and R. Falter. 1997. Determination of elemental, inorganic and organic mercury in North German gas condesates and formation brines. In *SPE International Symposium on Oilfiled Chemistry*. Houston, Texas: Society of Petroleum Engineers, Inc. .

[13] Dessy, Raymond E., and Y. K. Lee. 1960. "The Mechanism of the Reaction of Mercuric Halides with Dialkyl and Diarylmercury Compounds." *Journal of the Americal Chemical Society* no. 82 (3):689-693. doi: 0.1021/ja01488a047.

[14] Pollard, D. R., and J. V. Westwood. 1965. "Kinetic Studies of Exchange between Metallic Mercury and Mercury Compounds in Solution. I." *Journal of the American Chemical Society* no. 87 (13):2809-2815. doi: 10.1021/ja01091a006.

[15] Lobana, Tarlok S. 2006. Organometallics. In *Inorganic Chemistry*. Amritsar 143005 Guru Nanak Dev University

[16] Baughman, George L., John A. Gordon, N. Lee Wolde, and Richard G. Zepp. 1973. Chemistry of Organomercurials in Aquatic Systems. edited by National Environmental Research Center. Corvallis, Oregon: United States Environmental Protection Agency.

[17] McCutchan, Roy T., and Kenneth A. Kobe. 1954. "Diphenylmercury Synthesis." *Industrial & Engineering Chemistry* no. 46 (4):675-680. doi: 10.1021/ie50532a027.

[18] McAuliffe, C. A. 1977. *The Chemistry of Mercury* London The Macmillan Press Ltd.

[19] (ECHA), European Chemicals Agency. 2011. Background document to the Opinions on the Annex XV dossier proposing restrictions on five Phenylmercury compounds. https://echa.europa.eu/documents/10162/4a71bea0-31f0-406d-8a85-59e4bf2409da.

[20] Sloot, H. A. van der, C. Blomberg, and H. A. Das. 1974. "Solubility and adsorption of some organo-mercury compounds " *Reactor Centrum Nederland*.

[21] Okamoto, G., and M. Nagayama. 1952. "Physiochemical properties of aqueous solutions of mercury compounds." *Japan Journal of Pharmacy and Chemistry* no. 24:358-362.

[22] Haynes, William M. Internet Version 2017. "CRC Handbook of Chemistry and Physics." In: CRC Press/Taylor & Francis, Boca Raton, FL.

[23] Gallup, Darrell L., Dennis J. O'Rear, and Ron Radford. 2017. "The behavior of mercury in water, alcohols, monoethylene glycol and triethylene glycol." *Fuel* no. 196:179-184. doi: 10.1016/j.fuel.2017.01.100.

[24] Clever, H. Lawrence, Susan A. Johnson, and M. Elizabeth Derrick. 1985. "The Solubility of Mercury and Some Sparingly Soluble Mercury Salts in Water and Aqueous Electrolyte Solutions." *Journal of Physical and Chemical Reference Data* no. 14 (3).

[25] Abraham, Michael H., Javier Gil-Lostes, Jr William E. Acree, J. Enrique Cometto-Muñizc, and William S. Cainc. 2008. "Solvation parameters for mercury and mercury(II) compounds: calculation of properties of environmental interest." *Journal of Environmental Monitoring* no. 10 (2):453-442. doi: 10.1039/B719685G.

[26] Carson, A. S., D. R. Stranks, and B. R. Wilmshurst. 1958. "The Measurement of Very Low Vapour Pressures Using Radioactive Isotopes: The Latent Heat of Sublimation of Mercury Diphenyl." *Proceedings of the Royal Society A* no. 244 (1236):72-84. doi: 10.1098/rspa.1958.0026.

[27] Wilke, C. R., and Pin Chang. 1955. "Correlation of diffusion coefficients in dilute solutions " *AIChE Journal* no. 1 (2):264-270.

[28] Corwin, Alsoph H., and Marcus A. Naylor Jr. 1947. "Aromatic Substitution. The Cleavage of Diphenylmercury." *Journal of the American Chemical Society* no. 69 (5):1004-1009. doi: 10.1021/ja01197a008.

[29] Kaufman, Frederick, and Alsoph H. Corwin. 1955. "Aromatic Substitution. II. The Acid Cleavage of Diphenylmercury." *Journal of the American Chemical Society* no. 77 (23):6280-6284. doi: 10.1021/ja01628a065.

[30] Ruckenstein, E., and I. Shulgin. 2002. "Salting-Out or -In by Fluctuation Theory." *Industrial & Engineering Chemistry Research* no. 41 (18):4674-4680. doi: 10.1021/ie020348y.

[31] Tokumura, Masahiro, Mayumi Baba, and Yoshinori Kawase. 2007. "Dynamic modeling and simulation of absorption of carbon dioxide into seawater." *Chemical Engineering Science* no. 62 (24):7305-7311. doi: 10.1016/j.ces.2007.08.074.

[32] Jamnongwong, Marupatch, Karine Loubiere, Nicolas Dietrich, and Gilles Hébrard. 2010. "Experimental study of oxygen diffusion coefficients in clean water containing salt, glucose or surfactant: Consequences on the liquid-side mass transfer coefficients." *Chemical Engineering Journal* no. 165 (3):758-768. doi: 10.1016/j.cej.2010.09.040.

[33] Taweel, A.M. Al, A.O. Idhbeaa, and A. Ghanem. 2013. "Effect of electrolytes on interphase mass transfer in microbubble-sparged airlift reactors." *Chemical Engineering Science* no. 100:474-485. doi: 10.1016/j.ces.2013.06.013.

[34] Hill, Gordon A. 2009. "Oxygen Mass Transfer Correlations for Pure and Salt Water in a Well-Mixed Vessel." *Industrial & Engineering Chemistry Research* no. 48 (7):3696-3699. doi: 10.1021/ie8019906.

[35] Iverfeldt, Åke, and Oliver Lindqvist. 1982. "Distribution equilibrium of methyl mercury chloride between water and air." *Atmospheric Environment* no. 16 (12):2917-2925. doi: 10.1016/0004-6981(82)90042-7.

[36] Xie, Wen Hui, Wan Ying Shiu, and Donald Mackay. 1997. "A review of the effect of salts on the solubility of organic compounds in seawater." *Marine Environmental Research* no. 44 (4):429-444. doi: 10.1016/S0141-1136(97)00017-2.

[37] Hyde, Alan M., Susan L. Zultanski, Jacob H. Waldman, Yong-Li Zhong, Michael Shevlin, and Feng Peng. 2017. "General Principles and Strategies for Salting-Out Informed by the Hofmeister Series." *Organic Process Research & Development* no. 21 (9):1355-1370. doi: 10.1021/acs.oprd.7b00197.

[38] Copolovici, Lucian, and Ülo Niinemets. 2007. "Salting-in and salting-out effects of ionic and neutral osmotica on limonene and linalool Henry's law constants and octanol/water partition coefficients." *Chemosphere* no. 69 (4):621-629. doi: 10.1016/j.chemosphere.2007.02.066.

[39] Haslam, R. T., R. L. Hershey, and R. H. Keen. 1924. "Effect of gas velocity and temperature on rate of absorption " *Industrial and Engineering Chemistry* no. 16 (12):1224-1230. doi: 10.1021/ie50180a004.

[40] Mehta, V. D., and M. M. Sharma. 1966. "Effect of diffusivity on gas-side mass transfer coefficient " *Chemical Engineering Scienc* no. 21:361-365.

[41] Griffith, Donald Edwin. 1956. *The Effect of Sodium Oleate on the Absorption of Ammonia by Water in a Spray Column* Georgia Institute of Technology

CHAPTER 6:
BEHAVIOUR OF INORGANIC AND ORGANIC MERCURY IN AQUEOUS ENVIRONMENT

6.1 Introduction

It is highlighted in Chapter 2 that trace levels of mercury have been reported to exist in three different phases (gas, organic and water phase) within the petroleum and natural gas processing. Mercury as a contaminant have several detrimental effects to the processing facilities, the operators as well as the environment. This issue has raised concerns and interests for engineers to study its behaviours among the gas, water and condensate phase.

The aim of this chapter is to consolidate and apply the findings obtained from Chapter 4 and 5 to predict the mercury species behaviour in aqueous environment. Comparison of the absorption parameters and characteristics of the three different types of mercury species will be utilised to help map out their distribution in a liquid natural gas (LNG) processing facility as well as upon release into the environment (atmospheric and waste water emissions).

Aspects of absorption characteristics, equilibrium condition and potential species interconversion will be discussed to help predict emission pathways of mercury from the processing facility to the environment (atmosphere and water streams). Based on the current results and knowledge learnt in this project, current uncertainties and knowledge gaps in predicting distribution of mercury within the environment will be analysed and addressed to.

Likewise, kinetic results obtained on effect of NaCl and MEG will also provide aid in determining potential for conversion between the mercury species during transport and at the MEG regeneration facility.

6.2 Mercury in Liquid Natural Gas Processing

A diverse petroleum and natural gas processing schemes are utilised depending on the composition of the hydrocarbon chain and the market objectives, however majority of the facilities follow the same basic configurations. A typical process flow diagram in an oil and gas processing facilities is summarised in Fig. 6.1.

Mercury is naturally present in the gas reservoir with highly variating concentration across the world (details are discussed in Chapter 2, section 2.2). Hence, mercury is introduced throughout the different parts of the process upon extraction and transportation of natural gas into the processing facility. During transportation, accumulation of mercury on the pipeline surfaces can occur. Mercury is known to get adsorbed on both carbon and stainless steel by chemisorption and adsorption respectively [1, 2]. Consequently, Hg^0 is known to react with iron oxide and iron sulphide which formed on the pipe walls as a product of corrosion [3]. Presence of H_2S is found to have a catalytic effect on the reaction.

$$H_2S + Fe_2O_3 \rightarrow FeO + S + H_2O \qquad (1)$$

$$Hg^0 + S \rightarrow HgS \qquad (2)$$

Steel pipelines scavenging of mercury during transportation may lead to its long-term delays entering the downstream processes. These contaminated pipelines will pose serious health hazards to workers when emission of mercury vapours occur during inspection and maintenance. Moreover, during the life cycle of the project, treatment and disposal of high level of mercury in scrap steel will be both a challenge and great expense.

As natural gas undergoes a series of processes, mercury is known to have the tendency to accumulate in various process equipment. In 2014, IPIECA has estimated that around 20% of mercury entering the refineries accumulates in process equipment and end up in multiple portion of waste released [4]. It has been reported that mercury has been detected in the slug catcher, gas dehydration, sour gas (CO_2/H_2S) removal system and in the wastewaters [5], with majority tending to accumulate in the CO_2/H_2S removal system.

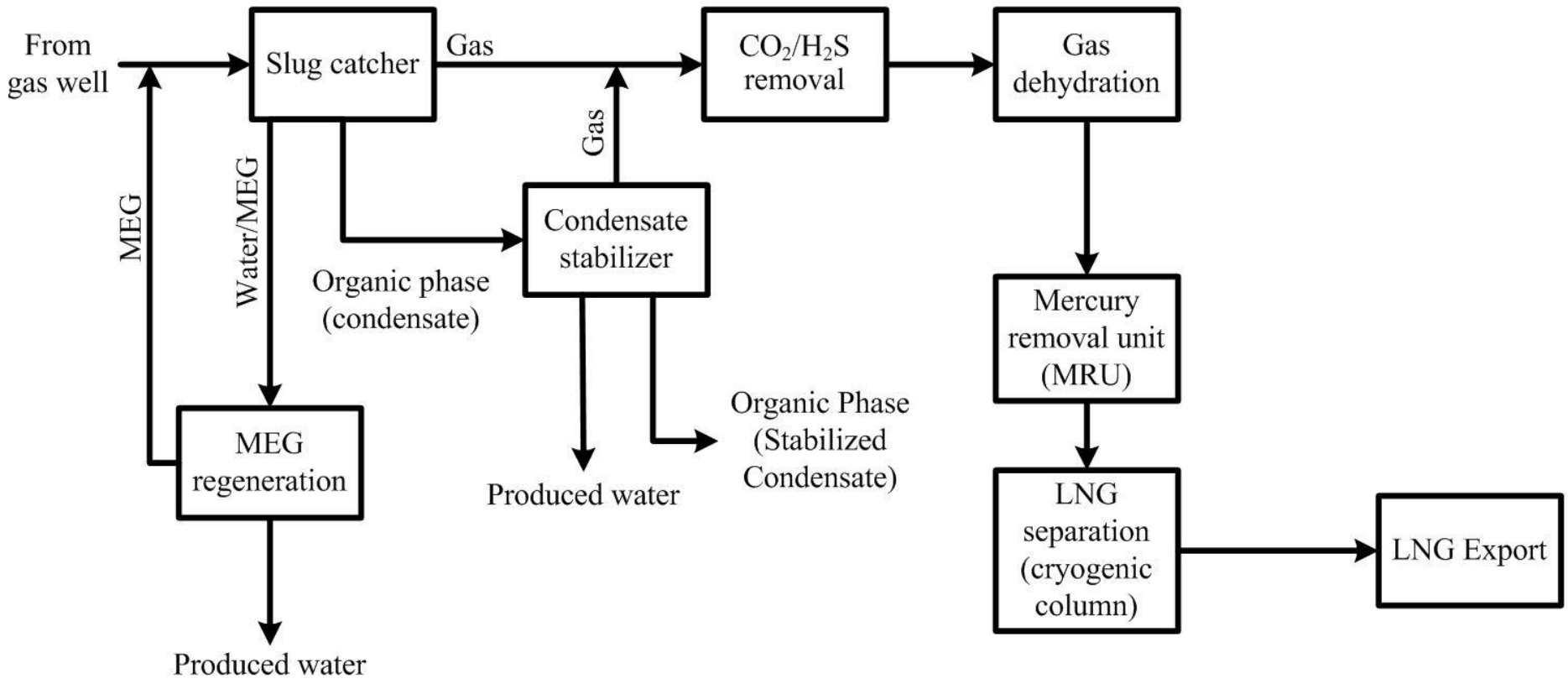

Fig. 6.1 Schematic of Liquid Natural Gas Processing

Although majority of the mercury will stay in the CO_2/H_2S removal system, some residual mercury will eventually end up condensing in the cryogenic section during natural gas liquid separation. The equipment used in the natural gas liquid (NGL) separation is most susceptible to mercury attack within the entire LNG processing facility. This is due to the use of aluminium alloy as the main construction material. Mercury even in small amount would cause major corrosion via liquid metal embrittlement (LME) and amalgam corrosion (AMC) as it deposits on the surface of the aluminium heat exchangers [6]. Mercury related failure and incidents on aluminium based equipment have been demonstrated and documented over the years [6, 7], one well known example being the Skikda gas plant explosion. Due to the high susceptibility and consequence of failure, gas processes often include a mercury removal (MRU) unit upstream of the NGL separation units to protect these cryogenic equipment.

Mercury that is present in the gas phase comes into contact with the water phase at numerous locations within the LNG processing equipment. Mercury location mapping within the LNG processes can be predicted using computer analyses. However, the current analyses techniques available take into assumption that all mercury are elemental in species along with equilibrium condition takes place when mercury partitions to different phases [6]. Unfortunately, this case is not valid in real life operations and it is still a major challenge to design appropriate safeguards to perform operations and maintenance tasks in the field.

Within the slug catcher where most of the partitioning to different phases occur (gas, water and organic phase), complete equilibrium is seldom reached due to the short residence time. This agrees with the results obtained in this work; outlined in detail in Chapter 4 and 5. Absorption of inorganic and organic mercury into water phase did not reach equilibrium in the contactor used in this work, despite the high gas concentration used and contact time of over 50 hours. Currently, information reported regarding mercury within the LNG processes rely heavily on knowledge gained from manual inspections and amount detected in various waste streams. Predictions using thermodynamic models require a lot of modifications to take into considerations non-equilibrium conditions. Transient results evaluated from this work will help improve the current mercury distribution models and accurate identification of emission points.

-Chapter 2, section 2.2 outlined the presence of several mercury species within the LNG processing facilities. However most have assumed the major cause of mercury related failure being solely Hg^0 due to its relative abundance and the limitations of current methods to analyse mercury gases. Majority of gaseous mercury monitoring in the industry utilises capture of gas using gold trap and analysed using atomic absorption spectroscopy (AAS) [8-10]. As discussed in Chapter 2 and 3, the use of this analysis method is not able to provide information in terms of mercury species present as AAS detects total mercury as Hg^0. In terms of gold trap, it is well known to be a good mercury capture material, but again, it is not selective to a particular mercury species as amalgamation is involved. According to literature reviews in Chapter 2, most speciation work involving mercury in oil and gas is mostly conducted on condensate and water phase.

Overlooking mercury speciation may cause serious unexpected errors associated with mercury deposition and damage within the LNG processes. It has been found in this work that varying mercury species (elemental; Hg^0, inorganic; $HgCl_2$ and organic; Ph_2Hg) behaves differently when being exposed to process liquids present in different locations of the LNG processes. Nevertheless, LME and AMC corrosions can occur with both Hg^0 and its other species whereby organic mercury (DMM) has been reported to cause more corrosion in aluminium and carbon steel compared to $HgCl_2$ [11]. Due to the serious implications that may arise, information regarding existing mercury species other than Hg^0 needed to be explored immediately.

Behaviour of the various mercury species present within the LNG processing facility is discussed in detail in the following sections. The mercury species in focus will be elemental mercury; Hg^0, inorganic mercury (represented by $HgCl_2$) and organic mercury (represented by Ph_2Hg). A summary detailing the possible pathways of distribution and reactions between the three mercury species with each other and the compounds present in the LNG processing system is illustrated in Fig. 6.2.

6.2.1 Behaviour of Mercury in Gas Phase

Several mercury species have been detected in natural gas, however its distribution and concentration remain a difficulty to be identified and quantified accurately. One aspect of distribution within the gas phase may be closely related to the compound's volatility. Table 6.1 summarises the vapour pressure of three different mercury species

(elemental, inorganic and organic) at 293 K. From Table 6.1, Hg^0 is most volatile among the other mercury species having a vapour pressure of several magnitudes higher than $HgCl_2$ and Ph_2Hg. Therefore, it is expected that Hg^0 has the tendency to stay in gaseous phase within the process. One would expect the distribution of mercury species within the gas phase to follow their volatility.

Table 6.1 Vapour Pressure of Various Mercury Species at 293 K

Mercury Species	Vapour Pressure (Pa)	Reference
Hg^0	0.171	[12]
$HgCl_2$	0.0128	[13]
Ph_2Hg	0.00015	[14]

Some have reported presence of other mercury species such as inorganic and organic mercury in the gas phase, but at a very small concentration (<1%) [15]. This small concentration detected might come from the partial pressure overhead of their dissolved compound in water phase, governed by H law. A document by S. Mark Wilhelm [16] reported the maximum concentration of mercury in produced waters to be 27 ppb in the Gulf of Mexico. Using the reported concentration as a basis, a simple calculation was performed to estimate the partial pressure (P_{gas}) of mercury gas that is in the overhead of the produced waters at 298 K. The results have been summarised in Table 6.2.

Table 6.2 Partial Pressure at the Overhead of Produced Waters Containing Mercury (Concentration = 27 μg Hg/L) at 298 K

Mercury Species	H ($Pa.m^3/mol$) (298 K)	P_{gas} (Pa)
Hg^0	769.23	0.104
$HgCl_2$	7.14×10^{-5}	7.10×10^{-9}
Ph_2Hg	0.980	7.46×10^{-5}

Results from Table 6.2 is similar with that seen in Table 6.1, where most of mercury species present in the gas phase will be Hg^0. These two simple analyses further justify the claims of Hg^0 being the major species in natural gas detected [16-22]. However, in Table 6.2 the order of distribution abundance with regards to $HgCl_2$ and Ph_2Hg is the other way around. Most inorganic mercury species have a relatively low He which means that they have the tendency to stay in the water phase, emitting gas at very low partial pressure. Vapour pressure of Ph_2Hg is much lower compared to $HgCl_2$ (Table 6.1), however at equilibrium, it can exert a higher partial pressure when the same amount is dissolved in water. It can be seen from Table 6.2 that the calculated equilibrium partial pressure of Ph_2Hg is a few degrees of magnitude higher than that

of $HgCl_2$. This finding suggest that Ph_2Hg has less tendency to stay in the water body compared to $HgCl_2$, resulting in higher concentration in gas phase. Hence, mercury in gas phase should be distributed as Hg^0 > Ph_2Hg (organic) > $HgCl_2$ (inorganic) in the order of decreasing abundancy.

Majority of gaseous mercury species that enter and accumulate within the CO_2/H_2S removal system is suspected to be Hg^0. Accumulation will mostly occur as HgS and some Hg^0 may be dissolved in the amine solutions. The accumulation of Hg^0 in the CO_2/H_2S gas removal system may be caused by two main ways:

1. Mercury is well known to have a strong affinity with sulphur compounds to form insoluble HgS [23].

   $$Hg^0 + H_2S \rightarrow HgS + H_2 \qquad (3)$$

   This reaction has a high occurrence during the CO_2/H_2S removal process and may cause accumulation of mercury in the equipment as suspended HgS. The reaction aforementioned will more likely to occur in solution (dissolved H_2S in amine solution) as Hall et al. [24] observed no chemical reaction between mercury and H_2S in gas phase. This reaction can also happen between dissolved mercury and H_2S gas, leading to formation of red HgS and reduced amount of mercury in solution [25]. Moreover, mercury in the presence of H_2S is known to have a significant increase in corrosion of aluminium and steel surfaces [11]. The presence of the two chemicals would lead to equipment damage within a fairly short period of time.
2. CO_2/H_2S removal often involve the use of amine solvents such as MEA (monoethanolamine), MDEA (methyl diethanolamine), DEA (diethanol amine) and DIPA (di-isopropanol amine) to remove both CO_2 and H_2S from product gas [26-28]. Aqueous MEA solution have been known to be able to absorb a certain amount of mercury, with removal efficiency reported at 15% for 3 kmol/m^3 MEA solution [29]. In the case of MDEA, absorption of mercury by the liquid will be quite unlikely as poor absorption (almost 0% efficiency) reported for 45% MDEA solution [28].

6.2.2 Behaviour of Mercury in Water Phase

Mercury of multiple species (Hg^0, inorganic and organic) have been reported to co-exist within the water phase with majority being the inorganic species, $HgCl_2$. Assumptions of gas/liquid equilibrium may be true in the case of Hg^0 due to its high H value (769.23 $Pa.m^3/mol$, 298 K, Table 6.2). The ease of reaching equilibrium has also been observed in this work, whereby Hg^0 reached equilibrium with water within a day of contact time (refer to Chapter 3, section 3.6). Using the calculated absorption parameters obtained from this work, absorption of Hg^0 gas overhead a water body is expected to occur at flux of 8.21×10^{-8} mol/m^2. h to reach equilibrium. This absorption flux is true if the concentration of Hg^0 gas phase is within the range reported; 0.02-1930 $\mu g/m^3$. Hence, based on the findings detailed, trace amount of Hg^0 may be present at equilibrium when gas phase comes into contact with the produced water stream, mostly at the slug catcher. Hg^0 equilibrium concentration in the water phase is expected to not exceed 60 ppb of the total mercury present.

$HgCl_2$ is classified to be a very soluble compound as its absorption into water is controlled by the gas phase resistance (Chapter 4, section 4.2). At equilibrium condition, its H is reported to be 7.14×10^{-5} $Pa.m^3/mol$ (Table 6.2) and its maximum solubility in water is 73 g/L at 298 K. As a result, $HgCl_2$ would be the prevalent species in the water phase separated in the slug catcher. According to the dynamic solubility studies of $HgCl_2$ in pure water conducted, it can be observed that equilibrium was still far away even at high gas concentration of $HgCl_2$ (500-4500 μg Hg/m^3) and contact time of over 50 hours. It is to be expected that gas/liquid equilibrium for $HgCl_2$ gases above a body of water will take much longer in the process plant. This assumption is due to the fact that lower concentration of these gases have been detected in field compared to the concentration used in this work. k_G was observed to have been constant in Chapter 4, section 4.3, regardless of gas concentration. Due to this absorption characteristics of $HgCl_2$, this will lead to lower absorption flux due to the lack of concentration gradient to promote the absorption.

Based on the absorption parameter in Chapter 4, $HgCl_2$ absorption flux in water can be estimated to reach a maximum of 1.93×10^{-5} $mol/m^2.h$ at 298 K for the highest detected concentration of 1930 $\mu g/m^3$. Based on this estimated absorption flux, it will take at least a few months under constant $HgCl_2$ in the gas to reach equilibrium. It is

to be noted that the estimated flux will be an overestimation as majority of mercury species in the gas detected comprises of >90% Hg^0 [16].

Water streams present in the LNG process has been reported to contain NaCl [30], especially very high concentration of Cl^-. Presence of NaCl will promote the absorption of enhancement of $HgCl_2$ in the overhead gas by formation of stable and very water-soluble complex; $Na_2[HgCl_4]$. According to the findings from Chapter 4, the reaction between $HgCl_2$ and NaCl follows second order reaction, with reaction constant $k_2 = 1.09 \times 10^9 \exp(\frac{-123.32\ \mathrm{kJ/mol}}{\mathrm{RT}})$. Its reaction mechanism can be represented as follows:

$$2NaCl \rightarrow 2Na^+ + 2Cl^- \quad (1)$$
$$HgCl_2 + Cl^- \rightarrow HgCl_3^- \quad (2)$$
$$HgCl_3^- + Cl^- \rightarrow HgCl_4^{2-} \quad (3)$$
$$HgCl_4^{2-} + 2Na^+ \rightarrow Na_2[HgCl_4] \quad (4)$$
$$2\ NaCl + HgCl_2 \rightarrow Na_2[HgCl_4]$$

The reaction mentioned although is very slow, it is very sensitive with temperature and will cause significant increase in absorption. Having said that, slug catchers typically operate within a temperature range of 290 – 300 K, around ambient temperature. At a lower temperature, enhancement of absorption caused by the reaction of $HgCl_2$ and NaCl would only result in enhancement of absorption by a factor of ~2 in 3.5 wt. % NaCl solution.

Solubility of Ph_2Hg sits in between Hg^0 and $HgCl_2$ at 0.0104 g/L at 293 K (Chapter 5, section 5.2). It is a challenge to predict Ph_2Hg equilibrium condition with water phase as there is no conclusive information with regards to its equilibrium constant. Currently, the H reported for Ph_2Hg/water system is 0.98 [31] $Pa.m^3/mol$ at 298 K. Taking into consideration its dynamic solubility studied in Chapter 5, gas/liquid equilibrium between Ph_2Hg gas and water might require a fair bit of time to be achieved. Comparison of Ph_2Hg absorption profile with Hg^0, suggest equilibrium to be achieved within the LNG process at absorption flux of 7.74×10^{-6} $mol/m^2.h$. Presence of NaCl up to 3.5 wt. % within the water phase have been shown to slightly decrease the absorption flux of Ph_2Hg into water due to salting-out effect.

As outlined in Chapter 2, mercury and its species are well known to readily react with each other and other compounds present to be converted into other mercury

compounds. When Hg^0 and $HgCl_2$ co-exist in the water phase, it is highly likely that they will react to form Hg_2Cl_2 which is less soluble in water [32]. Furthermore, this reaction will also occur between gaseous Hg^0 and dissolved $HgCl_2$, which results in an increased amount of total mercury in the water phase.

$$Hg^0 + HgCl_2 \rightarrow Hg_2Cl_2 \quad (4)$$

As previously discussed, formation of insoluble HgS will also occur between Hg^0, $HgCl_2$ and Ph_2Hg [33-35] with H_2S within the water phase.

$$Hg^0 + H_2S \rightarrow HgS + H_2 \quad (5)$$

$$HgCl_2 + H_2S \rightarrow HgS + 2HCl \quad (6)$$

$$Hg(C_6H_5)_2 + H_2S \rightarrow HgS + 2C_6H_6 \quad (7)$$

Ph_2Hg being one of the more stable mercury compounds has the highest tendency to undergo species transformation when exposed to other mercury species. Ph_2Hg undergoes decomposition in the presence of high heat and light to evolve Hg^0 gas [36]. This reaction might be one of the reasons why there is a lack of dialkyl mercury detected around the LNG facilities and the abundance of Hg^0.

$$Hg(C_6H_5)_2 \rightarrow Hg^0 + \text{phenyl radicals} \quad (8)$$

Moreover, in the presence $HgCl_2$, Ph_2Hg is known to react to form phenyl mercuric salts [37]. Some has reported the possibility of the reaction being reversible [38] and the conditions haven't been specified.

$$Hg(C_6H_5)_2 + HgCl_2 \leftrightarrow 2(C_6H_5)HgCl \quad (9)$$

Based on the analysis and findings from this work, distribution of mercury in the water phase would follow $HgCl_2 > Ph_2Hg > Hg^0$ in the order of decreasing abundancy.

6.2.3 Behaviour of Mercury in MEG Solution

MEG has been commonly injected into the pipeline for flow assurance purposes by inhibiting formation of hydrate. Some of the mercury present in both the gas and water phase have been reported have partitioned into the MEG solutions injected into the pipeline and in the glycols used in the gas dehydration stage. In the case of Hg^0, some of the dissolved Hg^0 has a high chance to accumulate in the equipment within the MEG

regeneration process by means of adsorption discussed earlier [39, 40]. If the concentration of Hg^0 in the gas is sufficiently high, it can be expected to condense to form liquid mercury in the MEG regeneration unit. Similar to the water phase, it is likely for Hg^0 to be at equilibrium condition in MEG solution with equilibrium concentration not exceeding 182 ppm in MEG at 293 K [41].

In Chapter 4 and Chapter 5, dynamic solubility study of $HgCl_2$ and Ph_2Hg in MEG solution of up to 50 v/v% show similar behaviour in water. No enhancement of absorption was observed when MEG concentration was increased up to 50 v/v% for both $HgCl_2$ and Ph_2Hg. The findings from this work suggest that there will be no sudden enrichment of mercury in the liquid phase when MEG is injected in the system. Consequently, as MEG concentration further increased, it would be expected for absorption rate to decrease due to the change of physical properties of the liquid (viscosity) acting as resistance (shown in Chapter 5, section 5.5.2). Several authors have reported the possibility of reaction between $HgCl_2$ and polyethylene glycol to form a metal complex; $[(HgCl_2)_3[EO3]]$ and $[HgCl_2[EO5]]$ [42]. Unfortunately, such reactions were not detected for the experimental conditions performed in this work.

Although enhancement of absorption rate was not observed, it is to be noted that Ph_2Hg is around 20 times more soluble in 50 v/v% MEG compared to in water (Chapter 5, section 5.5). Moreover, Ph_2Hg being an organic species, is more soluble in organic solvents [38]. Based on these findings, it is more likely to find higher concentration of Ph_2Hg in the MEG stream rather than in the water stream.

Finally, the interconversion between the mercury species resulting from several chemical reactions discussed in section 6.2.2 should be applicable in MEG solution as well.

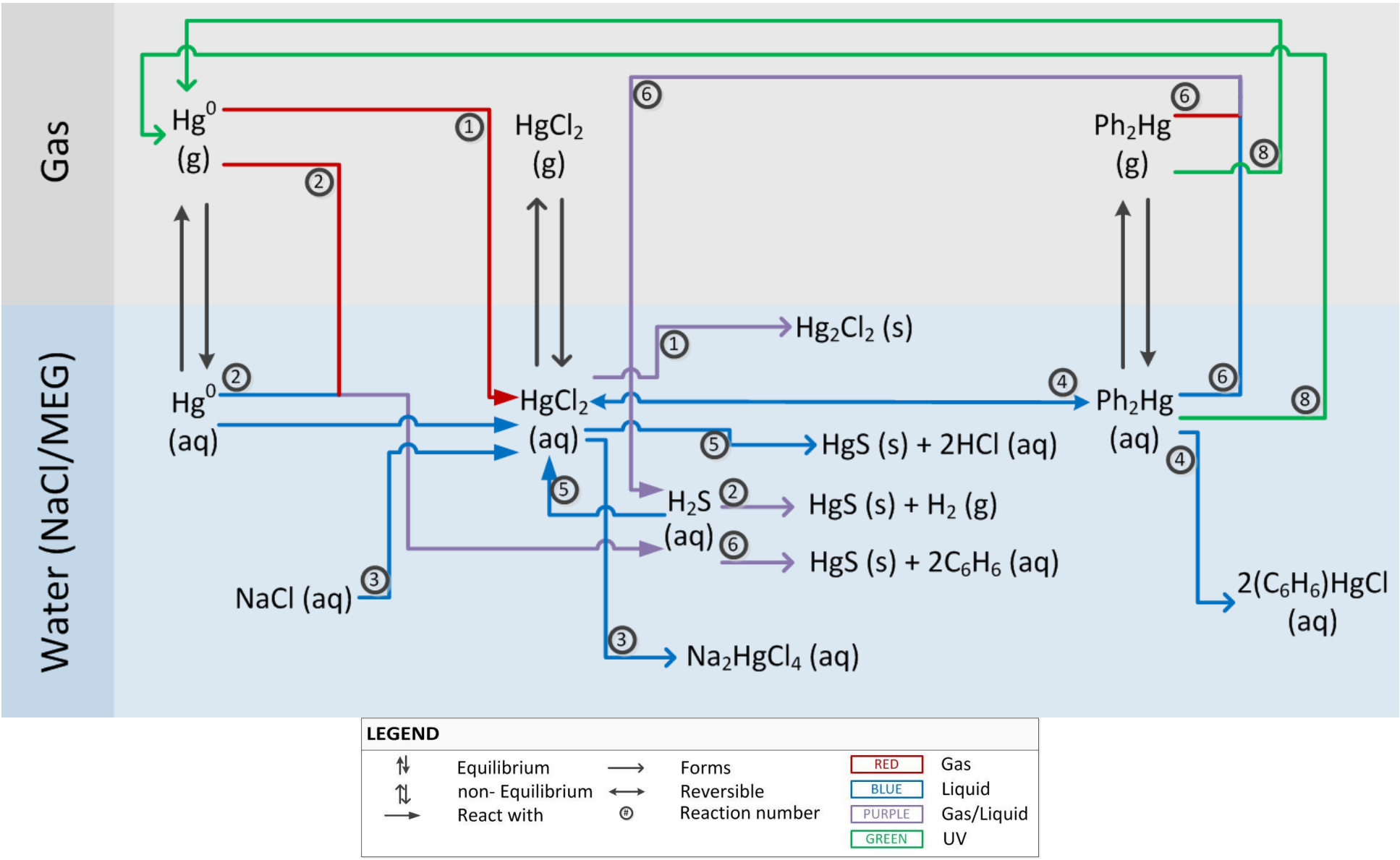

Fig. 6.2 Behaviour of Mercury Species in Aqueous Environment within LNG Processing Facility

6.2.4 Mercury Emission from LNG Processing

Mercury that is within the LNG processing facility has a possibility to be emitted into the environment by several means. Several means of mercury emissions may come from three main ways, namely waste water, solid waste and gas phase. The produced water that is associated to the LNG processing would mainly come from the slug catcher and the condensed water from the gas dehydration, the MEG regeneration and condensate stabilization unit. Point of mercury release through the gas phase would originate from process equipment via means of possible leaks and through the CO_2/H_2S removal, gas dehydration stage, glycol regeneration and MRU. Consequently, solid waste that are produced may contain high concentration of mercury.

Produced waters from Gulf of Thailand have been reported to contain suspended HgS , Hg^0 and ionic mercury (Hg^{2+}) [43, 44]. Concentration of up to 235 ppb was detected prior to treatment [44]. Most of these produced waters enter the environment by two ways, namely during discharge to a water body (oceans, lakes, evaporation pond, etc) and/or injected back into the gas reservoir. Prior to being discharged, produced waters are usually treated to remove as much mercury as possible to comply with government regulations. In the Gulf of Thailand, discharged water must not exceed 10 ppb of total mercury [44]. Re-injection of produced water is often selected to both reduce emission of mercury into the environment while at the same time provide benefit of enhancing oil recovery by maintaining well pressure [45, 46]. This method however is not simple and poor design may lead to production loss and a safety risk, hence produced waters are usually discharged, sometimes without treatment in areas that are not well-regulated.

Mercury release through gas phase would escape from CO_2/H_2S removal, gas dehydration stage and MRU. This is because most of the feed gas will pass through these stages prior to being condensed for production. Mercury would mainly release to the environment as vent gases from the three stages mentioned.

In gas dehydration stage, a stream of glycol (usually MEG or EO3) at ambient temperature is used to scrub the wet gases after removal of CO_2 and H_2S [47, 48]. As the glycol solution comes into contact with the wet gas, water, mercury and other impurities will be accumulated. The water-rich glycol stream will be sent to a glycol

recovery unit whereby it is filtered and heated to remove the water vapour. The accumulated mercury that is present in the water-rich glycol stream would be released along with the water vapour from this stage.

In CO_2/H_2S removal stage, the 'rich' amine solution used to remove these acid gases are usually sent to a regeneration unit where the solution is heated to release a CO_2/H_2S 'rich' gas. This CO_2/H_2S 'rich' gas is commonly burned to release any mercury present to enter the atmosphere. Several data from the literature estimated that 10% and 1.4% of total mercury is lost at the CO_2/H_2S removal and gas dehydration unit respectively [48].

Sources of solid mercury waste mainly comes from the sorbent materials used in the MRUs and from sludge and suspended solids accumulating in separators and filters [49]. Another possible location that produces solid mercury waste would be at the glycol regeneration units. It has been reported by Zaboon et al. [50] that presence of salt in the water phase leads to precipitation of salts such as $CaCO_3$ and $FeCO_3$. Mercury species may react with these salt-precipitate and deposit within the process equipment.

A diagram illustrating the potential location of mercury release from LNG process is provided in Fig. 6.3.

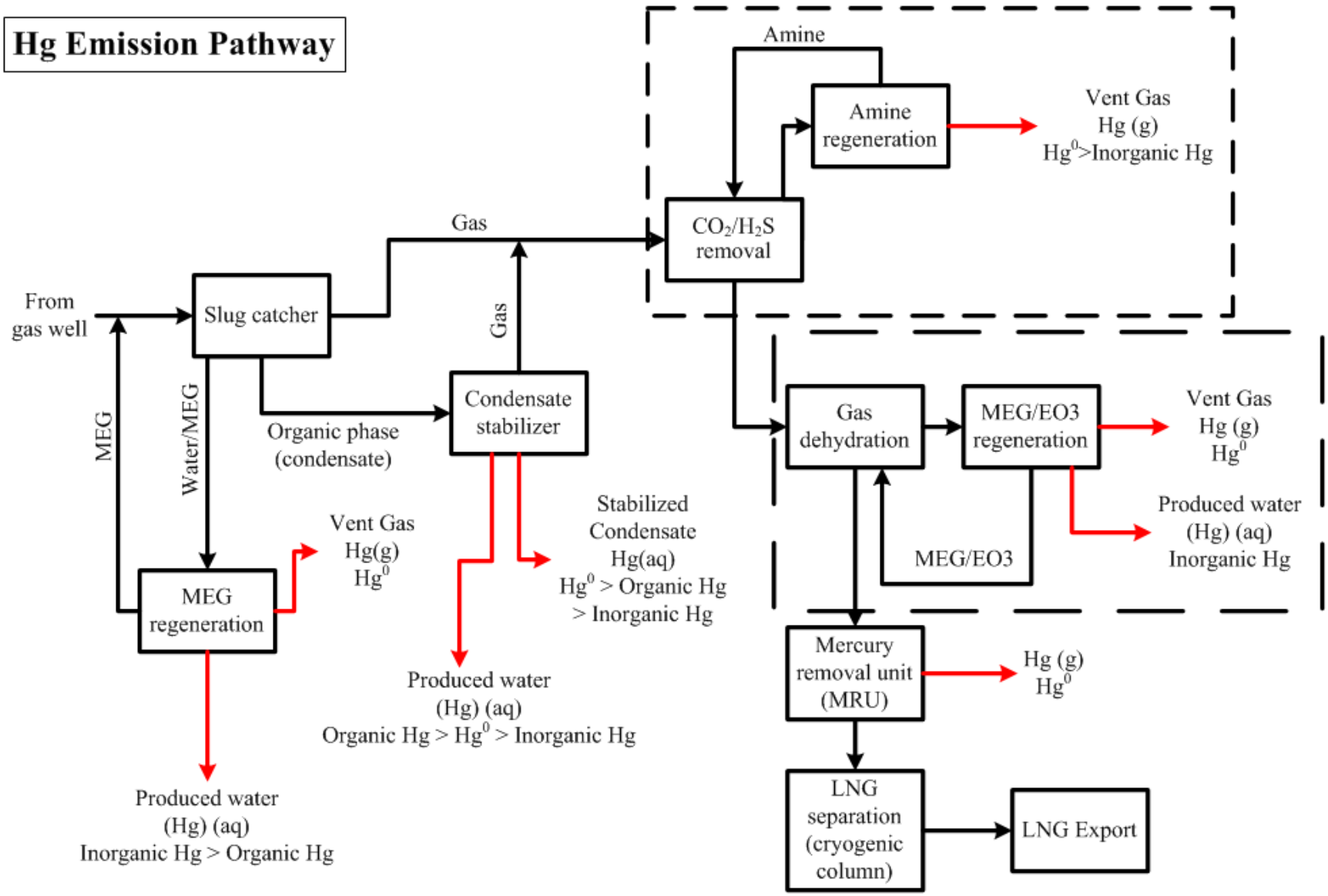

Fig. 6.3 Main Emission Pathway of Mercury from LNG Processing Facility

6.3 Mercury in the Environment Emitted from LNG Facility

As previously discussed, mercury is released from the LNG processing facility as gas and waste water, both introduced into the environment through the atmosphere and the aquatic environment such as the ocean and wetlands. Wetlands are defined as areas where a body of water is present at different periods of time during the year. Some examples of types of wetlands include ponds, lakes, floodplains, etc. Released waste waters containing mercury from LNG processing facilities may be introduced into the wetlands via aquatic cycling of sea water. However, deposition from atmospheric mercury has been reported to be the main entry point into several wetlands [51].

The atmosphere provides transportation pathways for mercury species as they may get transported over a long distance before being deposited either in surface waters or land (wet and dry deposition) [52]. The distance at which gaseous mercury can travel is highly dependent on its residence time within the atmosphere. This residence time is closely related to mercury's tendency to be deposited and varies depending on the species. According to the analysis in section 6.2, Hg^0 is the major mercury species emitted from LNG processing facility, followed by $HgCl_2$ and Ph_2Hg in much smaller abundance.

The atmospheric residence time of $HgCl_2$ has been reported to be within the range of hours and a day [51, 53]. The results from the literature generally agrees with the findings from Chapter 4. $HgCl_2$ is readily absorbed into the water phase almost immediately, around 60% of the gas phase is absorbed within the first few hours of contact time. Absorption of $HgCl_2$ into water is heavily affected by the change in temperature and the partial pressure of the gas; Chapter 4 section 4.2 and 4.3. Increase in temperature has a positive impact on the mercury flux, which means that mercury exchange between atmosphere and water will occur more during the warmer months. This agrees with Selin et al. [54] and Wängberg et al. [55], whereby they've reported an increase gaseous mercury flux during summer and fall. Equilibrium condition might occur within a span of a few months, however within that period, any $HgCl_2$ presence in the gas phase will be absorbed immediately into the water bodies. It has been reported that vented gas from the glycol regeneration and acid gas removal process have mercury concentration of up to 150 $\mu g/m^3$ [48]. Assuming that all of the mercury in the vent gas enters the atmosphere, the equilibrium concentration within the nearby water body is quite high; 7.9 g/L at 298 K.

The atmospheric residence time of Ph_2Hg of 1 day has been reported [31]. Similar to $HgCl_2$, absorption of Ph_2Hg is enhanced with the increase in temperature and its concentration in gas phase as the driving force. Ph_2Hg does not dissociate in water, however this result is still within expectation as Ph_2Hg will decompose to form Hg^0 in the presence of UV light (Rxn. 8). Presence of UV light in the atmosphere is unavoidable with exposure of up to 12 hours in most part of the hemisphere. Henceforth, due to its relatively short lifetime, one would expect deposition of Ph_2Hg from the atmosphere to occur within proximity of its emission source.

The atmospheric residence time of Hg^0 has been predicted by several methods to be quite long, most estimates 1 – 2 years [53, 56]. This predicted residence time has helped explained the presence of mercury in remote locations on the hemisphere; the Arctic and Antartic regions. A comprehensive review on the presence of mercury in Arctic terrestrial have detected ~3% of the total dissolved mercury from lake waters found in the arctic area [57]. The findings support the claim of mercury transportation in the atmosphere as they concentration detected were far too high to have come from local sources. Although assumption is likely valid, Hedgecock and Pirrone have calculated residence time of Hg^0 to be only within 10 days within marine boundary layer (MBL) [58], which is quite contradicting. Based on the discrepancy of the two results, the basis of the calculations needs to be analysed further. Fig. 6.4 provides a visual representation of the current mercury transfer and transformation within the atmosphere. The sections shown labelled in Fig. 6.4 will be analysed subsequently to identify possible sources that yield to uncertainties in atmospheric modelling of mercury.

The method to estimate the residence time of Hg^0 is dictated by its oxidation process. Hg^0 upon released into the atmosphere will eventually get oxidised by ozone and other gases present to form inorganic Hg(II) species. This process is denoted (I) in Fig. 6.4. The resulting inorganic Hg(II) species are water soluble in nature and will combine with water vapours and travel back the Earth's surface as rain via absorption (wet deposition). A summary of the oxidation process used as basis in the estimation method has been summarised in Table 6.3.

Table 6.3 Estimation of Hg^0 Residence Time in the Atmosphere

Oxidation Process	**Residence Time of Hg^0**	**Source**
O_3, HCl, SO_2, OH	~1.7 years	[56]
O_3	0.3 – 2 years	[53]
O_3, H_2O_2, NH_3, NO_2, HNO_3, CH_4, HCHO, CO, CO_2, HCl, SO_2, OH, halogens	10 days	[58]

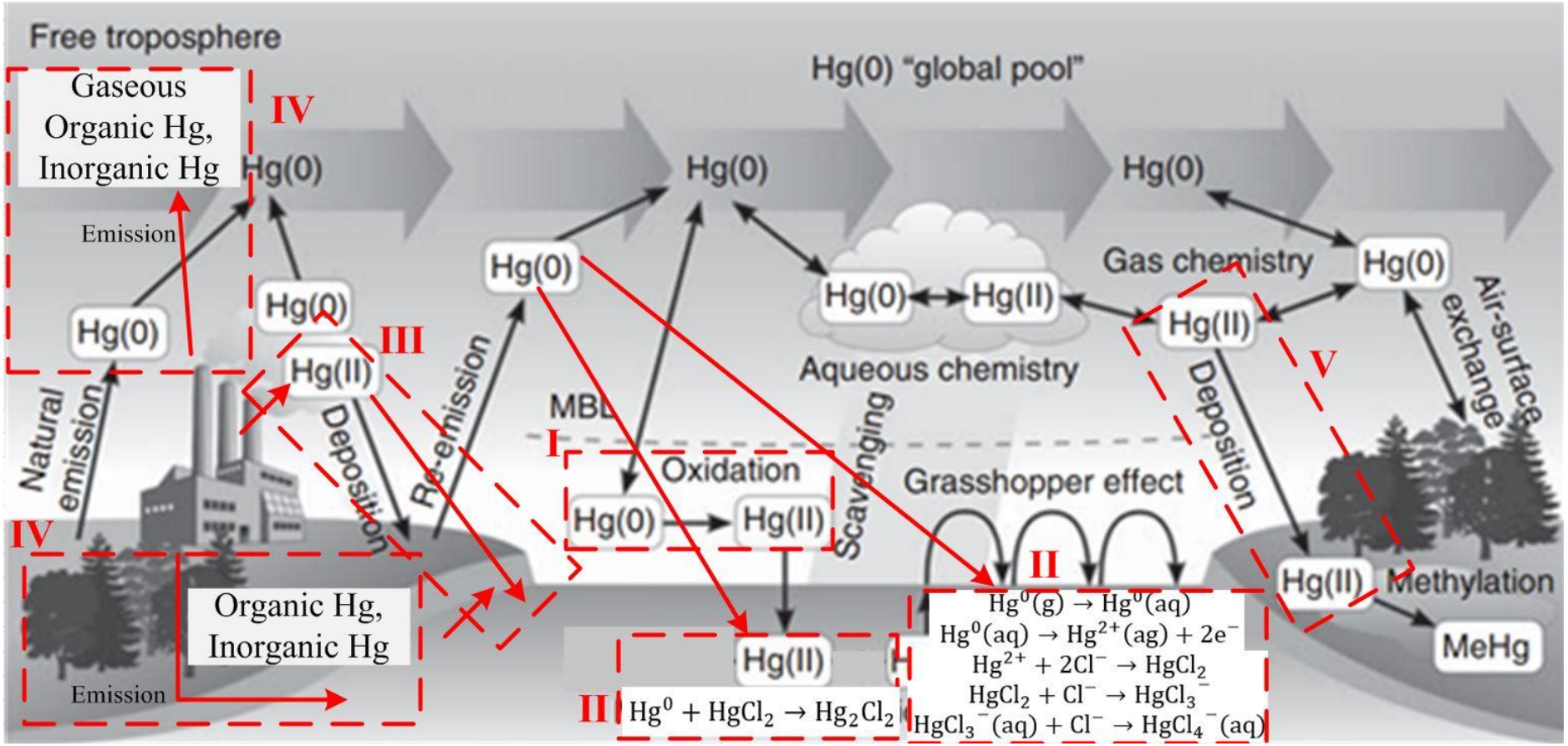

Fig. 6.4 Overall Mercury Transfer and Distribution in the Environment [59]

Result from Table 6.3 shows a decrease in overall Hg^0 residence time as more oxidation process are added into the equation. The oxidation of Hg^0 to Hg(II) is commonly known to readily occur in the gas phase with O_3. However, addition of several possible reaction pathways with existing gases in the atmosphere, leads to a big reduction of residence time from 1 – 2 years to as low as 10 days. The varying estimates of residence time shows the lack of understanding and data to accurately model mercury behaviour in the atmosphere. Other than formation of water-soluble mercury species, Hg^0 may undergo deposition when $HgCl_2$ is present in the surface waters. It has been reported by Ma et al. that solution of $HgCl_2$ is able to effectively absorb some Hg^0 by Rxn. 4 to form Hg_2Cl_2 [32]. Due to the likeliness of this reaction from occurring, it is necessary to include this into the current mercury atmospheric modelling.

Other than reactions involved in deposition of Hg^0, atmospheric residence time is also dependent on the kind atmospheric conditions and the season of the year (most likely associated with wind speed, temperature and rainfall). Hedgecock and Pirrone [58] have also observed a decrease in residence time of Hg^0 at low temperature with high sunlight and aerosol particles. Most of the oxidation reaction with the gases and contaminants present in the atmosphere are highly endothermic, hence likelihood of reaction happening at lower temperature is expected. This suggests that Hg^0 released from LNG process would get deposited within the surrounding area. The area surrounding the processing facility will have substantial number of contaminants as they are simultaneously released with mercury in the waste streams [60]. The presence of these contaminants will encourage oxidation of Hg, thus reducing its residence time in the atmosphere. Reduction of residence time will result in Hg^0 having less time to be transported further away, hence accumulating within close proximity of the release point. This effect of contaminants has been reported by several authors [61-63] whereby mercury was detected within 5 – 10 km from a chlor-alkali plant. Deposition close to the emission source is also applicable for $HgCl_2$ and Ph_2Hg as they have a very short residence time to begin with.

(II) in Fig. 6.4 refers the possible pathways for direct mercury deposition in sea water. Presence of high concentration of NaCl, typically from the sea has been observed to increase deposition rate of Hg^0 by promoting oxidation and stabilise formation of

$HgCl_2$ and its chloro-complexes ($HgCl_3^-$ and $HgCl_4^{2-}$) [64, 65]. The oxidation reaction within the water phase has been reported to follow a pseudo zero-order [65]. This means that oxidation into Hg (II) is likely to happen after Hg^0 is deposited into the water phase. Reaction pathways of Hg^0 oxidation in NaCl solutions occurs following Rxn. 10 up to 14.

$$Hg^0(g) \rightarrow Hg^0(aq) \quad (10)$$

$$Hg^0(aq) \rightarrow Hg^{2+}(aq) + 2e^- \quad (11)$$

$$Hg^{2+} + 2Cl^- \rightarrow HgCl_2 \quad (12)$$

$$HgCl_2 + Cl^- \rightarrow HgCl_3{}^- \quad (13)$$

$$HgCl_3{}^-(aq) + Cl^- \rightarrow HgCl_4{}^-(aq) \quad (14)$$

Direct deposition is also possible as the deposited $HgCl_2$ act as a good absorber of Hg^0 (discussed in detail in previous sections). Hence, one could expect some deposition of Hg^0 to occur directly rather than only through deposition of Hg(II). Result from Chapter 3, section 3.6 observes absorption of Hg^0 into water phase, reaching its maximum concentration of 57 µg/L at 298 K within 20 hours of contact. Absorption and kinetic parameters of the absorption of $HgCl_2$ in NaCl solution has been provided in Chapter 4, section 4.4 This information will prove useful to add onto and improve existing mercury atmospheric modelling.

(III) in Fig. 6.4 illustrates the pathways for direct deposition of Hg(II) gas as $HgCl_2$ upon release to the atmosphere. Many of these pathways assumed gas/liquid equilibrium to have been reached which does not agree with the findings of this work. Analysis of equilibrium condition of $HgCl_2$ with water phase has been discussed in the prior section. Moreover, aqueous reactions involving $HgCl_2$ have assumed dissociation of $HgCl_2$ to Hg^{2+} and Cl^- [56, 66]. This assumption is debatable as earlier study of $HgCl_2$ [67] has proven non-dissociation of the compound in water (Chapter 4, section 4.4). In addition, deposition of $HgCl_2$ into the water body should occur readily and not just through re-emission of Hg^0. Presence of high concentration of NaCl, such as in sea water will promote higher deposition rate as absorption of $HgCl_2$ gas is enhanced by a factor of 2 through the formation of $Na_2[HgCl_4]$ in the water phase (Chapter 4, section 4.4.1).

(IV) in Fig. 6.4 refers the emission pathway for inorganic and organic mercury into the atmosphere and the aquatic phase. It has been discussed in prior that mercury released into the environment from the anthropogenic sources (such as LNG processing) exist in all three species; elemental, inorganic and organic. Despite this knowledge, many mercury atmospheric pathways still include only Hg^0 into their work. Especially with organic mercury, presence of this mercury species within the aquatic environment is mostly assumed to have indirectly resulted from the conversion of dissolved Hg^0 and Hg(II) via the methylation process [68]. Although not as soluble as $HgCl_2$ in water, results from Chapter 5 suggest that organic mercury has a comparable absorption flux when present at similar gas concentrations; around 3 times slower than absorption flux of $HgCl_2$. This introduction of organic mercury through this additional pathway may lead to higher overall concentration of organic mercury in these natural water bodies. This finding needs to be reviewed and added into the current mercury behaviour in the aquatic environment.

(V) in Fig. 6.4 represents the deposition pathway for gaseous inorganic mercury; $HgCl_2$ into the fresh waters such as lakes and ponds. Presence of NaCl in sea water contribute to higher absorption flux of $HgCl_2$. Having said that, a study of the reaction between these two compounds is found to be very slow and resulted in small enhancements (Chapter 4, section 4.4). From the finding of this work, it is expected that absorption of $HgCl_2$ into fresh water sources to be comparable to its absorption in sea water. As absorption of $HgCl_2$ in water is controlled by its gas-film resistance, flux will mainly depend on the temperature of the environment and its concentration in the gas phase.

6.4 Summary

This work evaluated the behaviour of several mercury species (elemental, inorganic and organic) within the aqueous environment based on the findings from Chapter 3, 4 and 5. The aqueous environment encompasses those within the LNG processing facility and in the environment upon mercury being released in the waste streams. From the discussion presented, the following conclusions can be drawn.

Within the LNG processing facility:

- Mercury exists in various species, including elemental, inorganic ($HgCl_2$) and organic (Ph_2Hg) species. Based on their respective dynamic solubility studies, $HgCl_2$ present in the gas phase will be the fastest to get absorbed into the water and MEG phase, followed by Ph_2Hg and Hg^0.
- Hg^0 and Ph_2Hg gas will most likely reach equilibrium with water and MEG system within a span of a few weeks. On the other hand, $HgCl_2$ will take at least a few months to reach equilibrium, provided a constant $HgCl_2$ being supplied at all time from the feed gas.
- $HgCl_2$ will be the major species prevalent in the water and MEG phase. Presence of NaCl in all water and MEG streams will enhance absorption of $HgCl_2$ from the overhead gas and keep the species stable as $Na[HgCl_4]$ metal complex.
- Hg^0 and Ph_2Hg will have the tendency to be more prevalent in MEG solutions compared to water phase. This is contributed by their increased solubility in MEG. Ph_2Hg is 20 times more soluble in solution of 50 v/v% MEG compared to just in water. Hg^0 concentration in MEG should be expected to not exceed 182 ppm. Moreover, presence of NaCl will reduce absorption of Ph_2Hg due to salting-out effect.
- Mercury is emitted to the environment as gas and liquid phase. Gaseous mercury escapes process equipment, entering the atmosphere at the CO_2/H_2S removal stage, gas dehydration stage, condensate stabilization stage and MRU as vent gases. Mercury is released in liquid phase as produced waters from the slug catcher, condensate stabilization stage and the glycols regeneration unit.

Within the environment:

- Hg^0 will be present mostly in the atmosphere upon release from the LNG processing facility. Current method to estimate the residence time of Hg^0 in the atmosphere of 1-2 years have some uncertainties and lead to overestimation. Factors used to estimate the residence time is limited to the oxidation reactions of Hg^0 to form Hg(II) that will exist the atmosphere and enter the water phase. Direct deposition of Hg^0 is often not considered. Presence of NaCl in water (sea water) show an increment in Hg^0 deposition by enhancing the oxidation process and forming a stable mercury chloro complexes.
- $HgCl_2$ will be present in the environment in aqueous form. Some of total deposition of Hg(II) gas into the water phase comes from direct deposition of $HgCl_2$ gas upon release into the environment. Sea water and saltwater wetlands will have the highest deposition of $HgCl_2$ due to the formation of stable mercury-chloro complexes. Although absorption flux into sea water will be higher, this enhancement will not exceed a factor of 3 compared to absorption in fresh waters. This is because of the slow reaction between $HgCl_2$ and NaCl.
- Ph_2Hg will have a short life time upon entering the atmosphere and surface waters, estimated to be around 1 days. Ph_2Hg will decompose to release Hg^0 gas and phenyl radicals in the presence of UV light. Direct introduction into the aquatic environment should be re-considered as sources of organic mercury in wetlands and sea water when reviewing the methylation of elemental and inorganic mercury.

6.5 Reference

[1] Wilhelm, S. Mark, and Mark Nelson. 2010. "Interaction of Elemental Mercury with Steel Surfaces." *The Journal of Corrosion Science and Engineering* no. 13 (Preprint 38).

[2] Widyanto, Bambang, Iryanni Dewi Tanto, and Secta Ariardi Aviananto. 2014. The Effect of Elemental and Mercury Compound Presence in Solution on Corrosion Phenomena of Aluminum and Low Carbon Steel. In *The 19th International Corrosion Conference*. Jeju Island, Korea

[3] Nengkoda, Ardian, and Zaher Mohammed Al-Hinai. 2009. Understanding of Mercury Corrosion attack on Stainless Steel Material at Gas Wells: Case Study. Paper read at International Petroleum Technology Conference, 7 - 9 December at Doha, Qatar.

[4] IPIECA. 2014. Mercury management in petroleum refining. *An IPIECA Good Practice Guide*.

[5] Radford, Ron. 2010. Mercury Management and Chemical Decontamination White Paper 2010. http://cdn2.hubspot.net/hub/22765/file-599028159-pdf/docs/mmsmercurydecontaminationwhitepaperfinal-100314092414-phpapp01.pdf?t=1405621888413&submissionGuid=4ee9e069-34e3-4815-a622-c38282787f1e),.

[6] Wilhelm, S. Mark. 2009. "Risk Analysis for Operation of Aluminum Heat Exchangers Contaminated by Mercury." *Process Safety Progress* no. 28 (3):259-266. doi: 10.1002/prs.10322.

[7] Coade, R., and D. Coldham. 2006. "The interaction of mercury and aluminium in heat exchangers in a natural gas plants." *International Journal of Pressure Vessels and Piping* no. 83 (5):336-342. doi: 10.1016/j.ijpvp.2006.02.022.

[8] El-Feky, A.A., W. El-Azab, M.A. Ebiad, Mohamed B. Masod, and S. Faramawy. 2018. "Monitoring of elemental mercury in ambient air around an Egyptian natural gas processing plant." *Journal of Natural Gas Science and Engineering* no. 54:189-201. doi: 10.1016/j.jngse.2018.01.019.

[9] Liu, QuanYou. 2013. "Mercury concentration in natural gas and its distribution in the Tarim Basin." *Science China Earth Science* no. 56 (8):1371-1379. doi: 10.1007/s11430-013-4609-2.

[10] Ezzeldin, Mohamed F., Zuzana Gajdosechova, Mohamed B. Masod, Tamer Zaki, Jörg Feldmann, and Eva M. Krupp. 2016. "Mercury Speciation and Distribution in an Egyptian Natural Gas Processing Plant." *Energy & Fuels* no. 30 (12):10236-10243. doi: 10.1021/acs.energyfuels.6b02035.

[11] Wongkasemjit, S., and A. Wasantakorn. 2000. "Laboratory Study of Corrosion Effect of Dimethyl-Mercury on Natural Gas Processing Equipment." *The Journal of Corrosion Science and Engineering* no. 1 (12).

[12] Huber, Marcia L., Arno Laesecke, and Daniel G. Friend. 2006. "Correlation for the Vapor Pressure of Mercury." *Industrial & Engineering Chemistry Research* no. 45 (21):7351-7361. doi: 10.1021/ie060560s.

[13] Bernard, L., K. Awitor, J. Badaud, O. Bonnin, B. Coupat, J. Fournier, and P. Verdier. 1997. "D´etermination de la pression de vapeur de HgCl2 par la m´ethode d'effusion de Knudsen." *Journal de Physique III* no. 7 (2):311-319. doi: 10.1051/jp3:1997124.

[14] Carson, A. S., D. R. Stranks, and B. R. Wilmshurst. 1958. "The Measurement of Very Low Vapour Pressures Using Radioactive Isotopes: The Latent Heat

of Sublimation of Mercury Diphenyl." *Proceedings of the Royal Society A* no. 244 (1236):72-84. doi: 10.1098/rspa.1958.0026.

[15] Wilhelm, S. Mark, and Nicholas Bloom. 2000. "Mercury in Petroleum." *Fuel Processing Technology* no. 63 (2000):1-27.

[16] Wilhelm, S. Mark. 2001. Mercury in Petroleum and Natural Gas: Estimation of Emissions from Production, Processing, and Combustion. Tomball, Texas.

[17] Corvini, Giacomo, Julie Stiltner, and Keith Clark. 2016. Mercury removal from natural gas and liquid streams https://www.uop.com/?document=mercury-removal-from-natural-gas-and-liquid-streams&download=1.

[18] Zettlitzer, M., R. Scholer, and R. Falter. 1997. Determination of elemental, inorganic and organic mercury in North German gas condesates and formation brines. In *SPE International Symposium on Oilfiled Chemistry*. Houston, Texas: Society of Petroleum Engineers, Inc. .

[19] Schickling, C., and J. A. C. Broekaert. 1995. "Determination of mercury species in gas condensates by on-line coupled High-performance liquid Chromatography and Cold-vapor atomic absorption spectrometry." *Applied Organometallic Chemistry* no. 9:29-36.

[20] Tao, Hiroaki, Tadahiko Murakami, Mamoru Tominaga, and Akira Miyazaki. 1998. "Mercury speciation in natural gas condensate by gas chromatography-inductively coupled plasma mass spectrometry." *Journal of Analytical Atomic Spectrometry* no. 13 (1998):1086-1093.

[21] Bingham, Mark D. 1990. "Field Detection and Implications of Mercury in Natural Gas." *Society of Petroleum Engineers Production Engineering*:120-124.

[22] Abbas, Tauqeer, Girma Gonfa, Kallidanthiyil Chellappan Lethesh, M.I. Abdul Mutalib, Mahpuzah bt Abai, Kuah Yong Cheun, and Eakalak Khan. 2016. "Mercury capture from natural gas by carbon supported ionic liquids: Synthesis, evaluation and molecular mechanism." *Fuel* no. 177:296-303. doi: 10.1016/j.fuel.2016.03.032.

[23] Bebout, Deborah C. 2006. "Mercury: Inorganic & Coordination Chemistry." *Encyclopedia of Inorganic Chemistry*. doi: 10.1002/0470862106.ia131.

[24] Hall, B., P. Schager, and O. Lindqvist. 1991. "Chemical Reactions of Mercury in Combustion Flue Gases " *Water, Air, and Soil Pollution* no. 56:3-14.

[25] Audeh, Costi A. 1993. Hydrogen Sulphide: An Effective Reagent for Reducing the Elemental Mercury Content of Liquid Hydrocarbons. Paper read at 206th ACS National Meeting, 22-26 Augustus at Chicago.

[26] Aliabad, H. Zare, and S. Mirzaei. 2009. "Removal of CO2 and H2S using Aqueous Alkanolamine Solusions " *International Journal of Chemical, Molecular, Nuclear, Materials and Metallurgical Engineering* no. 3 (1):50-59. doi: 10.1999/1307-6892/15675.

[27] Chevron. 2015. Gorgon Gas Development and Jansz Feed Gas Pipeline: Best Practice Pollution Control Design Report Chevron Australia Pty Ltd.

[28] O'Rear, Dennis John, Russell Evan Cooper, Feng-Ran Sheu, and Jordan Taylor Belue. 2014. Process, Method, and System for Removing Mercury from Fluids Chevron U.S.A. Inc.,.

[29] Cui, Zheng, Adisorn Aroonwilas, and Amornvadee Veawab. 2010. "Simultaneous Capture of Mercury and CO2 in Amine-Based CO2 Absorption Process." *Industrial & Engineering Chemistry Research* no. 49 (24):12576-12586. doi: 10.1021/ie100687a.

[30] Igunnu, Ebenezer T., and George Z. Chen. 2012. "Produced water treatment technologies." *International Journal of Low-Carbon Technologies* no. 9 (3):157-177. doi: 10.1093/ijlct/cts049.

[31] (ECHA), European Chemicals Agency. 2011. Background document to the Opinions on the Annex XV dossier proposing restrictions on five Phenylmercury compounds. https://echa.europa.eu/documents/10162/4a71bea0-31f0-406d-8a85-59e4bf2409da.

[32] Ma, Yongpeng, Haomiao Xu, Zan Qu, Naiqiang Yan, and Wenhua Wang. 2014. "Absorption characteristics of elemental mercury in mercury chloride solutions." *Journal of Environmental Sciences* no. 26 (11):2257-2265. doi: 10.1016/j.jes.2014.09.011.

[33] Jacobson, C. A. 1951. *Encyclopedia of chemical reactions*. Vol. Volume 4. New York, USA: Reinhold Publishing Corp. .

[34] Ralston, A. W., and J. A. Wilkinson. 1928. "Reactions in liquid hydrogen sulfide. III Thiohydrolysis of chlorides[1]." *Journal of the American Chemical Society* no. 50 (2):258-264. doi: 10.1021/ja01389a002.

[35] McCutchan, Roy T., and Kenneth A. Kobe. 1954. "Diphenylmercury Synthesis." *Industrial & Engineering Chemistry* no. 46 (4):675-680. doi: 10.1021/ie50532a027.

[36] Bamford, C.H., and C.F.H. Tipper. 1972. *Reactions of Aromatic Compounds*. Vol. 13, *Comprehensive Chemical Kinetics*.

[37] Dessy, Raymond E., and Y. K. Lee. 1960. "The Mechanism of the Reaction of Mercuric Halides with Dialkyl and Diarylmercury Compounds." *Journal of the Americal Chemical Society* no. 82 (3):689-693. doi: 0.1021/ja01488a047.

[38] Lobana, Tarlok S. 2006. Organometallics. In *Inorganic Chemistry*. Amritsar 143005 Guru Nanak Dev University

[39] Sabri, Y. M., S. J. Ippolito, J. Tardio, S. Bee Abd Hamid, and S. K. Bhargava. 2015. "Mercury Migration and Speciation Study during Monoethylene Glycol Regeneration Processes." *Industrial & Engineering Chemistry Research* no. 54 (19):5349-5355. doi: 10.1021/acs.iecr.5b00492.

[40] Sabri, Y.M., S.J. Ippolito, J. Tardio, P.D. Morrison, and S.K. Bhargava. 2015. "Studying mercury partition in monoethylene glycol (MEG) used in gas facilities." *Fuel* no. 159:917-924. doi: 10.1016/j.fuel.2015.07.047.

[41] Gallup, Darrell L., Dennis J. O'Rear, and Ron Radford. 2017. "The behavior of mercury in water, alcohols, monoethylene glycol and triethylene glycol." *Fuel* no. 196:179-184. doi: 10.1016/j.fuel.2017.01.100.

[42] Rogers, Robin D., Andrew H. Bond, and Janice L. Wolff. 2006. "Structural Studies of Polyether Coordination to Mercury (II) Halides: Crown Ether Versus Polyethylene Glycol Complexation " *Journal of Coordination Chemistry* no. 29 (4):187-207. doi: 10.1080/00958979308037425.

[43] Pancharoen, Ura, Sawatpop Somboonpanya, Srestha Chaturabul, and Anchaleeporn Waritswat Lothongkum. 2010. "Selective removal of mercury as HgCl42− from natural gas well produced water by TOA via HFSLM." *Journal of Alloys and Compounds* no. 489 (1):72-79. doi: 10.1016/j.jallcom.2009.08.145.

[44] Gallup, Darrell L., and James B. Strong. 2007. Removal of Mercury and Arsenic from Produced Water http://citeseerx.ist.psu.edu/viewdoc/download?doi=10.1.1.626.7356&rep=rep1&type=pdf.

[45] Ochi, Jalel, Dominique Dexheimer, and Vincent Corpel. 2013. Produced Water Re-Injection Design and Uncertainties Assessment In *SPE European Formation Damage Conference & Exhibition*. Noordwijk, The Netherlands.

[46] Rongponsumrit, Manisa, Suwat Athichanagorn, and Thotsaphon Chaiananansutcharit. 2006. Optimal Strategy of Disposing Mercury Contaminated Waste. In *International Oil & Gas Conference and Exhibition in China*. Beijing, China.

[47] Dreher, Trina, Courtney Hocking, Michael Cavill, and Adam Geard. 2014. Increasing Sales Gas Output From Glycol Dehydration Plants In *SPE Asia Pacific Oil & Gas Conference and Exhibition*. Adelaide, Australia.

[48] Lang, David, Murray Gardner, and John Holmes. 2012. Mercury arising from oil and gas production in the United Kingdom and UK continental shelf. University of Oxford.

[49] Avellan, Astrid, John P. Stegemeier, Ke Gai, James Dale, Heileen Hsu-Kim, Clément Levard, Dennis O'Rear, Thomas P. Hoelen, and Gregory V. Lowry. 2018. "Speciation of Mercury in Selected Areas of the Petroleum Value Chain." *Environmental Science & Technology* no. 52 (3):1655-1664. doi: 10.1021/acs.est.7b05066.

[50] Zaboon, Sami, Adam Soames, Varun Ghodkay, Rolf Gubner, and Ahmed Barifcani. 2017. "Recovery of mono-ethylene glycol by distillation and the impact of dissolved salts evaluated through simulation of field data." *Journal of Natural Gas Science and Engineering* no. 44:214-232. doi: 10.1016/j.jngse.2017.04.007.

[51] Driscoll, Charles T., Robert P. Mason, Hing Man Chan, Daniel J. Jacob, and Nicola Pirrone. 2013. "Mercury as a Global Pollutant: Sources, Pathways, and Effects." *Environmental Science & Technology* no. 47 (10):4967-4983. doi: 10.1021/es305071v.

[52] Morel, Francois M. M., Anne M. L. Kraepiel, and Marc Amyot. 1998. "The Chemical Cycle and Bioaccumulation of Mercury." *Annual Review Ecology and Systematics* no. 29:543-566.

[53] Lindqvist, Oliver, and Henning Rodhe. 1985 "Atmospheric mercury—a review." *Tellus* no. 27V (3):136-159. doi: 10.1111/j.1600-0889.1985.tb00062.x.

[54] Selin, Noelle E., Daniel J. Jacob, Rokjin J. Park, Robert M. Yantosca, Sarah Strode, Lyatt Jaeglé, and Daniel Jaffe. 2007. "Chemical cycling and deposition of atmospheric mercury: Global constraints from observations." *Journal of Geophysical Research: Atmospheres* no. 112 (D2). doi: 10.1029/2006JD007450.

[55] Wängberg, Ingvar, Jana Moldanová, and John Munthe. 2010. Mercury cycling in the Environment - Effects of Climate Change IVL Swedish Environmental Research Institute

[56] Shia, Run‐Lie, Christian Seigneur, Prasad Pai, Malcolm Ko, and Nien Dak Sze. 1999. "Global simulation of atmospheric mercury concentrations and deposition fluxes." *Journal of Geophysical Research: Atmospheres* no. 104 (D19):23747-23760 doi: 10.1029/1999JD900354.

[57] Douglas, Thomas A., Lisa L. Loseto, Robie W. Macdonald, Peter Outridge, Aurélien Dommergue, Alexandre Poulain, Marc Amyot, Tamar Barkay, Torunn Berg, John Chételat, Philippe Constant, Marlene Evans, Christophe Ferrari, Nikolaus Gantner, Matthew S. Johnson, Jane Kirk, Niels Kroer, Catherine Larose, David Lean, Torkel Gissel Nielsen, Laurier Poissant, Sigurd

Rognerud, Henrik Skov, Søren Sørensen, Feiuye Wang, Simon Wilson, and Christian M. Zdanowicz. 2012. "The fate of mercury in Arctic terrestrial and aquatic ecosystems, a review." *Environmental Chemistry* no. 9 (4):321-355. doi: 10.1071/EN11140.

[58] Hedgecock, Ian M., and Nicola Pirrone. 2004. "Chasing Quicksilver: Modeling the Atmospheric Lifetime of Hg0(g) in the Marine Boundary Layer at Various Latitudes." *Encironmental Science & Technology* no. 38 (1):69-76. doi: 10.1021/es034623z.

[59] Travnikov, Oleg. 2011. Atmospheric Transport of Mercury. In *Environmental Chemistry and Toxicology of Mercury*, edited by Guangliang Liu, Yong Cai and Nelson O'Driscoll: John Wiley & Sons, Inc.

[60] Pichtel, John. 2016. "Oil and Gas Production Wastewater: Soil Contamination and Pollution Prevention." *Applied and Environmental Soil Science* no. 2016:1-24. doi: 10.1155/2016/2707989.

[61] Wallin, Thomas. 1976. "Deposition of airborne mercury from six Swedish chlor-alkali plants surveyed by moss analysis." *Environmental Pollution (1970)* no. 10 (2):101-114. doi: 10.1016/0013-9327(76)90100-2.

[62] Lodenius, Martin. 1998. "Dry and wet deposition of mercury near a chlor-alkali plant." *The Science of the Total Environment* no. 23 (1-3):53-56. doi: 10.1016/S0048-9697(98)00073-4.

[63] Lodenius, Martin, and Esa Tulisalo. 1984. "Environmental Mercury Contamination Around a Chlor-Alkali Plant " *Bulletin of Environmental Contamination and Toxicology* no. 32 (1):439-444. doi: 10.1007/BF01607520.

[64] Han, Yeongcheol, Youngsook Huh, Soon Do Hur, Sungmin Hong, Ji Woong Chung, and Hideaki Motoyama. 2017. "Net deposition of mercury to the Antarctic Plateau enhanced by sea salt." *Science of The Total Environment* no. 583:81-87. doi: 10.1016/j.scitotenv.2017.01.008.

[65] Magalhães, Maria Elizabeth Afonso de, and Matthieu Tubino. 1995. "A possible path for mercury in biological systems: the oxidation of metallic mercury by molecular oxygen in aqueous solutions." *The Science of the Total Environment* no. 170 (3):229-239. doi: 10.1016/0048-9697(95)04711-5.

[66] Seigneur, Christian, Jacek Wrobel, and Elpida Constantinou. 1994. "A Chemical Kinetic Mechanism for Atmospheric Inorganic Mercury." *Environmental Science & Technology* no. 28 (9):1589-1597. doi: 10.1021/es00058a009.

[67] Kozin, Leonid F, and Steve Hansen. 2013. "Mercury Handbook: Chemistry, Applications and Environmental Impact." In: Royal Society of Chemistry.

[68] Clarkson, Thomas W., and Laszlo Magos. 2006. "The Toxicology of Mercury and Its Chemical Compounds." *Critical Reviews in Toxicology* no. 36 (8):609-662. doi: 10.1080/10408440600845619.

CHAPTER 7:
CONCLUSIONS AND RECOMMENDATIONS

7.1 Introduction

The aim of this chapter is to summarize the major results and findings achieved from this PhD work. The objective of the work carried out is to study the behaviour characteristics of gaseous inorganic and organic mercury species in reservoir fluids and aqueous environment. The mercury species selected for this work comprise of Hg^0, $HgCl_2$ and Ph_2Hg, each representing the various mercury species (elemental, inorganic and organic mercury) found within the oil and gas processes. At different working conditions and presence of different impurities, their effects on the dynamic solubility of these mercury species have been investigated. Key parameters such as absorption characteristics, reaction pathways and reaction constant have been evaluated to improve understanding and prediction of the absorption of the selected mercury species in fresh and sea water. Main findings achieved are summarized in the following sections. Based on the conclusions of this research work, recommendations are proposed for future studies to further close the knowledge gaps in this research area.

7.2 Conclusions

Results from the dynamic solubility of mercury species into liquids with similar composition to the reservoir fluids yield higher understanding of their behaviour in the oil and gas processes. As mercury species characterizes differently both physically and chemically, their behaviour when exposed to aqueous environment greatly varies as well. Aspects of operating condition such as temperature and chemical reaction with existing compounds within the oil and gas process fluids have been investigated and inferred.

7.2.1 Behaviour of $HgCl_2$ in Aqueous Environment

- Dynamic solubility of gaseous $HgCl_2$ into water phase show characteristics of ‘highly soluble gas’ where the absorption process is controlled the gas phase resistance. Absorption has been reported to increase significantly with

elevation of temperature. However, this enhancement is minimal with increase in $HgCl_2$ concentration in the gas phase. This result finding suggest that absorption of $HgCl_2$ into streams of produced waters and waste waters would occur very fast. Vapour/liquid equilibrium is not expected to be achieved within any section of the LNG processes.

- Presence of NaCl (NaCl concentration of up to 3.5 wt. %) within the reservoir fluids will caused a chemical-reaction-enhanced absorption of $HgCl_2$ due to the formation highly soluble and stable $Na_2[HgCl_4]$ complex.
- The chemical reaction between $HgCl_2$ and NaCl follows second-order; reaction constant, k_2 as a function of temperature is as follows:

$$k_2 = 1.09 \times 10^9 \exp\left(\frac{-123.32\ \mathrm{kJ/mol}}{RT}\right)$$

The chemical reaction is classified as a 'slow reaction' due to its high activation energy, hence it is relatively sensitive when temperature aspect comes into play. Therefore, absorption of $HgCl_2$ will be expected to occur more at process streams/equipment with higher operating temperature, such as the distillation step at the glycol and amine regeneration units. As the used MEG, amine and condensate were heated to remove the water vapour, the $HgCl_2$ present in the gas will partition into the re-circulated MEG and amine solution. This increased in absorption contributes to the prevalence of $HgCl_2$ reported in the recycled MEG and amine streams.

- Absorption of $HgCl_2$ into MEG solution (2 – 30 v/v %) did not show significant outcome on the process. Chemical reaction between $HgCl_2$ and MEG yielding organically-bound mercury was not detected despite long-term contact of the two compounds. The result findings suggest $HgCl_2$ absorption behaviour to follow physical absorption. Absorption of $HgCl_2$ at process streams with higher MEG content will occur less due to the increase in physical properties of the liquid (increase in viscosity resulting in higher mass transfer resistance).

7.2.2 Behaviour of Ph_2Hg in Aqueous Environment

- Dynamic solubility of Ph_2Hg gas into water is similar to Hg^0, and is controlled by the mass transfer resistance at the liquid phase. Absorption rate of Ph_2Hg is promoted at conditions of elevated temperature.

- Presence of NaCl (up to 3.5 wt. % NaCl concentration) have been found to depress absorption flux of Ph_2Hg due to the effect of salting out. This finding suggest that partitioning of Ph_2Hg would most likely occur in process streams containing higher portion of organic phase, such as the condensation stabilization unit.
- Ph_2Hg is found to be 20 times more soluble in solution with 50 v/v% MEG compared to in fresh water. However, there is no enhancement of absorption flux when Ph_2Hg was exposed to solutions of 10 – 30 v/v% MEG. Further increase of MEG concentration to 50 v/v% show a decrease in the overall absorption of the compound. The findings show that absorption process of Ph_2Hg into the aqueous environment follow a physical absorption and that no chemical reaction was detected to enhance the mass transfer.

7.3 Recommendations

Based on the outcome of the current work achieved, the following recommendations for future studies to further close the knowledge gaps are suggested:

1. Numerous equipment within the oil and gas process operates at variable conditions (pressure and temperature) to achieve the desired production outcome. It's been observed during maintenance that deposition of mercury occurs mainly at cryogenic heat exchangers that operate at these extreme conditions. Reactor design that operate at high pressure and temperature would need to be developed and tested to emulate real-life production conditions. This is imperative to further close the knowledge gap on the effect of extended pressure and temperature on solubility kinetics of mercury species.
2. It has been reviewed in Chapter 2 that inorganic and organic mercury in the oil and gas processes are not limited to just $HgCl_2$ and Ph_2Hg. Therefore, dynamic solubility of other detected inorganic and organic mercury species such as $Hg(CH_3)_2$, $Hg(C_2H_5)_2$, Hg_2Cl_2 and Hg-sulphur compounds should be evaluated. This is necessary to have a better understanding of the overall behaviour of mercury within the oil and gas processes.
3. Mercury speciation is a very important aspect in understanding and predicting mercury behaviour within a process. However, this aspect of mercury studies still remain a challenge and limited techniques are available to characterize the

various mercury species that partition into the phases. To this date, mercury speciation is mainly done on condensate samples and not a lot of information are available for gas samples. Thus, the next important step would be to incorporate mercury speciation into the dynamic solubility study. Being able to qualify and quantify the various mercury species present in the absorbed liquids would lead to more accurate kinetics evaluation and compound specific mass balance.

4. Liquid in a conventional oil and gas process consists of a very complex matrix. Effect of impurities such as divalent salts; $CaCO_3$, $FeCO_3$ and FeS on the solubility kinetics of different mercury species should be studied.
5. Mercury and its species are known to be reactive. Hence, interconversion of these species when they come into contact with each other and at different operating conditions should be investigated.

APPENDIX:

STATEMENT OF CONTRIBUTION BY OTHERS

To Whom It May Concern,

I, Fenny Anggreni Kho, contributed all aspects (experiments, analysis, write-up, etc.) of the work to the publications entitled:

1. Kho, Fenny, and Gia Hung Pham. 2018. "Absorption kinetics of mercury (II) chloride into water and aqueous sodium chloride solution." Fuel Processing Technology no. 174:78-87. doi: 10.1016/j.fuproc.2018.02.017
2. Kho, Fenny, and Gia Hung Pham. 2019. "Absorption kinetics of mercury (II) chloride into mono-ethylene glycol (MEG) solution." Fuel Processing Technology no. 185:46-55. doi: 10.1016/j.fuproc.2018.11.018.

.....

I, as a Co-Author, endorse that this level of contribution by the candidate indicated above is appropriate.

Dr. Gia Hung Pham .....